Universidade de Lisboa

Faculdade de Farmácia

S-Adenosylhomocysteine Promotes Endothelial Dysfunction and Activation: a Role for Hypomethylation in Vascular Disease

Maria Madalena Henriques Serras Vicente Barroso

Orientadores: - Prof. Doutora Maria Rita Mouzinho de Albuquerque de Azevedo e Castro
- Prof. Doutora Diane Elizabeth Handy

Tese especialmente elaborada para obtenção do grau de Doutor em Farmácia

(Especialidade: Biologia Celular e Molecular)

2015

Universidade de Lisboa
Faculdade de Farmácia

S-Adenosylhomocysteine Promotes Endothelial Dysfunction and Activation: a Role for Hypomethylation in Vascular Disease

Maria Madalena Henriques Serras Vicente Barroso

Orientadores: - Prof. Doutora Maria Rita Mouzinho de Albuquerque de Azevedo e Castro
- Prof. Doutora Diane Elizabeth Handy

Tese especialmente elaborada para obtenção do grau de Doutor em Farmácia
(Especialidade: Biologia Celular e Molecular)

Júri:
Presidente: Prof. Doutora Cecília Maria Pereira Rodrigues
Vogais:
- Prof. Doutor Joseph Loscalzo
- Prof. Doutora Diane E. Handy
- Prof. Doutor João António Nave Laranjinha
- Prof. Doutora Paula Alexandra Quintela Videira
- Prof. Doutor Luís Afonso Brás Simões do Rosário
- Prof. Doutora Maria Isabel Ginestal Tavares de Almeida
- Prof. Doutora Maria Rita Mouzinho de Albuquerque de Azevedo e Castro

2015

Universidade de Lisboa

Faculdade de Farmácia

S-Adenosylhomocysteine Promotes Endothelial Dysfunction and Activation: a Role for Hypomethylation in Vascular Disease

S-Adenosilhomocisteína Promove Disfunção e Ativação Endotelial: um Papel para a Hipometilação na Doença Vascular

Tese especialmente elaborada para obtenção do grau de Doutor em Farmácia

(Especialidade: Biologia Celular e Molecular)

2015

The studies presented in this thesis were performed at the Metabolism and Genetics Group, The Research Institute for Medicines (iMed.ULisboa), and at the Department of Biochemistry and Human Biology, Faculdade de Farmácia da Universidade de Lisboa, Portugal, under the supervision of Professor Rita Azevedo e Castro, and at the Cardiovascular Division, Department of Medicine, Brigham and Women's Hospital and Harvard Medical School, Harvard University, Boston, USA, under the supervision of Professor Diane E. Handy. This work was financially supported by Fundação para a Ciência e a Tecnologia (F.C.T.), Lisboa, Portugal (SFRH/BD/73021/2010).

Para os meus pais…

TABLE OF CONTENTS

ABBREVIATIONS

5-aza-dC	5-aza-2'-deoxycytidine
5-mC	5-methylcytosine
5-MTHF	5-methyltetrahydrofolate
5,10-meTHF	5,10-methylenetetrahydrofolate
ADA	adenosine-2',3'-dialdehyde
AdCtrl	control adenoviral vector
AdGPx-1	adenoviral construct with the human glutathione peroxidase-1 cDNA
AdIkBDN	adenovirus carrying the dominant negative IkB
ADMA	asymmetric dimethylarginine
Ad-βGal	adenoviral construct with a CMV-LacZ cassette
ALKBH8	alkylation repair homolog 8
Am	2′-O-methyladenosine
ATP	adenosine triphosphate
BHMT	betaine-homocysteine methyltransferase
BNIP3	BCL2/adenovirus E1B 19kDa interacting protein 3
CBS	cystathionine β-synthase
CDKN1A	cyclin-dependent kinase inhibitor 1A
CDKN2A	cyclin-dependent kinase inhibitor 2A
CGL	cystathionine γ-lyase
Cm	2′-O-methylcytidine
cm^5U	5-carboxymethyluridine
Ctrl	control
CVD	cardiovascular disease
DAPI	4',6-diamidino-2-phenylindole
DNMT	DNA-methyltransferase
DTNB	5,5'-dithio-bis(2-nitrobenzoic acid)
DTT	dithiothreitol
eNOS	endothelial nitric oxide synthase
EZH2	enhancer of zeste homolog 2
FoxO1	forkhead box O 1
Gm	2′-O-methylguanosine
GPx1	glutathione peroxidase-1
GRP	glucose-regulated protein

H_2O_2	hydrogen peroxide
H3K9me3	histone H3 lysine 9 trimethylation
H3K27me3	histone H3 lysine 27 trimethylation
HCAEC	human coronary artery endothelial cells
Hcy	homocysteine
HDM	histone demethylase
HHcy	hyperhomocysteinemia
HKMT	histone lysine methyltransferase
HUVEC	human umbilical vein endothelial cells
i^6A	isopentenyladenosine
ICAM-1	intercellular adhesion molecule-1
IkB	inhibitor of kappa B
IkBDN	inhibitor of kappa B dominant negative mutant
IKK	IκB kinase complex
IL	interleukin
JMJD3	jumonji domain containing 3 demethylase
LC-MS/MS	liquid chromatography-tandem mass spectrometry
LDH	lactate dehydrogenase
LDL	low-density lipoprotein
LDLR	low-density lipoprotein receptor
L-NNA	L-N^G-nitroarginine
m^1A	1-methyladenosine
m^1G	1-methylguanosine
$m_2{}^6A$	N^6,N^6-dimethyladenosine
m^2G	N^2-methylguanosine
m^5C	5-methylcytidine
m^5U	5-methyluridine
m^6A	N^6-methyladenosine
m^7G	7-methylguanosine
MAT	methionine adenosyltransferase
mcm^5U	5-methoxycarbonylmethyluridine
mcm^5Um	5-methoxycarbonylmethyl-2′-O-methyluridine
MFI	mean fluorescence intensity
MS	methionine synthase
MsrB1	methionine sulfoxide reductase B1
MTHFR	5,10-methylenetetrahydrofolate reductase

MTT	3-(4,5-dimethylthiazol-2-yl)-2,5-diphenyltetrazolium bromide
NAC	N-acetylcysteine
NFκB	nuclear factor kappa B
NIK	NFkB-interacting kinase
NO	nitric oxide
NOX	NADPH oxidase
NT	no treatment
PBS	phosphate-buffered saline
PDGF	platelet-derived growth factor
PECAM-1	platelet endothelial cell adhesion molecule-1
PKC	protein kinase C
PRC	polycomb repressive complex
PRMT1	protein arginine methyltransferase-1
qRT-PCR	quantitative reverse transcription polymerase chain reaction
ROS	reactive oxygen species
SAH	S-adenosylhomocysteine
SAHH	S-adenosylhomocysteine hydrolase
SAM	S-adenosylmethionine
Sec	selenocysteine
SELE	E-selectin coding gene
SelH	selenoprotein H
SelM	selenoprotein M
Shc	Src homology 2 domain containing
SHMT	serine hydroxymethyltransferase
siRNA	small interference RNA
SOD	superoxide dismutase
SREBF1	sterol regulatory element binding transcription factor-1
TET	ten-eleven translocation enzymes
THF	tetrahydrofolate
TNF	tumor necrosis factor
TRM112	tRNA methyltransferase 112 homolog
$tRNA^{[Ser]Sec}$	selenocysteine-carrying tRNA (Sec-tRNA)
TrxR	thioredoxin reductase
Um	2′-O-methyluridine
UPR	unfolded protein response

UTX	ubiquitously transcribed tetratricopeptide repeat on X chromosome demethylase
VCAM-1	vascular adhesion molecule-1
WBC	white blood cells

SUMMARY

Homocysteine has been established as a risk factor for cardiovascular disease (CVD) by mechanisms incompletely defined. S-Adenosylhomocysteine (SAH) is the metabolic precursor of homocysteine that accumulates in the setting of hyperhomocysteinemia and is a negative regulator of most cell methyltransferases.

This thesis project investigated whether methylation imbalance, caused by excess SAH, disrupts endothelium homeostasis and favors the establishment of a pro-atherogenic phenotype.

To experimentally address this possibility, studies were conducted in human endothelial cells, in which SAH accumulation was induced using either a pharmacologic or a siRNA approach. As the major regulator of vascular homeostasis, the endothelium exerts a number of vasoprotective effects that are largely mediated by nitric oxide (NO), the most potent endogenous vasodilator. Decreased NO bioavailability is a principal manifestation of underlying endothelial dysfunction, an early marker of atherosclerosis and CVD. To determine whether excess SAH alters NO bioavailability, the expression and activity of endothelial nitric oxide synthase (eNOS), and NO production were monitored in cells. These experiments showed that excess SAH increased the levels of eNOS mRNA but caused a decrease in eNOS protein and activity, to decrease cellular production of NO.

Another important feature of endothelial dysfunction is oxidative stress. Studies in endothelial cells revealed that a hypomethylating environment, induced by excess SAH, impairs, not only NO production, but also the cellular redox state. Glutathione peroxidase-1 (GPx-1) is a selenoprotein and a major cellular antioxidant. A link between homocysteine-associated suppression of GPx-1 and endothelial dysfunction had been reported previously; however, the causal molecular mechanisms remained unresolved. The experiments presented here demonstrate a specific mechanism by which SAH-mediated hypomethylation suppresses GPx-1 expression and leads to inflammatory activation of endothelial cells. The expression of a subset of selenoproteins (including GPx-1) is dependent on a specific methylation of the selenocysteine-tRNA (Sec-tRNA). Thus, SAH accumulation was found to inhibit the formation of this methylated isoform of Sec-tRNA resulting in decreased GPx-1 expression, as well as alterations in the expression of other selenoproteins, to promote oxidative stress and a pro-inflammatory activation state in endothelial cells.

The observation that Sec-tRNA methylation is decreased by excess SAH, suggests that other RNA species may also be targets for SAH-mediated hypomethylation. Therefore, the effect of SAH on methylation modifications was determined in total and size-fractionated RNA samples from our cell model. Additionally, to confirm these observations, RNA methylation was analyzed in tissue samples from a hyperhomocysteinemic mouse model, where SAH accumulation results from a genetic disorder affecting homocysteine metabolism. Conditions of excess SAH altered the content of some

RNA methylation modifications, suggesting that specific RNA methyltransferases may be more susceptible to inhibition by SAH.

The activation of endothelial cells that occurs during atherogenesis is characterized by the up-regulation of adhesion molecules, which by recruiting circulating leukocytes favor their transendothelial migration. In a series of studies, the physiological relevance of SAH-induced endothelial cell activation was demonstrated by determining that these SAH-activated cells promoted leukocyte adhesion and migration. Further, the role of DNA hypomethylation on the SAH-induced up-regulation of adhesion molecules was examined. ICAM-1 (intercellular adhesion molecule 1) was found to be up-regulated by SAH accumulation as well as by a DNA methyltransferase inhibitor, suggesting that its expression may be regulated by DNA methylation. Analysis of its promoter methylation; however, showed that it was demethylated in untreated cells, suggesting that it may be regulated by factors other than DNA promoter methylation in response to excess SAH.

To understand better the factors involved in the pro-inflammatory activation of endothelial cells, the role of NFkB (nuclear factor kappa B) in SAH-induced responses was examined. These studies establish a role for NFkB in the endothelial cell response to SAH and further link these responses to a suppression of the epigenetic regulator EZH2 (enhancer of zeste homolog 2). EZH2 is a methyltransferase that regulates gene expression by mediating a repressive histone methylation. These results identify EZH2 as a new target of SAH regulation important in inflammatory responses, demonstrating that EZH2 suppression and NFkB activation mediated by excess SAH accumulation may contribute to its adverse effects in the vasculature.

Overall, these studies implicate SAH as a key modulator of epigenetic mechanisms by compromising RNA, DNA, and histone methylation. More importantly, our results clearly present SAH as a key player in the disruption of endothelial homeostasis, supporting a role for SAH as an important mediator of homocysteine-associated vascular disease.

Key words: S-Adenosylhomocysteine, hyperhomocysteinemia, hypomethylation stress, endothelial dysfunction, pro-inflammatory phenotype.

SUMÁRIO

A doença cardiovascular é a principal causa de morte nos países desenvolvidos, facto que reflete a insuficiência das atuais medidas terapêuticas e de prevenção para esta patologia. O aumento do conhecimento sobre os mecanismos moleculares na origem da doença cardiovascular poderá assim contribuir para a resolução deste importante problema de saúde pública. A elevação dos níveis circulantes de homocisteína é um fator de risco para a ocorrência de doença cardiovascular; no entanto, os mecanismos fisiopatológicos subjacentes à relação entre a hiperhomocisteinémia e a doença cardiovascular, embora intensamente estudados, permanecem ainda por elucidar.

A homocisteína é um aminoácido sulfurado, em cujo metabolismo as vitaminas do grupo B atuam como importantes cofatores ou substratos. Em estudos clínicos, nos quais a concentração de homocisteína plasmática foi significativamente reduzida através da administração destas vitaminas, não foram observados os efeitos cardio-protetores esperados. Uma teoria alternativa propõe a S-adenosilhomocisteína (SAH), o precursor metabólico da homocisteína que se acumula em situações em que esta se encontra elevada, como um marcador mais fidedigno do risco de doença cardiovascular associado a situações de hiperhomocisteinémia. Sendo a SAH um regulador negativo da atividade enzimática da maioria das metiltransferases celulares, que atuam sobre diversos compostos (incluindo moléculas como DNA, RNA e proteínas), a sua acumulação poderá originar, teoricamente, um ambiente celular de hipometilação.

A presente tese investigou a possibilidade de o desequilíbrio das reações de metilação celulares, provocado pela elevação dos níveis intracelulares de SAH, perturbar a homeostase endotelial, favorecendo o estabelecimento de um fenótipo pró-aterogénico e a ocorrência de doença cardiovascular. Para tal, desenvolveu-se um modelo de estudo com base em células endoteliais humanas, nas quais a acumulação de SAH foi induzida através de abordagens genéticas (RNA de interferência) ou farmacológicas (inibição da atividade da enzima responsável pela síntese de SAH, a SAH hidrolase).

O endotélio é o principal regulador da homeostasia vascular, exercendo uma série de efeitos vasoprotetores que são largamente mediados pelo óxido nítrico (NO), um potente vasodilatador endógeno. A diminuição da biodisponibilidade do NO é uma manifestação importante da disfunção endotelial e um marcador precoce de aterosclerose e doença cardiovascular. O trabalho experimental desenvolvido revelou que o excesso de SAH diminui os níveis endoteliais de NO, os quais estão diretamente relacionados com a diminuição, quer dos níveis de proteína eNOS (sintase do óxido nítrico endotelial), quer da sua atividade enzimática.

Outra característica importante da disfunção endotelial é um aumento de *stress* oxidativo. Várias selenoproteínas, incluindo a glutationa peroxidase-1 (GPx-1), são componentes enzimáticos

dos principais sistemas antioxidantes celulares. Estudos anteriores relataram a existência de uma associação entre a supressão de GPx-1, induzida por um excesso de homocisteína, e a ocorrência de disfunção endotelial, sem no entanto conseguir esclarecer os mecanismos moleculares subjacentes. Adicionalmente, encontra-se descrito que a expressão de um subconjunto de selenoproteínas, entre as quais a GPx-1, depende da metilação específica do RNA de transferência necessário à incorporação do aminoácido selenocisteína (Sec-tRNA). Interessantemente, os resultados das nossas experiências revelaram que um ambiente de hipometilação, induzido por um excesso de SAH, altera não só a produção de NO, mas também o estado redox celular. Efetivamente, as experiências aqui apresentadas demonstraram a existência de um mecanismo específico através do qual a hipometilação suprime a expressão de GPx-1 e leva à ativação inflamatória das células endoteliais. Os resultados revelaram que a acumulação de SAH inibe a formação da isoforma metilada do Sec-tRNA, o que resulta na diminuição da expressão da GPx-1, bem como em alterações na expressão de outras selenoproteínas, promovendo, desta forma, um estado de *stress* oxidativo e de ativação pró-inflamatória das células endoteliais.

A observação de que a metilação do Sec-tRNA é reduzida por um excesso de SAH sugere a possibilidade de que outras espécies de RNA possam ser igualmente alvos da hipometilação mediada pela acumulação intracelular de SAH. Para averiguar esta possibilidade, foram quantificadas modificações de metilação, quer em RNA total, quer em diferentes espécies de RNA obtidas por fracionamento de acordo com o seu tamanho molecular, extraídas de amostras do nosso modelo celular. Adicionalmente, estas observações foram avaliadas em amostras de tecido obtidas a partir de um modelo animal de hiperhomocisteinémia, no qual a acumulação de SAH resulta de uma deficiência da enzima CBS (cistationina β-sintetase) envolvida no catabolismo da homocisteína. Em ambas as condições estudadas, os resultados revelaram alterações nos níveis de modificações por metilação do RNA, sugerindo que as metiltransferases específicas de RNA são suscetíveis à inibição da sua atividade enzimática pela acumulação de SAH.

O estado de ativação de células endoteliais que ocorre durante a aterogénese caracteriza-se por um aumento da expressão de citocinas e moléculas de adesão, as quais recrutam leucócitos circulantes, favorecendo a sua migração transendotelial e a formação das placas de ateroma. A relevância fisiológica da ativação endotelial induzida pela SAH foi demonstrada numa série de estudos, nos quais se observou um aumento da expressão de moléculas de adesão e um acréscimo na capacidade das células endoteliais promoverem a adesão de leucócitos e a sua subsequente transmigração.

A metilação do DNA é um mecanismo epigenético que pode regular a expressão genética, estando a hipometilação das regiões promotoras tipicamente associada com a ativação da expressão dos genes correspondentes. Por esta razão, após a confirmação de que SAH induz uma hipometilação global do DNA no modelo celular utilizado, foi examinado o papel desta hipometilação

na sobre-expressão de moléculas de adesão. Os resultados revelaram que a expressão endotelial de ICAM-1 (*intercellular adhesion molecule*-1), uma importante molécula de adesão, era regulada positivamente não só por uma acumulação de SAH induzida no nosso modelo celular, mas também pela utilização de um inibidor específico das metiltransferases do DNA. No entanto, a quantificação dos níveis de metilação no promotor do gene *ICAM1* revelaram um estado de hipometilação nas células controlo, ou seja, com níveis normais de SAH. Estes dados demonstram que a indução da expressão de ICAM-1 por SAH é mediada por fatores independentes da hipometilação do seu promotor.

Como referido, o excesso de SAH induz um fenótipo pró-inflamatório nas células endoteliais. Assim, e com o intuito de compreender melhor os mecanismos moleculares subjacentes, foram examinadas as vias de ativação do NFkB (*nuclear factor kappa B*), um conhecido promotor da resposta inflamatória. Os resultados estabelecem um papel da ativação do NFkB nesta resposta inflamatória, sugerindo que a supressão do regulador epigenético EZH2 (*enhancer of zeste homolog 2*) possa contribuir para esta resposta. O EZH2 é uma histona metiltransferase que regula negativamente a expressão genética através da metilação específica das histonas (nomeadamente ao estabelecer a trimetilação da lisina 27 na histona H3, ou seja a marca epigenética H3K27me3). A acumulação de SAH em células endoteliais resultou numa diminuição da expressão e atividade de EZH2, que subsequentemente determinou um aumento de expressão de citocinas pro-inflamatórias e moléculas de adesão celular. Estes resultados revelaram assim um novo alvo para a SAH na regulação da resposta inflamatória endotelial, demonstrando que a supressão de EZH2 e a ativação de NFkB, mediadas pelo excesso de SAH, contribuem para os seus efeitos adversos no endotélio.

Considerados em conjunto, estes estudos implicam a SAH como um metabolito chave na modulação de mecanismos epigenéticos, ao comprometer a metilação do DNA, do RNA e das histonas, e mostram claramente que a acumulação de SAH desempenha um papel determinante na perturbação da homeostasia do endotélio. Como referido anteriormente, a SAH é o precursor metabólico da homocisteína. Os resultados aqui apresentados demonstram um papel importante da SAH como mediador da doença vascular associada à hiperhomocisteinémia, suportando a hipótese da SAH ser um possível marcador mais fidedigno do que a própria homocisteína.

Palavras-chave: S-adenosilhomocisteína, hiperhomocisteinémia, *stress* de hipometilação, disfunção endotelial, fenótipo pro-inflamatório.

CHAPTER

1

General Introduction

1. Homocysteine Metabolism

Homocysteine was identified by the Nobel laureate Vincent DuVigneaud in 1932 during his pioneering studies on sulfur amino-acid chemistry. In fact, he first discovered the disulfide homocystine, and only later identified its reduced form, an intermediate of methionine metabolism, which he named homocysteine (1).

Homocysteine metabolism is shown in Figure 1. Homocysteine is formed by the demethylation of the essential amino acid, methionine, via the formation of two intermediate compounds, S-adenosylmethionine (SAM) and S-adenosylhomocysteine (SAH) (2). Methionine is first converted to SAM through the catalytic action of methionine adenosyltransferase enzymes (MATs). MAT transfers the adenosyl moiety of ATP to the methionine molecule, forming SAM, a highly energetic compound. SAM is the major methyl-donor compound for cellular methylation reactions, which are catalyzed by specific methyltransferases that target important biomolecules, such as DNA, RNA, proteins, and lipids (2). Nevertheless, in mammals, most methyl groups transferred from SAM are used in creatine formation, in phosphatidylcholine synthesis, and in the generation of sarcosine from glycine (3). After the transfer of a methyl group, the methylated product is formed and SAM is converted to SAH. Importantly, because SAH has nearly the same, or even higher affinity for the catalytic site of most SAM-dependent methyltransferases than SAM, SAH is a potent inhibitor of these methyltransferases and the SAM/SAH ratio is often used as an indicator for intracellular methylation capacity (4).

SAH is further converted into homocysteine and adenosine by SAH hydrolase (SAHH), which is ubiquitously expressed in mammalian tissues. The formation of homocysteine from methionine via the transmethylation pathway is the only pathway for homocysteine biosynthesis in humans (2).

Importantly, the SAH hydrolase reaction is reversible and presents a thermodynamic equilibrium that strongly favors SAH synthesis rather than its hydrolysis (5). However, under normal physiological conditions the reaction is directed towards SAH hydrolysis due to the rapid metabolism or export of homocysteine. Homocysteine is located at a metabolic branch point and can be either conserved by remethylation back to methionine or irreversibly degraded to cysteine via the transsulfuration pathway (5).

Homocysteine can be remethylated back to methionine by two alternative metabolic pathways, the folate-dependent or independent remethylation pathways (Figure 1). 5-Methyltetrahydrofolate (5-MTHF) is the active folate derivative and the main circulating form of folate in plasma. In the folate dependent-pathway, 5-MTHF supplies the methyl group used by methionine synthase (MS) to remethylate homocysteine and produce methionine and tetrahydrofolate (THF). THF is then converted to 5,10-methylenetetrahydrofolate (5,10-MeTHF) in the presence of serine and vitamin B_6 by the enzyme serine hydroxymethyltransferase (SHMT). After reduction by 5,10-methylenetetrahydrofolate reductase (MTHFR), 5,10-MeTHF is converted into 5-MTHF, which will be available for the remethylation of a second molecule of homocysteine. MTHFR uses flavin

adenine dinucleotide (FAD; the active form of vitamin B_2) as a cofactor. The folate-dependent remethylation pathway is present in nearly all cells (3, 6). Additionally, in liver and kidney, remethylation also occurs by the folate independent pathway in which methyl groups are donated by betaine (also known as trimethylglycine, a derivative of choline oxidation), in a reaction catalyzed by the enzyme betaine-homocysteine methyltransferase (BHMT) (3, 6).

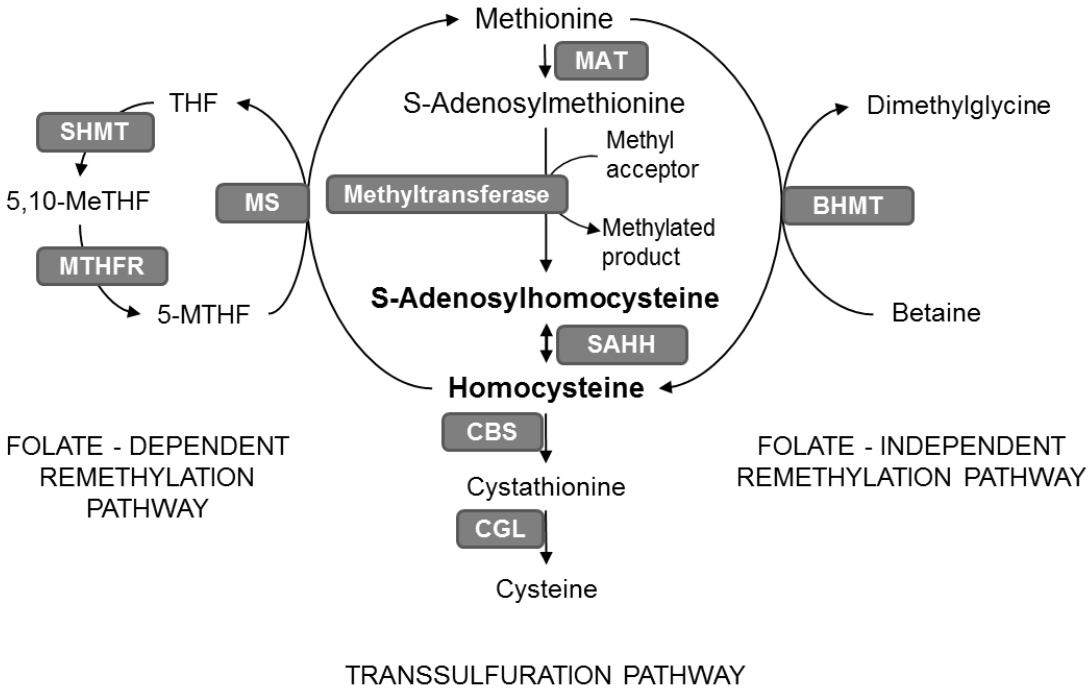

Figure 1 - Schematic representation of homocysteine metabolism. MAT (methionine adenosyltransferase), SAHH (S-adenosylhomocysteine hydrolase), CBS (cystathionine β-synthase), CGL (cystathionine γ-lyase), MS (methionine synthase), SHMT (serine hydroxymethyltransferase), MTHFR (5,10-methylenetetrahydrofolate reductase), BHMT (betaine-homocysteine methyltransferase).

Homocysteine can be irreversibly metabolized through the transsulfuration pathway, which is mainly confined to the liver, kidney, small intestine and pancreas (7). In the first step of this pathway, cystathionine β-synthase (CBS) catalyzes the condensation of homocysteine and serine to form cystathionine using pyridoxal phosphate (PLP or vitamin B_6) as a co-factor (5). Cystathionine is further metabolized to produce cysteine by another PLP-requiring enzyme, cystathionine γ-lyase (CGL) (5, 8). In addition to protein synthesis, cysteine is used in the synthesis of glutathione, an important cellular antioxidant (5, 9). The sulfur end product of cysteine metabolism is sulfate, which can be excreted by the kidneys (10).

In addition to the homocysteine metabolic pathways, and to maintain the optimal intracellular levels of homocysteine, cells may also export homocysteine. The mechanisms that regulate homocysteine export into the extracellular compartment are not completed defined. Nevertheless, two types of transport of homocysteine across the cell membranes were suggested: one involving the

removal of the reduced form of homocysteine (with a free thiol group) to the extracellular compartment, and the other the transport of the oxidized, disulfide forms of homocysteine, that are most abundant in plasma, into cells (11). In plasma, the majority (98-99%) of homocysteine is rapidly oxidized, reacting with free thiol-containing molecules (including small thiol molecules such as homocysteine or cysteine, and proteins with free cysteines, such as albumin) to form disulfides. The remaining 1-2% of plasma homocysteine remains in its reduced form (5, 11). Total plasma homocysteine includes the sum of the circulating homocysteine molecules either in its reduced or oxidized forms.

Homocysteine can be cleared from the organism by urinary excretion, but 98-99% of plasma homocysteine is reabsorbed in the kidney (12). The remethylation and transsulfuration pathways play major roles in maintaining circulating homocysteine levels. Nevertheless, when renal function is compromised, homocysteine levels often become elevated (5, 12).

2. Hyperhomocysteinemia

The intracellular concentration of homocysteine is under tight control. Once formed in the cell, homocysteine is either metabolized to cysteine or remethylated to methionine or exported from the cell. Hence, cellular export of homocysteine reflects the balance between homocysteine production and its catabolism. Persistent elevation of homocysteine in the blood defines the condition called hyperhomocysteinemia. In healthy adults, fasting homocysteine concentrations in plasma are usually within a 5-15 µmol/L range (13–15). Hyperhomocysteinemia is classified according to the levels of homocysteine accumulated, as mild (15-30 µmol/L), moderate (31-100 µmol/L), or severe (>100 µmol/L) (14, 16, 17).

Several factors can contribute to the circulating levels of homocysteine. In fact, plasma homocysteine levels are influenced by various non-genetic as well as genetic determinants.

Non-genetic determinants of plasma homocysteine include inadequate concentrations of B vitamins that play a vital role in the metabolism of homocysteine. As mentioned in the previous section, folate is a primary substrate for homocysteine remethylation and other B vitamins, such as vitamin B_{12}, vitamin B_6, and vitamin B_2, are co-factors for the major homocysteine regulating enzymes (Figure 1). As such, plasma concentrations of homocysteine are inversely related to plasma concentrations of folate, vitamin B_{12} and vitamin B_6, as well as to the intake of these vitamins (18). The most consistent association has been found with lower folate intake or with lower plasma concentrations of folate (17). A modest inverse relationship has been reported between plasma concentrations of vitamin B_2 and homocysteine; however, this association is restricted to subjects carrying the *MTHFR* 677TT genotype (see below). In addition, normal kidney function maintains optimal plasma levels of homocysteine, and impaired renal function is often associated with mild to moderate hyperhomocysteinemia (5, 12). Plasma homocysteine concentrations increase with age. In

fact, homocysteine levels approximately double from childhood to old age (2, 5). Gender also significantly affects concentration of plasma homocysteine, with males having higher levels than females (5, 17). A rise in plasma homocysteine concentrations with menopause has been also described (17). Lifestyle factors can also modulate the circulating levels of homocysteine. Tobacco smoking, high coffee consumption, alcoholism, and lack of exercise are examples of lifestyle factors associated with mild hyperhomocysteinemia (19). Several pharmacological agents can also disturb homocysteine metabolism, such as certain anti-carcinogenic agents (e.g. methotrexate or sulfasalazine) and anticonvulsants (e.g. carbamazepine or phenytoin) (22). Lastly, pathologic conditions, such as hypothyroidism, psoriasis, lymphoblastic leukemia and other malignancies, were also associated with hyperhomocysteinemia (22).

Genetic determinants cause mild to severe hyperhomocysteinemia. Severe hyperhomocysteinemia is caused by rare genetic defects in either homocysteine transsulfuration or remethylation pathways. CBS deficiency or classical homocystinuria, an autosomal recessive disorder that affects the transsulfuration pathway, is the most common inborn error of homocysteine metabolism (20). In addition to severe hyperhomocysteinemia and homocystinuria, the biochemical phenotype of CBS deficiency also includes hypocysteinemia, and hypermethioninemia, due to increased homocysteine remethylation (20). Phenotypic consequences of CBS deficiency include thromboembolism and vascular occlusion, skeletal abnormalities, dislocation of the optic lenses, marfanoid features, and varying degrees of neurological impairment. In these patients, early homocysteine-lowering treatment significantly reduces the risk of life-threatening vascular events despite imperfect biochemical control of homocysteine levels (20).

Other genetic causes of hyperhomocysteinemia include disorders that cause cobalamin (vitamin B_{12}) deficiency. Inborn errors of cobalamin metabolism can affect its absorption, transport, as well as its intracellular metabolism, namely adenosylcobalamin synthesis, methionine synthase function, or both (21).

Several pieces of evidence lead to the conclusion that the more common mild forms of hyperhomocysteinemia are, at least partially, genetically based (22). For this reason, almost every gene involved in homocysteine metabolism has been analyzed for functional polymorphisms that could affect the circulating concentrations of homocysteine, and many genetic variants have been identified. However, one *MTHFR* polymorphism has been the most consistently associated with plasma homocysteine variability. In fact, the major known genetic determinant of plasma homocysteine levels in the general population is the 677C>T variation in the *MTHFR* gene (23). MTHFR is a FAD-dependent enzyme involved in the folate-dependent remethylation of homocysteine. The common *MTHFR* C677T polymorphism determines the synthesis of a thermolabile enzyme with reduced activity (24). Homozygosity for the thermolabile MTHFR variant increases the plasma concentrations of homocysteine by approximately 25% in individuals with low folate status (25).

3. Hyperhomocysteinemia and Cardiovascular Disease

Cardiovascular diseases (CVD) are the number one cause of death in the Western industrialized world. Meta-analyses have shown that, in the general population, mild hyperhomocysteinemia is an independent risk factor for CVD, with a prevalence around 5% (19, 26, 27).

The hypothesis that elevated homocysteine may contribute to vascular disease was suggested by McCully (1969) on the basis of postmortem observations of widespread arterial disease in young patients with markedly elevated homocysteine concentrations due to different genetic causes (1, 6, 28). These observations formed the basis for the so-called *Homocysteine Theory* that suggests the importance of hyperhomocysteinemia in the development of atherosclerosis. McCully raised the important question of whether mild to moderate elevations of homocysteine, common in the general population, would increase the risk of vascular disease (1, 29).

In 1976, Wilcken and Wilcken provided the first evidence for an association between impaired homocysteine metabolism and CVD in the general population (30). Since these observations, data from a large number of clinical and epidemiological studies have implied an important role for mild hyperhomocysteinemia as an independent risk factor for CVD and related-mortality (26). Large meta-analysis studies concluded that every increase of 5 μmol/L in plasma concentration of homocysteine increases the risk of CVD by approximately 20%, independently of traditional risk factors, such as diabetes, hypertension, smoking and hypercholesterolemia (31).

3.1. Homocysteine and Endothelial Dysfunction and Activation

Increased levels of plasma homocysteine are associated with various forms of vascular disease, including arterial and venous thrombosis, in which a common feature is endothelial dysfunction, an early step in atherogenesis. The term 'endothelial dysfunction' refers to the impairment of the normal homeostatic properties of the vascular endothelium, which include endothelium-dependent regulation of vascular tone, hemostasis, and inflammation. A decrease of nitric oxide bioavailability and an impairment of cell redox balance are major features of endothelial dysfunction (Figure 2). Endothelial dysfunction often leads to a pro-inflammatory state (endothelial activation) that precedes the formation of atherosclerotic plaques (32). The detrimental effect of homocysteine on the endothelium may explain the increased risk for CVD associated with hyperhomocysteinemia (33).

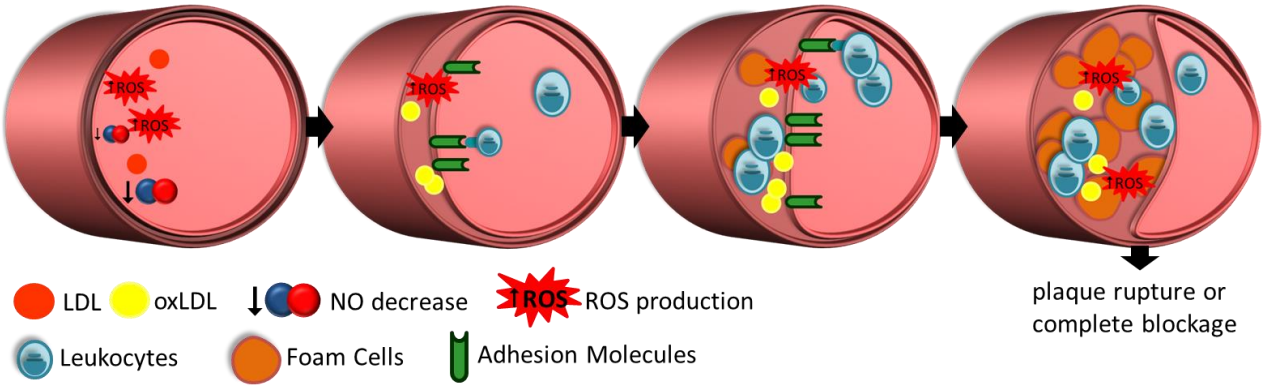

Figure 2 - Schematic representation of major steps of the atherosclerosis process.

The mechanisms by which homocysteine promotes endothelial dysfunction are not fully understood, although several effects known to disturb endothelial homeostasis have been associated with hyperhomocysteinemia (summarized in Figure 3).

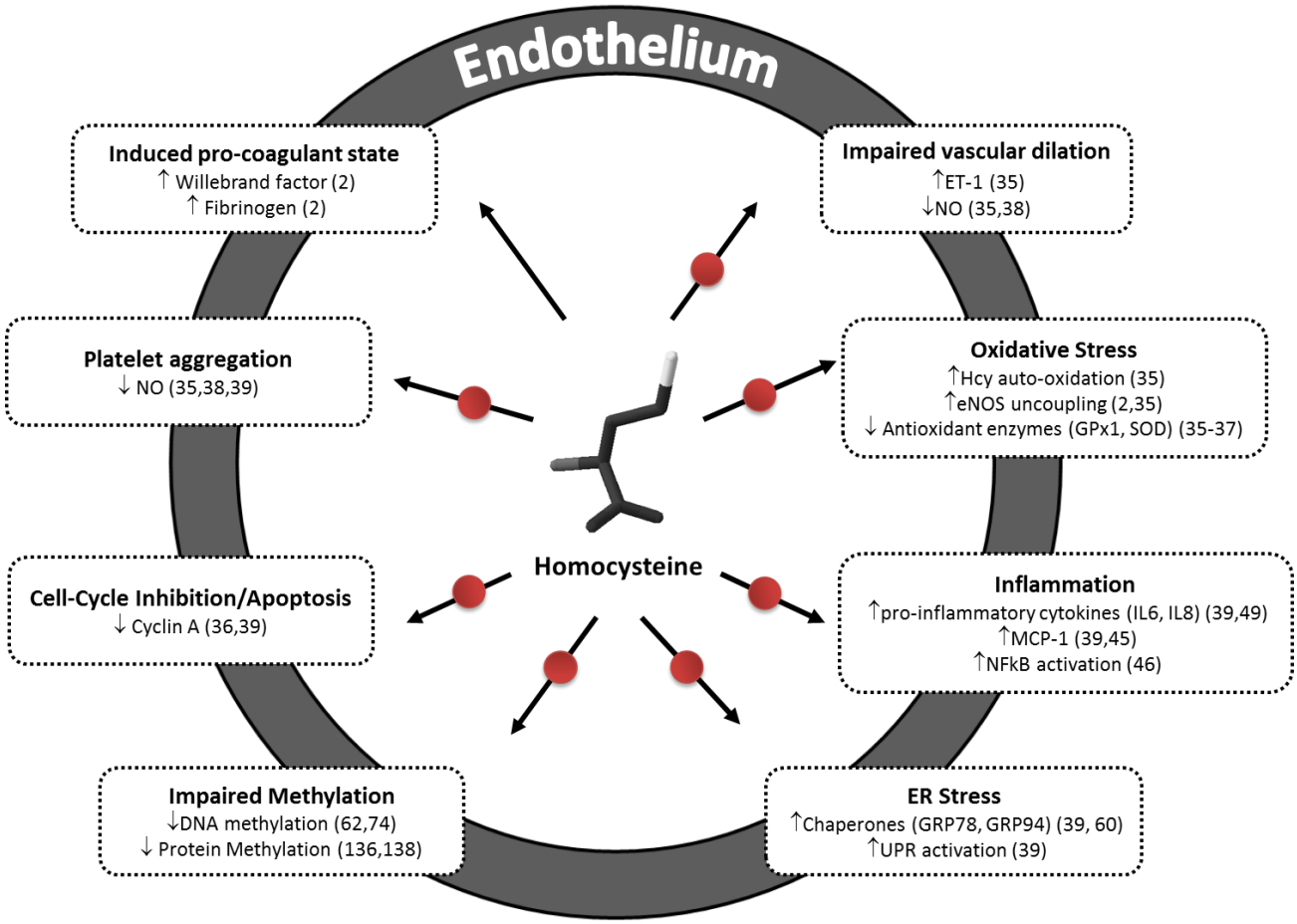

Figure 3 - The harmful effects of homocysteine in the endothelium (red dots indicate that these effects were previously suggested to be associated with elevated SAH).

Different studies have reported increased oxidative stress and impaired vasodilation, due to decreased nitric oxide (NO) bioavailability, in the context of hyperhomocysteinemia. Cellular oxidative stress is characterized by an increase in oxidants over antioxidants, which leads to an imbalance of the redox state. Increased levels of reactive oxygen species (ROS), such as hydrogen peroxide, superoxide anions and hydroxyl radicals, contribute to a more oxidant environment (34). There are several means by which homocysteine can promote ROS accumulation, these include: homocysteine's auto-oxidation, endothelial nitric oxide synthase (eNOS) uncoupling, and the inhibition of the activity of important antioxidant enzymes, such as glutathione peroxidase-1 (GPx-1) or superoxide dismutase (SOD) (35–37). The reaction of superoxide with NO produces the strong oxidant peroxynitrite ($ONOO^-$) and, simultaneously, decreases NO bioavailability (33). NO is considered a major endogenous anti-atherosclerotic molecule, as it is a potent vasodilator, and it inhibits monocyte and platelet adhesion, smooth muscle cell proliferation, and low density lipoprotein (LDL) oxidation (38, 39). Increased plasma levels of homocysteine have been associated with impaired vascular tone, due to the decrease in NO bioavailability and increase of endothelin-1 (ET-1), a potent vasoconstrictor (35). Vascular dysfunction was observed in an animal model of diet-induced mild hyperhomocysteinemia (40). Moreover, oxidative stress was shown to contribute to this association in various *in vivo* studies (41, 42). In addition, decreased levels of NO were observed in several vascular beds obtained from mice with mild hyperhomocysteinemia (35). Importantly, elevated homocysteine levels have also been associated with an increase of asymmetric dimethylarginine (ADMA) in endothelial cells (43). ADMA is a by-product of the hydrolysis of methylated proteins and an endogenous inhibitor of NO synthases (43). Therefore, ADMA has been suggested as a mediator of reduced NO availability during hyperhomocysteinemia (44).

Moreover, homocysteine induces endothelial inflammation and activation of the coagulation cascade, further contributing to the progression of atherosclerotic lesions. In studies using cell and animal models, homocysteine triggered the activation of NFkB, a transcription factor known to stimulate the production of cytokines, chemokines, leukocyte adhesion molecules, and hematopoietic growth factors (45). In other studies using vascular endothelial cells, homocysteine increased the expression of important adhesion molecules, such as E-selectin and vascular cell adhesion protein-1 (VCAM-1) (46, 47). These adhesion molecules and cytokines enhance the binding of leukocytes to the endothelium and promote their transmigration to the vessel wall. More recently, it was shown that in humans, plasma levels of homocysteine correlate with those of interleukin 6 (IL-6) and interleukin-1 (IL-1) receptor antagonist (39, 48). Cell culture studies also showed that homocysteine induces activation of the coagulation cascade, favoring a pro-coagulant state and platelet adhesion. Endothelial cells exposed to homocysteine had increased levels of tissue factor (TF) and enhanced activation of factor V to Va (2). Plasma of patients with coronary artery disease showed a correlation between homocysteine and fibrinogen, an acute-phase protein involved in vascular inflammation and

a marker of endothelial dysfunction. Von Willebrand factor, another marker of adverse changes to the endothelium, was also found increased in plasma from hyperhomocysteinemic patients with premature arterial disease (2).

Endoplasmic reticulum (ER) stress is another deleterious effect associated with high concentrations of homocysteine. ER stress is characterized by an accumulation of misfolded proteins in the ER lumen, which triggers the unfolded protein response (UPR) and increases the expression of stress response genes, such as *GRP78* and *GRP94*. ER stress can induce inflammation and apoptosis, which can favor the progression of atherosclerotic lesions (39).

Several pathways contribute to homocysteine's harmful effects on the endothelium to promote vascular disease progression. For example, both ROS release and ER stress can activate apoptosis (45). Oxidative stress contributes to LDL oxidation and the formation of foam cells, which are determinants of atherosclerotic plaque growth. Together with enhanced activation of coagulation pathways, decreased NO levels lead to increased platelet aggregation. Furthermore, as has been shown in vascular cells from animal models of hyperhomocysteinemia, homocysteine-induced peroxynitrite can induce apoptosis and reduce cyclin A levels, promoting cell cycle arrest and preventing replacement of damaged endothelial cells (36, 39). Thus, effects of excess homocysteine on the endothelium promote a cascade of events that will affect surrounding cells and tissue, contributing to CVD.

3.2. S-Adenosylhomocysteine and Cardiovascular Disease

As discussed above, several studies concluded that elevations of plasma homocysteine in the mild to moderate range were an independent risk factor for CVD in general population. Subsequently, to unequivocally establish the causal effect of increased plasma homocysteine in the promotion of CVD, several randomized controlled studies were conducted to examine whether homocysteine-lowering B-vitamin therapy would decrease the occurrence of adverse cardiovascular events. Surprisingly, despite a substantial, quick and long lasting effect on lowering the concentrations of plasma homocysteine, the majority of these intervention trials and the subsequent follow-up meta-analysis studies have shown no clear clinical benefit of these vitamin treatments on vascular disease risk and mortality (49–53). An alternative theory proposes that SAH, rather than homocysteine, may be a more accurate measure of CVD risk (54–57). SAH is the homocysteine precursor that accumulates in the setting of hyperhomocysteinemia and growing evidence shows that B-vitamin treatments that reduce plasma homocysteine fail to lower plasma (58) and intracelular SAH (59).

To date, association studies between SAH and CVD are still scarce, possibly due, in part, to the sample preparation methodologies necessary to preserve SAH that can be difficult in large-scale studies. Nevertheless, experiments in mice have established an association between excess SAH

and CVD (60), suggesting SAH as a more sensitive biomarker for atherosclerosis than homocysteine (56). A prospective cohort study in coronary angiographic patients showed that increased plasma SAH levels are significantly correlated with an increase in CVD events (57). Moreover, a cross-sectional cohort study of 402 individuals with low CVD risk, found an association between SAH and subclinical atherosclerosis, implicating SAH as a marker of early atherosclerotic disease (61). Taken together, these observations support the concept that SAH, rather than homocysteine, may be the culprit in the CVD risk that has been associated with hyperhomocysteinemia. Nevertheless, the underlying molecular mechanisms are still elusive.

4. S-Adenosylhomocysteine and Cell Hypomethylation

SAH is the homocysteine precursor that accumulates in the setting of hyperhomocysteinemia due to the reversibility of SAH hydrolase reaction. As discussed above, the SAH hydrolase reaction is reversible and presents a thermodynamic equilibrium that strongly favors SAH synthesis rather than its hydrolysis. Therefore, increased homocysteine levels can lead to SAH accumulation as well. In fact, several studies report SAH accumulation under conditions of hyperhomocysteinemia in humans and in animal models (62–65).

Homocysteine metabolism is biochemically linked to the methylation status of several biomolecules. In fact, cell methyltransferases use SAM as a methyl donor to methylate various targets, including DNA, RNA, and proteins (66). A common feature of these reactions is the production of SAH. SAH is, simultaneously, a by-product and a potent inhibitor of the activity of SAM-dependent methyltransferases. In fact, SAH has nearly the same (or greater) affinity for the catalytic site of most methyltransferases than SAM (4). Hence, homocysteine-induced SAH accumulation may inhibit the activity of cell methyltransferases, thereby disrupting methylation homeostasis and promoting a hypomethylating environment. Targets of SAH-mediated methylation inhibition include key determinants of gene expression: DNA, RNA, and proteins. Therefore, DNA, RNA, or protein hypomethylation are potential mechanistic links between hyperhomocysteinemia and CVD and may contribute to the molecular basis of homocysteine-induced vascular toxicity.

4.1. Targets of S-Adenosylhomocysteine-Mediated Methylation Inhibition

4.1.1. DNA

DNA methylation plays an important role in the epigenetic regulation of gene expression. Epigenetics refers to heritable traits that are not a consequence of the DNA sequence (67, 68). Epigenetic marks, such as DNA methylation, regulate gene expression during development and adulthood, and they can determine cell and tissue specific gene expression.

Methylation of the carbon 5 position of the cytosine ring (Figure 4) is the most common modification on the double helix, and this cytosine methylation can modulate the transcriptional potential of genomic DNA (69).

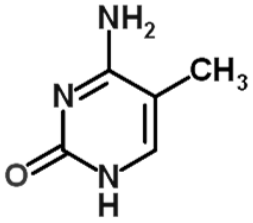

Figure 4 – Chemical structure of 5-methylcytosine.

In differentiated mammalian cells, cytosine methylation can occur in any nucleotide context; however, more than 98% occurs in cytosines (C) that are followed by guanines (G), in a CpG dinucleotide context (70).

CpG islands are sequences present in the genome that have a CG-rich base composition and high density of CpG dinucleotides (71). The majority of the annotated gene promoters, including promoters of housekeeping genes, tissue-specific genes and developmental regulator genes, contain CpG islands (71).

DNA methylation is generally associated with a repressed chromatin state and inhibition of transcriptional initiation. Repression by DNA methylation has been demonstrated for promoters that contain CpG islands and also for promoters with low CpG density (72).

Cytosine methylation in DNA is accomplished by the action of three DNA methyltransferases (DNMTs): DNMT1, DNMT3A, and DNMT3B. DNMT1 is responsible for maintenance of the DNA methylation patterns during replication, while the DNMT3A and DNMT3B function as *de novo* methyltransferases (69). Importantly, SAH has been shown to inhibit the *in vitro* methyltransferase activity of each of the DNMT enzymes (73). Accordingly, excess SAH levels have been strongly associated with altered gene expression in several studies (74–76). Therefore, SAH-induced damage to the endothelium can be partially due to impaired activity of DNMTs.

SAH has been shown to disturb promoter methylation of different genes, including, the *PDGF* (platelet-derived growth factor) gene (74), the stress response-related *p66Shc* (76), genes involved in the regulation of cholesterol biosynthesis, such as *SREBF1* (sterol regulatory element binding transcription factor-1) and *LDLR* (LDL receptor) (75), and those involved in cell stress and cell cycle regulation, such as the *BNIP3* (BCL2/adenovirus E1B 19kDa interacting protein 3) gene (77). Additionally, the inflammatory genes *IL1B* (interleukin 1 beta), *IL6*, *IL8* (interleukin 8), and *ICAM1* (intercellular adhesion molecule-1), that were shown to be regulated by DNA methylation in cancer cells (78, 79), are possible targets of SAH-mediated regulation.

Several lines of evidence support the notion that an elevation of homocysteine can lead to DNA hypomethylation, secondary to inhibition of DNMTs by SAH, and that DNA hypomethylation may contribute to atherosclerotic disease mechanisms (62, 64, 68, 80, 81). For instance, plasma

homocysteine concentration correlates positively with SAH levels and negatively with lymphocyte DNA methylation status in healthy individuals and in patients with CVD (64, 65). In another example, a significant reduction in the genomic methyl cytosine content was detected in advanced human atherosclerotic lesions (82) and in vascular lesions of mice lacking apolipoprotein E (ApoE), a well-established animal model of atherosclerosis (83). Similarly, another recent study showed that DNA hypomethylation is present in human atherosclerotic carotid plaques (84). Although several studies report global hypomethylation in atherosclerotic plaques (67, 84), some report global hypermethylation (85). The basis for these differences is unclear, but may relate to the stage of the plaque (86), or whether or not the plaque is symptomatic (i.e., had a rupture) (80). Nonetheless, many studies have identified specific genes that are hypomethylated in atherosclerotic plaques and can be determinants for disease (81). Additional analysis is necessary to determine whether SAH or homocysteine can potentiate the hypomethylation of specific genes that contribute to atherosclerosis.

4.1.2. RNA

Although much less studied than other SAM-methylation targets, RNA is highly methylated. There are almost one hundred different methylation modifications in RNA described so far (87). However, due, in part, to the highly demanding techniques necessary for studying RNA modifications, the function of most RNA modifications is unknown. Different RNA species, such as tRNA, rRNA, mRNA, snRNA, and miRNA, are differently methylated. Interestingly, some RNA methyltransferases target different RNA species, while others are specific for a single RNA species (88).

The importance of RNA methylation is illustrated by the 5' methylation cap in mRNA, which is critical for mRNA stability and efficient gene expression (89). Several mechanisms have been proposed for tRNA and rRNA methylation-mediated regulation of translation and codon decoding (88). RNA methylation has been shown to affect basic cellular processes, such as RNA decoding and synthesis, maturation, transport, and splicing. The role of methylation in RNA function depends on the RNA molecule that is being methylated, as well as the location within that molecule, and within the nucleotide.

Even though RNA methylation can occur on nitrogen, oxygen, and carbon, nitrogen is the most modified atom within the pyrimidine or purine base rings (88). Nucleotides are usually methylated on the nucleotide base or ribose, and 2′-O-methylation is the most common type of ribose methylation (90). Recently, the fat mass and obesity-associated protein (FTO) and the alkylation repair homolog-5 (ALKBH5) were reported to mediate m^6A (N6-methyladenosine)* demethylation (89, 91, 92). The discovery that RNA methylation can be a highly dynamic modification raises the question

* Chemical structure of various RNA modifications can be found in Chapter 4.2.

of whether these modifications can regulate gene expression. RNA methylation is *per se* an addition of information to the RNA sequence and its flexibility further increases RNA complexity and diversity.

The lack of information on the function of specific RNA methylations, as well as the fact that several RNA methyltransferases still lack characterization, makes the study of these modifications in normal and disease conditions challenging. There are no studies on the effects of hyperhomocysteinemia on RNA methylation, although cell culture studies, as well as studies using purified enzymes, have shown that specific RNA methylation modifications are sensitive to SAH accumulation (93–96). One study conducted in rabbits experiencing myocardial infarction reported altered patterns of liver tRNA methylation in these stressed rabbits compared to controls (97). In particular, m^1A (1-methyladenosine)* content was decreased in rabbits experiencing myocardial infarction, whereas m^7G (7-methylguanosine)* and m^1G (1-methylguanosine)* content was increased (97); however, the specific function of each of these modifications remains unclear as is the molecular basis for these changes (97). Several studies have also reported hypo- and hyper-methylation of specific tRNA modifications in different types of cancers, such as, hepatoma, adenocarcinoma, breast and lymphoid cancers (90, 98–103). Likewise, impaired rRNA methylation was found in leukemic blast cells, where rRNA maturation was compromised (104, 105). Additionally, genome-association studies have also implicated different gene variants of the mRNA demethylase *FTO* gene in cancer, neuronal development, and renal and cardiovascular diseases (92, 106).

tRNA is the most heavily modified RNA species and some of these modification may have important roles in mediating cellular stress responses (107). In 2010, the activity of ALKBH8, a mammalian methyltransferase that is able to methylate a number of different tRNA residues, was reported (107). Its activity includes modifications that are essential for the correct translation of a subset group of selenoproteins (proteins that contain selenocysteine in their polypeptide chain) (107, 108). Selenocysteine (Sec) carrying tRNA (Figure 5) recognizes a UGA codon, which is a common signal for translation termination, as a target for Sec incorporation (107, 109, 110). Thus, Sec-tRNA is essential for efficient translation of selenoproteins. There are two major Sec-tRNA isoforms, mcm^5U (5-methoxycarbonylmethyluridine) and mcm^5Um (5-methoxycarbonyl-methyl-2'-O-methyluridine), which differ by a single methyl group at the ribose of the U at position 34 (Figure 5) (107, 109). ALKBH8 is responsible for the conversion of cm^5U (5-carboxymethyluridine) to mcm^5U, and the 2'-O-ribose methylation to form mcm^5Um doesn't occur without the prior synthesis of the mcm^5U (107, 108). Several selenoproteins rely on the presence of mcm^5Um to be efficiently translated, including GPx-1. GPx-1 is a major antioxidant in human cells and its impaired translation is associated with high homocysteine levels (37). Songe-Møller *et al*. found that mice lacking ALKBH8 showed decreased mcm^5U and mcm^5Um content in tRNA with a consequent decrease in GPx-1 expression and increased susceptibility for oxidative stress (107). Subsequent studies have also shown that a deficiency of ALKBH8 suppresses the expression of GPx-1 and other selenoproteins to

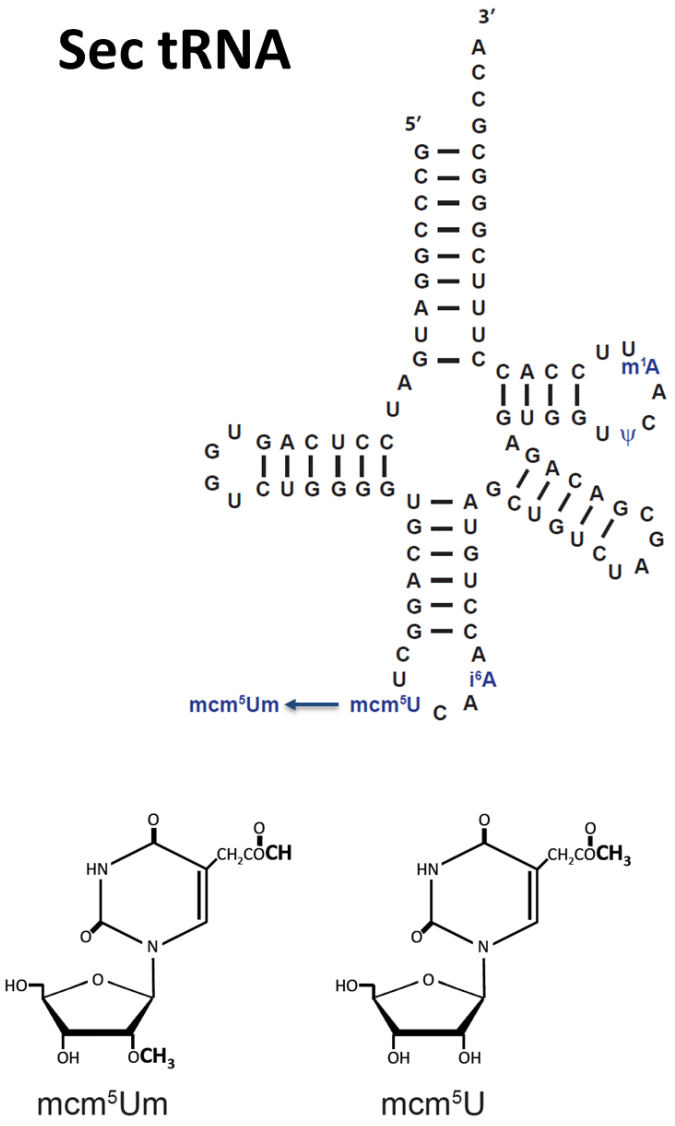

cause oxidative stress in mouse embryonic fibroblasts (111). Importantly, in addition to GPx-1, many other selenoproteins are involved in cell detoxification and redox regulation. Furthermore, selenium deficiency has also been associated with oxidative stress and cancer (109, 112). Therefore, impaired Sec-tRNA methylation may contribute to endothelial dysfunction due to its key role in the expression of the selenoproteome.

Figure 5 - Human selenocysteine (Sec)-tRNA. The sequence and structure of the Sec-tRNA is shown at the top and the chemical modifications of the wobble uridine at position 34 of the anticodon (U34) are shown at the bottom. mcm^{5}U, 5-methoxycarbonyl-methyluridine; mcm^{5}Um, 5-methoxycarbonyl-methyl-2′-O-methyluridine.

4.1.3. Protein

Protein methylation is a widespread post-translational modification that modulates protein function and increases the structural diversity of the proteome. Furthermore, protein methylation can be reversible, similar to phosphorylation or acetylation, adding another means to regulate protein-protein interactions, protein stability, protein localization, and/or enzymatic activity (113). Protein methylation has been reported for many different amino acids, such as histidine, cysteine, aspartic acid, glutamic acid, serine, and threonine, although methylation has been most commonly observed on lysine and arginine residues (114). Currently, 50 different protein lysine methyltransferases (PKMTs) and 11 protein arginine methyltransferases (PRMTs) are known (115). PKMTs can catalyze the transfer of one, two, or three methyl groups from SAM to lysine residues in a protein polypeptide chain, producing mono-, di-, or tri-methyl-lysine residues. Likewise, PRMTs can also mono-, di-, or tri-methylate arginine residues. Additionally, PRMTs-mediated di-methylation can

be symmetric, generating symmetric dimethylarginine (SDMA) residues, or asymmetric, producing ADMA residues (116, 117).

PKMTs and PRMTs methylate a wide variety of proteins involved in diverse cell processes, such as transcriptional regulation, protein localization, signal transduction, RNA metabolism, and DNA repair (117–119).

The methylation of histones is a well-known epigenetic mechanism that regulates gene expression. Histones are nuclear proteins that package the DNA into units referred to as nucleosomes, which constitute the fundamental units of chromatin (67). Histones are susceptible to different types of modifications, including lysine and arginine methylation. Methylation of histone can influence gene expression by modulating chromatin structure (67, 120). The effects of histone methylation on chromatin activation depend on the specific residues that are methylated (120). Methylation of lysines 4, 36 and 79 in histone H3 are mainly associated with active transcription, while methylation at lysines 9 and 27 are associated with gene repression and heterochromatin formation. Furthermore, the methylation status (mono-, di-, or trimethylation) of a single lysine residue can be determinant for gene expression. For example, trimethylated histone H3 lysine 4 (H3K4) is a mark of active promoters, while di- and trimethylated histone H3 lysine 9 (H3K9) residues are strongly associated with transcriptional repression (120). Methylation of the histone H3 arginines 17 and 26 is associated with active chromatin, whereas the methylation of histone H3 arginine 2 and 8, and methylation of histone H4 arginine 3, are associated with gene repression and heterochromatin formation (121, 122).

Histone methylation is also highly dynamic. The removal of methyl moieties at arginine and lysine residues is carried out by histone demethylases. JMJD6 is the only known histone arginine demethylase in humans and it is responsible for the removal of the H3R2me2, H4R3me1, and H4R3me2 marks (123). Histone lysine methylation is also reversible, and several demethylases have been identified. Histone lysine demethylases (KDM) were classified into different families (KDM 1-7) based on their substrate specificities and protein domain organization (117).

The establishment and maintenance of epigenetic gene silencing is fundamental to cell homeostasis (124). The Polycomb group (PcG) of proteins are negative epigenetic regulators of transcription and represent evolutionarily conserved multiprotein complexes: the Polycomb repressive complexes (PRCs) (125). There are two main PRCs: PRC1 and PRC2. PRC2 catalyzes the di-methylation and tri-methylation of histone H3 at lysine 27 (H3K27me2/3), which is a central feature of PcG-silenced chromatin; while PRC1 catalyzes lysine 119 mono-ubiquitylation of histone H2A (H2AUb1) (126). PRC2 complex is involved in the initiation of gene silencing, whereas PRC1 is responsible for stabilizing and maintaining gene repression. Enhancer of zeste homolog 2 (EZH2) is a SAM-dependent histone lysine methyltransferase (HKMT) that is the catalytic component of PCR2 and epigenetically silences gene expression by mediating the H3K27me3 methylation (124, 127).

UTX (ubiquitously transcribed tetratricopeptide repeat on X chromosome demethylase) and JMJD3 (jumonji domain containing 3 demethylase) are H3K27-specific histone demethylases, which are capable of removing di- and tri-methylation of H3K27 (117).

G9a/GLP is another major epigenetic silencing machinery in eukaryotes. G9a and G9a-Like Protein (GLP) are two H3K9 HKMTs (128). Several different demethylases were reported to remove H3K9 methylation, including members of the KDM families 1, 3, 4, 5 and 7 (117). Very recently, functional crosstalk between PCR2 and G9a/GLP was reported (128). Notably, G9a enzymatic activity in stem cells was shown to control EZH2 recruitment and H3K27me3 content at a subset PRC2-target genes genome wide. In a more targeted study in differentiated cells, the activities of G9a and EZH2 were coordinately linked with the suppression of cyclooxygenase 2 (129). Experimental evidence suggests that G9a may contribute to the monomethylation of H3K27 to facilitate the docking of EZH2 and promote the establishment of the repressive H3K27me3 mark on PCR2 target genes (128). Interestingly, similar to EZH2, G9a also relies on SAM as the methyl-donor compound for its HKMT activity (129, 130).

Recent studies revealed that EZH2 epigenetically regulates cell proliferation, spreading, and angiogenesis in endothelial cells (131). Additionally, EZH2 target genes encode several inflammation mediators, including pro-inflammatory cytokines that can induce endothelial cell expression of adhesion molecules (131). As SAM-dependent HKMTs, EZH2 and G9a may be targets for SAH-dependent inhibition of their methyltransferases activities. As such, these observations raise the possibility that deregulation of epigenetic control mediated by EZH2/G9a, via SAH accumulation, may contribute to endothelial dysfunction and CVD. In support of this idea, excess SAH was found to cause a loss of the repressive histone marks, H3K27me3 and H3K9me3 (132, 133). Moreover, a reduction in global histone H3K27me3 in atherosclerotic plaques was just reported (134).

Nonetheless, the methylation of non-histone proteins has also been associated with disease. Perna *et al.* suggested, for the first time, the involvement of protein hypomethylation in hyperhomocysteinemia, reporting that SAH induced a decrease of methyl esterification of erythrocyte membrane proteins of patients with renal function impairment (135). Garcia and colleagues also observed that a decrease in the SAM/SAH ratio in rats resulted in impaired arginine methylation of proliferator-activated receptor-γ co-activator-1 (PGC-1α), a transcriptional co-activator that regulates genes involved in energy metabolism (136).

Our group reported the SAH-mediated effects on global protein arginine methylation *in vitro* and *in vivo* (137, 116, 138). In these studies, we observed that protein arginine methylation is a more susceptible target for SAH-mediated inhibition than DNA methylation (116). Furthermore, we found hypomethylation of proteins, including histones, in two independent animal models of hyperhomocysteinemia (137, 138). These results provide evidence that protein methylation is a target for SAH-mediated inhibition during hyperhomocysteinemia and lay the groundwork for further studies

of specific protein methylation targets that may contribute to vascular disease. In support of these findings, an alteration of histone (and DNA) methylation in human atherosclerotic carotid plaques has been recently reported (84).

References

1. McCully, K. S. (2001) The biomedical significance of homocysteine. *J. Sci. Explor.* **15**, 5–20
2. Durand, P., Prost, M., Loreau, N., Lussier-Cacan, S., and Blache, D. (2001) Impaired Homocysteine Metabolism and Atherothrombotic Disease. *Lab. Investig.* **81**, 645–672
3. Schalinske, K. L., and Smazal, A. L. (2012) Homocysteine imbalance: a pathological metabolic marker. *Adv. Nutr.* **3**, 755–62
4. Ueland, P. M. (1982) Pharmacological and biochemical aspects of S-adenosylhomocysteine and S-adenosylhomocysteine hydrolase. *Pharmacol. Rev.* **34**, 223–53
5. Castro, R., Rivera, I., Blom, H. J., Jakobs, C., and Tavares de Almeida, I. (2006) Homocysteine metabolism, hyperhomocysteinaemia and vascular disease: an overview. *J. Inherit. Metab. Dis.* **29**, 3–20
6. Eldibany, M. M., and Caprini, J. A. (2007) Hyperhomocysteinemia and thrombosis: an overview. *Arch. Pathol. Lab. Med.* **131**, 872–84
7. Finkelstein, J. D. (1998) The metabolism of homocysteine: pathways and regulation. *Eur. J. Pediatr.* **157 Suppl** , S40–4
8. Locasale, J. W. (2013) Serine, glycine and one-carbon units: cancer metabolism in full circle. *Nat. Rev. Cancer*. **13**, 572–83
9. Taysi, S., Keles, M. S., Gumustekin, K., Akyuz, M., Boyuk, A., Cikman, O., and Bakan, N. (2015) Plasma homocysteine and liver tissue S-adenosylmethionine, S-adenosylhomocysteine status in vitamin B6-deficient rats. *Eur. Rev. Med. Pharmacol. Sci.* **19**, 154–60
10. Stipanuk, M. H., and Ueki, I. (2011) Dealing with methionine/homocysteine sulfur: cysteine metabolism to taurine and inorganic sulfur. *J. Inherit. Metab. Dis.* **34**, 17–32
11. Blom, H. J. (2000) Consequences of homocysteine export and oxidation in the vascular system. *Semin. Thromb. Hemost.* **26**, 227–32
12. Van Guldener, C. (2006) Why is homocysteine elevated in renal failure and what can be expected from homocysteine-lowering? *Nephrol. Dial. Transplant*. **21**, 1161–6
13. Clarke, R., Halsey, J., Bennett, D., and Lewington, S. (2011) Homocysteine and vascular disease: review of published results of the homocysteine-lowering trials. *J. Inherit. Metab. Dis.* **34**, 83–91
14. Cacciapuoti, F. (2011) Hyper-homocysteinemia: a novel risk factor or a powerful marker for cardiovascular diseases? Pathogenetic and therapeutical uncertainties. *J. Thromb. Thrombolysis*. **32**, 82–8
15. Cheng, X. (2013) Updating the relationship between hyperhomocysteinemia lowering therapy and cardiovascular events. *Cardiovasc. Ther.* **31**, e19–26
16. Abraham, J. M., and Cho, L. (2010) The homocysteine hypothesis: still relevant to the prevention and treatment of cardiovascular disease? *Cleve. Clin. J. Med.* **77**, 911–8
17. Maron, B. A., and Loscalzo, J. (2009) The treatment of hyperhomocysteinemia. *Annu. Rev. Med.* **60**, 39–54
18. Graham, I. M., and O'Callaghan, P. (2002) Vitamins, homocysteine and cardiovascular risk. *Cardiovasc. Drugs Ther.* **16**, 383–9
19. Kuo, H.-K., Sorond, F. A., Chen, J.-H., Hashmi, A., Milberg, W. P., and Lipsitz, L. A. (2005) The role of homocysteine in multisystem age-related problems: a systematic review. *J. Gerontol. A. Biol. Sci. Med. Sci.* **60**, 1190–201
20. Mudd, S. H., Skovby, F., Levy, H. L., Pettigrew, K. D., Wilcken, B., Pyeritz, R. E., Andria, G., Boers, G. H., Bromberg, I. L., and Cerone, R. (1985) The natural history of homocystinuria due to cystathionine beta-synthase deficiency. *Am. J. Hum. Genet.* **37**, 1–31
21. Whitehead, V. M. (2006) Acquired and inherited disorders of cobalamin and folate in children. *Br. J. Haematol.* **134**, 125–36

22. Lievers, K. J. A., Afman, L. A., Kluijtmans, L. A. J., Boers, G. H. J., Verhoef, P., den Heijer, M., Trijbels, F. J. M., and Blom, H. J. (2002) Polymorphisms in the transcobalamin gene: association with plasma homocysteine in healthy individuals and vascular disease patients. *Clin. Chem.* **48**, 1383–9

23. Semmler, A., Moskau, S., Stoffel-Wagner, B., Weller, M., and Linnebank, M. (2009) The effect of MTHFR c.677C>T on plasma homocysteine levels depends on health, age and smoking. *Clin. Invest. Med.* **32**, E310

24. Kang, S. S., Zhou, J., Wong, P. W., Kowalisyn, J., and Strokosch, G. (1988) Intermediate homocysteinemia: a thermolabile variant of methylenetetrahydrofolate reductase. *Am. J. Hum. Genet.* **43**, 414–21

25. Devlin, A. M., Arning, E., Bottiglieri, T., Faraci, F. M., Rozen, R., and Lentz, S. R. (2004) Effect of Mthfr genotype on diet-induced hyperhomocysteinemia and vascular function in mice. *Blood*. **103**, 2624–9

26. Boers, G. H. (2000) Mild hyperhomocysteinemia is an independent risk factor of arterial vascular disease. *Semin. Thromb. Hemost.* **26**, 291–5

27. Cate, H. Ten (2009) *Encyclopedia of Molecular Mechanisms of Disease* (Lang, F. ed), Springer Science & Business Media

28. D'Angelo, A., and Selhub, J. (1997) Homocysteine and thrombotic disease. *Blood*. **90**, 1–11

29. McCully, K. S., and Wilson, R. B. (1975) Homocysteine theory of arteriosclerosis. *Atherosclerosis*. **22**, 215–27

30. Wilcken, D. E., and Wilcken, B. (1976) The pathogenesis of coronary artery disease. A possible role for methionine metabolism. *J. Clin. Invest.* **57**, 1079–82

31. Humphrey, L. L., Fu, R., Rogers, K., Freeman, M., and Helfand, M. (2008) Homocysteine level and coronary heart disease incidence: a systematic review and meta-analysis. *Mayo Clin. Proc.* **83**, 1203–12

32. Papatheodorou, L., and Weiss, N. (2007) Vascular oxidant stress and inflammation in hyperhomocysteinemia. *Antioxid. Redox Signal.* **9**, 1941–58

33. Antoniades, C., Antonopoulos, A. S., Tousoulis, D., Marinou, K., and Stefanadis, C. (2009) Homocysteine and coronary atherosclerosis: from folate fortification to the recent clinical trials. *Eur. Heart J.* **30**, 6–15

34. Drummond, G. R., Selemidis, S., Griendling, K. K., and Sobey, C. G. (2011) Combating oxidative stress in vascular disease: NADPH oxidases as therapeutic targets. *Nat. Rev. Drug Discov.* **10**, 453–71

35. Cheng, Z., Yang, X., and Wang, H. (2009) Hyperhomocysteinemia and Endothelial Dysfunction. *Curr. Hypertens. Rev.* **5**, 158–165

36. Splaver, A., Lamas, G. A., and Hennekens, C. H. (2004) Homocysteine and cardiovascular disease: biological mechanisms, observational epidemiology, and the need for randomized trials. *Am. Heart J.* **148**, 34–40

37. Handy, D. E., Zhang, Y., and Loscalzo, J. (2005) Homocysteine down-regulates cellular glutathione peroxidase (GPx1) by decreasing translation. *J. Biol. Chem.* **280**, 15518–25

38. Naseem, K. M. (2005) The role of nitric oxide in cardiovascular diseases. *Mol. Aspects Med.* **26**, 33–65

39. Zhou, J., and Austin, R. C. (2009) Contributions of hyperhomocysteinemia to atherosclerosis: Causal relationship and potential mechanisms. *Biofactors*. **35**, 120–9

40. Lentz, S. R., Sobey, C. G., Piegors, D. J., Bhopatkar, M. Y., Faraci, F. M., Malinow, M. R., and Heistad, D. D. (1996) Vascular dysfunction in monkeys with diet-induced hyperhomocyst(e)inemia. *J. Clin. Invest.* **98**, 24–9

41. Eberhardt, R. T., Forgione, M. A., Cap, A., Leopold, J. A., Rudd, M. A., Trolliet, M., Heydrick, S., Stark, R., Klings, E. S., Moldovan, N. I., Yaghoubi, M., Goldschmidt-Clermont, P. J., Farber, H. W., Cohen, R., and Loscalzo, J. (2000) Endothelial dysfunction in a murine model of mild hyperhomocyst(e)inemia. *J. Clin. Invest.* **106**, 483–91

42. Lentz, S. R., Rodionov, R. N., and Dayal, S. (2003) Hyperhomocysteinemia, endothelial dysfunction, and cardiovascular risk: the potential role of ADMA. *Atheroscler. Suppl.* **4**, 61–5

43. Dayal, S., and Lentz, S. R. (2005) ADMA and hyperhomocysteinemia. *Vasc. Med.* **10 Suppl 1**, S27–33

44. Stühlinger, M. C., and Stanger, O. (2005) Asymmetric dimethyl-L-arginine (ADMA): a possible link between homocyst(e)ine and endothelial dysfunction. *Curr. Drug Metab.* **6**, 3–14

45. Austin, R. C., Lentz, S. R., and Werstuck, G. H. (2004) Role of hyperhomocysteinemia in endothelial dysfunction and atherothrombotic disease. *Cell Death Differ.* **11 Suppl 1**, S56–64

46. Silverman, M. D., Tumuluri, R. J., Davis, M., Lopez, G., Rosenbaum, J. T., and Lelkes, P. I. (2002) Homocysteine upregulates vascular cell adhesion molecule-1 expression in cultured human aortic endothelial cells and enhances monocyte adhesion. *Arterioscler. Thromb. Vasc. Biol.* **22**, 587–92

47. Koga, T., Claycombe, K., and Meydani, M. (2002) Homocysteine increases monocyte and T-cell adhesion to human aortic endothelial cells. *Atherosclerosis*. **161**, 365–74

48. Gori, A. M., Corsi, A. M., Fedi, S., Gazzini, A., Sofi, F., Bartali, B., Bandinelli, S., Gensini, G. F., Abbate, R., and Ferrucci, L. (2005) A proinflammatory state is associated with hyperhomocysteinemia in the elderly. *Am J Clin Nutr*. **82**, 335–341

49. Bazzano, L. A., Reynolds, K., Holder, K. N., and He, J. (2006) Effect of folic acid supplementation on risk of cardiovascular diseases: a meta-analysis of randomized controlled trials. *JAMA*. **296**, 2720–6

50. Albert, C. M., Cook, N. R., Gaziano, J. M., Zaharris, E., MacFadyen, J., Danielson, E., Buring, J. E., and Manson, J. E. (2008) Effect of folic acid and B vitamins on risk of cardiovascular events and total mortality among women at high risk for cardiovascular disease: a randomized trial. *JAMA*. **299**, 2027–36

51. Ebbing, M., Bleie, Ø., Ueland, P. M., Nordrehaug, J. E., Nilsen, D. W., Vollset, S. E., Refsum, H., Pedersen, E. K. R., and Nygård, O. (2008) Mortality and cardiovascular events in patients treated with homocysteine-lowering B vitamins after coronary angiography: a randomized controlled trial. *JAMA*. **300**, 795–804

52. Armitage, J. M., Bowman, L., Clarke, R. J., Wallendszus, K., Bulbulia, R., Rahimi, K., Haynes, R., Parish, S., Sleight, P., Peto, R., and Collins, R. (2010) Effects of homocysteine-lowering with folic acid plus vitamin B12 vs placebo on mortality and major morbidity in myocardial infarction survivors: a randomized trial. *JAMA*. **303**, 2486–94

53. Clarke, R., Halsey, J., Lewington, S., Lonn, E., Armitage, J., Manson, J. E., Bønaa, K. H., Spence, J. D., Nygård, O., Jamison, R., Gaziano, J. M., Guarino, P., Bennett, D., Mir, F., Peto, R., and Collins, R. (2010) Effects of lowering homocysteine levels with B vitamins on cardiovascular disease, cancer, and cause-specific mortality: Meta-analysis of 8 randomized trials involving 37 485 individuals. *Arch. Intern. Med.* **170**, 1622–31

54. Wagner, C., and Koury, M. J. (2007) S-Adenosylhomocysteine: a better indicator of vascular disease than homocysteine? *Am. J. Clin. Nutr.* **86**, 1581–5

55. Wagner, C., and Koury, M. J. (2008) Plasma S-Adenosylhomocysteine Versus Homocysteine as a Marker for Vascular Disease. *J. Nutr.* **138**, 980–

56. Liu, C., Wang, Q., Guo, H., Xia, M., Yuan, Q., Hu, Y., Zhu, H., Hou, M., Ma, J., Tang, Z., and Ling, W. (2008) Plasma S-adenosylhomocysteine is a better biomarker of atherosclerosis than homocysteine in apolipoprotein E-deficient mice fed high dietary methionine. *J. Nutr.* **138**, 311–5

57. Xiao, Y., Zhang, Y., Wang, M., Li, X., Su, D., Qiu, J., Li, D., Yang, Y., Xia, M., and Ling, W. (2013) Plasma S-adenosylhomocysteine is associated with the risk of cardiovascular events in patients undergoing coronary angiography: a cohort study. *Am. J. Clin. Nutr.* **98**, 1162–9

58. Green, T. J., Skeaff, C. M., McMahon, J. A., Venn, B. J., Williams, S. M., Devlin, A. M., and Innis, S. M. (2010) Homocysteine-lowering vitamins do not lower plasma S-adenosylhomocysteine in older people with elevated homocysteine concentrations. *Br. J. Nutr.* **103**, 1629–34

59. Smith, D. E. C., Hornstra, J. M., Kok, R. M., Blom, H. J., and Smulders, Y. M. (2013) Folic acid supplementation does not reduce intracellular homocysteine, and may disturb intracellular one-carbon metabolism. *Clin. Chem. Lab. Med.* **51**, 1643–50

60. Xiao, Y., Huang, W., Zhang, J., Peng, C., Xia, M., and Ling, W. (2015) Increased plasma S-adenosylhomocysteine-accelerated atherosclerosis is associated with epigenetic regulation of endoplasmic reticulum stress in apoE-/- mice. *Arterioscler. Thromb. Vasc. Biol.* **35**, 60–70

61. Zawada, A. M., Rogacev, K. S., Hummel, B., Berg, J. T., Friedrich, A., Roth, H. J., Obeid, R., Geisel, J., Fliser, D., and Heine, G. H. (2014) S-adenosylhomocysteine is associated with subclinical atherosclerosis and renal function in a cardiovascular low-risk population. *Atherosclerosis*. **234**, 17–22

62. Caudill, M. A., Wang, J. C., Melnyk, S., Pogribny, I. P., Jernigan, S., Collins, M. D., Santos-Guzman, J., Swendseid, M. E., Cogger, E. A., and James, S. J. (2001) Intracellular S-adenosylhomocysteine concentrations predict global DNA hypomethylation in tissues of methyl-deficient cystathionine beta-synthase heterozygous mice. *J. Nutr.* **131**, 2811–8

63. Choumenkovitch, S. F., Selhub, J., Bagley, P. J., Maeda, N., Nadeau, M. R., Smith, D. E., and Choi, S.-W. (2002) In the cystathionine beta-synthase knockout mouse, elevations in total plasma homocysteine increase tissue S-adenosylhomocysteine, but responses of S-adenosylmethionine and DNA methylation are tissue specific. *J. Nutr.* **132**, 2157–60

64. Castro, R., Rivera, I., Struys, E. A., Jansen, E. E. W., Ravasco, P., Camilo, M. E., Blom, H. J., Jakobs, C., and Tavares de Almeida, I. (2003) Increased homocysteine and S-adenosylhomocysteine concentrations and DNA hypomethylation in vascular disease. *Clin. Chem.* **49**, 1292–6

65. Yi, P., Melnyk, S., Pogribna, M., Pogribny, I. P., Hine, R. J., and James, S. J. (2000) Increase in plasma homocysteine associated with parallel increases in plasma S-adenosylhomocysteine and lymphocyte DNA hypomethylation. *J. Biol. Chem.* **275**, 29318–23

66. Xiao, Y., Su, X., Huang, W., Zhang, J., Peng, C., Huang, H., Wu, X., Huang, H., Xia, M., and Ling, W. (2015) Role of S-adenosylhomocysteine in cardiovascular disease and its potential epigenetic mechanism. *Int. J. Biochem. Cell Biol.* 10.1016/j.biocel.2015.06.015

67. Handy, D. E., Castro, R., and Loscalzo, J. (2011) Epigenetic modifications: basic mechanisms and role in cardiovascular disease. *Circulation*. **123**, 2145–56

68. Loscalzo, J., and Handy, D. E. (2014) Epigenetic modifications: basic mechanisms and role in cardiovascular disease (2013 Grover Conference series). *Pulm. Circ.* **4**, 169–74

69. Subramaniam, D., Thombre, R., Dhar, A., and Anant, S. (2014) DNA methyltransferases: a novel target for prevention and therapy. *Front. Oncol.* **4**, 80

70. Jin, B., Li, Y., and Robertson, K. D. (2011) DNA methylation: superior or subordinate in the epigenetic hierarchy? *Genes Cancer*. **2**, 607–17

71. Deaton, A. M., and Bird, A. (2011) CpG islands and the regulation of transcription. *Genes Dev.* **25**, 1010–22

72. Han, H., Cortez, C. C., Yang, X., Nichols, P. W., Jones, P. A., and Liang, G. (2011) DNA methylation directly silences genes with non-CpG island promoters and establishes a nucleosome occupied promoter. *Hum. Mol. Genet.* **20**, 4299–310

73. Saavedra, O. M., Isakovic, L., Llewellyn, D. B., Zhan, L., Bernstein, N., Claridge, S., Raeppel, F., Vaisburg, A., Elowe, N., Petschner, A. J., Rahil, J., Beaulieu, N., MacLeod, A. R., Delorme, D., Besterman, J. M., and Wahhab, A. (2009) SAR around (l)-S-adenosyl-l-homocysteine, an inhibitor of human DNA methyltransferase (DNMT) enzymes. *Bioorg. Med. Chem. Lett.* **19**, 2747–51

74. Han, X.-B., Zhang, H.-P., Cao, C.-J., Wang, Y.-H., Tian, J., Yang, X.-L., Yang, A.-N., Wang, J., Jiang, Y.-D., and Xu, H. (2014) Aberrant DNA methylation of the PDGF gene in homocysteine-mediated VSMC proliferation and its underlying mechanism. *Mol. Med. Rep.* **10**, 947–54

75. Adaikalakoteswari, A., Finer, S., Voyias, P. D., McCarthy, C. M., Vatish, M., Moore, J., Smart-Halajko, M., Bawazeer, N., Al-Daghri, N. M., McTernan, P. G., Kumar, S., Hitman, G. A., Saravanan, P., and Tripathi, G. (2015) Vitamin B12 insufficiency induces cholesterol biosynthesis by limiting s-adenosylmethionine and modulating the methylation of SREBF1 and LDLR genes. *Clin. Epigenetics*. **7**, 14

76. Kim, C.-S., Kim, Y.-R., Naqvi, A., Kumar, S., Hoffman, T. A., Jung, S.-B., Kumar, A., Jeon, B.-H., McNamara, D. M., and Irani, K. (2011) Homocysteine promotes human endothelial cell dysfunction via site-specific epigenetic regulation of p66shc. *Cardiovasc. Res.* **92**, 466–75

77. Lakshmi, S. V. V., Naushad, S. M., Reddy, C. A., Saumya, K., Rao, D. S., Kotamraju, S., and Kutala, V. K. (2013) Oxidative stress in coronary artery disease: epigenetic perspective. *Mol. Cell. Biochem.* **374**, 203–11

78. Tekpli, X., Landvik, N. E., Anmarkud, K. H., Skaug, V., Haugen, A., and Zienolddiny, S. (2013) DNA methylation at promoter regions of interleukin 1B, interleukin 6, and interleukin 8 in non-small cell lung cancer. *Cancer Immunol. Immunother.* **62**, 337–45

79. Roebuck, K. A., and Finnegan, A. (1999) Regulation of intercellular adhesion molecule-1 (CD54) gene expression. *J. Leukoc. Biol.* **66**, 876–88

80. Nazarenko, M. S., Markov, A. V, Lebedev, I. N., Freidin, M. B., Sleptcov, A. A., Koroleva, I. A., Frolov, A. V, Popov, V. A., Barbarash, O. L., and Puzyrev, V. P. (2015) A comparison of genome-wide DNA methylation patterns between different vascular tissues from patients with coronary heart disease. *PLoS One*. **10**, e0122601

81. Aavik, E., Lumivuori, H., Leppänen, O., Wirth, T., Häkkinen, S.-K., Bräsen, J.-H., Beschorner, U., Zeller, T., Braspenning, M., van Criekinge, W., Mäkinen, K., and Ylä-Herttuala, S. (2014) Global DNA methylation analysis of human atherosclerotic plaques reveals extensive genomic hypomethylation and reactivation at imprinted locus 14q32 involving induction of a miRNA cluster. *Eur. Heart J.* **36**, 993–1000

82. Hiltunen, M. O., Turunen, M. P., Häkkinen, T. P., Rutanen, J., Hedman, M., Mäkinen, K., Turunen, A.-M., Aalto-Setälä, K., and Ylä-Herttuala, S. (2002) DNA hypomethylation and methyltransferase expression in atherosclerotic lesions. *Vasc. Med.* **7**, 5–11

83. Lund, G., Andersson, L., Lauria, M., Lindholm, M., Fraga, M. F., Villar-Garea, A., Ballestar, E., Esteller, M., and Zaina, S. (2004) DNA methylation polymorphisms precede any histological sign of atherosclerosis in mice lacking apolipoprotein E. *J. Biol. Chem.* **279**, 29147–54

84. Greißel, A., Culmes, M., Napieralski, R., Wagner, E., Gebhard, H., Schmitt, M., Zimmermann, A., Eckstein, H.-H., Zernecke, A., and Pelisek, J. (2015) Alternation of histone and DNA methylation in human atherosclerotic carotid plaques. *Thromb. Haemost.* 10.1160/TH14-10-0852

85. Zaina, S., Heyn, H., Carmona, F. J., Varol, N., Sayols, S., Condom, E., Ramírez-Ruz, J., Gomez, A., Gonçalves, I., Moran, S., and Esteller, M. (2014) DNA methylation map of human atherosclerosis. *Circ. Cardiovasc. Genet.* **7**, 692–700

86. Zaina, S., Gonçalves, I., Carmona, F. J., Gomez, A., Heyn, H., Mollet, I. G., Moran, S., Varol, N., and Esteller, M. (2015) DNA Methylation Dynamics in Human Carotid Plaques After Cerebrovascular Events. *Arterioscler. Thromb. Vasc. Biol.* 10.1161/ATVBAHA.115.305630

87. Machnicka, M. A., Milanowska, K., Osman Oglou, O., Purta, E., Kurkowska, M., Olchowik, A., Januszewski, W., Kalinowski, S., Dunin-Horkawicz, S., Rother, K. M., Helm, M., Bujnicki, J. M., and Grosjean, H. (2013) MODOMICS: a database of RNA modification pathways--2013 update. *Nucleic Acids Res.* **41**, D262–7

88. Motorin, Y., and Helm, M. (2011) RNA nucleotide methylation. *Wiley Interdiscip. Rev. RNA*. **2**, 611–31

89. Li, S., and Mason, C. E. (2014) The pivotal regulatory landscape of RNA modifications. *Annu. Rev. Genomics Hum. Genet.* **15**, 127–50

90. Towns, W. L., and Begley, T. J. (2012) Transfer RNA methytransferases and their corresponding modifications in budding yeast and humans: activities, predications, and potential roles in human health. *DNA Cell Biol.* **31**, 434–54

91. Sibbritt, T., Patel, H. R., and Preiss, T. (2013) Mapping and significance of the mRNA methylome. *Wiley Interdiscip. Rev. RNA*. **4**, 397–422

92. Jia, G., Fu, Y., and He, C. (2013) Reversible RNA adenosine methylation in biological regulation. *Trends Genet.* **29**, 108–15

93. Glick, J. M., Ross, S., and Leboy, P. S. (1975) S-adenosylhomocysteine inhibition of three purified tRNA methyltransferases from rat liver. *Nucleic Acids Res.* **2**, 1639–51

94. Leboy, P. S., Glick, J. M., Steiner, F. G., Haney, S., and Borchardt, R. T. (1978) S-adenosylhomocysteine analogues as inhibitors of specific tRNA methylation. *Biochim. Biophys. Acta - Nucleic Acids Protein Synth.* **520**, 153–163

95. Hildesheim, J., Hildesheim, R., Blanchard, P., Farrugia, G., and Michelot, R. (1973) Studies on synthetic inhibitors of t-RNA methyl transferases: analogs of S-adenosyl homocysteine. *Biochimie*. **55**, 541–6

96. Backlund, P. S., Carotti, D., and Cantoni, G. L. (1986) Effects of the S-adenosylhomocysteine hydrolase inhibitors 3-deazaadenosine and 3-deazaaristeromycin on RNA methylation and synthesis. *Eur. J. Biochem.* **160**, 245–51

97. Tarasiavichene, L. E., Iasaĭtis, A. A., Rachiauskaĭte, D. V, Ivanov, L. L., and Prashkiavichius, A. K. (1989) [Comparative characteristics of tRNA-methyltransferases from rabbit liver and myocardium under normal conditions and in experimental ischemia]. *Biokhimiia (Moscow, Russ.* **54**, 427–33

98. Stern, P. H., and Hoffman, R. M. (1984) Elevated overall rates of transmethylation in cell lines from diverse human tumors. *In Vitro*. **20**, 663–70

99. Chauhan, M. A., Ali, M., Vedeckis, W. V, and Salas, C. E. (1991) Transfer RNA nucleoside composition in 13762 rat adenocarcinoma. *Braz. J. Med. Biol. Res.* **24**, 547–58

100. Lin, W., MacKenzie, J. W., McCoy, J. R., and Clark, I. (1983) Metabolism of tRNA in rats with aflatoxin B1-induced hepatomas. *Cancer Biochem. Biophys.* **7**, 61–8

101. Li, H.-Y., Wang, S.-M., Liu, H.-M., Li, J., Han, D., Bu, S.-S., and Zhang, M.-Z. (2008) Analysis of modified nucleosides in the urine of patients with malignant cancer by liquid chromatography/electrospray ionization mass spectrometry. *Rapid Commun. Mass Spectrom.* **22**, 3161–71

102. Okamoto, M., Hirata, S., Sato, S., Koga, S., Fujii, M., Qi, G., Ogawa, I., Takata, T., Shimamoto, F., and Tatsuka, M. (2012) Frequent increased gene copy number and high protein expression of tRNA (cytosine-5-)-methyltransferase (NSUN2) in human cancers. *DNA Cell Biol.* **31**, 660–71

103. Wainfan, E., Dizik, M., Hluboky, M., and Balis, M. E. (1986) Altered tRNA methylation in rats and mice fed lipotrope-deficient diets. *Carcinogenesis*. **7**, 473–6

104. Gallo, R. C. (1971) Transfer RNA and transfer RNA methylation in growing and “resting” adult and embryonic tissues and in various oncogenic systems. *Cancer Res.* **31**, 621–9

105. Torelli, U. L., Torelli, G. M., Andreoli, A., and Mauri, C. (1971) Impaired of ribosomal precursor RNA in blast cells of acute leukemia. *Acta Haematol.* **45**, 201–8

106. Lappalainen, T., Kolehmainen, M., Schwab, U. S., Tolppanen, A. M., Stančáková, A., Lindström, J., Eriksson, J. G., Keinänen-Kiukaanniemi, S., Aunola, S., Ilanne-Parikka, P., Herder, C., Koenig, W., Gylling, H., Kolb, H., Tuomilehto, J., Kuusisto, J., and Uusitupa, M. (2011) Association of the FTO gene variant (rs9939609) with cardiovascular disease in men with abnormal glucose metabolism--the Finnish Diabetes Prevention Study. *Nutr. Metab. Cardiovasc. Dis.* **21**, 691–8

107. Songe-Møller, L., van den Born, E., Leihne, V., Vågbø, C. B., Kristoffersen, T., Krokan, H. E., Kirpekar, F., Falnes, P. Ø., and Klungland, A. (2010) Mammalian ALKBH8 possesses tRNA methyltransferase activity required for the biogenesis of multiple wobble uridine modifications implicated in translational decoding. *Mol. Cell. Biol.* **30**, 1814–27

108. Fu, D., Brophy, J. A. N., Chan, C. T. Y., Atmore, K. A., Begley, U., Paules, R. S., Dedon, P. C., Begley, T. J., and Samson, L. D. (2010) Human AlkB homolog ABH8 Is a tRNA methyltransferase required for wobble uridine modification and DNA damage survival. *Mol. Cell. Biol.* **30**, 2449–59

109. Kryukov, G. V, Castellano, S., Novoselov, S. V, Lobanov, A. V, Zehtab, O., Guigó, R., and Gladyshev, V. N. (2003) Characterization of mammalian selenoproteomes. *Science*. **300**, 1439–43

110. Itoh, Y., Chiba, S., Sekine, S.-I., and Yokoyama, S. (2009) Crystal structure of human selenocysteine tRNA. *Nucleic Acids Res.* **37**, 6259–68

111. Endres, L., Begley, U., Clark, R., Gu, C., Dziergowska, A., Małkiewicz, A., Melendez, J. A., Dedon, P. C., and Begley, T. J. (2015) Alkbh8 Regulates Selenocysteine-Protein Expression to Protect against Reactive Oxygen Species Damage. *PLoS One*. **10**, e0131335

112. Babaknejad, N., Sayehmiri, F., Sayehmiri, K., Rahimifar, P., Bahrami, S., Delpesheh, A., Hemati, F., and Alizadeh, S. (2014) The relationship between selenium levels and breast cancer: a systematic review and meta-analysis. *Biol. Trace Elem. Res.* **159**, 1–7

113. Polevoda, B., and Sherman, F. (2007) Methylation of proteins involved in translation. *Mol. Microbiol.* **65**, 590–606

114. Afjehi-Sadat, L., and Garcia, B. A. (2013) Comprehending dynamic protein methylation with mass spectrometry. *Curr. Opin. Chem. Biol.* **17**, 12–9

115. Tan, J., Yan, Y., Wang, X., Jiang, Y., and Xu, H. E. (2014) EZH2: biology, disease, and structure-based drug discovery. *Acta Pharmacol. Sin.* **35**, 161–74

116. Esse, R., Rocha, M. S., Barroso, M., Florindo, C., Teerlink, T., Kok, R. M., Smulders, Y. M., Rivera, I., Leandro, P., Koolwijk, P., Castro, R., Blom, H. J., and de Almeida, I. T. (2013) Protein arginine methylation is more prone to inhibition by S-adenosylhomocysteine than DNA methylation in vascular endothelial cells. *PLoS One*. **8**, e55483

117. Zhang, X., Wen, H., and Shi, X. (2012) Lysine methylation: beyond histones. *Acta Biochim. Biophys. Sin. (Shanghai).* **44**, 14–27

118. Huang, J., and Berger, S. L. (2008) The emerging field of dynamic lysine methylation of non-histone proteins. *Curr. Opin. Genet. Dev.* **18**, 152–8

119. Pahlich, S., Zakaryan, R. P., and Gehring, H. (2006) Protein arginine methylation: Cellular functions and methods of analysis. *Biochim. Biophys. Acta*. **1764**, 1890–903

120. Schleithoff, C., Voelter-Mahlknecht, S., Dahmke, I. N., and Mahlknecht, U. (2012) On the epigenetics of vascular regulation and disease. *Clin. Epigenetics*. **4**, 7

121. Migliori, V., Phalke, S., Bezzi, M., and Guccione, E. (2010) Arginine/lysine-methyl/methyl switches: biochemical role of histone arginine methylation in transcriptional regulation. *Epigenomics*. **2**, 119–37

122. Di Lorenzo, A., and Bedford, M. T. (2011) Histone arginine methylation. *FEBS Lett.* **585**, 2024–2031

123. Chang, B., Chen, Y., Zhao, Y., and Bruick, R. K. (2007) JMJD6 Is a Histone Arginine Demethylase. *Science (80-.).* **318**, 444–447

124. Margueron, R., and Reinberg, D. (2011) The Polycomb complex PRC2 and its mark in life. *Nature*. **469**, 343–9

125. Tan, J., Yang, X., Zhuang, L., Jiang, X., Chen, W., Lee, P. L., Karuturi, R. K. M., Tan, P. B. O., Liu, E. T., and Yu, Q. (2007) Pharmacologic disruption of Polycomb-repressive complex 2-mediated gene repression selectively induces apoptosis in cancer cells. *Genes Dev.* **21**, 1050–63

126. Morey, L., and Helin, K. (2010) Polycomb group protein-mediated repression of transcription. *Trends Biochem. Sci.* **35**, 323–32

127. Deb, G., Singh, A. K., and Gupta, S. (2014) EZH2: not EZHY (easy) to deal. *Mol. Cancer Res.* **12**, 639–53

128. Mozzetta, C., Pontis, J., Fritsch, L., Robin, P., Portoso, M., Proux, C., Margueron, R., and Ait-Si-Ali, S. (2014) The histone H3 lysine 9 methyltransferases G9a and GLP regulate polycomb repressive complex 2-mediated gene silencing. *Mol. Cell*. **53**, 277–89

129. Coward, W. R., Feghali-Bostwick, C. A., Jenkins, G., Knox, A. J., and Pang, L. (2014) A central role for G9a and EZH2 in the epigenetic silencing of cyclooxygenase-2 in idiopathic pulmonary fibrosis. *FASEB J.* **28**, 3183–96

130. Shinkai, Y., and Tachibana, M. (2011) H3K9 methyltransferase G9a and the related molecule GLP. *Genes Dev.* **25**, 781–8

131. Dreger, H., Ludwig, A., Weller, A., Stangl, V., Baumann, G., Meiners, S., and Stangl, K. (2012) Epigenetic regulation of cell adhesion and communication by enhancer of zeste homolog 2 in human endothelial cells. *Hypertension*. **60**, 1176–83

132. Hayden, A., Johnson, P. W. M., Packham, G., and Crabb, S. J. (2011) S-adenosylhomocysteine hydrolase inhibition by 3-deazaneplanocin A analogues induces anti-cancer effects in breast cancer cell lines and synergy with both histone deacetylase and HER2 inhibition. *Breast Cancer Res. Treat.* **127**, 109–19

133. Fiskus, W., Wang, Y., Sreekumar, A., Buckley, K. M., Shi, H., Jillella, A., Ustun, C., Rao, R., Fernandez, P., Chen, J., Balusu, R., Koul, S., Atadja, P., Marquez, V. E., and Bhalla, K. N. (2009) Combined epigenetic therapy with the histone methyltransferase EZH2 inhibitor 3-deazaneplanocin A and the histone deacetylase inhibitor panobinostat against human AML cells. *Blood*. **114**, 2733–43

134. Wierda, R. J., Rietveld, I. M., van Eggermond, M. C. J. A., Belien, J. A. M., van Zwet, E. W., Lindeman, J. H. N., and van den Elsen, P. J. (2014) Global histone H3 lysine 27 triple methylation levels are reduced in vessels with advanced atherosclerotic plaques. *Life Sci.* 10.1016/j.lfs.2014.10.010

135. Perna, A. F., Ingrosso, D., Zappia, V., Galletti, P., Capasso, G., and De Santo, N. G. (1993) Enzymatic methyl esterification of erythrocyte membrane proteins is impaired in chronic renal failure. Evidence for high levels of the natural inhibitor S-adenosylhomocysteine. *J. Clin. Invest.* **91**, 2497–503

136. Garcia, M. M., Guéant-Rodriguez, R.-M., Pooya, S., Brachet, P., Alberto, J.-M., Jeannesson, E., Maskali, F., Gueguen, N., Marie, P.-Y., Lacolley, P., Herrmann, M., Juillière, Y., Malthiery, Y., and Guéant, J.-L. (2011) Methyl donor deficiency induces cardiomyopathy through altered methylation/acetylation of PGC-1α by PRMT1 and SIRT1. *J. Pathol.* **225**, 324–35

137. Esse, R., Florindo, C., Imbard, A., Rocha, M. S., de Vriese, A. S., Smulders, Y. M., Teerlink, T., Tavares de Almeida, I., Castro, R., and Blom, H. J. (2013) Global protein and histone arginine methylation are affected in a tissue-specific manner in a rat model of diet-induced hyperhomocysteinemia. *Biochim. Biophys. Acta*. **1832**, 1708–14

138. Esse, R., Imbard, A., Florindo, C., Gupta, S., Quinlivan, E. P., Davids, M., Teerlink, T., Tavares de Almeida, I., Kruger, W. D., Blom, H. J., and Castro, R. (2014) Protein arginine hypomethylation in a mouse model of cystathionine β-synthase deficiency. *FASEB J.* **28**, 2686–95

CHAPTER

2

Aims and Outline

Cardiovascular diseases (CVD) are the number one cause of death globally, therefore it is important to improve our understanding of the molecular mechanisms contributing to these diseases. Hyperhomocysteinemia is a common risk factor for CVD; however, the mechanisms underlying this association, although extensively studied, remain to be fully elucidated. The overall hypothesis of the thesis is that accumulation of the homocysteine precursor, S-adenosylhomocysteine (SAH), may contribute to the vascular toxicity associated with hyperhomocysteinemia by disturbing cellular methylation via its effects as an inhibitor of methyltransferases. To explore this possibility, the main goals of the thesis are:

- to clarify the role of SAH accumulation in endothelial dysfunction and activation;
- to identify molecular targets that are disturbed under excess SAH in endothelial cells;
- to investigate whether hypomethylation contributes to the harmful effects of SAH in endothelial cells.

In **Chapter 3** we characterize an endothelial cell model of SAH intracellular accumulation used in this and subsequent studies. Additionally, we investigate the role of excess SAH in nitric oxide (NO) bioavailability, by monitoring endothelial nitric oxide synthase expression and activity, as well as NO production in our cell model. NO is an endogenous major player in endothelial homeostasis.

Chapter 4 explores the effects of SAH-mediated hypomethylation in RNA, and it encompasses two sub-chapters. In **Chapter 4.1**, we demonstrate that excess SAH modulates the expression of selenoproteins by impairing the methylation of a uridine within the tRNA that carries selenocysteine (tRNASec). Glutathione peroxidase-1 (GPx-1) is a selenoprotein and major antioxidant enzyme. Oxidative stress is a hallmark of endothelial dysfunction. We monitored GPx-1 expression and activity in our cell model. Moreover, we demonstrated that suppression of GPx-1 by SAH promoted oxidative stress by increasing hydrogen peroxide accumulation and that exposure to SAH also resulted in inflammatory activation of endothelial cells. In **Chapter 4.2**, we expanded our studies of RNA methylation by assessing the effect of SAH on methylation modifications in total and size-fractionated RNA samples from our cell model. Further, to confirm our observations we additionally analyzed RNA methylation in tissue samples from a hyperhomocysteinemic mouse model, where SAH accumulation results from endogenously disturbed homocysteine metabolism.

DNA is an established target for the SAH-mediated inhibition of methyltransferase activity. In **Chapter 5**, we investigate the effects of excess SAH in endothelial activation, to examine further the expression of adhesion molecules in response to SAH and the effects of their up-regulation on leukocyte transmigration. Here, we also compared the effects of SAH accumulation to those of a DNA

methyltransferase inhibitor, identifying specific adhesion molecules that are affected by both of these stresses and assessing the role of DNA hypomethylation in these effects.

Chapter 6 clarifies the role of the inflammatory mediator NFkB in the endothelial activation promoted by excess SAH. Recent evidence suggests that histone hypomethylation may be a consequence of SAH accumulation. To understand better the effects of excess SAH on endothelial cell activation, we additionally examine whether SAH suppresses the activity of the histone methyltransferase EZH2 to contribute to endothelial cell activation via the activation of NFkB.

Lastly, in **Chapter 7**, the results presented in the previous chapters are considered together and discussed in the light of the initial aims of this thesis. Then, some possible paths for future investigation are also discussed.

CHAPTER

3

Cellular Hypomethylation is Associated with Impaired Nitric Oxide Production by Cultured Human Endothelial Cells

Amino Acids. ***42****, 1903–11 (2012)*

Cellular Hypomethylation is Associated with Impaired Nitric Oxide Production by Cultured Human Endothelial Cells

Madalena Barroso[a], Mónica S Rocha[a,b], Ruben Esse[a], Israel Gonçalves Jr[a], Anita Q Gomes[c], Tom Teerlink[b], Cornelis Jakobs [b], Henk J Blom[b], Joseph Loscalzo[d], Isabel Rivera[a], Isabel Tavares de Almeida[a], Rita Castro[a].

[a] *Research Institute for Medicines and Pharmaceutical Sciences (iMed.ULisboa), Faculty of Pharmacy, University of Lisbon, Lisbon, Portugal;*
[b] *Department of Clinical Chemistry, Metabolic Unit, VU University Medical Center, Amsterdam, The Netherlands.*
[c] *Escola Superior de Tecnologia da Saúde de Lisboa, Portugal / Instituto de Medicina Molecular, Faculty of Medicine, University of Lisbon, Portugal.*
[d] *Cardiovascular Division, Department of Medicine, Brigham and Women's Hospital and Harvard Medical School, Boston, MA, US.*

ABSTRACT

Hyperhomocysteinemia (HHcy) is a risk factor for vascular disease, but the underlying mechanisms remain incompletely defined. Reduced bioavailability of nitric oxide (NO) is a principal manifestation of underlying endothelial dysfunction, which is an initial event in vascular disease. Inhibition of cellular methylation reactions by S-adenosylhomocysteine (SAH), which accumulates during HHcy, has been suggested to contribute to vascular dysfunction. However, thusfar, the effect of intracellular SAH accumulation on NO bioavailability has not yet been fully substantiated by experimental evidence. The present study was carried out to evaluate whether disturbances in cellular methylation status affect NO production by cultured human endothelial cells. Here, we show that a hypomethylating environment, induced by the accumulation of SAH, impairs NO production. Consistent with this finding, we observed decreased endothelial NO synthase (eNOS) expression and activity, but, by contrast, enhanced *NOS3* (gene encoding eNOS) transcription. Taken together, our data supports the existence of regulatory post-transcriptional mechanisms potentially modulated by cellular methylation leading to impaired NO production by cultured human endothelial cells. As such, our conclusions may have implications for the HHcy-mediated reductions in NO bioavailability and endothelial dysfunction.

Key Words: **S-adenosylhomocysteine, methylation, endothelial dysfunction, nitric oxide bioavailability, endothelial nitric oxide synthase.**

1. INTRODUCTION

Hyperhomocysteinemia (HHcy) is a risk factor for vascular disease, but the underlying mechanisms remain incompletely defined (1).

Cellular methylation potential is determined by the concentrations of the homocysteine precursor, S-adenosylhomocysteine (SAH). SAH inhibits virtually all S-adenosylmethionine (SAM)-dependent-methyltransferases, which in turn, catalyze the transfer of a methyl group from SAM to a wide variety of target molecules (including DNA and proteins), forming SAH and the methylated substrate (2). SAH is further converted into homocysteine and adenosine by a reversible reaction catalyzed by SAH hydrolase, which favors SAH production. When homocysteine accumulates, its precursor, SAH, will accumulate, as well. Elevated homocysteine was shown to be directly associated with increased extracellular and intracellular SAH concentrations *in vivo* (1). Increasing evidence indicates that homocysteine may be regarded as a cellular demethylating agent, at least at the DNA level. In fact, we and others have observed an association between high levels of homocysteine and SAH, which, in turn, is correlated with global DNA hypomethylation status (1). In addition, several studies support the existence of epigenetic mechanisms in the context of homocysteine-related endothelial dysfunction (2).

Vascular disease begins with endothelial dysfunction, a sensitive indicator of the atherosclerotic process, occurring even before the clinical manifestations of the pathology and predicting adverse clinical outcomes (3, 4). Reduced bioavailability of nitric oxide (NO) and consequent impairment of endothelium-dependent vasodilation result in endothelial dysfunction. Nitric oxide is synthesized by endothelial cells from the amino acid, L-arginine, via the enzymatic action of endothelial nitric oxide synthase (eNOS), and is an important mediator of intracellular signaling and a potent anti-atherogenic molecule responsible for the maintenance of vascular homeostasis (5). Endothelial NOS expression is subject to significant degrees of regulation from transcriptional to post-translational levels (3, 4). Asymmetric dimethylarginine (ADMA) is an endogenous competitive inhibitor of eNOS, and is derived from the proteolysis of methylated arginine residues in proteins (6). Methylation of arginine in proteins is carried out by protein-arginine methyltransferases type 1 (PRMTs 1), transferring one methyl group from SAM to various proteins and forming, in addition, SAH (7). SAH is further hydrolysed to homocysteine. Because of the metabolic link between ADMA and homocysteine, ADMA has been suggested as a potential mediator of endothelial dysfunction in HHcy (8–10). Evidence from animal models and clinical studies have suggested that accumulation of ADMA contributes to impaired NO generation and disease pathogenesis (11).

Several *in vivo* studies, either in animal models (12–14) or in humans with severe (15), mild (16, 17), or transient (18, 19) HHcy, showed that endothelial dysfunction is a key vascular phenotype occurring in the setting of HHcy; however, the mechanistic understanding of the association between HHcy and impaired NO bioavailability remains to be completely defined. The present study was

designed to evaluate whether a hypomethylating environment, induced by accumulation of the homocysteine precursor, SAH, perturbs NO production by cultured human endothelial cells.

2. MATERIALS AND METHODS

Cell Culture and Treatments – Human umbilical vein endothelial cells (HUVEC) were obtained from umbilical cords of healthy fetuses from uncomplicated pregnancies and vaginal deliveries from healthy mothers, as described (20), or commercially obtained from Lonza. The cord was collected in buffered solution [4 mmol/L KCl, 140 mmol/L NaCl, 11 mmol/L D-glucose (Merck), 10 mmol/L HEPES (Gibco), and 1% antibiotic–antimycotic solution (Sigma)], and stored at −4ºC. Within 4 days, cells were isolated by collagenase (Gibco) treatment, and were cultured essentially as previously described (20). Cells were grown in coated six-well plates (6 x 10 cm^2), 75 cm^2 flasks or 100 cm^2 disks depending on subsequent analysis.

All experiments were performed at 80% confluence and between the fourth and sixth passage. After the removal of the culture medium, fresh medium, either without (control) or with increasing concentrations of an SAH hydrolase inhibitor (adenosine dialdehyde, ADA) (5, 10, and 20 μmol/L) was added. After 24 h of incubation, lactate dehydrogenase (LDH) release was evaluated in the cell culture medium using the Cytotoxicity Detection Kit (Roche Diagnostic GmbH).

Metabolite Analysis – Aliquots of the medium were collected from cells grown in six-well plates after 24h of incubation and stored at –20°C for further homocysteine and ADMA analysis. HUVEC were then extensively washed with ice-cold phosphate-buffered saline (PBS) and exposed to denaturation buffer for 15 min at 4°C. Denaturation buffer consisted of 1.5 mmol/L $MgCl_2$, 10 mmol/L KCl, 1 mmol/L DTT (Merck), 10 mmol/L HEPES (Gibco), and 1.0 mmol/L PMSF (Sigma) (pH 7.9), containing containing 1% (V/V) Triton X-100 (Merck). The cell lysate was centrifuged at 4°C, 1,200 rpm, for 10 min. The supernatant (cytosol) was collected, and two aliquots were taken. One was promptly deproteinized with an equal volume of 10% perchloric acid and stored at –20°C for further SAM and SAH evaluation, and the remainder was immediately frozen and kept at –20°C until protein determination.

Extracellular total homocysteine levels, defined as the total concentration of homocysteine after reductive cleavage of all disulfide bonds, was determined by HPLC analysis according to Araki and Sako (21), with minor modifications. Extracellular ADMA concentrations were measured by HPLC with fluorescence detection as described previously (22), using modified chromatographic separation conditions (23). Intracellular SAH and SAM concentrations were analyzed by LC-MS/MS (24).

NO Levels – Nitric oxide production in response to intracellular SAH accumulation was measured by the Griess reaction (25). For this purpose, cells were grown in six-well plates. Culture

medium was replaced 24 h before incubations, which were conducted in 0.8 mL of basal endothelial cell culture medium without phenol red. After 12 h and 24 h of incubation, aliquots of culture medium were collected for NO_2^- quantification. In addition, incubations for 18 h with 1 mmol/L of L-N^G-nitroarginine (L-NNA) (Cayman Chemicals), an eNOS inhibitor, in the presence and in the absence of 20 μmol/L of ADA, were also performed. Freshly collected (200 μL) cell culture supernatants were mixed with 200 μL Griess reagent (1:1 mixture of 1% sulphanilamide in 5% H_3PO_4 and 0.1% naphthylethylenediamine dihydrochloride in water) and incubated in 96-well plates for 10 minutes at room temperature. Absorbance at 543 nm was recorded. Cells were lysed and protein concentrations were determined. Nitrite concentration was calculated using sodium nitrite standards and normalized by cellular protein concentration (μmoles of NO_2^- / mg of cell protein).

Western Blotting – Western blot was performed for analysis of eNOS levels, using four independent cultures. 30 cm^2 of 80% confluent HUVEC was used for each sample. Cells were washed 3 times with ice-cold PBS, directly lysed in cell lysis buffer containing protease inhibitors (Sigma), collected with a cell scraper, and sonicated. After centrifugation, the obtained supernatant was used for total protein determination and Western blot analysis. Protein concentrations were quantified using the DC Protein Assay (Biorad).

Protein samples (20-30 μg) were separated on 10 % SDS-polyacrylamide gels and transferred onto nitrocellulose membranes (Amersham, GE Healthcare). The membranes were incubated with anti-eNOS (at a 1:500 dilution; Cell Signalling) and anti-β-actin (at a 1:400 dilution; Sigma) antibodies. A secondary anti-rabbit IgG HRP secondary antibody (Cell Signaling) at a 1:2000 dilution was used. Primary antibody incubation was performed overnight at 4°C, and secondary antibody incubation was performed for 1–1.5 hours at room temperature. An ECL Plus Western Blotting Detection System was used for protein detection (GE Healthcare), membranes were exposed to Amersham Hyperfilm HCl (GE Healthcare), and a VersaDoc scanning system (BioRad) was used for densitometric analysis.

eNOS Activity – eNOS activity was determined by measuring the efficacy of conversion of [^{3}H]-Arg to [^{3}H]-citrulline in protein extracts from cultured cells using a commercial kit (Cayman Chemicals), according to the manufacturer's instructions. Four independent cultures were used.

Briefly, cells were grown to confluence in 100 cm^2 disks, treated with 20 μmol/L of ADA for 24 hours, washed with PBS, harvested in PBS containing 1mmol/L of EDTA, and centrifuged. The obtained pellet was lysed in 100 μL of lysis buffer, centrifuged, and 10 μL of the obtained supernatant were incubated with 40 μL of reaction buffer containing [^{3}H]-Arg for 60 minutes at 37ºC. Reactions were terminated by addition of 400 μL of Stop Buffer from the kit. Cell lysates were applied to a cation exchange resin column from the kit. The citrulline was eluted, radioactivity determined, and normalized via protein concentration.

Reverse Transcription and Quantitative PCR – Total RNA was extracted from three independent cultures using the RNeasy Minikit (Qiagen) and was reverse transcribed (2 μg) into cDNA using oligo(dT) SuperScript II Reverse Transcriptase (Invitrogen). Specific primers for *NOS3* gene (NM_000603.3): 5'-CGTCCCTGTGGAAAGACAAG-3' and 5'-CACGATGGTGACTTTGGCTA-3', were designed with the Universal Probe Library Assay Design Center (Roche Applied Science). EIF4A2 gene (NM_001967.3) was used as an internal control gene (primers: 5'-GTGTGAACTGGACCCTGTTG-3' and 5'-TATTTAACATTCAAACTTCATTAAGACATG-3'). Amplification reaction assays were performed in triplicate and contained 1×SYBR Green PCR Mastermix (Applied Biosystems) and primers at optimal concentration. A hot start at 50ºC for 2 min, was followed by an extension period at 95ºC for 10 minutes and then for 40 cycles at 95ºC for 15s and 60ºC for 1 min, using the 7300 Real Time PCR System (Applied Biosystems). Fluorescence emission was detected for each PCR cycle and the Ct (threshold cycle) values were determined.

Statistical Analysis – Data are presented as means ± *SD*. Statistical evaluation of the data was performed by paired Student's t test for comparisons between two groups, and by one-way analysis of variance followed by Dunnett's test for comparisons between more than two groups. A value of $p<0.05$ was regarded as significant.

3. RESULTS

Intracellular SAH and SAM levels – As shown in Figure 1A, ADA was effective in promoting a significant SAH intracellular accumulation, confirming its inhibitory effect on SAH hydrolase. SAM levels remained unaltered (189 ± 50, 216 ± 22, 169 ± 50 and 203 ± 30 pmol/mg protein for ADA 0, 5, 10 and 20 μmol/L, respectively, p=NS for trend). A significant ($p<0.01$ *versus* control) decrease in intracellular SAM/SAH ratio was observed (5.8 ± 1.6, 1.8 ± 0.2, 1.0 ± 0.3 and 0.8 ± 0.1 for ADA 0, 5, 10 and 20 μmol/L, respectively), which was exclusively defined by the increasing levels of SAH.

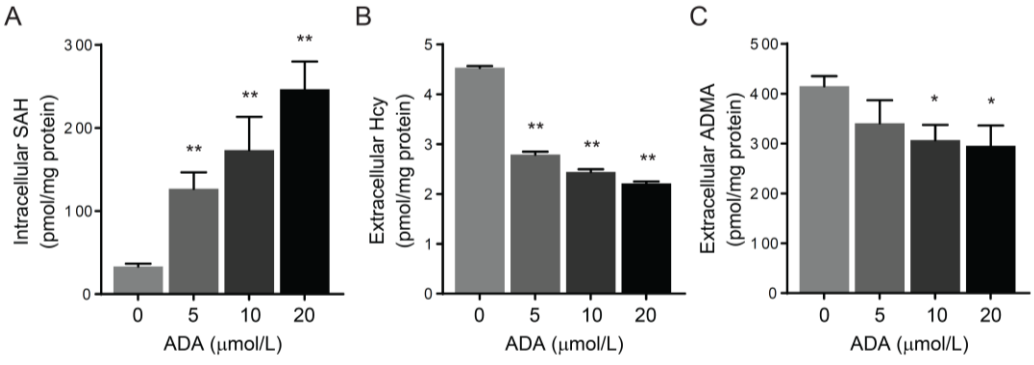

Figure 1 - Intracellular SAH **(A)**, and extracellular homocysteine (Hcy) **(B)** and ADMA **(C)** concentrations in HUVEC incubated in culture medium supplemented with increasing concentrations of ADA for 24 h. Data are presented as means ± *SD*. (**p< 0.01 *versus* control, n≥3; *p< 0.05 *versus* control, n=6).

Lactate dehydrogenase (LDH) – Cell LDH release (average ± *SD,* n=3), an indicator of cytotoxicity, after 24 h of incubation, in the absence (control: 100 ± 8 %) or presence of the tested ADA concentrations [(ADA 5 μmol/L: 111 ± 16 %; ADA 10 μmol/L: 110 ± 17 % and ADA 20 μmol/L: 105 ± 12 %] were similar. Therefore, a possible cytotoxic effect for the ADA was ruled out in the present study.

NO levels under intracellular SAH accumulation – We measured nitrite, a metabolite of NO, as an index of endothelial NO production. We observed a decrease in extracellular nitrite concentrations, after 12 and 24 h of incubation, which, for the highest ADA concentration tested, reached statistical significance (Fig. 2). The observed difference of extracellular nitrite concentrations, observed in the absence and the presence of 20 μmol/L of ADA, was abolished by co-incubation with 1 mmol/L of L-NNA, an eNOS inhibitor (Fig. 3).

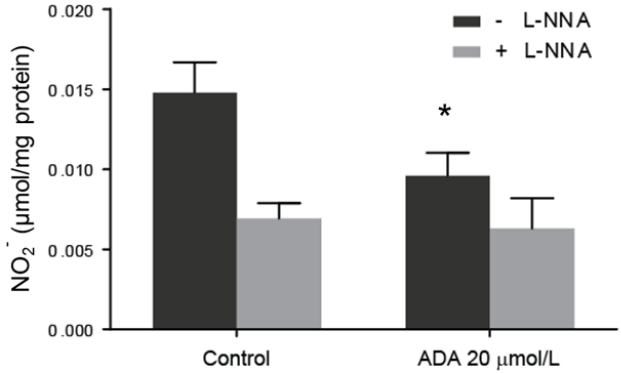

Figure 2 - Nitrite levels in HUVEC culture medium measured by the Griess reaction. HUVEC were incubated in culture medium supplemented with increasing concentrations of ADA for 12 or 24h. Data are presented as means ± *SD,* and are representative of 3 different cell lines (*p< 0.05 *versus* control).

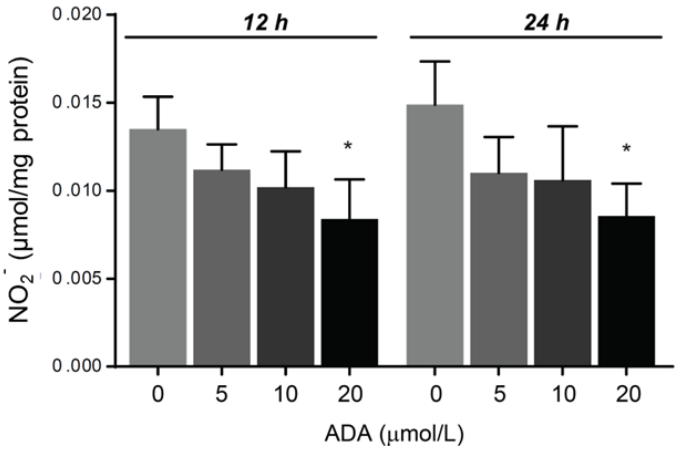

Figure 3 - Nitrite levels in HUVEC culture medium supplemented with 0 and 20 μmol/L concentrations of ADA in the absence and in the presence of L-NNA (1 mmol/L) after 18 h of incubation. Data are presented as means ± *SD* (*p< 0.05 *versus* control, n=3).

eNOS: transcriptional and translational levels and enzymatic activity under intracellular SAH accumulation (eNOS protein and activity) – The expression of eNOS protein was studied using Western blot analysis. A typical band with a molecular mass of approximately 140 kDa was detected with an anti-eNOS antibody, with β-actin used as reference. Relative expression of eNOS was significantly reduced by intracellular SAH accumulation (Fig. 4A1).

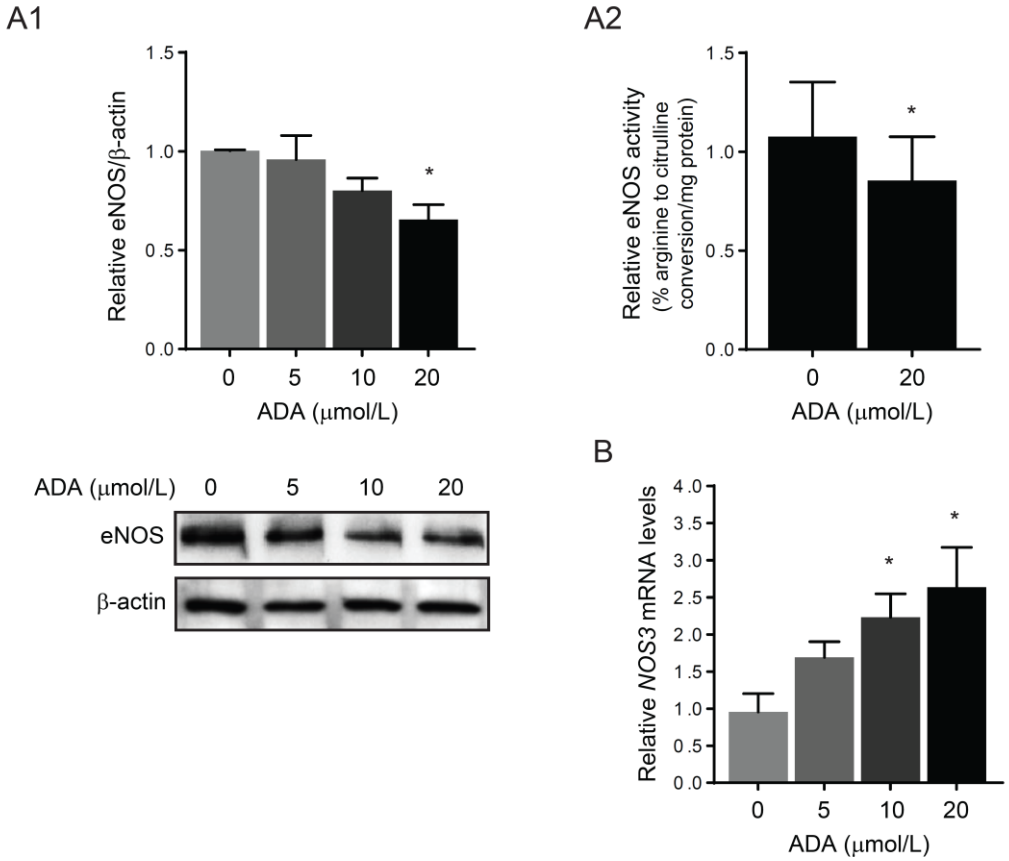

Figure 4 - **eNOS expression in HUVEC cultured with increasing concentrations of ADA after 24 h of incubation**. Data are means ± *SD*. **(A1)**, relative eNOS expression was determined by Western blotting with antibodies against eNOS and β-actin. Densitometry was performed on 4 blots. A representative blot is shown. (*p<0.05 *versus* control). **(A2)**, eNOS activity was measured in HUVEC incubated in the absence or presence of 20 μmol/L of ADA after 24 h by measuring the conversion of L-arginine to L-citrulline in cell lysates. Four different experiments were performed each in duplicate. (*p<0.05 paired Student t-test *versus* control). **(B)**, Real-time quantitative RT-PCR of relative *NOS3* mRNA levels of three or more independently prepared cDNA pools representing independent RNA isolations. (*p<0.05 *versus* control).

The functionality of the eNOS protein was assessed by monitoring the efficacy of L-arginine to L-citrulline conversion in cell lysates. Compared to controls, cells incubated with 20 μmol/L ADA for 24 h showed a significant decrease in eNOS activity (p<0.05) (Fig. 4A2).

eNOS: transcriptional and translational levels and enzymatic activity under intracellular SAH accumulation (*NOS3* mRNA) – *NOS3* mRNA levels were quantified by RT-qPCR. As opposed to the ADA-induced decrease of eNOS protein and activity, a significant increase of *NOS3* gene transcription was found directly related to the intracellular accumulation of SAH (Fig. 4B).

4. DISCUSSION

The major finding of the present study is that intracellular accumulation of SAH resulted in impaired NO production by cultured human endothelial cells. Furthermore, decreased eNOS protein expression and corresponding enzymatic activity were observed, but increased *NOS3* mRNA levels were found.

Homocysteine metabolism is biochemically linked to the principal epigenetic tag (5-methylcytosine) found in DNA (2). Inhibition of cellular methylation reactions by SAH, which accumulates in the setting of HHcy, has been suggested to contribute to vascular dysfunction. Accordingly, several studies support the existence of epigenetic mechanisms in the context of homocysteine-related endothelial dysfunction (2). However, thus far, the effect of intracellular SAH accumulation on NO bioavailability has not yet been fully examined. The present study was designed to evaluate whether a hypomethylating environment, caused by intracellular SAH accumulation, contributes to the impairment of endothelium-dependent NO production in cultured human endothelial cells.

Because SAH hardly crosses the cell membrane (20, 26), the intracellular accumulation of the homocysteine precursor, SAH, was achieved through the pharmacological inhibition of SAH hydrolase by an adenosine analogue, ADA. As shown in Figure 1, increasing concentrations of ADA were effective in increasing intracellular SAH levels. Supporting our previous observations, the levels of SAH exclusively determined the decrease in SAM/SAH ratio since SAM levels remained constant over the range of ADA concentrations used (20). Homocysteine export from the HUVEC reflects an imbalance between its intracellular production and metabolism. Therefore, and as expected, a decrease in the concentration of extracellular homocysteine was observed (Fig. 1B), confirming the inhibitory effect of ADA upon SAH hydrolase.

The rapid metabolism and short half-life of NO brings additional difficulties to its analytical assessment (25). However, the measurement of nitrite, a metabolite of NO, is currently used as an index of endothelial NO production (25). As shown in Figure 2, with increasing concentrations of ADA, a dose-dependent decrease in extracellular nitrite levels was observed in our system. This effect was abolished in the presence of the eNOS inhibitor, the L-NNA (Fig. 3). This finding confirmed that the decreased nitrite formation caused by intracellular SAH accumulation was due to impaired NO synthesis by eNOS. Previous studies also found that NO release from cultured endothelial cells was impaired in the presence of elevated homocysteine (27). In addition, in hyperhomocysteinemic mice with endothelial dysfunction, elevated SAH and decreased SAM/SAH ratio were observed (12). ADMA is an endogenous and potent inhibitor of eNOS that was found to accumulate in different study models including in humans with HHcy and vascular disease (11). Consequently, the accumulation of ADMA was suggested to contribute to reduced NO generation in homocysteine-dependent endothelial dysfunction (11). Our results suggest that the accumulation of the homocysteine precursor, SAH, is

not responsible for the ADMA accumulation observed in the setting of HHcy. In fact, an SAH intracellular accumulation (Fig. 1A) was associated with decreased extracellular ADMA levels (Fig. 1C) in our cellular model. In addition, a significant impaired NO production was observed (Figs. 2-4). Therefore, our results suggest the existence of an ADMA-independent mechanism triggered by SAH accumulation that may contribute to the HHcy-related impaired NO bioavailability. Interestingly, it has been recently suggested that the increase in ADMA levels, seen in humans with HHcy and vascular disease, is probably due to the decline of renal function and is not directly related to HHcy-dependent metabolic changes, nor contribute to endothelial dysfunction (28, 29).

Nitric oxide is generated in endothelial cells from conversion of L-arginine to L-citrulline by the enzymatic action of eNOS, which in turn is encoded by the *NOS3* gene. To investigate whether the observed impairment in endothelial NO bioavailability was caused by decreased eNOS expression, we focused on its translational and transcriptional expression. As shown in Figure 4A1, decreased eNOS protein levels were observed, suggesting eNOS down-regulation by intracellular SAH accumulation. In agreement with these observations, an homocysteine-induced decrease in eNOS protein levels was seen using human aortic endothelial cells in a prior study (30).

We also examined the functionality of eNOS protein, monitoring the efficacy of L-arginine to L-citrulline conversion by cell lysates. Compared to controls, cells incubated with 20 μmol/L of ADA for 24 h showed a significant decrease in eNOS activity (Fig. 4A2), which is consistent with our findings of decreased nitrite levels (Fig. 2) and decreased eNOS levels (Fig. 4A1). Previous reports concerning homocysteine-induced disturbances in eNOS activity are controversial. In fact, no effect (31) or down-regulation (32) by homocysteine upon eNOS activity had been reported previously in cultured endothelial cells.

Surprisingly, we found that relative *NOS3* mRNA levels were significantly increased by intracellular SAH accumulation (Fig. 4B). We, and others, have already shown that global DNA hypomethylation is induced by SAH accumulation (1, 20). It is well known that DNA methylation is an epigenetic mechanism of gene regulation and that decreased methylation patterns usually are related to increased transcription of target genes by several mechanisms (2). However, it has been previously shown that in eNOS-expressing cells the core promoter CpG dinucleotides are fully demethylated (33). Accordingly, it was reported that treatment of human endothelial cells with a DNA methyltransferase inhibitor did not alter the levels of *NOS3* mRNA, as it did in eNOS non-expressing cells (33). These observations led us to exclude DNA hypomethylation as causing the increase in *NOS3* mRNA levels observed in our model. However, DNA is not the only target for the SAH-mediated inhibition of SAM-dependent methyltransferases, and multiple targets may be affected, including proteins implicated in eNOS expression in human endothelial cells. An example of this point is the forkhead box O 1 (FoxO1) transcription factor, which acts as transcriptional repressor of *NOS3* expression. Recent data showed that protein arginine methyltransferase 1 (PRMT1) methylates

FoxO1, which in turn hinders its phosphorylation and export to cytoplasm, thus augmenting the expression of FoxO1 target genes (34). The same authors showed that, in a HUVEC model, the knockdown of PRMT1 induced *NOS3* expression (34). Moreover, our data show that intracellular SAH accumulation was associated with decreased extracellular ADMA concentrations, as well as increased relative *NOS3* mRNA levels. Recent observations by our group showed that protein-incorporated ADMA is strongly decreased by SAH intracellular accumulation in HUVEC (35), indicating that PRMT1 is a target for SAH-mediated inhibition and suggesting that FoxO1-methylation may be subsequently reduced by SAH. Taken together, these findings suggest that PRMT1 was subjected to SAH-mediated inhibition, causing FoxO1 hypomethylation and the observed SAH-dependent enhanced *NOS3* transcription (Fig. 4B).

Regulation of eNOS protein levels is a complex process that is mediated at several levels, including post-transcriptionally (36). In fact, our paradoxal observations concerning eNOS transcriptional and translational levels disclose the existence of post-transcriptional events to be ascertained. Similar observations have been reported in different contexts. For example, in livers from patients with alcoholic hepatitis, *NOS3* mRNA was found to be increased, but eNOS activity decreased, despite no differences in eNOS protein expression compared with non-alcoholic livers (37). In addition, exercise training of diabetic animals was shown to lead to an increase in left ventricular eNOS protein and a concomitant decrease in *NOS3* mRNA (38).

In conclusion, we observed that a hypomethylating environment, due to increased intracellular levels of SAH, impairs NO production by cultured human endothelial cells. This finding may have implications in the HHcy-mediated reduction in NO bioavailability and endothelial dysfunction. Taken together, our results clearly suggest that post-transcriptional events may be crucial mechanisms in the regulation of NO synthesis, and their modulation by the cellular methylation potential demands further investigation.

ACKNOWLEDGEMENTS

We thank Diane E. Handy and Jane A. Leopold for scientific advice. We also thank Scott R. Oldebeken, Desiree Smith, and Sigrid de Jong for theirs excellent technical assistance.

FUNDING

This work was partially supported by FCT (Fundação para a Ciência e Tecnologia) (PTDC/SAUGMG/68714/2006 and SFRH/BSAB/921/2009 [RC], SFRH/BD/41970/2007 [MR], SFRH/BD/48585/2008 [RE]) and Fundação Calouste Gulbenkian (grant 105783/2009 [RC]), and by the NIH grants HL61795, HL81587, HL70819, and HL48743 (JL).

REFERENCES

1. Castro, R., Rivera, I., Blom, H. J., Jakobs, C., and Tavares de Almeida, I. (2006) Homocysteine metabolism, hyperhomocysteinaemia and vascular disease: an overview. *J. Inherit. Metab. Dis.* **29**, 3–20
2. Handy, D. E., Castro, R., and Loscalzo, J. (2011) Epigenetic modifications: basic mechanisms and role in cardiovascular disease. *Circulation*. **123**, 2145–56
3. Tai, S. C., Robb, G. B., and Marsden, P. A. (2004) Endothelial nitric oxide synthase: a new paradigm for gene regulation in the injured blood vessel. *Arterioscler. Thromb. Vasc. Biol.* **24**, 405–12
4. Weiss, N., Keller, C., Hoffmann, U., and Loscalzo, J. (2002) Endothelial dysfunction and atherothrombosis in mild hyperhomocysteinemia. *Vasc. Med.* **7**, 227–39
5. Luksha, L., Agewall, S., and Kublickiene, K. (2009) Endothelium-derived hyperpolarizing factor in vascular physiology and cardiovascular disease. *Atherosclerosis*. **202**, 330–44
6. Cardounel, A. J., Cui, H., Samouilov, A., Johnson, W., Kearns, P., Tsai, A.-L., Berka, V., and Zweier, J. L. (2007) Evidence for the pathophysiological role of endogenous methylarginines in regulation of endothelial NO production and vascular function. *J. Biol. Chem.* **282**, 879–87
7. Böger, R. H. (2006) Asymmetric dimethylarginine (ADMA): a novel risk marker in cardiovascular medicine and beyond. *Ann. Med.* **38**, 126–36
8. Lentz, S. R., Rodionov, R. N., and Dayal, S. (2003) Hyperhomocysteinemia, endothelial dysfunction, and cardiovascular risk: the potential role of ADMA. *Atheroscler. Suppl.* **4**, 61–5
9. Dayal, S., and Lentz, S. R. (2005) ADMA and hyperhomocysteinemia. *Vasc. Med.* **10 Suppl 1**, S27–33
10. Stühlinger, M. C., and Stanger, O. (2005) Asymmetric dimethyl-L-arginine (ADMA): a possible link between homocyst(e)ine and endothelial dysfunction. *Curr. Drug Metab.* **6**, 3–14
11. Teerlink, T., Luo, Z., Palm, F., and Wilcox, C. S. (2009) Cellular ADMA: regulation and action. *Pharmacol. Res.* **60**, 448–60
12. Dayal, S., Bottiglieri, T., Arning, E., Maeda, N., Malinow, M. R., Sigmund, C. D., Heistad, D. D., Faraci, F. M., and Lentz, S. R. (2001) Endothelial dysfunction and elevation of S-adenosylhomocysteine in cystathionine beta-synthase-deficient mice. *Circ. Res.* **88**, 1203–9
13. Devlin, A. M., Arning, E., Bottiglieri, T., Faraci, F. M., Rozen, R., and Lentz, S. R. (2004) Effect of Mthfr genotype on diet-induced hyperhomocysteinemia and vascular function in mice. *Blood*. **103**, 2624–9
14. Celotto, A. C., Fukada, S. Y., Laurindo, F. R. M., Haddad, R., Eberlin, M. N., and de Oliveira, A. M. (2010) Chronic hyperhomocysteinemia impairs vascular function in ovariectomized rat carotid arteries. *Amino Acids*. **38**, 1515–22
15. Celermajer, D. S., Sorensen, K., Ryalls, M., Robinson, J., Thomas, O., Leonard, J. V, and Deanfield, J. E. (1993) Impaired endothelial function occurs in the systemic arteries of children with homozygous homocystinuria but not in their heterozygous parents. *J. Am. Coll. Cardiol.* **22**, 854–8
16. Tawakol, A., Omland, T., Gerhard, M., Wu, J. T., and Creager, M. A. (1997) Hyperhomocyst(e)inemia is associated with impaired endothelium-dependent vasodilation in humans. *Circulation*. **95**, 1119–21
17. Woo, K. S., Chook, P., Lolin, Y. I., Cheung, A. S., Chan, L. T., Sun, Y. Y., Sanderson, J. E., Metreweli, C., and Celermajer, D. S. (1997) Hyperhomocyst(e)inemia is a risk factor for arterial endothelial dysfunction in humans. *Circulation*. **96**, 2542–4
18. Chambers, J. C., Obeid, O. A., and Kooner, J. S. (1999) Physiological increments in plasma homocysteine induce vascular endothelial dysfunction in normal human subjects. *Arterioscler. Thromb. Vasc. Biol.* **19**, 2922–7
19. Chao, C. L., Kuo, T. L., and Lee, Y. T. (2000) Effects of methionine-induced hyperhomocysteinemia on endothelium-dependent vasodilation and oxidative status in healthy adults. *Circulation*. **101**, 485–90
20. Castro, R., Rivera, I., Martins, C., Struys, E. A., Jansen, E. E. W., Clode, N., Graça, L. M., Blom, H. J., Jakobs, C., and de Almeida, I. T. (2005) Intracellular S-adenosylhomocysteine increased levels are associated with DNA hypomethylation in HUVEC. *J. Mol. Med. (Berl).* **83**, 831–6

21. Araki, A., and Sako, Y. (1987) Determination of free and total homocysteine in human plasma by high-performance liquid chromatography with fluorescence detection. *J. Chromatogr.* **422**, 43–52

22. Teerlink, T., Nijveldt, R. J., de Jong, S., and van Leeuwen, P. A. M. (2002) Determination of arginine, asymmetric dimethylarginine, and symmetric dimethylarginine in human plasma and other biological samples by high-performance liquid chromatography. *Anal. Biochem.* **303**, 131–7

23. De Jong, S., and Teerlink, T. (2006) Analysis of asymmetric dimethylarginine in plasma by HPLC using a monolithic column. *Anal. Biochem.* **353**, 287–9

24. Struys, E. A., Jansen, E. E., de Meer, K., and Jakobs, C. (2000) Determination of S-adenosylmethionine and S-adenosylhomocysteine in plasma and cerebrospinal fluid by stable-isotope dilution tandem mass spectrometry. *Clin. Chem.* **46**, 1650–6

25. Guevara, I., Iwanejko, J., Dembińska-Kieć, A., Pankiewicz, J., Wanat, A., Anna, P., Gołabek, I., Bartuś, S., Malczewska-Malec, M., and Szczudlik, A. (1998) Determination of nitrite/nitrate in human biological material by the simple Griess reaction. *Clin. Chim. Acta.* **274**, 177–88

26. Ueland, P. M. (1982) Pharmacological and biochemical aspects of S-adenosylhomocysteine and S-adenosylhomocysteine hydrolase. *Pharmacol. Rev.* **34**, 223–53

27. Upchurch, G. R., Welch, G. N., Fabian, A. J., Freedman, J. E., Johnson, J. L., Keaney, J. F., and Loscalzo, J. (1997) Homocyst(e)ine decreases bioavailable nitric oxide by a mechanism involving glutathione peroxidase. *J. Biol. Chem.* **272**, 17012–7

28. Wilcken, D. E. L., Wang, J., Sim, A. S., Green, K., and Wilcken, B. (2006) Asymmetric dimethylarginine in homocystinuria due to cystathionine beta-synthase deficiency: relevance of renal function. *J. Inherit. Metab. Dis.* **29**, 30–7

29. Van Guldener, C., Nanayakkara, P. W. B., and Stehouwer, C. D. A. (2007) Homocysteine and asymmetric dimethylarginine (ADMA): biochemically linked but differently related to vascular disease in chronic kidney disease. *Clin. Chem. Lab. Med.* **45**, 1683–7

30. Jiang, X., Yang, F., Tan, H., Liao, D., Bryan, R. M., Randhawa, J. K., Rumbaut, R. E., Durante, W., Schafer, A. I., Yang, X., and Wang, H. (2005) Hyperhomocystinemia impairs endothelial function and eNOS activity via PKC activation. *Arterioscler. Thromb. Vasc. Biol.* **25**, 2515–21

31. Heydrick, S. J., Weiss, N., Thomas, S. R., Cap, A. P., Pimentel, D. R., Loscalzo, J., and Keaney, J. F. (2004) L-Homocysteine and L-homocystine stereospecifically induce endothelial nitric oxide synthase-dependent lipid peroxidation in endothelial cells. *Free Radic. Biol. Med.* **36**, 632–40

32. Dayal, S., Rodionov, R. N., Arning, E., Bottiglieri, T., Kimoto, M., Murry, D. J., Cooke, J. P., Faraci, F. M., and Lentz, S. R. (2008) Tissue-specific downregulation of dimethylarginine dimethylaminohydrolase in hyperhomocysteinemia. *Am. J. Physiol. Heart Circ. Physiol.* **295**, H816–25

33. Chan, Y., Fish, J. E., D'Abreo, C., Lin, S., Robb, G. B., Teichert, A.-M., Karantzoulis-Fegaras, F., Keightley, A., Steer, B. M., and Marsden, P. A. (2004) The cell-specific expression of endothelial nitric-oxide synthase: a role for DNA methylation. *J. Biol. Chem.* **279**, 35087–100

34. Yamagata, K., Daitoku, H., Takahashi, Y., Namiki, K., Hisatake, K., Kako, K., Mukai, H., Kasuya, Y., and Fukamizu, A. (2008) Arginine methylation of FOXO transcription factors inhibits their phosphorylation by Akt. *Mol. Cell*. **32**, 221–31

35. Esse, R., Rocha, M. S., Barroso, M., Gonçalves Jr, I., Leandro, P., Teerlink, T., Jakobs, C., Blom, H. J., Castro, R., and Tavares de Almeida, I. (2010) S-Adenosyl homocysteine accumulation decreases global protein arginine methylation status in cultured human endothelial cells. *J. Inherit. Metab. Dis.* **33 Suppl 1**, S35

36. Fish, J. E., and Marsden, P. A. (2006) Endothelial nitric oxide synthase: insight into cell-specific gene regulation in the vascular endothelium. *Cell. Mol. Life Sci.* **63**, 144–62

37. Mookerjee, R. P., Wiesenthal, A., Icking, A., Hodges, S. J., Davies, N. A., Schilling, K., Sen, S., Williams, R., Novelli, M., Müller-Esterl, W., and Jalan, R. (2007) Increased gene and protein expression of the novel eNOS regulatory protein NOSTRIN and a variant in alcoholic hepatitis. *Gastroenterology*. **132**, 2533–41

38. Grijalva, J., Hicks, S., Zhao, X., Medikayala, S., Kaminski, P. M., Wolin, M. S., and Edwards, J. G. (2008) Exercise training enhanced myocardial endothelial nitric oxide synthase (eNOS) function in diabetic Goto-Kakizaki (GK) rats. *Cardiovasc. Diabetol.* **7**, 34

CHAPTER

4

CHAPTER

4.1

Inhibition of Cellular Methyltransferases Promotes Endothelial Cell Activation by Suppressing Glutathione Peroxidase-1 Expression

J. Biol. Chem. ***289****, 15350–62 (2014)*

Inhibition of Cellular Methyltransferases Promotes Endothelial Cell Activation by Suppressing Glutathione Peroxidase-1 Expression

Madalena Barroso[a,c], Cristina Florindo[c], Hermann Kalwa[a], Zélia Silva[d], Anton A. Turanov[b], Bradley A. Carlson[e], Isabel Tavares de Almeida[c], Henk J. Blom[f], Vadim N. Gladyshev[b], Dolph L. Hatfield[e], Thomas Michel[a], Rita Castro[c], Joseph Loscalzo[a], and Diane E. Handy[a]

[a] *From the Cardiovascular and* [b] *Genetics Divisions, Department of Medicine, Brigham and Women's Hospital and Harvard Medical School, Boston, MA, 02115 USA;*
[c] *Research Institute for Medicines and Pharmaceutical Sciences (iMed.ULisboa), Faculty of Pharmacy, University of Lisbon, Lisbon, Portugal;*
[d] *Departamento de Imunologia, Faculdade de Ciências Médicas, Universidade Nova de Lisboa, Lisboa, Portugal;*
[e] *Molecular Biology of Selenium Section, Mouse Cancer Genetics Program, National Cancer Institute, National Institutes of Health, Bethesda, MD, USA;*
[f] *Department of General Pediatrics, Center for Pediatrics and Adolescent Medicine University Hospital, Freiburg, Germany.*

ABSTRACT

S-Adenosylhomocysteine (SAH) is a negative regulator of most methyltransferases and the precursor for the cardiovascular risk factor homocysteine. We have previously identified a link between the homocysteine-induced suppression of the selenoprotein glutathione peroxidase-1 (GPx-1) and endothelial dysfunction. Here, we demonstrate a specific mechanism by which hypomethylation, promoted by the accumulation of the homocysteine precursor SAH, suppresses GPx-1 expression and leads to inflammatory activation of endothelial cells. The expression of GPx-1 and a subset of other selenoproteins is dependent on the methylation of the $tRNA^{Sec}$ to the Um34 form; the formation of methylated $tRNA^{Sec}$ facilitates translational incorporation of selenocysteine at a UGA codon. Our findings demonstrate that SAH accumulation in endothelial cells suppresses the expression of GPx-1 to promote oxidative stress. Hypomethylation stress, caused by SAH accumulation, inhibits the formation of the methylated isoform of the $tRNA^{Sec}$ and reduces GPx-1 expression. In contrast, under these conditions, the expression and activity of thioredoxin reductase-1, another selenoprotein, is increased. Furthermore, SAH-induced oxidative stress creates a pro-inflammatory activation of endothelial cells characterized by up-regulation of adhesion molecules and an augmented capacity to bind leukocytes. Taken together, these data suggest that SAH accumulation in endothelial cells can induce $tRNA^{Sec}$ hypomethylation which alters the expression of selenoproteins, such as GPx-1, to contribute to a pro-atherogenic endothelial phenotype.

Key Words: **tRNA methylation, S-adenosylhomocysteine, selenoprotein, oxidative stress, cell adhesion, endothelial cell, glutathione peroxidase.**

1. INTRODUCTION

S-Adenosylhomocysteine (SAH) is an intermediate of homocysteine metabolism, which in excess is a feedback inhibitor of most cellular methylation processes. Methyltransferases use S-adenosylmethionine (SAM) to methylate a wide range of substrates, such as DNA, RNA, proteins and other biomolecules, and SAH is generated by every SAM-dependent methylation reaction (1,2). During hyperhomocysteinemia, which is an independent risk factor for cardiovascular disease, homocysteine's precursor SAH accumulates as well, since the reaction catalyzed by SAH hydrolase (SAHH) thermodynamically favors SAH synthesis over its hydrolysis to homocysteine. DNA hypomethylation has been correlated with increased levels of SAH in mice and humans with hyperhomocysteinemia (3,4). More recently, we have shown that increased levels of SAH also lead to protein arginine hypomethylation in rodents (5,6).

We have previously reported that homocysteine can induce oxidative stress through glutathione peroxidase-1 (GPx-1) down-regulation by decreasing its translation; however, the underlying mechanism remains unknown (7). GPx-1 is a major antioxidant protein that uses GSH as a cofactor to reduce hydrogen peroxide (H_2O_2) to water and other hydroperoxides to their corresponding alcohols (8). Antioxidant agents, such as GPx-1, are crucial for maintaining endothelial homeostasis. In fact, antioxidant deficiency may lead to intracellular accumulation of reactive oxygen species (ROS) creating oxidative stress (8,9). Oxidative stress is a major contributor to atherosclerosis and vascular dysfunction. An increase in ROS leads to LDL oxidation, decreases nitric oxide (NO) bioavailability, and induces the activation of transcription factors such as nuclear factor κB (NFκB) to promote the expression of adhesion molecules, such as intercellular adhesion molecule-1 (ICAM-1) and vascular cell adhesion molecule-1 (VCAM-1) (10-12). The binding and transmigration of leukocytes from the lumen of vessels into the vessel wall is mediated by the presence of these adhesion molecules at the endothelial cell surface (10,13). Work by us and others has shown that GPx-1 deficiency can induce the expression of these key adhesion molecules by regulating ROS flux, thus, promoting atherogenesis (14-17). Furthermore, decreased activity of GPx-1 was shown to be independently associated with an increased risk of cardiovascular events in human subjects (17).

GPx-1 and its several paralogs (GPx-2, GPx-3, GPx-4 and GPx-6) are part of the human selenoproteome, which comprises proteins that carry selenium incorporated in their polypeptide chain in the form of the amino acid, selenocysteine (Sec) (18). Selenoprotein expression relies on the ability of a Sec-carrying tRNA ($tRNA^{[Ser]Sec}$) to recognize UGA, not as a stop codon, but as the site of incorporation of Sec during translation. For this, additional cofactors are necessary (19). The selenoprotein-encoding transcripts contain a stem-loop structure (Sec insertion sequence) within their 3'-UTR which, together with translational cofactors, contribute to Sec incorporation (18,19). Sec is synthesized on $tRNA^{[Ser]Sec}$, which is first aminoacylated with Ser, and then enzymatically converted to

Sec (20). The mammalian $tRNA^{[Ser]Sec}$ population consists of two major isoforms that differ by a single methyl group on the ribosyl moiety at position 34, 2'-*O*-methylribose (21). The highly modified base at position 34 is 5-methoxycarbonylmethyluridine (mcm^5U), and thus, the two isoforms are designated: mcm^5U and 5-methoxycarbonylmethyluridine-2'-*O*-methylribose (mcm^5Um) (21). Loss of the isopentenyladenosine (iA6) at position 37 (e.g., by site substitution of A37 with G) prevents 2'-*O*-methylribose (Um34) formation at position 34 (22). The A37>G37 mutation or selenium-deficiency conditions reduce Um34 formation and decrease the expression of a subset of selenoproteins, designated stress-related selenoproteins, such as GPx-1 and selenoprotein W. On the other hand, these changes have less effect on the expression of another subset of selenoproteins, designated housekeeping selenoproteins, such as the thioredoxin reductases, TrxR1 and TrxR2 (21,23).

In the current study, we analyzed the link between SAH-induced hypomethylation and the expression of selenoproteins. We determined that SAH accumulation suppresses GPx-1 expression, in part, by altering the methylation of $tRNA^{[Ser]Sec}$. Additionally, hypomethylation of the $tRNA^{[Ser]Sec}$ altered the expression of other selenoproteins, as shown by [^{75}Se]- incorporation. Furthermore, the SAH-induced hypomethylation environment caused an increase in ROS levels and a subsequent up-regulation of adhesion molecules. These findings illustrate the functional consequences of hypomethylation on selenoprotein synthesis and cellular homeostasis, and their clear implications for vascular pathology.

2. MATERIALS AND METHODS

Cell Culture, Treatments and siRNA Transfection – Human umbilical vein endothelial cells (HUVEC) were cultured in EBM-2 media (Lonza) supplemented with EGM-2 additives (Lonza) without antibiotics at 37ºC in 5% CO_2. These culture conditions included 2% FBS, which added 7.5 nM Se, to the basal level of 30 nM Se (in the form of selenious acid) in the basal media. Selenium was added in the form of sodium selenite in some experiments, as noted in the figure legend. Experiments were performed between passage five and eight with cells 70-80% confluent. Cells were treated with 5-20 μM adenosine-2′,3′-dialdehyde (ADA) (Sigma) for 12-48 h. Eight mM N-acetylcysteine (NAC) was used as an antioxidant in some experiments, as designated in the figure legend.

Transfections with small interference RNA (siRNA) were performed using Lipofectamine® 2000 (Life Technologies) and 60 nM of stealth siRNA (Life Technologies) to SAHH mRNA (5'-ACGCCGUGGAGAAGGUGAACAUCAA-3') or GPx-1 mRNA (5'-GGUUCGAGCCCAACUUCAUGCUCUU-3'). All transfections were performed in parallel with scrambled control siRNAs, (5'-UUGGGAUUGUCCACUCUUCACCCGU-3'), for the SAHH control, or (5'- GGUAGCGCCAAUCCUUACGUCUCUU-3') for the GPx-1 control.

SAM/SAH Analysis and SAHH Activity – In order to measure SAH and SAM intracellular metabolites, cell lysates were promptly deproteinized with an equal volume of 10 % perchloric acid and then quantified using tandem mass spectrometry, as described (24).

SAHH activity was measured in the hydrolytic direction using an assay based on the reduction of MTT (3-(4,5-dimethylthiazol-2-yl)-2,5-diphenyltetrazolium bromide) to formazan according to published methods (25,26). The assay was performed on cell lysates, comparing equivalent amounts of protein for each condition. Lysates were pre-incubated with MTT for 5 m prior to adding SAH to monitor SAHH specific reduction of MTT.

Real-time PCR – Total RNA was isolated using RNeasy Mini kit (Qiagen) and 0.5 µg of each sample was reverse transcribed using Advantage RT-for-PCR kit (Clontech). Relative mRNA quantification was performed by TaqMan Assays, using the PRISM 7900 HT Sequence Detector (Applied Biosystems). The $\Delta\Delta$Ct method of relative quantification was used to compare gene expression, using β-actin as an endogenous control. Real time PCR reactions used the TaqMan Universal PCR Master Mix (Life Technologies) and the following specific gene expression primers: 4352935E, β-actin; Hs00829989_gH, GPx-1; Hs00164932_m1, ICAM-1; Hs04183463_g1, SAHH; and Hs00365485_m1, VCAM-1 (Life Technologies).

Western Blotting – Antibodies to β-actin (Sigma-Aldrich), GPx-1 (Abcam), SAHH (RD Systems), ICAM-1, VCAM-1 (Santa Cruz), or the antibodies previously described for TrxR1 or TrxR2 (27) were used as primary antibodies for Western blotting. After 2 h of incubation with a secondary antibody linked to HRP, membranes were visualized using the ECL detection system (Amersham Biosciences).

GPx Activity Assay – An indirect assay, based on absorbance changes after NADPH oxidation, was used to measure GPx-1 activity (27).

TrxR Activity Assay – The assay is based on the direct reduction of DTNB (5,5'-dithio-bis(2-nitrobenzoic acid)) by thioredoxin reductase. To account for nonspecific reduction of DTNB by other cellular enzymes, the change in DTNB reduction over time in the presence of the TxR inhibitor aurothioglucose is subtracted from the activity in the absence of inhibitor to determine TrxR-specific activity (28,29).

GPx-1 Overexpression – GPx-1 was expressed in endothelial cells using an adenoviral vector (AdGPx-1) as described (30). HUVEC were incubated with adenovirus for 24 h, prior to exposure to ADA or control media. An adenovirus expressing β-galactosidase (Ad-βGal) was used as a control.

ROS Measurements – ROS were assessed by two independent methods. First, hydrogen peroxide (H_2O_2) released by endothelial cells was measured by the Amplex Red assay (Molecular Probes), using previously described methods (14). Intracellular H_2O_2 was monitored using the highly specific biosensor HyPer2 expressed in lentivirus (31-33). HUVECs were infected with virus particles (10^6 pfu/mL) in the presence of polybrene (4mM). Upon treatment, live cells were monitored, in parallel with control samples, for 13 h using a microscope stage incubator (Tokai) and an Olympus IX81 inverted microscope with a DSU spinning disk confocal system and a Hamamatsu Orca ER cooled CCD camera. Image acquisition was performed using a 40× oil immersion objective lens (Olympus), every 5 min. The HyPer2 fluorescence ratio was calculated as described (32,33). For imaging of fixed cells, lentivirus-infected HUVEC were treated for 24 h, then washed and fixed with 4% paraformaldehyde in PBS for 20 min. Fixed cells were mounted using DAPI-containing mounting media or DAPI-free mounting media (SouthernBiotech) and imaged. Methamorph imaging software (Universal Imaging) was used for analysis.

Flow Cytometry and Static Adhesion Assay – ICAM-1 surface expression was analyzed after cell staining with FITC-conjugated anti-ICAM-1 antibody (Santa Cruz Biotechnology). Briefly, cells were trypsinized, washed with PBS, then incubated with antibody for 30 min, washed with PBS containing 0.1% NaN_3, and analyzed using GUAVA EasyCyte 5HT FACS and InCyte software (Millipore).

An adhesion assay using human leukocytes was performed under static conditions. Leukocytes (WBC) were isolated from blood samples of healthy individuals using a RBC lysis solution (Citogene). The ethics committee at the Faculty of Pharmacy, University of Lisbon approved the study and a written informed consent was obtained from all participants. After three washes with PBS, WBCs were resuspended at 6×10^6 cells/mL in PBS with Ca^{2+} and Mg^{2+} with 0.1% human serum and added to the confluent HUVEC monolayer. The cell mixture was incubated for 20 min at 37ºC, 5% CO_2, after which cells were thoroughly washed with PBS without Ca^{2+} and Mg^{2+}, trypsinized, and assessed for cell specific markers by flow cytometry. An antibody mixture of PE anti-human CD31 antibody (BioLegend) and PerCP anti-human CD45 antibody (BioLegend) was used to distinguish endothelial and leukocyte cell populations, respectively.

[^{75}Se] Labeling – HUVEC were labeled with 10 µCi/mL of [^{75}Se]-selenious acid (1000 Ci/mmol, Research Reactor Facility, University of Missouri, Columbia, MO) for 24 h in cell culture media supplemented with or without ADA (20 µM). Cells were then washed, lysed, and protein extracts separated on 10 % Bis-Tris gels (NuPage, Novex, Invitrogen). Proteins were then transferred to a PVDF membrane (Invitrogen), exposed to Storage Phosphor Screen (GE) for 24 h, and analyzed with PhosphorImager (GE) (34). Finally, membranes were used for immunoblotting: anti-β-actin antibody was used to confirm equal protein loading of the samples.

Sec-tRNA Analysis – One gram of HUVEC cells was used for total RNA isolation and aminoacylation with [^{3}H]-serine and 19 unlabelled amino acids as described (35,36). The aminoacylated seryl-tRNA was fractionated on a RPC-5 column, first in the absence of Mg^{2+} and subsequently, in the presence of Mg^{2+}. Using this sequential chromatography approach, it is possible to quantify the relative $tRNA^{[Ser]Sec}$ to the total $tRNA^{Ser}$, and separate the two major isoforms of $tRNA^{[Ser]Sec}$, mcm^5U and mcm^5Um (35,36).

Statistical Analysis – Means are provided ± standard deviations. Statistical analysis was performed on experiments repeated in 3-5 independent assays. The statistical significance of differences among means ($p<0.05$) in experiments with more than two conditions was determined by ANOVA, followed by pairwise *post-hoc* comparisons with the Student-Newman-Keuls test. Alternatively, the Student's t-test was used for comparison, in experiments with only two groups.

3. RESULTS

SAH accumulation in endothelial cells – SAH is a metabolite of methionine metabolism and an endogenous inhibitor of SAM-dependent methyltransferases. SAH accumulation was induced by two different approaches: direct inhibition of SAHH by ADA or targeted knockdown of SAHH using siRNA. ADA, an adenosine analog, is a strong inhibitor of SAHH activity that has been used previously by us and others (2,37). Following HUVEC incubation with 20 µM ADA for 24 h, SAHH activity was reduced by 99.5 ± 0.8% ($p<0.0001$) (Fig. 1). This treatment significantly decreased SAHH mRNA by 27.1 ± 2.9 % ($p<0.0001$) and 45.3 ± 2.9 % ($p<0.0001$) after 24 h and 48 h, respectively, with no statistically significant change in protein expression over this time course. Using a specific siRNA against SAHH, enzymatic activity was suppressed by 66.5 ± 3.7% ($p<0.0001$) 48 h after transfection with corresponding decreases of 88.5 ± 6.5% ($p<0.001$) and 48.3 ± 15.8% ($p<0.01$) at the mRNA and protein level, respectively. The SAM/SAH ratio, commonly used as an indicator of cell methylation status, was decreased by 6.1 ± 0.2-fold ($p<0.001$) after 24 h incubation with 20 µM of ADA, and 1.3 ± 0.2-fold ($p<0.005$) after 72 h of siSAHH transfection.

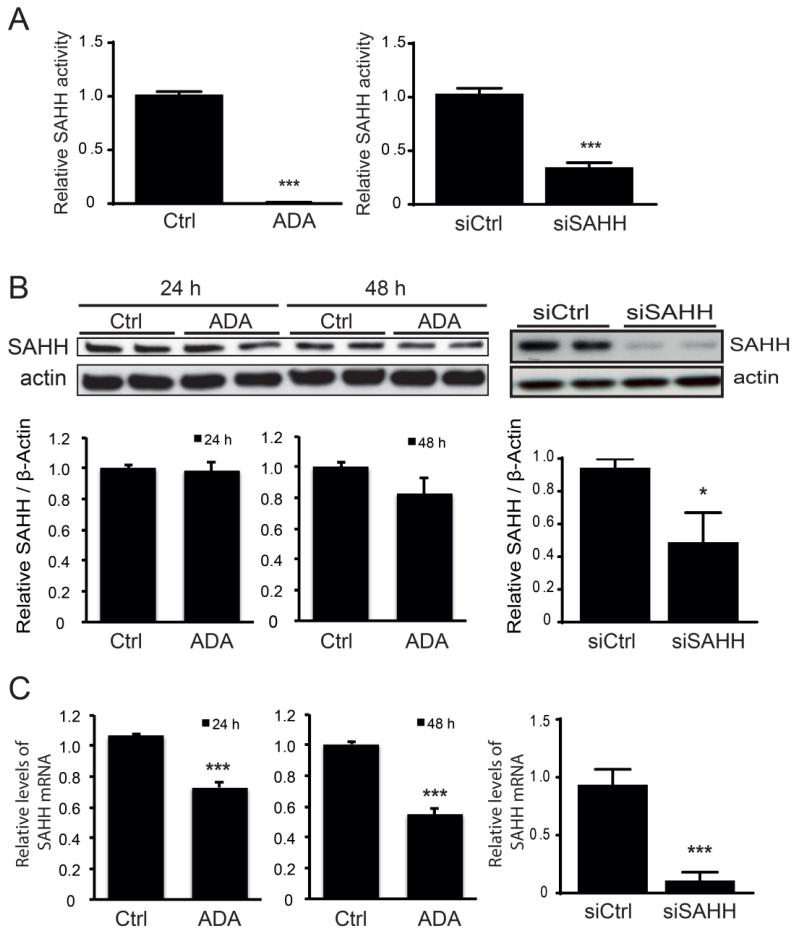

Figure 1 - **Inhibition of cellular SAHH activity**. **(A)**. Adenosine dialdehyde (ADA) or siSAHH was used to decrease SAHH activity. Means are significantly different by t-test. (***p<0.0001 *versus* control, n=3-4). **(B)**. The effects of ADA or siSAHH on SAHH protein expression was examined by Western blotting. Summary densitometry measurements, corrected for β-actin (actin) intensity, are shown below the immunoblots (n=3-4). **(C)**. The effects of ADA or siSAHH on SAHH mRNA were measured by qRT-PCR using actin as an endogenous control. (**p<0.001, ***p<0.0001 *versus* control, n=3-4).

GPx-1 activity under SAH accumulation – Homocysteine levels and GPx-1 activity are strong biomarkers for cardiovascular risk, with clinical studies suggesting that those with the lowest GPx-1 activity are at the greatest risk (17,38). Our previous studies have shown that excess homocysteine suppresses GPx-1 expression by decreasing Se-dependent translation; however, although these findings linked suppression of GPx-1 to conditions that favored the intracellular formation of SAH, a role for SAH in the translational regulation of GPx-1 remained unresolved (7,39). To determine whether SAH modulates GPx-1 expression, we treated cells with ADA or siSAHH. Incubation of endothelial cells with increasing concentrations of the SAHH inhibitor, from 5 to 20 µM, resulted in a significant decrease of GPx-1 activity in a dose-dependent manner (Fig. 2A). ADA (20 µM) or the siRNA-mediated knockdown of SAHH significantly reduced GPx-1 protein expression by more than 27% (Fig. 2B). Under these conditions, however, GPx-1 mRNA levels were not significantly altered, which is consistent with the hypothesis that SAH-induced hypomethylation affects GPx-1 expression at a translational level (Fig. 2C).

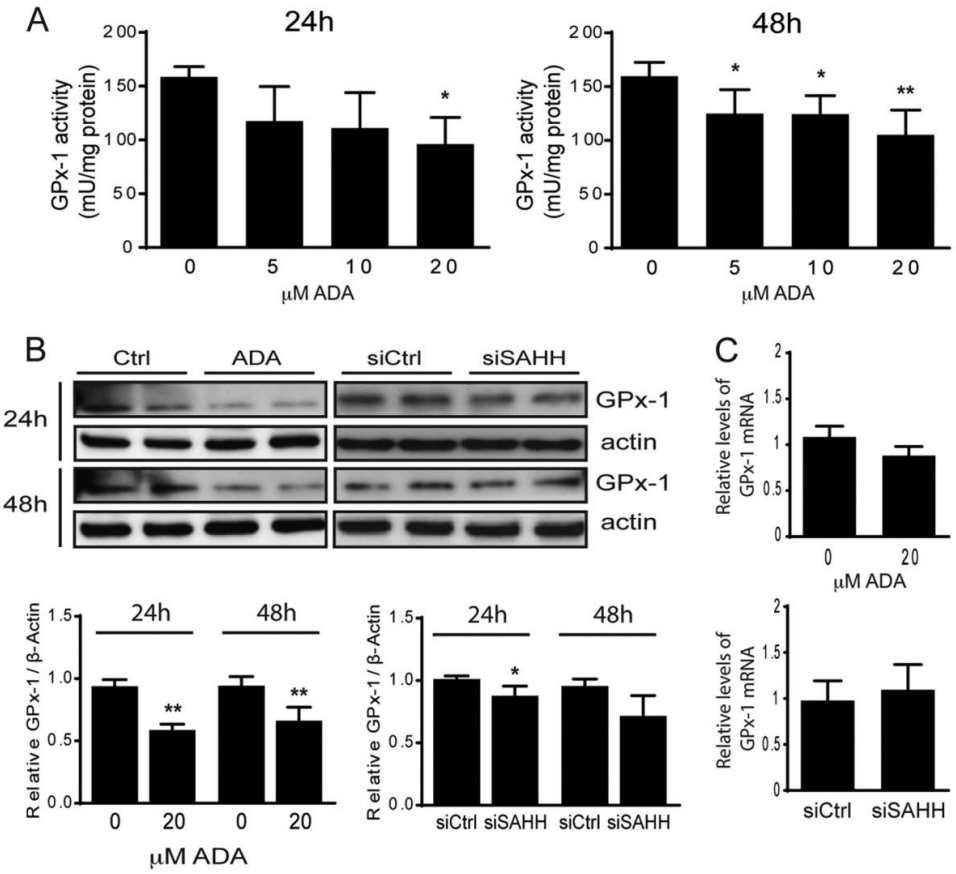

Figure 2 - Effect of SAH accumulation on GPx-1. **(A)**. GPx-1 activity was measured by an indirect coupled enzymatic assay. Means were significantly different by ANOVA, followed by *posthoc* pairwise comparisons (n=4-5, *p<0.05, **p<0.005). **(B)**. The effect of SAHH inhibition on the expression of GPx-1 was examined by Western blotting. A representative blot (top) and summary densitometry measurements, corrected for actin intensity (bottom) are shown, for 24 and 48 h in the presence and absence of ADA or siSAHH (n=3, *p<0.05, **p<0.005). **(C)**. mRNA levels from the same experiments were measured by qRT-PCR using actin as an endogenous control. No significant difference was found between treatment groups.

Hypomethylation induces endothelial oxidative stress – The enzymatic actions of GPx-1 and other antioxidants diminish the damaging effects of ROS, like H_2O_2 (8). Thus, we next assessed whether the ADA-induced suppression of GPx-1 altered cellular H_2O_2 accumulation in endothelial cells. To do so, we measured cellular H_2O_2 levels by two different methods. First, we used the Amplex Red assay to quantitate extracellular H_2O_2 levels. After 24 h of exposure, we found an increase in H_2O_2 released to the media with increasing ADA concentrations (Fig. 3A). Next, we used the biosensor Hyper2 to monitor intracellularly H_2O_2 flux. Hyper2 is a biosensor that uses the regulatory domain of the *E. coli* H_2O_2–sensing protein, OxyR. The HyPer2 probe has a fluorescent protein (circularly permuted yellow fluorescence protein) inserted into the OxyR domain, which allows the detection of fluorescence changes when the domain undergoes oxidation by H_2O_2 (31). ADA induced a 2.5-fold increase in the production of intracellular H_2O_2 (Fig. 3B). These findings suggest that hypomethylation stress promotes an oxidative imbalance in endothelial cells, most likely, due to the suppression of GPx-1.

.

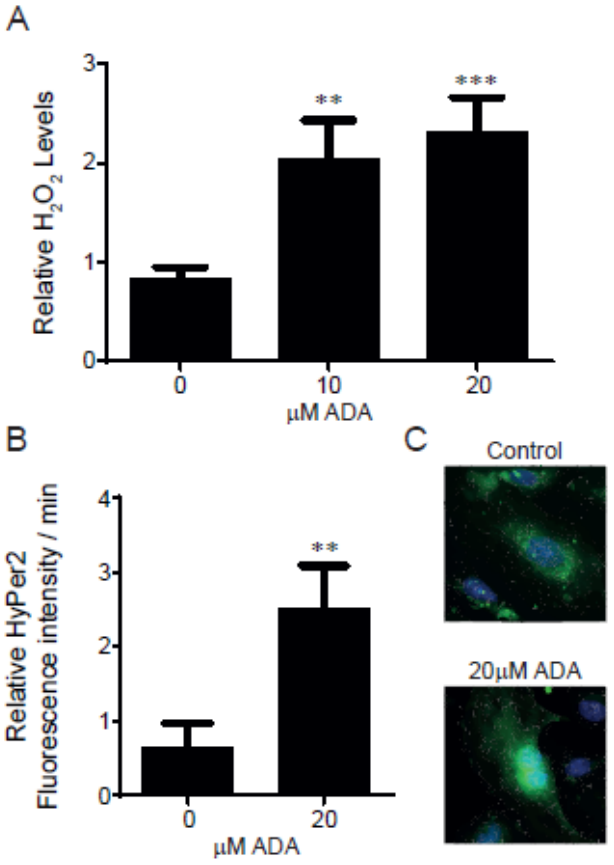

Figure 3 - H_2O_2 levels are increased by SAHH inhibition. **(A)**. After 24 h of ADA exposure H_2O_2 release from cells was measured by Amplex Red. The results represent means from 3 independent experiments that were analyzed by ANOVA, followed by pairwise *post hoc* analysis (**p<0.005, ***p<0.0005 compared to control). **(B)**.Intracellular H_2O_2 production was detected using the HyPer2 fluorescence ratio. The graph shows the means of 3 independent experiments, for which fluorescence ratios were measured for 3-5 cells *per* condition over 13 h (**p<0.005 compared to control). **(C)**. Representative images of HyPer2 transfected cells 24 h following exposure to ADA-containing or control media are shown on the right.

Oxidative stress induced by SAH accumulation promotes endothelial cell activation – Endothelial activation is a consequence of oxidative stress characterized by an increase in the expression of inflammatory cytokines and adhesion molecules, which promote adhesion and trans-endothelial migration of leukocytes (40,41). Thus, to determine whether SAH-induced oxidant stress augmented endothelial cell activation, we measured the expression of the adhesion molecules ICAM-1 and VCAM-1 following SAHH inhibition. Figure 4 shows a positive correlation between a hypomethylation environment and adhesion molecule expression. Both ADA and siSAHH significantly induced ICAM-1 and VCAM-1 expression detectable at the protein (Fig. 4A and 5A) and transcript levels (Fig. 4B).

ICAM-1 and VCAM-1 expression has been associated with ROS levels, both in normal and in pathogenic conditions (10,41,42). Therefore, in order to causally link endothelial activation with SAH-induced oxidative stress, endothelial cells were co-incubated with ADA and various antioxidants. Both ICAM-1 and VCAM-1 were induced by approximately two-fold ($p<0.05$) following ADA or siSAHH exposure (Fig. 4 and 5A). Treatment with the antioxidant N-acetyl-cysteine (NAC) significantly attenuated the ADA-induced up-regulation of these adhesion molecules (Fig. 5A). A similar effect was found with the antioxidants butylated hydroxyanisole (100 µM) and allopurinol (150 µM) (data not shown). Similarly, overexpression of GPx-1 in endothelial cells minimized the effect of ADA exposure on adhesion molecules expression (Fig. 5B).

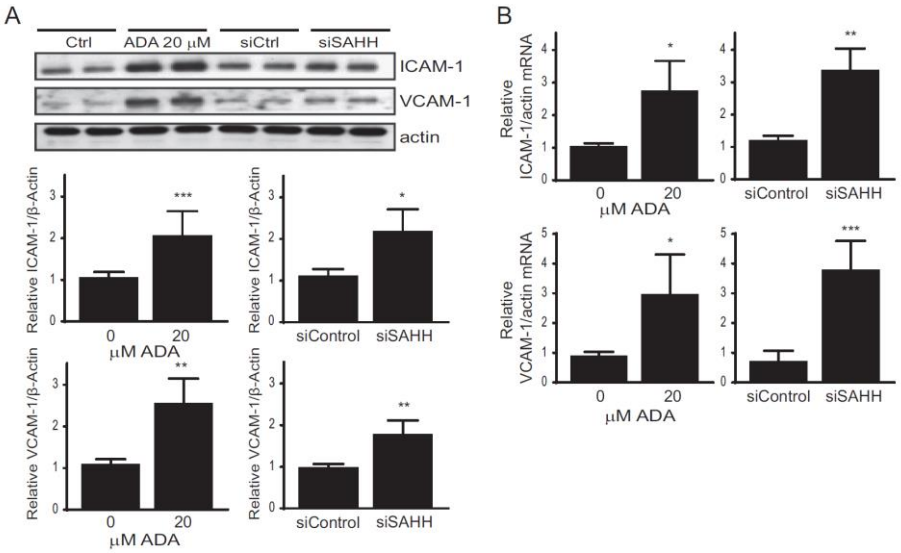

Figure 4 - Adhesion molecules expression is increased by pharmacological or siRNA-mediated suppression of SAHH. (A). The effect of 48 h SAHH inhibition on the expression of ICAM-1 and VCAM-1 was evaluated by Western blotting. On the top, a representative blot is shown; on the bottom relative mean densitometry measurements are given, corrected for actin, for each protein and treatment condition. Mean densitometry measurements were compared by the Student's t-test (n=3-5, *p<0.05, **p<0.005, ***p<0.0005). **(B)**. Gene expression levels from the same experiments were measured by qRT-PCR, using β-actin gene expression as a control (*p<0.05, **p<0.005, ***p<0.0005).

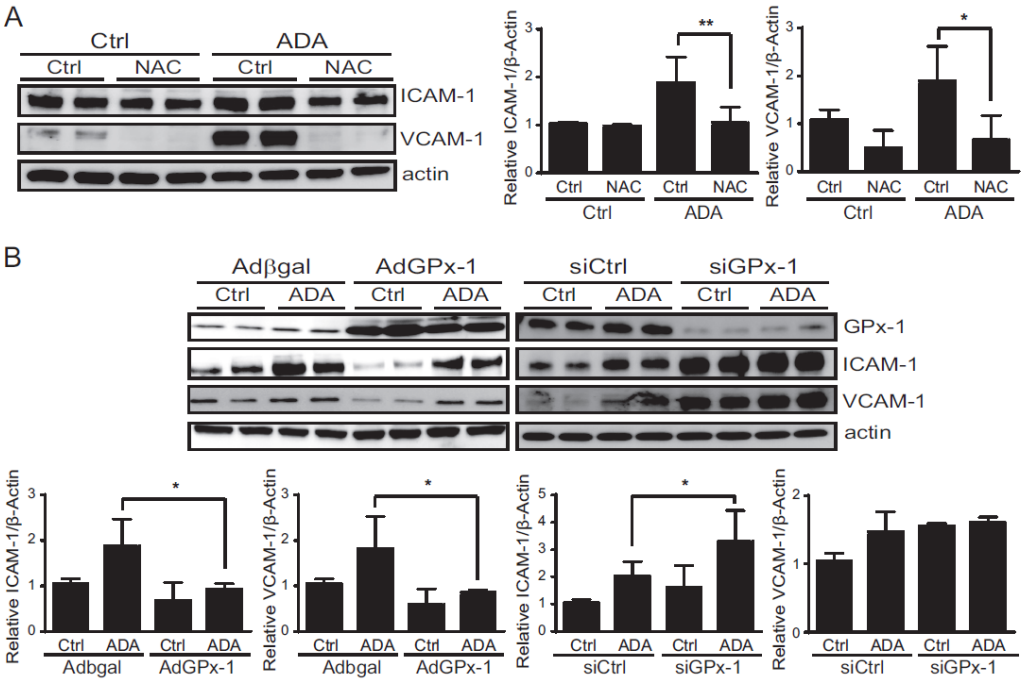

Figure 5 - Oxidative stress contributes to endothelial cell activation following SAHH inhibition. (A). Control cells or cells exposed to ADA were incubated in the presence or absence of the antioxidant NAC (8mM). Western blot analysis was performed to evaluate ICAM-1 and VCAM-1 protein expression. A representative blot is shown (left), as well as mean densitometry measurements, corrected for actin, for each protein and treatment condition (right). Densitometry results were analyzed by ANOVA, followed by pairwise *post hoc* analysis (*p<0.05, **p<0.005; n=3). **(B)**. In the left panel, cells with overexpression of a control gene (β-Gal) or GPx-1 were incubated in the presence or absence of ADA (n=3). Western blotting was used to evaluate ICAM-1 and VCAM-1 expression. In the right panel, ICAM-1 and VCAM-1 expression was evaluated in the presence or absence of ADA and GPx-1 knockdown. Mean densitometry measurements, normalized for actin, were analyzed as in A.

The specific role of GPx-1 in regulating adhesion molecule expression was further assessed by performing a knockdown of this antioxidant protein. As shown in Figure 5B, GPx-1 knockdown potentiated the ADA effect: ADA-induced ICAM-1 expression was increased 47.3% by the combination of siGPx-1 plus ADA compared with ADA alone ($p<0.05$). VCAM-1 expression was also up-regulated by GPx-1 suppression, although the increase in expression was not significantly different between ADA and ADA treatment with GPx-1 knockdown. These findings are consistent with a role for excess ROS, caused by the suppression of GPx-1, in mediating the SAH-induced up-regulation of endothelial adhesion molecules.

Hypomethylation increases endothelium leukocyte-binding capacity – We next sought to determine whether the ADA-induced up-regulation of ICAM-1 and VCAM-1 was sufficient to enhance leukocyte binding. We first confirmed that the induced up-regulation of ICAM-1 expression resulted in a corresponding increase in ICAM-1 at the cell surface where it is capable of leukocyte binding. To do so, we used a fluorescently-tagged antibody to ICAM-1 and evaluated changes in the mean fluorescence intensity (MFI) by flow cytometry. Using this method, cell surface detection of ICAM-1 was significantly up-regulated by 1.6-fold at 48 h and by 2.1-fold at 72 h ($p<0.05$) following ADA exposure (Fig. 6A). Next, to assess the leukocyte binding capacity of these endothelial cells following hypomethylation stress, we performed an adhesion assay. In this assay, we co-incubated endothelial cells (control cells or those previously exposed to ADA) with leukocytes for 20 min in static conditions. After several washes, cells were detached and stained with fluorescent anti-CD31 or anti-CD45 antibody in order to quantitate the number of endothelial cells (CD31+) and leukocytes (CD45+) by flow cytometry and to evaluate the number of leukocytes that remained attached to endothelial cells during the procedure. Pre-exposure to ADA increased the number of leukocytes attached to the endothelial monolayer by 33.0% at 48 h ($p<0.05$) and 40.8% ($p<0.05$) at 72 h (Fig. 6B). These findings are consistent with the increase of cell surface-detectable ICAM-1. The mean fluorescence intensity of the endothelial marker CD31 (platelet endothelial cell adhesion molecule-1 or PECAM-1), used to distinguish endothelial cells during the assay, was increased by 33.3% after 72 h of ADA treatment ($p<0.0001$), suggesting that it may also be up-regulated under hypomethylating stress.

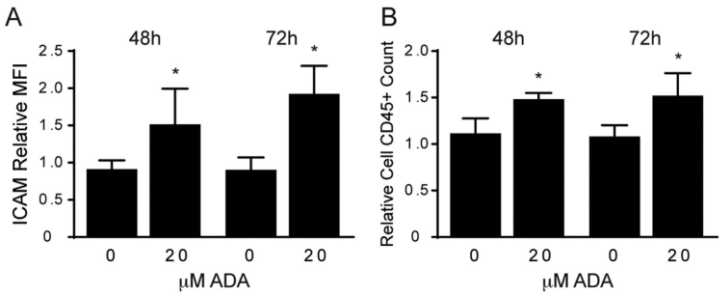

Figure 6 - Cell surface adhesion of leukocytes is enhanced by ADA exposure. (A). Flow cytometry was used to detect cell surface expression of ICAM-1 tagged with a fluorescent antibody following exposure to ADA for 48 h and 72 h (n=3). Means were compared at each time point between ADA treatment and no treatment by Student's t-test (* $p<0.05$). **(B)**. Following a static adhesion assay, leukocytes that remained attached to the endothelial monolayer were labeled with a fluorescent-conjugated antibody (CD45) and counted by FACS. Results are shown as means from 3 independent assays, normalized to the control and analyzed as in A (*$p<0.05$).

GPx-1 expression deregulation by Sec-tRNA hypomethylation – During Sec incorporation, Sec-tRNA$^{[Ser]Sec}$ recognizes the stop codon, UGA, as a site for Sec insertion (8,19,43). As noted in the Introduction, mammalian tRNA$^{[Ser]Sec}$ is present in two main isoforms that differ by a methyl group in the wobble uridine (U34) of the anticodon (Fig. 7A) (21). The mcm^{5}Um isoform of tRNA$^{[Ser]Sec}$ has been shown to be required for the expression of stress-related selenoproteins that include GPx-1 (21,23). To determine whether excess SAH altered the methylation state of the tRNA$^{[Ser]Sec}$, we treated cells with ADA and measured the levels of both isoforms, mcm^{5}U and mcm^{5}Um, following the specific labeling and chromatographic separation of [^{3}H]-Ser-tRNA$^{[Ser]Sec}$. Figure 7B shows the chromatographic separation of the tRNA$^{[Ser]Sec}$ isoforms from control cells or cells under SAHH inhibition. Preparations from control cells (Fig. 7B – left) show two different peaks that represent the presence of the mcm^{5}U form (earlier-eluting peak) and the mcm^{5}Um form (later-eluting peak). Following ADA exposure, the tRNA$^{[Ser]Sec}$ mcm^{5}Um isoform is practically undetectable, suggesting that ADA-treatment blocks the formation of the critical isoform of tRNA$^{[Ser]Sec}$ necessary for optimal Sec incorporation in GPx-1 and other selenoproteins. Interestingly, total tRNA$^{[Ser]Sec}$ levels were increased 1.7-fold with ADA exposure.

We next used [^{75}Se]-labeling, followed by gel electrophoresis, to study the expression of key proteins in the selenoproteome (Fig. 7C). Overall, there are more than 25 selenoproteins that are encoded in 25 genes in humans (18,44). To confirm the absence of changes in protein synthesis or other gel loading issues, β-actin immunoblotting was performed following radioautography of [^{75}Se]-labeled proteins. There were no differences detected in β-actin between control and treated samples. In contrast, examination of the [^{75}Se]-labeled proteins indicates alterations in selenoprotein expression in control cells compared with those in which SAH accumulation was induced. The molecular mass of selenoproteins, such as GPx-1, GPx-4, thioredoxin reductase (TrxR) 1, Sep15 and MsrB1, have been previously characterized in mammalian cells and tissues (23) and these can be identified by their relative migration in the gel imaged in Figure 7C. Consistent with the results of Western blotting and activity assays, ADA and siSAHH decreased the [^{75}Se]-labeling of GPx-1. The selenoproteins, GPx-4, Sep15 and/or MsrB1, were also suppressed by these treatments. Interestingly, the TrxR enzymes (TrxR1 and, to a lesser extent, TrxR2) showed increased expression. Western blot analysis was used to confirm the up-regulation of these TrxRs (Fig. 7D), illustrating the significant ($p<0.05$) up-regulation of TrxR1 by 36.8% and TrxR2 by 23.1% following ADA treatment. TrxR1 but not TrxR2 mRNA was also significantly up-regulated (Fig. 7E) and cellular TrxR activity was also significantly increased by ADA exposure ($p<0.05$) (Fig. 8A). These findings are consistent with previous studies, which suggest that the expression of the TrxRs is less reliant on methylated tRNA$^{[Ser]Sec}$ than other selenoproteins, including GPx-1 (21,23,43).

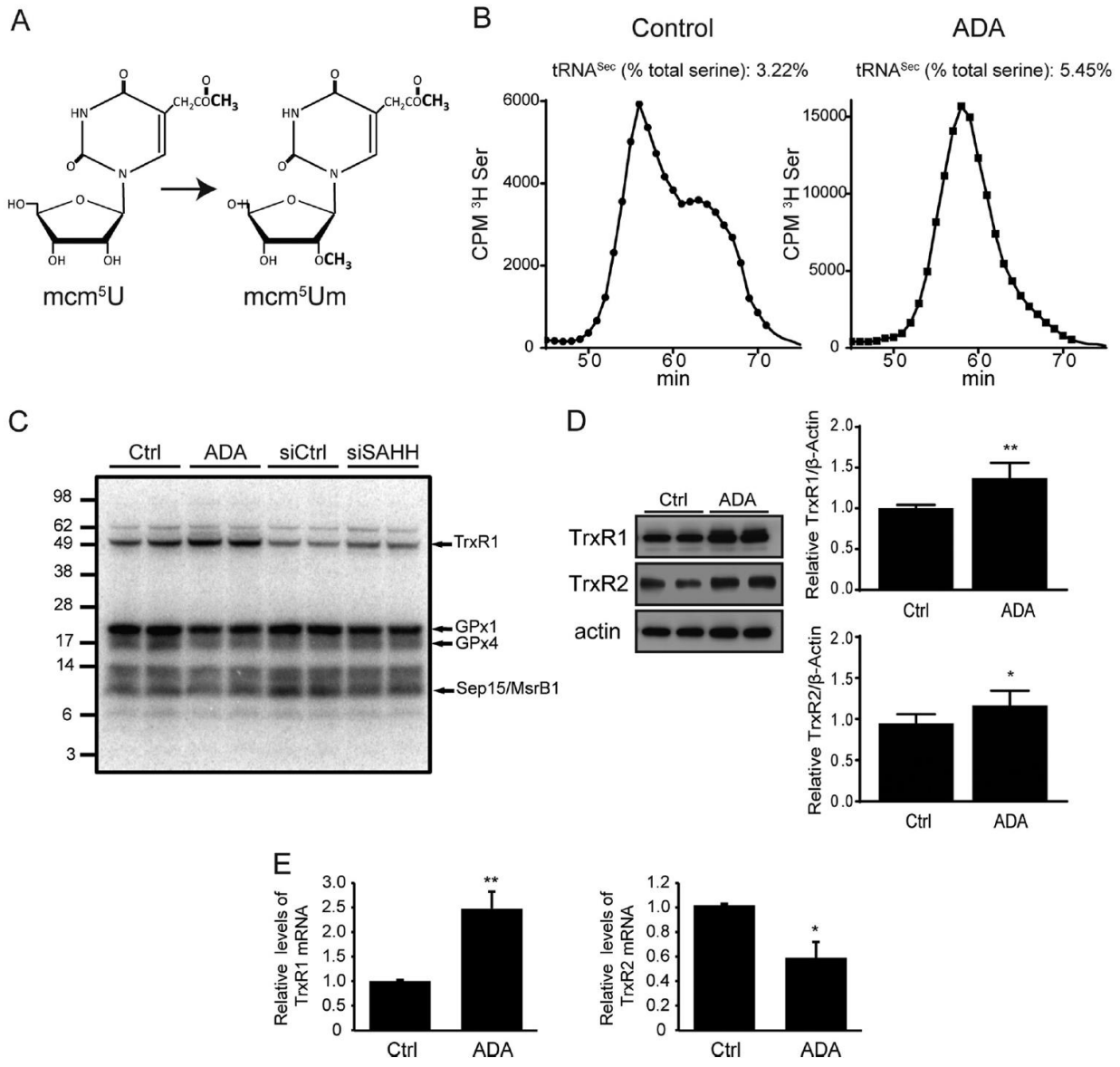

Figure 7 - tRNA$^{[Ser]Sec}$ hypomethylation and its effect on selenoproteome expression. (A). Structures of the mcm^{5}U and mcm^{5}Um isoforms of the wobble uridine (Um34). **(B)**. Following aminoacylation with [^{3}H]-serine, tRNA$^{[Ser]Sec}$ isoforms were separated by reverse phase chromatography. A normal profile is shown on the left chromatogram (control cells), where mcm^{5}U elutes earlier than the mcm^{5}Um isoform. On the right chromatogram, cells exposed to ADA are lacking the peak corresponding to the later-eluting mcm^{5}Um isoform. Note the differences in the Y-axis scale. **(C)**. Duplicates of control cells or cells exposed to ADA or siRNA treatment were labeled for 24 h with ^{75}Se. Proteins were extracted, separated by gel electrophoresis, and labeled selenoproteins were detected using a PhosphoImager. The protein marker sizes (in KDa) and select selenoprotein bands are indicated on the left and right sides of the image, respectively. **(D)**. Protein extracts were prepared from total cell lysates treated and untreated with ADA, and Western blots were used to detect TrxR1 and TrxR2. A representative blot is shown; on the right relative mean densitometry measurements are shown, corrected for actin, for each protein and treatment condition. Mean densitometry measurements were compared by the Student's t-test (n=3, *p<0.05, **p<0.005). **(E)**. TrxR1 and TrxR2 mRNA levels were measured in treated and untreated control samples by qRT-PCR using actin as endogenous control.

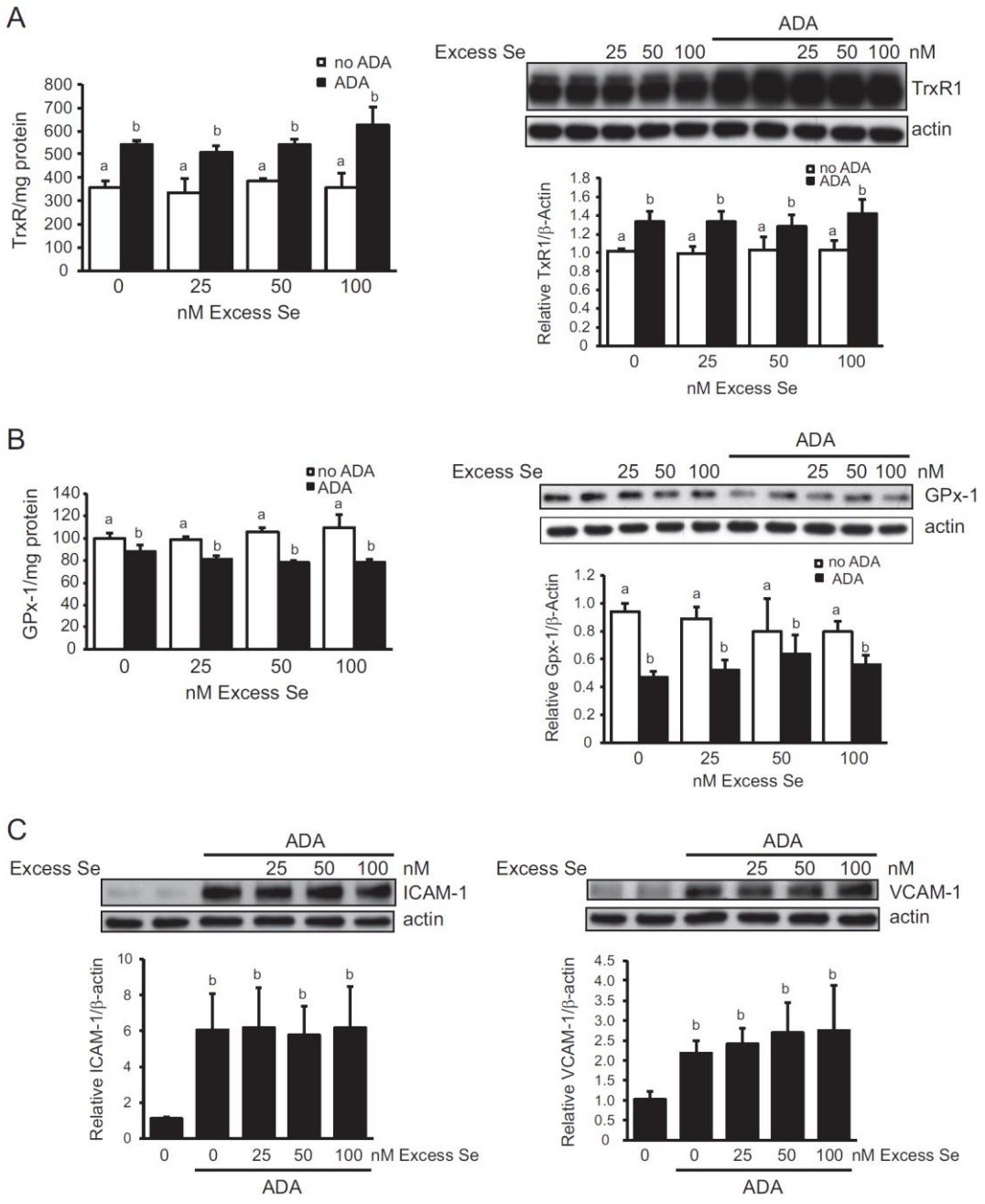

Figure 8 - The effects of excess selenium on TrxR1 and GPx-1 expression. Selenium in the form of sodium selenite was added to media that contained 37 nM selenium for 48 h prior to exposure to ADA for an additional 48h in the presence and absence of Se. **(A)**. Effect of excess selenium on TrxR enzyme activity and TrxR1 protein expression. Excess Se had no effect on TrxR1 activity (n=3) or expression (n=4) in the absence of ADA. In the presence of ADA, the TrxR1 up-regulation of TrxR1 was not altered by excess Se. **(B)**. Effect of excess selenium on GPx-1 activity (n=4) and GPx-1 protein expression (n=4) in the presence and absence of ADA. Selenium did not significantly alter GPx-1 in the absence of ADA. In the presence of ADA, the suppression of GPx-1 was not decreased by excess Se. **(C)**. Effect of excess selenium on ICAM-1 and VCAM-1 protein. Excess Se did not lessen ADA-induced up-regulation of the ICAM-1 or VCAM-1. For each graph, values that are not significantly different from no treatment or ADA are labeled a or b, respectively.

Se supplementation and hypomethylation – To determine whether excess selenium would mitigate the effects of ADA on GPx-1 and TrxR expression, we added additional Se to the culture media, which has 37.5 nM Se. Addition of up to 100 nM Se for 4 d did not increase GPx-1 or TrxR1 in the absence of ADA (Fig. 8 A & B). Similarly, in the presence of ADA, exposure to additional Se did not significantly alter the effects of ADA alone on GPx-1 or TrxR activity and expression, although at 50 nM Se plus ADA there was a (non-significant) increase in GPx-1 protein. We next determined whether additional Se altered ADA-induced adhesion molecule up-regulation (Fig. 8C). Western blot analysis shows that the ADA-induced up-regulation of ICAM-1 and VCAM-1 is unchanged by excess Se.

4. DISCUSSION

Methylation is essential for critical cell processes, including gene expression and protein function (45,46). SAH, which is one of the most potent *in vivo* modulators of SAM-dependent methylation reactions, is an important regulator of cellular homeostasis. The SAM-to-SAH ratio is thought to regulate intracellular methylation reactions, with many methyltranferases showing diminished activity when this ratio decreases (4,45). Altered methylation patterns have been related to cellular dysfunction and disease, including cancer and cardiovascular disease (45,47,48). RNA methylation can regulate the structure and function of various RNA species. tRNA is the most heavily modified RNA species and modifications to nucleotides in the anticodon loop, especially at the Wobble position (position 34), play an essential role in efficient mRNA decoding at the ribosome (49).

SAH, which accumulates in the setting of hyperhomocysteinemia, has gained attention as an intracellular metabolite that may be responsible for the deleterious actions on the vasculature previously attributed to excess homocysteine (46). Our studies are focused on the effects of SAH as a hypomethylating agent that alters endothelial function. In particular, our results indicate that excess SAH decreases methylation of $tRNA^{[Ser]Sec}$ to alter the expression of the selenoproteins GPx-1 and TrxR. We show that the resulting decrease in the expression of the antioxidant selenoprotein GPx-1 leads to an increase in cellular H_2O_2 and a subsequent up-regulation of endothelial adhesion molecules expression. Furthermore, the increase in adhesion molecules is sufficient to have a functional effect on cellular adhesion, augmenting the binding of leukocytes. Recent studies have reported possible links between methylation impairment and vascular dysfunction (2,50,51); here, we demonstrate a specific mechanism by which hypomethylation stress can lead to inflammatory activation of endothelial cells.

In our studies, we used two methodological approaches to promote SAH accumulation by targeting SAHH. First, we used the specific SAHH inhibitor, ADA, which is known to cause SAH-induced hypomethylation stress (1,2). Additionally, we used a targeted siRNA-mediated knockdown of SAHH. Two additional genes that encode the SAHH-like proteins -1 and -2 have also

been identified in mammalian systems (52,53), although a clear functional role for these proteins has yet to be made. Nonetheless, in our targeted siRNA knockdown studies, we confirmed that siSAHH did not affect the levels of SAHH-like-1 and SAHH-like-2 mRNA. Overall, the effects of siSAHH paralleled those of SAHH inhibition, although the magnitude of the changes was lower with the siSAHH. This difference may be explained by the time course of their action, since ADA has an almost immediate inhibitory action on SAHH activity, while the siRNA takes longer to achieve its maximal effect on SAHH expression. Moreover, siSAHH resulted in only a 67% reduction of SAHH activity compared to the complete suppression achieved with ADA. Nonetheless, targeted siRNA mediated knockdown of SAHH had qualitatively similar effects on altering the SAM/SAH ratio as the pharmacological approach. An unanticipated result was the ADA-induced suppression of SAHH mRNA, although under the time-frame examined, this did not significantly alter SAHH protein. This may be the result of a feedback mechanism in which excess SAH suppresses SAHH expression.

Here, we show that oxidative stress can be promoted by excess SAH. Our data is consistent with a role for hypomethylation in the suppression of GPx-1 expression (Fig. 2). Our previous studies indicated that excess exogenous homocysteine, or conditions that promote homocysteine production in cells, reduce GPx-1 expression by a mechanism that involved decreased Se-dependent translation (7). GPx-1 is one of the major antioxidants that can modulate overall oxidative stress (8). Its role in vascular dysfunction has been widely studied as an important regulator of endothelial oxidative balance and its deficiency contributes to atherosclerosis in susceptible mice and patients with coronary artery disease. Here, we observed a decrease in GPx-1 activity and protein expression following pharmacological inhibition or knockdown of SAHH with no significant decrease in GPx-1 transcript levels. Taken together, these findings suggest that GPx-1 is modulated by hypomethylation post-transcriptionally. Previously, it has been suggested that the GPx-1 promoter is a target for epigenetic regulation by DNA methylation, as exposure to the DNA methyltransferase inhibitor 5'-aza-2-deoxycytidine (5'-aza-dC) induced an up-regulation of GPx-1 in gastric carcinoma cells (54). In our study, however, hypomethylation stress did not increase GPx-1 expression. Furthermore, in endothelial cells exposed to 5'-aza-dC, we did not observe an up-regulation in GPx-1 expression (data not shown), suggesting that GPx-1 regulation by DNA methylation may be cell-type specific.

Our laboratory recently reported that GPx-1 deficiency is sufficient to augment the expression of ICAM-1 and VCAM-1 in human endothelial cells (14). Here, we show that SAH accumulation also induces up-regulation of these adhesion molecules, possibly via the suppression of GPx-1 and the subsequent increase in cellular ROS (Fig. 9), which can activate signaling pathways that promote up-regulation of adhesion molecules (14). Furthermore, we confirmed a role for GPx-1 in regulation of adhesion molecules by using gain and loss of function approaches. GPx-1 overexpression decreased ADA-induced adhesion molecule up-regulation, while its knockdown augmented the effects of hypomethylation on adhesion molecule up-regulation.

ICAM-1, VCAM-1 and PECAM-1 can mediate the adhesion of leukocytes to the endothelium and their transmigration (10,11,55). We demonstrated that hypomethylation stress in endothelial cells caused an increase in the cell surface expression of ICAM-1 and PECAM-1. Although the magnitude of the increase in cell surface ICAM-1 was less than the magnitude of the up-regulation in total ICAM-1 expression, increased cell-surface expression of adhesion molecules following ADA-exposure was sufficient to increase leukocyte binding. These findings suggest that the effects of hypomethylation may contribute to inflammatory pro-atherogenic changes in endothelial cells.

We further demonstrated a role for oxidants in the SAH-induced up-regulation of adhesion molecules, as treatment with antioxidants attenuated the ADA-induced up-regulation of ICAM-1 and VCAM-1 (Fig. 5). Interestingly, other studies in cancer-associated endothelial cells suggest that the *ICAM1* gene promoter is a target for DNA methylation; thus, its expression may also be regulated epigenetically (56). Nonetheless, a variety of antioxidant treatments lessened the expression of ICAM-1, as well as VCAM-1, in ADA-treated cells, suggesting that the SAH-induced reduction of GPx-1 and subsequent oxidant stress rather than DNA hypomethylation contribute to their up-regulation.

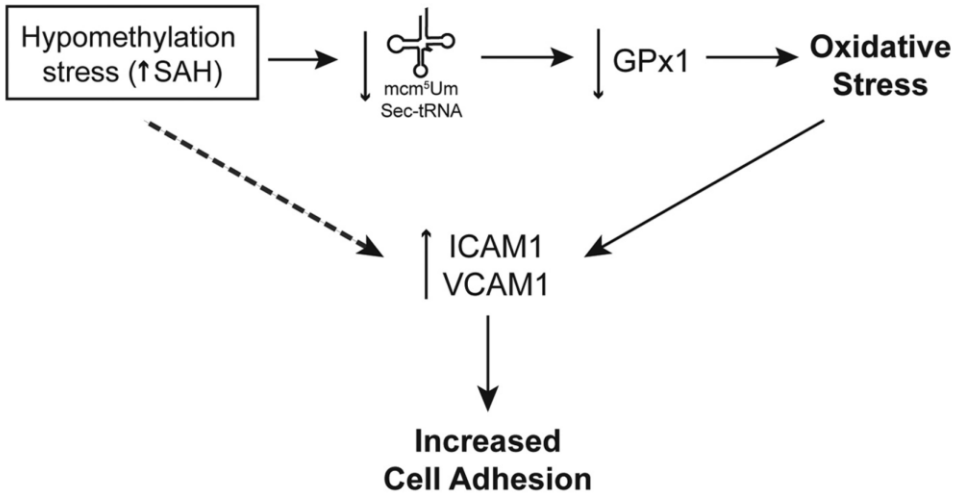

Figure 9 - The role of hypomethylation on endothelial dysfunction and activation. Excess SAH induces hypomethylation stress capable of decreasing the available $tRNA^{[Ser]Sec}$ isoform mcm^5Um. Lack of this $tRNA^{[Ser]Sec}$ isoform decreases the expression of the antioxidant GPx-1 (as well as other selenoproteins). Loss of GPx-1 causes an increase in cellular oxidants, promoting oxidative stress. Oxidant stress contributes to increased expression of adhesion molecules that are responsible for an increased capacity to bind leukocytes, contributing to a pro-atherogenic environment. Other possible mechanisms (represented by the dashed arrow), such as DNA hypomethylation, may also be involved in the up-regulation of adhesion molecules, such as ICAM-1 and VCAM-1.

GPx-1 is member of the selenoproteome, which comprises more than 25 proteins that contain selenium in the form of the Sec amino acid (18,21,44). More than 50% of the selenoproteome is known to be involved in redox homeostasis, and selenium deficiency has been associated with

oxidative stress and cancer (18). The unique translation mechanism exclusive to these proteins involves the recognition of the UGA codon, which in most circumstances signals translation termination, as a signal for Sec incorporation. Interestingly, Sec is synthesized directly on the tRNA that is initially charged with a Ser, which is subsequently enzymatically converted to Sec (20,57). The two major $tRNA^{[Ser]Sec}$ isoforms, mcm^5U and mcm^5Um, which differ by a single methyl group, Um34, at position 34, modulate the expression of selenoproteins (21). Theoretically, an effect of hypomethylation, due to SAH accumulation, on this tRNA will affect not only GPx-1 expression, but also expression of other members of the selenoproteome. By using [^{75}Se]-labeling, we found that many Sec-containing proteins were down-regulated following SAHH impairment. Previous studies have shown that some selenoproteins are less sensitive to the loss of the mcm^5Um isoform of $tRNA^{[Ser]Sec}$ than others. In particular, the mcm^5U isoform of $tRNA^{[Ser]Sec}$ supports the synthesis of a subclass of selenoproteins, designated as housekeeping selenoproteins (TrxR1 and TrxR2); whereas the methylated mcm^5Um form, supports the expression of the stress-related subclass of selenoproteins (GPx-1, GPx-3, GPx-4, SelR, SelT, SelW) (21). Accordingly, among the proteins that can be identified following selenium labeling, we found that hypomethylation results in an increase in TrxR1 expression, while GPx-1 and GPx-4 are diminished. One limitation of our study is that we have not confirmed the suppressive effects of ADA on selenoproteins other than GPx-1. Our results, however, clearly demonstrate a reciprocal regulation of TrxR1 and GPx-1, with a Pearson's correlation coefficient of -0.647, p=0.0006, between TrxR and GPx-1 enzyme activities. Interestingly, protein expression of the related TrxR1 and TrxR2 were both increased by ADA, although the mechanisms may be different: only the TrxR1 mRNA was increased with exposure to ADA. It is well known that TxR1 is a target for transcriptional regulation by the stress-activated nuclear factor Nrf2 (58-60). Thus, oxidant stress caused by GPx-1 suppression may contribute to TxR1 up-regulation, although other factors may also play a role in augmenting TxR1 expression. The reciprocal regulation of TrxR1 and GPx-1 has been reported previously in a variety of cancer cells (61) and these antioxidants enzymes may have complementary roles in regulating cellular redox. Thus, similar to loss of GPx-1, knockdown of TrxR1 may increase H_2O_2 in endothelial cells, although of the TrxR enzymes, the TrxR2 appears to have a greater role in modulating intracellular H_2O_2 (62). In our current study, however, modest up-regulation of TrxR enzymes was not sufficient to compensate for suppression of GPx-1 as H_2O_2 accumulated in ADA-treated endothelial cells.

In our cell culture system, HUVEC were cultured with media containing 30 nM selenious acid plus 7.5 nM selenium from serum. The addition of excess Se up to 100 nM had little effect on the expression of GPx-1 or TrxR as monitored by Western blots and enzyme activity assays (Fig. 8). The lack of an effect of additional Se in our cell system is consistent with previous studies reporting maximal expression of TrxR and GPx-1 when endothelial cells were cultured with 40 nM Se (63).

To date, the methyltransferase responsible for the methylation of mcm^5U $tRNA^{[Ser]Sec}$ has not been identified, but our studies suggest that it may be particularly sensitive to SAH accumulation as its product is virtually undetectable after ADA treatment (Fig. 7B). Recent studies have identified a methyltransferase, ALKBH8, which when complexed with TRM112, catalyzes the methyl esterification of cm^5U to mcm^5U (64,65). Absence of ALKBH8 also inhibited the decoding of the UGA stop codon to Sec, causing reduced levels of GPx-1 in the liver of ALKBH8 deficient mice (64).

Interestingly, besides the lack of the methylated form of $tRNA^{[Ser]Sec}$, cells under SAH accumulation appeared to respond to the absence of this isoform by inducing $tRNA^{[Ser]Sec}$ production: ADA treatment caused an approximate 1.7-fold increase in the overall levels of $tRNA^{[Ser]Sec}$. The mechanism that regulates this feedback response is not clear, and needs further investigation.

Our work elucidates a new mechanism by which hypomethylation can modulate selenoprotein expression. As excess SAH can be found in conditions of elevated homocysteine and it inhibits methylation reactions, we propose that SAH accumulation may explain the effects of homocysteine on GPx-1 suppression. Figure 9 summarizes the mechanism by which a hypomethylating environment can contribute to endothelial dysfunction and activation. Thus, an accumulation of SAH inhibits the methylation of the $tRNA^{[Ser]Sec}$ necessary for efficient translation of GPx-1 and other selenoproteins. The impairment of this important antioxidant can lead to oxidant stress and endothelial activation, contributing to the up-regulation of ICAM-1 and VCAM-1 adhesion molecules, which may augment leukocyte binding to contribute to an atherogenic phenotype.

ACKNOWLEDGEMENTS

We are very thankful to Derrick Kao (Brigham and Women's Hospital, Harvard Medical School, USA) for his technical assistance and to Desirée Smith (VU University Medical Center, The Netherlands) for her help with SAM and SAH quantification and analysis. The authors wish to thank Stephanie Tribuna for expert technical assistance.

FUNDING

This work was supported, in part, by NIH grants HL067195, HL070819, HL048743, HL107192, and HL108630 (JL), HL46457 and HL48743 (TM), GM061603 (VNG), by an American Heart Association Postdoctoral Fellowship Grant (HK), and by Fundação para a Ciência e a Tecnologia grants PTDC/SAU-ORG/112683/2009 (RC) and SFRH/BD/73021/2010 (MB).

CONFLICTS OF INTEREST

The authors have no conflict of interest.

REFERENCES

1. Barroso, M., Rocha, M. S., Esse, R., Goncalves, I., Jr., Gomes, A. Q., Teerlink, T., Jakobs, C., Blom, H. J., Loscalzo, J., Rivera, I., de Almeida, I. T., and Castro, R. (2012) Cellular hypomethylation is associated with impaired nitric oxide production by cultured human endothelial cells. *Amino Acids* **42**, 1903-1911

2. Esse, R., Rocha, M. S., Barroso, M., Florindo, C., Teerlink, T., Kok, R. M., Smulders, Y. M., Rivera, I., Leandro, P., Koolwijk, P., Castro, R., Blom, H. J., and de Almeida, I. T. (2013) Protein arginine methylation is more prone to inhibition by S-adenosylhomocysteine than DNA methylation in vascular endothelial cells. *PLoS One* **8**, e55483

3. Castro, R., Rivera, I., Struys, E. A., Jansen, E. E., Ravasco, P., Camilo, M. E., Blom, H. J., Jakobs, C., and Tavares de Almeida, I. (2003) Increased homocysteine and S-adenosylhomocysteine concentrations and DNA hypomethylation in vascular disease. *Clin. Chem.* **49**, 1292-1296

4. Caudill, M. A., Wang, J. C., Melnyk, S., Pogribny, I. P., Jernigan, S., Collins, M. D., Santos-Guzman, J., Swendseid, M. E., Cogger, E. A., and James, S. J. (2001) Intracellular S-adenosylhomocysteine concentrations predict global DNA hypomethylation in tissues of methyl-deficient cystathionine beta-synthase heterozygous mice. *J. Nutr.* **131**, 2811-2818

5. Esse, R., Florindo, C., Imbard, A., Rocha, M. S., de Vriese, A. S., Smulders, Y. M., Teerlink, T., Tavares de Almeida, I., Castro, R., and Blom, H. J. (2013) Global protein and histone arginine methylation are affected in a tissue-specific manner in a rat model of diet-induced hyperhomocysteinemia. *Biochim. Biophys. Acta* **1832**, 1708-1714

6. Esse, R., Imbard, A., Florindo, C., Gupta, S., Quinlivan, E. P., Davids, M., Teerlink, T., Tavares de Almeida, I., Kruger, W. D., Blom, H. J., and Castro, R. (2014) Protein arginine hypomethylation in a mouse model of cystathionine beta-synthase deficiency. *FASEB J.* 10.1096/fj.13-246579

7. Handy, D. E., Zhang, Y., and Loscalzo, J. (2005) Homocysteine down-regulates cellular glutathione peroxidase (GPx1) by decreasing translation. *J. Biol. Chem.* **280**, 15518-15525

8. Lubos, E., Loscalzo, J., and Handy, D. E. (2011) Glutathione peroxidase-1 in health and disease: from molecular mechanisms to therapeutic opportunities. *Antioxid. Redox Signal.* **15**, 1957-1997

9. Pastori, D., Carnevale, R., and Pignatelli, P. (2014) Is there a clinical role for oxidative stress biomarkers in atherosclerotic diseases? *Intern. Emerg. Med.* **9**, 123-131

10. Cook-Mills, J. M., Marchese, M. E., and Abdala-Valencia, H. (2011) Vascular cell adhesion molecule-1 expression and signaling during disease: regulation by reactive oxygen species and antioxidants. *Antioxid. Redox Signal.* **15**, 1607-1638

11. Forstermann, U. (2008) Oxidative stress in vascular disease: causes, defense mechanisms and potential therapies. *Nat. Clin. Pract. Cardiovasc. Med.* **5**, 338-349

12. Hulsmans, M., Van Dooren, E., and Holvoet, P. (2012) Mitochondrial reactive oxygen species and risk of atherosclerosis. *Curr. Atheroscler. Rep.* **14**, 264-276

13. Weber, C., and Noels, H. (2011) Atherosclerosis: current pathogenesis and therapeutic options. *Nat. Med.* **17**, 1410-1422

14. Lubos, E., Kelly, N. J., Oldebeken, S. R., Leopold, J. A., Zhang, Y. Y., Loscalzo, J., and Handy, D. E. (2011) Glutathione peroxidase-1 deficiency augments proinflammatory cytokine-induced redox signaling and human endothelial cell activation. *J. Biol. Chem.* **286**, 35407-35417

15. Lubos, E., Mahoney, C. E., Leopold, J. A., Zhang, Y. Y., Loscalzo, J., and Handy, D. E. (2010) Glutathione peroxidase-1 modulates lipopolysaccharide-induced adhesion molecule expression in endothelial cells by altering CD14 expression. *FASEB J.* **24**, 2525-2532

16. Lewis, P., Stefanovic, N., Pete, J., Calkin, A. C., Giunti, S., Thallas-Bonke, V., Jandeleit-Dahm, K. A., Allen, T. J., Kola, I., Cooper, M. E., and de Haan, J. B. (2007) Lack of the antioxidant enzyme glutathione peroxidase-1 accelerates atherosclerosis in diabetic apolipoprotein E-deficient mice. *Circulation* **115**, 2178-2187

17. Blankenberg, S., Rupprecht, H. J., Bickel, C., Torzewski, M., Hafner, G., Tiret, L., Smieja, M., Cambien, F., Meyer, J., Lackner, K. J., and AtheroGene, I. (2003) Glutathione peroxidase 1 activity and cardiovascular events in patients with coronary artery disease. *N. Engl. J. Med.* **349**, 1605-1613

18. Papp, L. V., Lu, J., Holmgren, A., and Khanna, K. K. (2007) From selenium to selenoproteins: synthesis, identity, and their role in human health. *Antioxid. Redox Signal.* **9**, 775-806

19. Donovan, J., and Copeland, P. R. (2010) Threading the needle: getting selenocysteine into proteins. *Antioxid. Redox Signal.* **12**, 881-892

20. Xu , X. T., A.A.; Carlson, B.A.; Yoo, M.; Gladyshev, V.N.; Hatfield, D.L. (2012) Selenocysteine biosynthesis and the replacement of selenocysteine with cysteine in the pathway. in Selenium: Its Molecular Biology and Role in Human Health (Hatfield, D. L. B., M.J.; Gladyshev, V.N. ed.), *Springer, New York.* pp 23-32

21. Hatfield, D. L., Carlson, B. A., Xu, X. M., Mix, H., and Gladyshev, V. N. (2006) Selenocysteine incorporation machinery and the role of selenoproteins in development and health. *Prog. Nucleic Acid Res. Mol. Biol.* **81**, 97-142

22. Kim, L. K., Matsufuji, T., Matsufuji, S., Carlson, B. A., Kim, S. S., Hatfield, D. L., and Lee, B. J. (2000) Methylation of the ribosyl moiety at position 34 of selenocysteine tRNA[Ser]Sec is governed by both primary and tertiary structure. *RNA* **6**, 1306-1315

23. Carlson, B. A., Xu, X. M., Gladyshev, V. N., and Hatfield, D. L. (2005) Selective rescue of selenoprotein expression in mice lacking a highly specialized methyl group in selenocysteine tRNA. *J. Biol. Chem.* **280**, 5542-5548

24. Struys, E. A., Jansen, E. E., de Meer, K., and Jakobs, C. (2000) Determination of S-adenosylmethionine and S-adenosylhomocysteine in plasma and cerebrospinal fluid by stable-isotope dilution tandem mass spectrometry. *Clin. Chem.* **46**, 1650-1656

25. Kloor, D., Hermes, M., Fink, K., Schmid, H., Klingel, K., Mack, A., Grenz, A., and Osswald, H. (2007) Expression and localization of S-adenosylhomocysteine-hydrolase in the rat kidney following carbon monoxide induced hypoxia. *Cell. Physiol. Biochem.* **19**, 57-66

26. Kloor, D., Stumvoll, W., Schmid, H., Kompf, J., Mack, A., and Osswald, H. (2000) Localization of S-adenosylhomocysteine hydrolase in the rat kidney. *J. Histochem. Cytochem.* **48**, 211-218

27. Turanov, A. A., Su, D., and Gladyshev, V. N. (2006) Characterization of alternative cytosolic forms and cellular targets of mouse mitochondrial thioredoxin reductase. *J. Biol. Chem.* **281**, 22953-22963

28. Arner, E. S., Zhong, L., and Holmgren, A. (1999) Preparation and assay of mammalian thioredoxin and thioredoxin reductase. *Methods Enzymol.* **300**, 226-239

29. Smith, A. D., and Levander, O. A. (2002) High-throughput 96-well microplate assays for determining specific activities of glutathione peroxidase and thioredoxin reductase. *Methods Enzymol.* **347**, 113-121

30. Handy, D. E., Lubos, E., Yang, Y., Galbraith, J. D., Kelly, N., Zhang, Y. Y., Leopold, J. A., and Loscalzo, J. (2009) Glutathione peroxidase-1 regulates mitochondrial function to modulate redox-dependent cellular responses. *J. Biol. Chem.* **284**, 11913-11921

31. Belousov, V. V., Fradkov, A. F., Lukyanov, K. A., Staroverov, D. B., Shakhbazov, K. S., Terskikh, A. V., and Lukyanov, S. (2006) Genetically encoded fluorescent indicator for intracellular hydrogen peroxide. *Nat. Methods* **3**, 281-286

32. Sartoretto, J. L., Kalwa, H., Pluth, M. D., Lippard, S. J., and Michel, T. (2011) Hydrogen peroxide differentially modulates cardiac myocyte nitric oxide synthesis. *Proc. Natl. Acad. Sci.* **108**, 15792-15797

33. Kalwa, H., Sartoretto, J. L., Sartoretto, S. M., and Michel, T. (2012) Angiotensin-II and MARCKS: a hydrogen peroxide- and RAC1-dependent signaling pathway in vascular endothelium. *J. Biol. Chem.* **287**, 29147-29158

34. Yoo, M. H., Xu, X. M., Turanov, A. A., Carlson, B. A., Gladyshev, V. N., and Hatfield, D. L. (2007) A new strategy for assessing selenoprotein function: siRNA knockdown/knock-in targeting the 3'-UTR. *RNA* **13**, 921-929

35. Moustafa, M. E., Carlson, B. A., El-Saadani, M. A., Kryukov, G. V., Sun, Q. A., Harney, J. W., Hill, K. E., Combs, G. F., Feigenbaum, L., Mansur, D. B., Burk, R. F., Berry, M. J., Diamond, A. M., Lee, B. J., Gladyshev, V. N., and Hatfield, D. L. (2001) Selective inhibition of selenocysteine tRNA maturation and selenoprotein synthesis in transgenic mice expressing isopentenyladenosine-deficient selenocysteine tRNA. *Mol. Cell. Biol.* **21**, 3840-3852

36. Kumaraswamy, E., Carlson, B. A., Morgan, F., Miyoshi, K., Robinson, G. W., Su, D., Wang, S., Southon, E., Tessarollo, L., Lee, B. J., Gladyshev, V. N., Hennighausen, L., and Hatfield, D. L. (2003) Selective removal of the selenocysteine tRNA [Ser]Sec gene (Trsp) in mouse mammary epithelium. *Mol. Cell. Biol.* **23**, 1477-1488

37. Dery, U., Coulombe, Y., Rodrigue, A., Stasiak, A., Richard, S., and Masson, J. Y. (2008) A glycine-arginine domain in control of the human MRE11 DNA repair protein. *Mol. Cell. Biol.* **28**, 3058-3069

38. Schnabel, R., Lackner, K. J., Rupprecht, H. J., Espinola-Klein, C., Torzewski, M., Lubos, E., Bickel, C., Cambien, F., Tiret, L., Munzel, T., and Blankenberg, S. (2005) Glutathione peroxidase-1 and homocysteine for cardiovascular risk prediction: results from the AtheroGene study. *J. Am. Coll. Cardiol.* **45**, 1631-1637

39. Weiss, N., Zhang, Y. Y., Heydrick, S., Bierl, C., and Loscalzo, J. (2001) Overexpression of cellular glutathione peroxidase rescues homocyst(e)ine-induced endothelial dysfunction. *Proc. Natl. Acad. Sci.* **98**, 12503-12508

40. Le, N. T., Corsetti, J. P., Dehoff-Sparks, J. L., Sparks, C. E., Fujiwara, K., and Abe, J. (2012) Reactive Oxygen Species, SUMOylation, and Endothelial Inflammation. *Int. J. Inflam.* 2012, 678190

41. Rahman, A., and Fazal, F. (2009) Hug tightly and say goodbye: role of endothelial ICAM-1 in leukocyte transmigration. *Antioxid. Redox Signal.* **11**, 823-839

42. Roebuck, K. A., and Finnegan, A. (1999) Regulation of intercellular adhesion molecule-1 (CD54) gene expression. *J. Leukoc. Biol.* **66**, 876-888

43. Howard, M. T., Carlson, B. A., Anderson, C. B., and Hatfield, D. L. (2013) Translational redefinition of UGA codons is regulated by selenium availability. *J. Biol. Chem.* **288**, 19401-19413

44. Kryukov, G. V., Castellano, S., Novoselov, S. V., Lobanov, A. V., Zehtab, O., Guigo, R., and Gladyshev, V. N. (2003) Characterization of mammalian selenoproteomes. *Science* **300**, 1439-1443

45. King, W. D., Ho, V., Dodds, L., Perkins, S. L., Casson, R. I., and Massey, T. E. (2012) Relationships among biomarkers of one-carbon metabolism. *Mol. Biol. Rep.* **39**, 7805-7812

46. Xiao, Y., Zhang, Y., Wang, M., Li, X., Su, D., Qiu, J., Li, D., Yang, Y., Xia, M., and Ling, W. (2013) Plasma S-adenosylhomocysteine is associated with the risk of cardiovascular events in patients undergoing coronary angiography: a cohort study. *Am. J. Clin. Nutr.* **98**, 1162-1169

47. Shen, H., and Laird, P. W. (2013) Interplay between the cancer genome and epigenome. *Cell* **153**, 38-55

48. Kim, G. H., Ryan, J. J., and Archer, S. L. (2013) The role of redox signaling in epigenetics and cardiovascular disease. *Antioxid. Redox Signal.* **18**, 1920-1936

49. Motorin, Y., and Helm, M. (2011) RNA nucleotide methylation. Wiley Interdiscip Rev. *RNA* **2**, 611-631

50. Yan, M. S., Matouk, C. C., and Marsden, P. A. (2010) Epigenetics of the vascular endothelium. *J. Appl. Physiol.* (1985) **109**, 916-926

51. Polotskaia, A., Wang, M., Patschan, S., Addabbo, F., Chen, J., and Goligorsky, M. S. (2007) Regulation of arginine methylation in endothelial cells: role in premature senescence and apoptosis. *Cell Cycle* **6**, 2524-2530

52. Jeong, W., Kim, J., Ahn, S. E., Lee, S. I., Bazer, F. W., Han, J. Y., and Song, G. (2012) AHCYL1 is mediated by estrogen-induced ERK1/2 MAPK cell signaling and microRNA regulation to effect functional aspects of the avian oviduct. *PLoS One* **7**, e49204

53. Frazier-Wood, A. C., Aslibekyan, S., Borecki, I. B., Hopkins, P. N., Lai, C. Q., Ordovas, J. M., Straka, R. J., Tiwari, H. K., and Arnett, D. K. (2012) Genome-wide association study indicates variants associated with insulin signaling and inflammation mediate lipoprotein responses to fenofibrate. Pharmacogenet. *Genomics* **22**, 750-757

54. Jee, C. D., Kim, M. A., Jung, E. J., Kim, J., and Kim, W. H. (2009) Identification of genes epigenetically silenced by CpG methylation in human gastric carcinoma. *Eur. J. Cancer* **45**, 1282-1293

55. Privratsky, J. R., Newman, D. K., and Newman, P. J. (2010) PECAM-1: conflicts of interest in inflammation. *Life Sci.* **87**, 69-82

56. Hellebrekers, D. M., Castermans, K., Vire, E., Dings, R. P., Hoebers, N. T., Mayo, K. H., Oude Egbrink, M. G., Molema, G., Fuks, F., van Engeland, M., and Griffioen, A. W. (2006) Epigenetic regulation of tumor endothelial cell anergy: silencing of intercellular adhesion molecule-1 by histone modifications. *Cancer Res.* **66**, 10770-10777

57. Xu, X. M., Carlson, B. A., Mix, H., Zhang, Y., Saira, K., Glass, R. S., Berry, M. J., Gladyshev, V. N., and Hatfield, D. L. (2007) Biosynthesis of selenocysteine on its tRNA in eukaryotes. *PLoS Biol.* **5**, e4

58. Sakurai, A., Nishimoto, M., Himeno, S., Imura, N., Tsujimoto, M., Kunimoto, M., and Hara, S. (2005) Transcriptional regulation of thioredoxin reductase 1 expression by cadmium in vascular endothelial cells: role of NF-E2-related factor-2. *J. Cell. Physiol.* **203**, 529-537

59. Fourquet, S., Guerois, R., Biard, D., and Toledano, M. B. (2010) Activation of NRF2 by nitrosative agents and H2O2 involves KEAP1 disulfide formation. *J. Biol. Chem.* **285**, 8463-8471

60. Brigelius-Flohe, R., Muller, M., Lippmann, D., and Kipp, A. P. (2012) The yin and yang of nrf2-regulated selenoproteins in carcinogenesis. Int. *J. Cell Biol.* 2012, 486147

61. Gladyshev, V. N., Factor, V. M., Housseau, F., and Hatfield, D. L. (1998) Contrasting patterns of regulation of the antioxidant selenoproteins, thioredoxin reductase, and glutathione peroxidase, in cancer cells. *Biochem. Biophys. Res. Commun.* **251**, 488-493

62. Sugiyama, T., and Michel, T. (2010) Thiol-metabolizing proteins and endothelial redox state: differential modulation of eNOS and biopterin pathways. *Am. J. Physiol. Heart Circ. Physiol.* **298**, H194-201

63. Miller, S., Walker, S. W., Arthur, J. R., Nicol, F., Pickard, K., Lewin, M. H., Howie, A. F., and Beckett, G. J. (2001) Selenite protects human endothelial cells from oxidative damage and induces thioredoxin reductase. *Clin. Sci.* (Lond.) **100**, 543-550

64. Songe-Moller, L., van den Born, E., Leihne, V., Vagbo, C. B., Kristoffersen, T., Krokan, H. E., Kirpekar, F., Falnes, P. O., and Klungland, A. (2010) Mammalian ALKBH8 possesses tRNA methyltransferase activity required for the biogenesis of multiple wobble uridine modifications implicated in translational decoding. *Mol. Cell. Biol.* **30**, 1814-1827

65. Fu, D., Brophy, J. A., Chan, C. T., Atmore, K. A., Begley, U., Paules, R. S., Dedon, P. C., Begley, T. J., and Samson, L. D. (2010) Human AlkB homolog ABH8 Is a tRNA methyltransferase required for wobble uridine modification and DNA damage survival. *Mol. Cell. Biol.* **30**, 2449-2459

CHAPTER

4.2

S-Adenosylhomocysteine Alters Methylation of Cellular RNA

(Manuscript in preparation for submission)

S-Adenosylhomocysteine Alters Methylation of Cellular RNA

Madalena Barroso[a,b,c], Kathrin Thüring[c], Lyudmil Tserovski[c], Sapna Gupta[d], Warren D. Kruger[d], Henk J. Blom[e], Isabel Tavares de Almeida[b], Joseph Loscalzo[a], Rita Castro[b,f], Diane E. Handy[a], and Mark Helm[c].

[a] *Cardiovascular Division, Department of Medicine, Brigham and Women's Hospital and Harvard Medical School, Boston, MA, USA;*
[b] *The Research Institute for Medicines (iMed.ULisboa), Faculty of Pharmacy, University of Lisbon, Lisbon, Portugal;*
[c] *Institute of Pharmacy and Biochemistry, Faculty of Chemistry, Pharmaceutical Sciences and Geoscience, Johannes Gutenberg-Universität Mainz, Mainz, Germany;*
[d] *Cancer Biology Program, Fox Chase Cancer Center, Philadelphia, Pennsylvania, USA.*
[e] *Department of General Pediatrics, Center for Pediatrics and Adolescent Medicine University Hospital, Freiburg, Germany;*
[f] *Department of Biochemistry and Human Biology, Faculty of Pharmacy, University of Lisbon, Lisbon, Portugal.*

ABSTRACT

S-Adenosylhomocysteine (SAH) is, simultaneously, a byproduct and a competitive inhibitor of most cellular methylation reactions, which is elevated in hyperhomocysteinemia. Hyperhomocysteinemia is a risk factor for vascular diseases by mechanisms incompletely defined. Our previous results have shown that elevated SAH levels suppress DNA and protein methylation and that SAH-induced hypomethylation can promote endothelial dysfunction. Recently, we have also found the hypomethylation of a specific tRNA modification under excess SAH. RNA methylation has essential functions in maintaining RNA structure and function. Here, we investigate the effects of SAH on 12 well-characterized RNA methylation modifications in total and size-fractionated RNA samples from human endothelial cells and mouse tissue samples.

We found that endothelial accumulation of SAH reduces the presence of Cm, m^1G, Gm, Am, and m^6A modifications in total RNA. Methylation of the tRNA fraction was significantly affected by excess SAH with decreased Cm and Gm modifications by 30% and 25%, respectively. Lastly, we evaluated RNA methylation levels in a hyperhomocysteinemic mouse model that has elevated levels of tissue SAH. Our results revealed that hyperhomocysteinemia can promote both hyper- and hypo-methylation of RNA *in vivo*, depending on the RNA modification, RNA fraction, and tissue. These findings show that alterations in intracellular SAH affect RNA methylation, and provide insights into new pathways that may be altered in hyperhomocysteinemia.

Key Words: ***S-adenosylhomocysteine, hyperhomocysteinemia, RNA modifications, RNA methylation.***

1. INTRODUCTION

High levels of homocysteine in plasma (hyperhomocysteinemia) have been associated with different pathologies (1–3). Homocysteine is a naturally occurring amino-acid formed during methionine metabolism, which begins with the synthesis of S-adenosylmethionine (SAM) (1). Each methylation reaction that uses SAM as a methyl donor results in the formation of S-adenosylhomocysteine (SAH), which can then be hydrolyzed to homocysteine by SAH hydrolase (SAHH) (1). Homocysteine is either rapidly exported from the cell, remethylated to methionine, or converted to cystathionine (1). Cystathionine β-synthase (CBS) catalyzes the synthesis of cystathionine from homocysteine (1, 4). CBS deficiency is the most common inborn error of metabolism and can lead to severe hyperhomocysteinemia (4, 5). Homocysteine's first association with vascular disease was noticed in patients with CBS deficiency (6). Later, homocysteine was found to be an independent risk factor for cardiovascular diseases, promoting endothelial dysfunction and atherosclerosis by mechanisms that are not completely understood (1, 2, 7, 8). Recently, SAH, rather than homocysteine itself, has been suggested as a more accurate measure of disease risk (9, 10). SAH, which accumulates in hyperhomocysteinemia, is not only a by-product of the majority of transmethylation reactions, but also a potent inhibitor of most SAM-dependent methyltransferases. Our previous work documented that excess SAH induces hypomethylation of DNA and proteins (including histones) (11–13).

Unlike DNA and protein, the biological role of most RNA methylation modifications is still unknown, in part, due to the demanding techniques necessary for their detection and quantification (14). RNA methylation occurs in a diverse range of RNA species, such as tRNA, rRNA, mRNA, lncRNA, and snRNA, and it was shown to have a role in RNA function and stability (15). We have recently shown that a specific tRNA methylation can be impaired by excess SAH resulting in pro-atherogenic changes in endothelial cells (8). Methyltransferases have varying degrees of sensitivity to the inhibitory effects of SAH (16, 17). Several reports show RNA methyltransferase inhibition by SAH analogues; however, most of these studies were performed *in vitro* using purified enzymes (16–18). Moreover, impaired activity of RNA methyltransferases and demethylases can lead to altered gene expression, supporting a possible role of RNA methylation in disease pathogenesis (8, 19, 20).

In this report, we analyzed the effects of SAH accumulation on global RNA methylation in order to identify specific RNA modifications altered by excess SAH. In endothelial cells, we found that inhibition of SAHH activity decreased specific RNA methylations. Additionally, we found significant changes in RNA methylation in liver, kidney, and brain tissue from a hyperhomocysteinemic mouse model in comparison to wild-type mice, indicating that aberrant RNA methylation patterns are also found *in vivo* under endogenously increased SAH levels.

2. MATERIALS AND METHODS

Cell Culture and Treatments – Human umbilical vein endothelial cells (HUVEC) (Lonza) were cultured in EBM-2 (Lonza) supplemented with EGM-2 aliquots excluding gentamicin/amphotericin-B (Lonza) at 37ºC and in 5% CO_2. Experiments were performed between passages five and eight, and initiated with cells that were 70-80% confluent. Forty-eight h incubations were performed using the SAHH inhibitor, adenosine-2',3'-dialdehyde (Sigma) 20 µM.

CBS Mice – CBS deficient mice were originally generated by crossing the transgenic strain, Tg C57BL6, which carries a human *CBS* gene construct with a 833T>C (I278T) missense mutation and the mice *Cbs* gene (Tg $Cbs^{+/+}$), with *Cbs* deficient animals ($Cbs^{+/-}$) to generate Tg $Cbs^{+/-}$ mice (4). Heterozygous $Cbs^{+/-}$ and Tg $Cbs^{+/-}$ animals were then crossed to create mice that only express the human I278T *CBS* gene (Tg $Cbs^{-/-}$). Transgenic CBS expression was under the control of a metallothionein promoter, which was activated by the addition of 25 mM zinc to the drinking water. Zinc-containing water was replaced by pure water after weaning. Prenatal transgenic gene expression allowed the mice to overcome the lethal phenotype of $Cbs^{-/-}$ (21). The animals were fed with standard rodent chow (Teklad 2018SX) and euthanized after day 50 after birth. Brain, liver, heart, and kidney tissues from five Tg $Cbs^{+/+}$ and five Tg $Cbs^{-/-}$ mice were collected and promptly frozen (-80ºC). Homocysteine, SAM, and SAH levels were previously determined in the same mice (4). In the remainder of this paper, we refer to Tg $Cbs^{+/+}$ and Tg $Cbs^{-/-}$ mice as $Cbs^{+/+}$ and $Cbs^{-/-}$, respectively.

RNA Extraction – RNA was extracted from HUVEC using TRI Reagent® (Sigma) following manufacturer's protocol. Tissue extraction (50-70 mg) was started by pestle homogenization in TRI Reagent; after lysis, the same protocol was used. RNA precipitation was achieved using ice-cold ethanol (100%).

RNA PAGE – RNA polyacrylamide gel electrophoresis (PAGE) was performed using a 10 % denaturing polyacrylamide gel with 8 M urea. We loaded 0.5-1 µg RNA with dye-free loading buffer (90% formamide, 1xTBE), and performed electrophoresis at 16W and room temperature. After PAGE, the gel was stained with SYBR® Gold (Life Technologies), and a fluorescence scanning (excitation 488 nm, emission 520nm BP40) was performed with the Typhoon 9400 (GE Healthcare).

IEX-Chromatography RNA Fractionation – RNA was analyzed by ion-exchange (IEX) chromatography with a DNAPac PA100 Column (Dionex) and the chromatography system BioLogic Duo-flow (BioRad) coupled to a diode array detector (DAD) (detection at 254 nm). Gradient-based chromatography was performed at 74ºC, with constant flow (1 ml/min), and using the pH 8 buffers: 20 mM Tris-HCl (buffer A) and 20 mM Tris-HCl with 0.4 M sodium perchlorate ($NaClO_4$, Sigma)

(buffer B). Buffers A and B were progressively mixed, starting with 20% of buffer B for 4 minutes, followed by 10% for 30 sec, and then gradually increasing from 20 to 100% during 30 min. Samples were collected at min: 17.5 (fraction *a*), 19.5 (fraction *b*), 21.5 (fraction *c*), and 25 (fraction *d*). After each run, RNA fractions were immediately precipitated by adding 0.1 vol 5 M ammonium acetate (Sigma) followed by 2.5 vol ice-cold ethanol. After precipitation, RNA was further washed with ice cold 70% ethanol and resuspended in water. The chromatography column was washed with a 0.4 M $NaClO_4$ solution (pH 12) before and between runs.

LC-MS/MS Analysis of Methylated Nucleosides – HPLC coupled to tandem mass spectrometry was used for detection and quantification of twelve well-characterized modified nucleosides (Fig. 1) in the total RNA collected from tissue and cell samples, as well as in the RNA fractions collected during IEX-chromatography. Briefly, RNA was digested to nucleosides by the action of nuclease P1 (Sigma), nuclease snake venom phosphodiesterase (Worthington), and alkaline phosphatase (Fermentas) as previously described in (22). A mixture containing stable isotope-labeled internal standard (IS) was then added in constant amounts to each sample.

The analysis of the modified nucleosides was performed on an Agilent 1260 HPLC series equipped with a DAD and a triple quadrupole mass spectrometer (Agilent 6460). A Synergi 4 µm Fusion-RP 80 Å LC Column (250 length and 2 mm inner diameter; Phenomenex) was used at 35°C. A chromatographic gradient was achieved using the solvents C (5 mM ammonium acetate buffer adjusted to pH 5.3 using acetic acid) and D (pure acetonitrile). The elution was performed at a constant flow rate (0.35 ml/min), starting with a linear gradient with buffer D increasing from 0% to 8% in 10 min, followed by an increase to 40% in the next 10 min, and then reaching 0% once more at 23 min. The column was then rinsed for 7 min with 100% buffer C. DAD detection at 254 nm allowed the identification of the 4 canonical nucleosides before the effluent entered the mass spectrometer. The triple quadruple mass spectrometer is equipped with an electrospray ion source (Agilent Jet Stream). The ESI parameters were: gas (N_2) temperature 350°C, flow 8 L/min, nebulizer pressure 50 psi, sheath gas temperature 350°C, sheath gas flow 12 L/min, and capillary voltage 3000 V. The MS was operated in the positive ion mode and modified nucleosides were monitored in the dynamic multiple reaction monitoring mode using the MassHunter software (Agilent). Commercially available modified nucleosides were used for the identification and determination of the specific retention times of m^1A, m^5C, m^7G, Cm, m^2G, Am (Sigma), Gm, m^5U, Um (Berry & Associates), m^1G, m^6A, and m_2^6A, were identified based on an *E. coli* nucleosides profile, where these modifications are highly abundant. All mass transitions and retention times used for identification of the modified nucleosides can be found in Supplementary Table 1. Agilent MassHunter qualitative analysis software was used for peak area determination. Comparison of modified nucleoside content between different samples was performed

after the normalization of the modified nucleoside peak to the corresponding IS peak area and, lastly, to the guanosine UV peak (23).

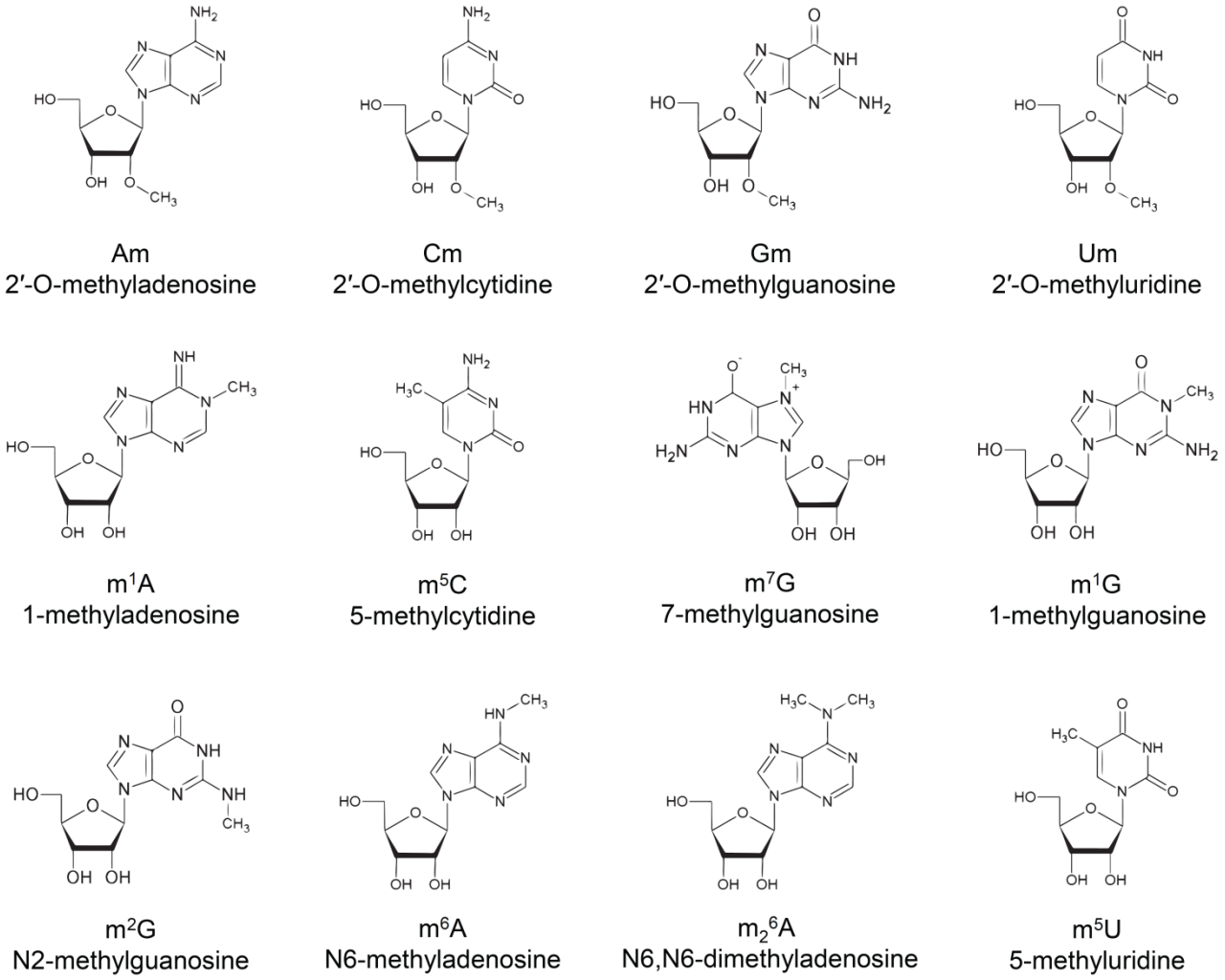

Figure 1 - RNA methylation modifications. Chemical structure of the methylated nucleotides.

3. RESULTS

Fractionation of total RNA – Although there are some methyltransferases that methylate different RNA species, others specifically target an RNA subtype. Therefore, the effects of excess SAH on RNA methylation may differ among RNA species. In order to achieve a sized-base separation of different RNA species, we used IEX chromatography. PAGE was used to confirm the composition of various chromatographic fractions (Fig. 2). The first eluting fraction collected (fraction *a*) was an attempt to recover RNA species that were smaller than tRNAs. However, the amount of RNA recovered after precipitation of this fraction was very low with no visible recovery of material on PAGE (Fig. 2A). tRNAs are usually easily identified after gel electrophoresis separation by 2 strong bands with sizes approximately between 76 and 100 nucleotides (nt) (24). Fraction *b* provided a good

enrichment in tRNA (below 100 bp; Fig. 2A). Separation of larger RNAs, such as mRNA and rRNA, is hard to achieve (24). We collected an intermediate-sized group of RNAs in fraction *c* (Fig. 2B). This fraction contained an enrichment of RNAs sized between 100 and 350 nt (fraction *c*, Fig. 2A).

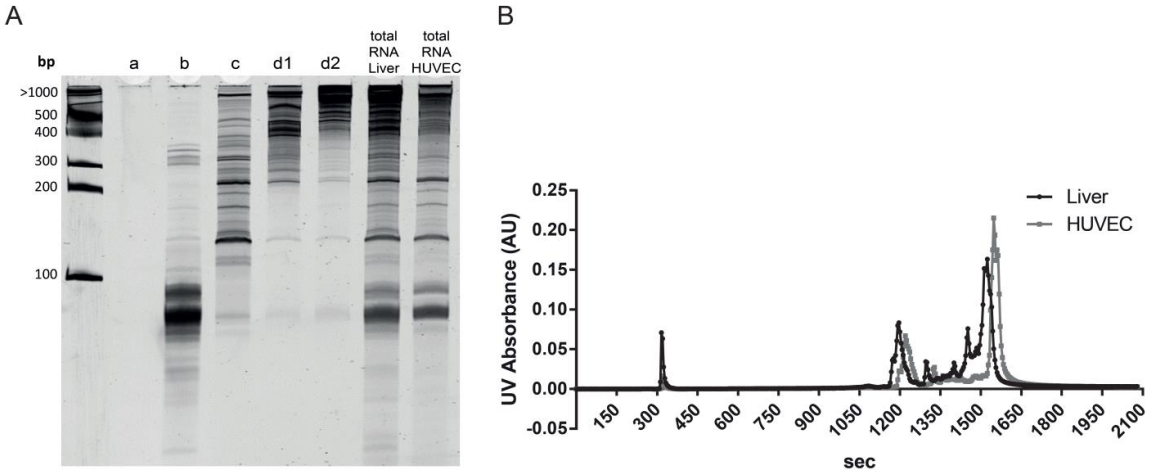

Figure 2 - RNA fractionation. (A), PAGE of RNA from HUVEC and from mice liver was performed and stained with SYBR® Gold. The different RNA fractions collected during IEX chromatography separation were loaded in the elution order: fraction *a* (15ng), *b* (0.94 µg), *c* (0.45 µg), *d1* (0.74 µg), and *d2* (1 µg). Total RNA from CBS liver (1 µg) and HUVEC total RNA (1 µg) were loaded for comparison. A DNA ladder (Thermo scientifc) was used and the DNA fragment sizes are indicated (left). **(B)**, IEX chromatograms of total RNA from CBS liver and cultured endothelial cells. A total of 60µg were injected for each sample.

The final eluting peaks were originally collected as separate fractions (*d1*) and (*d2*); however, there was a weak size-based separation of these larger and later eluting RNAs (Fig. 2). Therefore, in subsequent experiments, these fractions were pooled into a single fraction *d*. RNA recovery following chromatography was 20-30%. On average, fraction *d* represented about 60% of the total RNA recovered; fraction *c*, as well as *b*, represented 20% each, and fraction *a* less than 0.01%. Greater RNA complexity was observed for liver tissue when compared with endothelial cells (Fig. 2A). Additionally, RNA PAGE patterns differed between tissues, although, there were no significant observable changes between RNA profiles (from PAGE and IEX-chromatography) of cells treated and untreated, or between RNAs of wild-type and *Cbs* deficient mice within the same tissue (data not shown).

Endothelial SAH accumulation and RNA methylation – SAH impairs endothelial cell function, possibly contributing to vascular disease (8). For this reason and in light of our prior work, we determined the effects of SAH on global RNA methylation in endothelial cells. In order to achieve intracellular accumulation of SAH, we used ADA to inhibit its hydrolysis by SAHH, as previously (25). Endothelial cell treatment with ADA results in an intracellular increase of SAH by over 6-fold (25). Nine different key RNA methylation modifications were analyzed in total RNA, and the content of eight of these was reduced following ADA treatment (Fig. 3A). ADA significantly decreased Cm, m^1G, Gm, Am, and m^6A content in endothelial total RNA by 16 ± 2.6%, 18 ± 7.0%, 11 ± 6.1%, 7 ± 1.5%, and 9 ± 1.2%, respectively ($p < 0.05$).

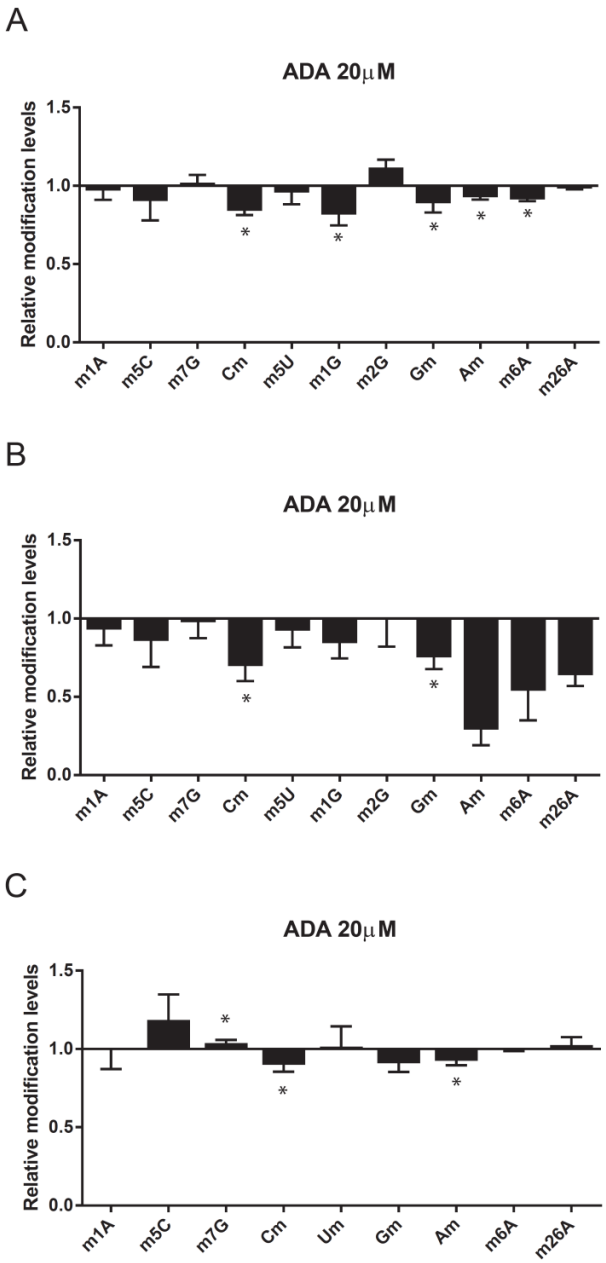

Figure 3 - Excess SAH effects on RNA methylation modifications in endothelial cells. Differences in the content of several methylated nucleosides following SAH accumulation were detected by LC-MS/MS. Each modified nucleoside was quantified using a stable isotope-labeled internal standard and normalized for total guanosine. The results obtained from RNA of ADA-treated cells were normalized to non-treated cells (Ctrl) and are shown on the left (n=3). The relative content of modified nucleosides from HUVEC total RNA. **(A)** and IEX-chromatography-obtained HUVEC RNA fractions *b* **(B)** and *d* **(C)** is shown. Statistical significance of the difference between means was determined, by Student's *t* test. *, $p < 0.05$ *versus* control. A(^{12}C), nucleoside peak area; A(^{13}C), nucleoside stable isotope labeled internal standard peak area; A(G) total guanosine UV peak area.

Like total RNA, RNA from fraction *b* showed decreased levels of methylated ribonucleosides following ADA treatment (Fig. 3B). However, only the Cm and Gm modifications showed statistically significant differences, with decreases of 30 ± 9.6% and 25 ± 7.6% following ADA treatment, respectively ($p < 0.05$).

Methylated nucleoside content in the intermediate-sized RNA fraction (fraction *c*), which includes RNAs like 5S and 5.8S rRNA and other non-coding RNAs, was not significantly different when comparing different treatment groups (Table 1). Interestingly, the methylated nucleosides that were found to be significantly decreased under ADA treatment in total RNA analysis also showed a trend toward a decrease in this intermediate fraction.

Finally, fraction *d*, which includes the larger RNAs, showed a significant reduction of Cm with ADA treatment by 10 ± 3.0 % ($p < 0.05$; Fig. 3C). ADA treatment also led to a significant reduction of Am ($p < 0.005$) and an increase in m^7G ($p < 0.05$).

Table 1 - Methylation modifications content from intermediate-sized RNA from HUVEC. RNA fraction *c* collected during IEX-chromatography of untreated and ADA treated cells, was analyzed by LC-MS/MS. Quantificated values of modified nucleosides are shown as mean ± standard error of the mean. Statistical significance of differences between means (*p* value) was calculated by Student's *t* test. A(^{12}C), nucleoside peak area; A(^{13}C), nucleoside stable isotope labeled internal standard peak area; A(G) total guanosine UV peak area.

	RNA (Fraction c)		
	A(12C)/A(13C)/A(G) * 10^3		*p* value
	Ctrl	**ADA**	**ADA vs Ctrl**
m1A	24.32 ± 0.32	56.96 ± 18.29	0.361
m5C	115.42 ± 5.99	224.79 ± 57.63	0.337
m7G	1.30 ± 0.07	2.44 ± 0.56	0.305
Cm	36.20 ± 1.07	33.36 ± 2.05	0.518
m5U	80.16 ± 7.81	130.23 ± 34.67	0.462
m1G	3.14 ± 0.33	10.49 ± 3.67	0.314
m2G	26.92 ± 2.91	92.50 ± 31.93	0.303
Gm	272.93 ± 3.43	251.85 ± 8.07	0.237
Am	1148.94 ± 21.01	1012.08 ± 30.66	0.101
m6A	42.55 ± 2.15	31.94 ± 2.10	0.111
m26A	121.09 ± 8.71	108.56 ± 2.14	0.465

SAH effects in RNA methylation *in vivo* – Human CBS deficiency significantly increases homocysteine levels in plasma and tissue (4). Similarly, SAH levels are significantly elevated in mice with impaired Cbs activity (4). To assess the effects of SAH on RNA methylation, we used RNA extracted from wild type ($Cbs^{+/+}$) and Cbs knockout mice ($Cbs^{-/-}$) liver, kidney, heart, and brain. RNA was fractionated by IEX chromatography and analyzed by LC-MS/MS for detection of methylated nucleosides (Table 2). Overall, most methylated nucleosides were not significantly altered in *Cbs* knockout mice compared with $Cbs^{+/+}$. m^5U levels were undetectable in fraction *c* and *d*. Moreover, m^2G levels were very low or undetectable in fraction *d*.

The comparison of the modified nucleoside content from different mice groups revealed a significant hypo- and hyper-methylation of specific moieties in *Cbs*-deficient mice compared to wild type. Specifically, Cm content was significantly decreased in RNA from liver fraction *b* and kidney fraction *c*, by 12 ± 6.8 and 11 ± 3.8 %, respectively ($p < 0.05$, $Cbs^{-/-}$ *versus* $Cbs^{+/+}$; Fig. 4). Moreover, Gm levels from $Cbs^{-/-}$ mice liver RNA were also 10 ± 6.6 % lower in fraction *b* ($p < 0.05$) and 14 ± 8.2 % lower in fraction *d* ($p = 0.05$). RNA Um content was also decreased in fraction *c* (8 ± 5.1 %, $p = 0.05$) and *d* (16 ± 6.8 %, $p < 0.05$) of $Cbs^{-/-}$ mice kidney. Finally, in brain, m^1A, m^5C, and m^7G showed a trend toward an increase during hyperhomocysteinemia across all fractions; in brain fraction *b*, m^1A, m^5C, m^1G, and m^5U from $Cbs^{-/-}$ were significantly up-regulated by 11 ± 6.8, 11 ± 5.6, 13 ± 5.9, and 12 ± 8.0 %, respectively ($p < 0.05$, $Cbs^{-/-}$ *versus* $Cbs^{+/+}$; Fig. 5).

Table 2. Methylation modifications content from control and Cbs-deficient mice. Different RNA modifications were analyzed for the IEX-chromatography-isolated fractions (b, c, and d) from liver, kidney, heart, and brain of control and Cbs deficient mice (n=3-5). LC-MS/MS results are shown as mean ± standard deviation. Statistical significance of differences between means (p value) was calculated by Student's t test. Values were not presented when the modification peak was undetectable. A(^{12}C), nucleoside peak area; A(^{13}C), nucleoside stable isotope labeled internal standard peak area; A(G) total guanosine UV peak area.

		Fraction b			***Fraction c***			***Fraction d***		
		A(12C)/A(13C)/A(G)		*p* value	A(12C)/A(13C)/A(G)		*p* value	A(12C)/A(13C)/A(G)		*p* value
		Cbs +/+	***Cbs -/-***		***Cbs +/+***	***Cbs -/-***		***Cbs +/+***	***Cbs -/-***	
Liver	m1A	1.651 ± 0.199	1.565 ± 0.215	0.528	0.008 ± 0.002	0.011 ± 0.005	0.336	0.007 ± 0.001	0.006 ± 0.000	0.057
	m5C	6.578 ± 1.440	6.512 ± 0.644	0.928	0.035 ± 0.009	0.049 ± 0.020	0.253	0.059 ± 0.007	0.052 ± 0.004	0.115
	m7G	0.045 ± 0.008	0.046 ± 0.003	0.774	0.000 ± 0.000	0.001 ± 0.000	0.316	0.000 ± 0.000	0.000 ± 0.000	0.853
	Cm	0.055 ± 0.004	0.048 ± 0.003	0.015	0.011 ± 0.002	0.014 ± 0.004	0.260	0.028 ± 0.002	0.025 ± 0.002	0.158
	m1G	0.356 ± 0.042	0.363 ± 0.031	0.766	0.001 ± 0.000	0.001 ± 0.001	0.371	0.001 ± 0.000	0.001 ± 0.000	0.667
	m2G	2.202 ± 0.337	2.343 ± 0.187	0.439	0.007 ± 0.001	0.009 ± 0.005	0.390			
	Gm	0.289 ± 0.024	0.261 ± 0.004	0.037	0.076 ± 0.009	0.090 ± 0.032	0.428	0.171 ± 0.012	0.146 ± 0.013	0.050
	Am	0.100 ± 0.033	0.115 ± 0.063	0.660	0.329 ± 0.030	0.408 ± 0.127	0.273	0.574 ± 0.062	0.522 ± 0.050	0.276
	m6A	0.012 ± 0.001	0.011 ± 0.002	0.567	0.011 ± 0.003	0.014 ± 0.005	0.361	0.013 ± 0.001	0.012 ± 0.001	0.335
	m26A	0.009 ± 0.002	0.006 ± 0.001	0.060	0.070 ± 0.019	0.085 ± 0.033	0.460	0.051 ± 0.004	0.051 ± 0.009	0.905
	m5U	0.020 ± 0.001	0.020 ± 0.002	0.385						
	Um				0.143 ± 0.020	0.165 ± 0.060	0.565	0.184 ± 0.022	0.186 ± 0.011	0.870
Kidney	m1A	0.705 ± 0.070	0.723 ± 0.024	0.703	0.013 ± 0.001	0.011 ± 0.001	0.075	0.006 ± 0.000	0.006 ± 0.001	0.693
	m5C	2.891 ± 0.327	3.015 ± 0.292	0.626	0.055 ± 0.007	0.055 ± 0.007	0.946	0.045 ± 0.006	0.046 ± 0.003	0.689
	m7G	0.019 ± 0.002	0.021 ± 0.001	0.160	0.001 ± 0.000	0.001 ± 0.000	0.684	0.000 ± 0.000	0.000 ± 0.000	0.452
	Cm	0.023 ± 0.003	0.023 ± 0.001	0.778	0.015 ± 0.001	0.013 ± 0.000	0.008	0.026 ± 0.002	0.025 ± 0.001	0.780
	m1G	0.168 ± 0.014	0.177 ± 0.008	0.336	0.001 ± 0.000	0.001 ± 0.000	0.834			
	m2G	1.070 ± 0.106	1.143 ± 0.036	0.311	0.015 ± 0.001	0.014 ± 0.002	0.536			
	Gm	0.107 ± 0.007	0.118 ± 0.007	0.084	0.105 ± 0.008	0.099 ± 0.007	0.287	0.146 ± 0.013	0.143 ± 0.003	0.670
	Am	0.036 ± 0.005	0.030 ± 0.006	0.178	0.450 ± 0.014	0.410 ± 0.026	0.062	0.514 ± 0.040	0.512 ± 0.042	0.971
	m6A	0.004 ± 0.000	0.005 ± 0.000	0.559	0.019 ± 0.001	0.016 ± 0.002	0.067	0.013 ± 0.001	0.013 ± 0.000	0.952
	m26A	0.007 ± 0.000	0.007 ± 0.001	0.101	0.108 ± 0.007	0.091 ± 0.005	0.012	0.053 ± 0.004	0.053 ± 0.001	0.941
	m5U	0.009 ± 0.001	0.010 ± 0.000	0.059						
	Um	0.270 ± 0.018	0.298 ± 0.039	0.245	0.171 ± 0.005	0.157 ± 0.010	0.053	0.226 ± 0.010	0.190 ± 0.016	0.019
Heart	m1A	0.797 ± 0.048	0.769 ± 0.213	0.836	0.019 ± 0.005	0.019 ± 0.005	0.936	0.007 ± 0.002	0.006 ± 0.000	0.571
	m5C	3.176 ± 0.279	2.721 ± 0.424	0.196	0.064 ± 0.012	0.063 ± 0.008	0.946	0.048 ± 0.003	0.047 ± 0.003	0.501
	m7G	0.018 ± 0.002	0.017 ± 0.004	0.673	0.001 ± 0.000	0.001 ± 0.000	0.604	0.001 ± 0.000	0.001 ± 0.000	0.768
	Cm	0.020 ± 0.004	0.017 ± 0.004	0.433	0.015 ± 0.002	0.013 ± 0.000	0.139	0.026 ± 0.002	0.026 ± 0.001	0.995
	m1G	0.177 ± 0.010	0.173 ± 0.048	0.897	0.002 ± 0.000	0.002 ± 0.000	0.719			
	m2G	1.211 ± 0.047	1.088 ± 0.281	0.495	0.025 ± 0.006	0.026 ± 0.008	0.947			
	Gm	0.102 ± 0.019	0.094 ± 0.021	0.653	0.110 ± 0.012	0.100 ± 0.008	0.295	0.143 ± 0.008	0.145 ± 0.008	0.854
	Am	0.030 ± 0.012	0.018 ± 0.003	0.156	0.428 ± 0.058	0.429 ± 0.013	0.982	0.593 ± 0.009	0.591 ± 0.064	0.962
	m6A	0.006 ± 0.001	0.005 ± 0.001	0.605	0.020 ± 0.004	0.023 ± 0.006	0.502	0.013 ± 0.000	0.013 ± 0.002	0.845
	m26A	0.007 ± 0.001	0.009 ± 0.006	0.541	0.115 ± 0.026	0.145 ± 0.041	0.351	0.062 ± 0.004	0.060 ± 0.014	0.758
	m5U	0.010 ± 0.001	0.010 ± 0.003	0.916						
	Um	0.253 ± 0.018	0.248 ± 0.069	0.906	0.175 ± 0.014	0.189 ± 0.012	0.284	0.210 ± 0.006	0.235 ± 0.079	0.613
Brain	m1A	0.701 ± 0.024	0.778 ± 0.047	0.021	0.013 ± 0.004	0.017 ± 0.003	0.109	0.006 ± 0.000	0.006 ± 0.001	0.525
	m5C	3.072 ± 0.111	3.404 ± 0.150	0.008	0.059 ± 0.013	0.072 ± 0.018	0.283	0.044 ± 0.004	0.045 ± 0.006	0.852
	m7G	0.020 ± 0.001	0.022 ± 0.002	0.074	0.001 ± 0.000	0.001 ± 0.000	0.080	0.000 ± 0.000	0.000 ± 0.000	0.411
	Cm	0.021 ± 0.001	0.022 ± 0.002	0.532	0.017 ± 0.002	0.017 ± 0.002	0.899	0.027 ± 0.002	0.026 ± 0.001	0.513
	m1G	0.172 ± 0.004	0.193 ± 0.010	0.006	0.001 ± 0.000	0.002 ± 0.000	0.079			
	m2G	1.114 ± 0.028	1.203 ± 0.081	0.078	0.017 ± 0.007	0.023 ± 0.003	0.148			
	Gm	0.049 ± 0.006	0.050 ± 0.006	0.829	0.107 ± 0.009	0.106 ± 0.011	0.830	0.143 ± 0.010	0.142 ± 0.001	0.786
	Am	0.023 ± 0.009	0.015 ± 0.002	0.118	0.465 ± 0.060	0.486 ± 0.069	0.649	0.557 ± 0.077	0.542 ± 0.038	0.737
	m6A	0.005 ± 0.000	0.005 ± 0.000	0.383	0.015 ± 0.003	0.016 ± 0.001	0.346	0.014 ± 0.001	0.014 ± 0.000	0.832
	m26A	0.005 ± 0.002	0.005 ± 0.002	0.816	0.058 ± 0.008	0.067 ± 0.008	0.141	0.060 ± 0.003	0.060 ± 0.002	0.955
	m5U	0.009 ± 0.000	0.010 ± 0.001	0.034						
	Um	0.260 ± 0.013	0.262 ± 0.017	0.822	0.179 ± 0.034	0.166 ± 0.034	0.576	0.189 ± 0.023	0.211 ± 0.005	0.110

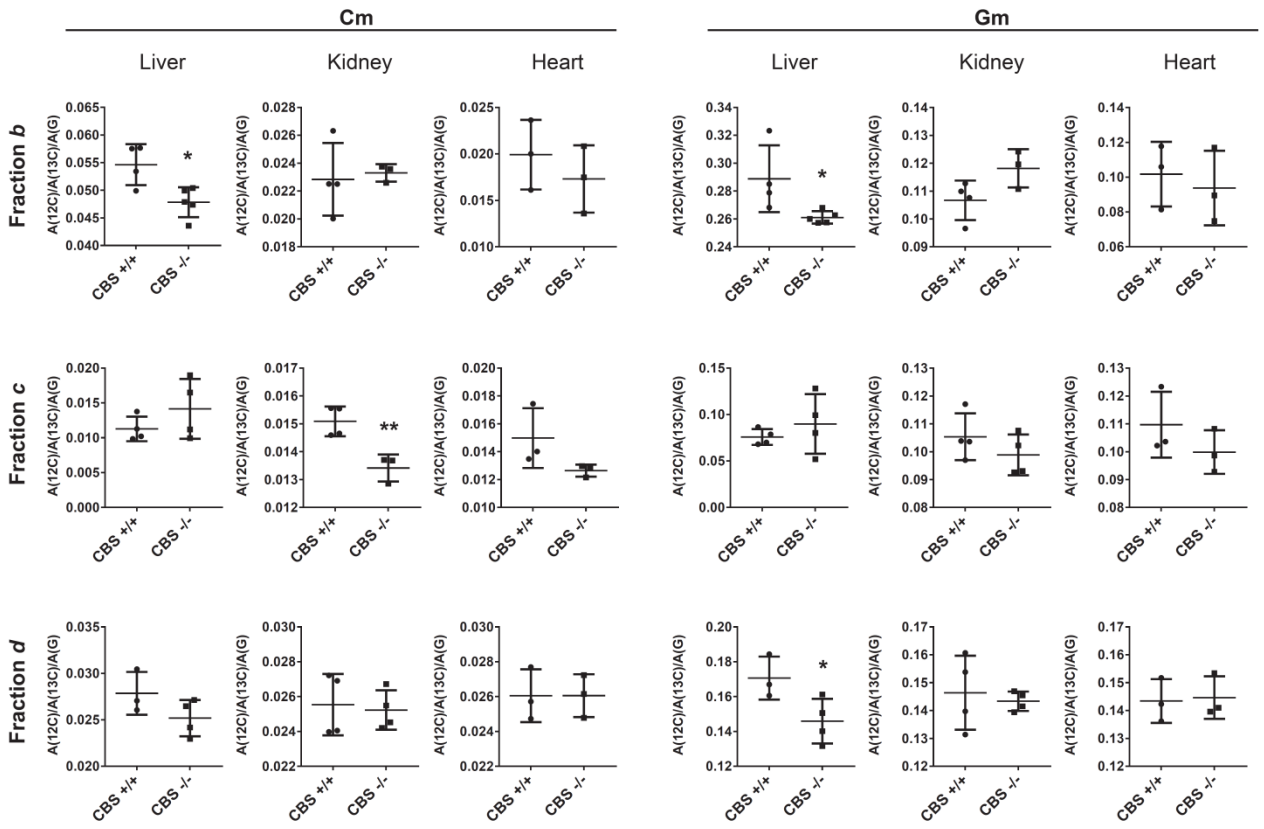

Figure 4 - Cm and Gm content from control and *Cbs* deficient mice liver, kidney and heart. Cm (left) and Gm (right) content from liver fractions *b*, *c*, and *d* of mice expressing Cbs (CBS +/+) and with Cbs deficiency (CBS-/-), was analyzed by LC-MS/MS. For each modified nucleoside, the detected peak area was normalized to the IS peak area and to total guanosine. The scatter plots show individual values, from three to five mice, mean ± SD. Statistical significance was evaluated by Student's *t* test. *, $p < 0.05$, **, $p < 0.005$ *versus* CBS +/+. A(^{12}C), nucleoside peak area; A(^{13}C), nucleoside stable isotope labeled internal standard peak area; A(G) total guanosine UV peak area.

4. DISCUSSION

Good separation of total RNA by chromatography is difficult to achieve especially for larger RNAs, such as mRNA and rRNA (24). IEX chromatography has been especially useful in the analysis and purification of short, single-stranded RNA molecules (24). Here, we optimized an anion-exchange liquid chromatography protocol in order to separate different RNA populations. Denaturing conditions were used in order to aid in the elution of larger RNA species. Using this method, we isolated and recovered three RNA populations based on their size (Fig. 2). Although we attempted to isolate smaller RNAs, such as miRNA (21-23 bp) and tRNA-derived RNA fragments (26), the recovery of RNA (in fraction *a*) was poor. Our method, however, reproducibly isolated a population of RNAs with a maximum size of 100 nt (fraction *b*). According to our PAGE results (Fig. 2A) and other reports (24), fraction *b* likely comprises the tRNA population and other non-coding RNAs, such as the small nuclear RNAs. The intermediate fraction (*c*) probably consists of rRNAs and other noncoding RNAs. The strongest band in fraction *c,* observable in the PAGE gel, may be the highly abundant 5S rRNA,

which is 121 nt in size (27). Size, polarity, and RNA conformation can influence chromatographic separation (24). In the case of the more abundant, large, and complex RNAs (fraction *d*), elution was compromised and column RNA retention could not be completely avoided; however, we were able to separate a fraction enriched in high-molecular-weight RNAs (> 400 nt), which should include mRNA, precursor mRNA, larger rRNAs (18S and 28S), and other long non-coding RNAs (24).

Although more than 150 RNA modifications have been described, most have an unknown function (28). Importantly, about two-thirds of these modifications are methylations (14). We analyzed a panel of 12 different ribonucleoside methylations (Fig. 1), which are well characterized (14). All of the identified human methyltransferases that catalyze these methylation additions are SAM-dependent and, therefore, targets for SAH inhibition (14, 29).

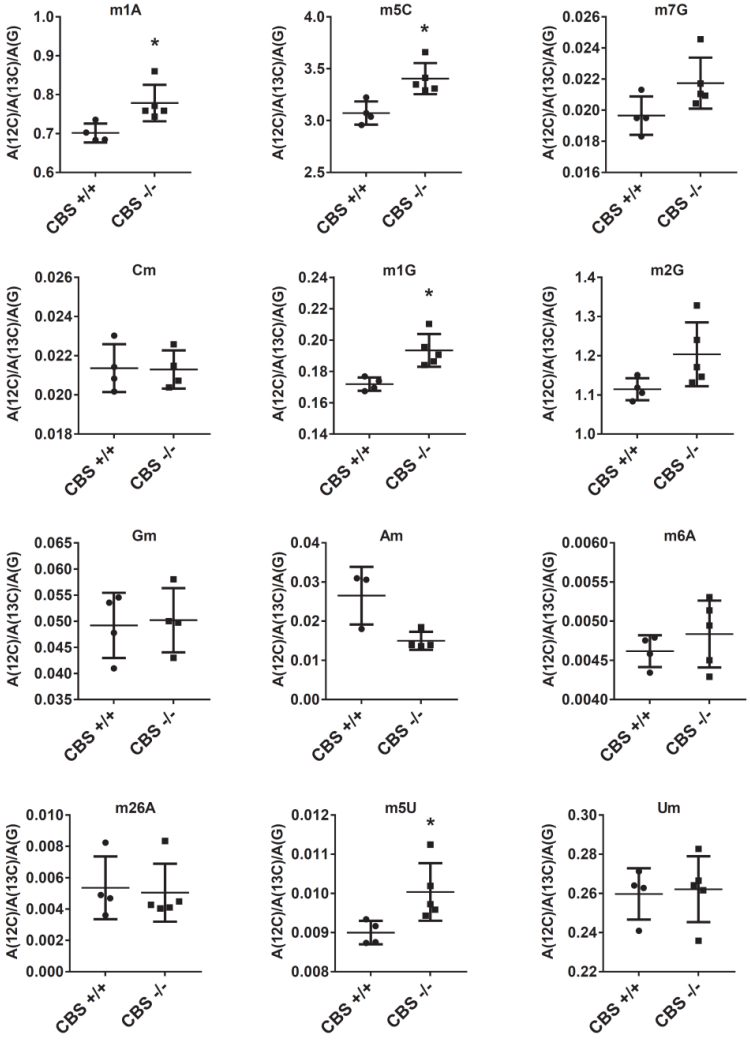

Figure 5 - Methylation modifications content from control and *Cbs* deficient mice brain tRNA. The tRNA-containing fraction obtained by IEX-chromatography (fraction *b*) of total RNA isolated from the brain of wild type (CBS +/+) and *Cbs*-deficient mice (CBS -/-) was analyzed by LC-MS/MS. Each scatter plot shows individual normalized peak areas from four mice, mean ± SD. Statistical significance was evaluated by Student's *t* test. *, $p < 0.05$ *versus* CBS +/+. A(^{12}C), nucleoside peak area; A(^{13}C), nucleoside stable isotope labeled internal standard peak area; A(G) total guanosine UV peak area.

Our previous studies in endothelial cells have shown that SAH inhibition by ADA induces a marked increase in intracellular SAH levels (8, 12, 25). Owing to the relevance of SAH in endothelial dysfunction, we used an endothelial cell model to test whether SAH promotes cellular RNA hypomethylation. ADA treatment reduced most of the methylated nucleosides studied. Five of these were significantly reduced ($p < 0.05$): three 2'-O-methylations (Cm, Gm, and Am), m^1G, and m^6A. These results suggest that 2'-O-methyltransferases may be particularly sensitive to SAH inhibition in endothelial cells. There are several classes of methyltransferases that can mediate the formation of these down-regulated modifications, such as the Rossmann-fold or SPOUT methyltransferases super-families (14, 29, 30). However, specific methyltransferase activity assays in the presence of excess SAH were not investigated in this report to address these possible specific mechanisms. Interestingly, a previous study using SAH analogues in a mouse macrophage cell line reported that m^6A synthesis was inhibited to a greater extent in mRNA than m^7G (31). In tRNA methyltransferases isolated from rat, the guanine-1 methyltransferase (m^1G) had a low K_i for SAH, whereas the N^2-guanine methyltransferase I (m^2G) had a high K_i for SAH (17, 32), consistent with our findings in endothelial cells that showed a significant suppression of global m^1G but not m^2G levels.

tRNA is the most heavily modified RNA species (14). Under excess SAH, greater differences were observed in the methylation content of the tRNA fraction than in the global RNA samples. For example, Cm and Gm were 14% more diminished in the tRNA fraction compared to total RNA. The fact that rRNA accounts for more than 80% of total RNA and that it is a stable RNA with a slow turnover may help to explain why modifications in total RNA show less variation. We observed a significant decrease in Cm and Gm in tRNA from ADA-treated cells. These 2'-O-methylation modifications are prevalent in the anticodon loop of the tRNA (14); thus, they may affect tRNA structure and decoding function.

Analysis of RNAs sized between 100 and 350 nt (fraction *c*) from endothelial cells showed no significant changes in RNA methylation following ADA (Table 1). This group of RNA includes mainly 5S and 5.8S rRNAs, which are heavily methylated but very stable, and, therefore, the effect of methyltransferases inhibition may be more difficult to detect. Nevertheless, the 2'-O-methylations detected, Cm, Gm and Am, showed a trend toward a decrease following ADA treatment. Likewise, 2'-O-methylations, which are known to be highly prevalent in rRNA (33), are decreased in the RNA fraction that includes the larger rRNAs and mRNA (fraction *d*).

Since excess SAH altered RNA methylation in cultured endothelial cells, we next explored the possibility that these effects would be observed in a hyperhomocysteinemic animal model. Due to the reversibility of the SAHH-catalyzed reaction, SAH accumulates during hyperhomocysteinemia (11). Growing evidence supports the relevance of SAH in homocysteine's associated pathology in the cardiovascular system (9, 34, 35). In order to investigate whether SAH impairs RNA methylation in hyperhomocysteinemia, we used a *Cbs*-deficient mouse model. Analyzing tRNA from liver, kidney,

heart, and brain, we observed that Cm and Gm were significantly reduced in the liver of Cbs-deficient mice. Total homocysteine and SAH liver levels were shown to be 33- and 9-fold higher, respectively, in $Cbs^{-/-}$ mice compared to $Cbs^{+/+}$ (4). The decrease of Cm and Gm in $Cbs^{-/-}$ liver was consistent with our observations in tRNA fractions isolated from ADA-treated cells, even though homocysteine metabolism is substantially different in hepatocytes and endothelial cells (1). Moreover Gm content is also significantly decreased in the rRNA- and mRNA-containing fraction from the liver of $Cbs^{-/-}$ mice. Importantly, these 2'-O-methylations can determine efficient translation by the ribosome (33, 36, 37); however, the consequences of these alterations for liver function remain unknown. Liver is a key regulator of homocysteine metabolism, and protein arginine hypomethylation was previously reported in this model (4). In other mouse models of hyperhomocysteinemia, DNA hypomethylation was reported for liver (38); however, in our previous studies using the reported Cbs-deficient mice we found no changes in global DNA methylation (4).

The kidney of *Cbs*-deficient mice presented significant hypomethylation in fraction *c* RNA, with significant reductions in the levels of Cm, Um (which was also significantly decreased in fraction *d*), and m_2^6A. Hyperhomocysteinemia is highly associated with renal disease even though the mechanisms underlying this association are not fully understood (39, 40). Interestingly, although SAH levels are 7-fold higher in $Cbs^{-/-}$ kidney, neither DNA nor protein hypomethylation was found previously in the kidney of the *Cbs*-deficient mice (4).

Most brain ribonucleoside methylations showed a trend toward an increase in detectable levels. In particular, the tRNA fraction in brain showed a significant increase in several base methylations, including m^5C. Previous studies associated the loss of this methylation with neurologic impairment (41). Due to the importance of RNA methylation for brain function, a feedback mechanism that leads to its up-regulation may be triggered in the context of excess SAH or homocysteine. However, the mechanisms by which hypermethylation may occur during hyperhomocysteinemia remain unresolved. The fact that these modifications differ among tissues in Cbs-deficient mice suggests that tissue-specific methyltransferases may contribute to these differences. Importantly, brain is a highly heterogeneous tissue. RNA methyltransferases less sensitive to SAH-mediated inhibition, and the increased levels of SAM observed in the brain of these mice (4), could contribute to the observed hypermethylation. Alternatively, differences in the regulation of the RNA methyltransferases or demethylases, may contribute to these tissue-specific differences. The biological relevance of human RNA demethylases has been reported for m^6A (19), but the existence of human or mouse demethylases for the remaining modifications have not yet been reported (29).

Our results support possible regulation of RNA methylation by SAH in the setting of hyperhomocysteinemia. Specifically, our findings suggest that SAH accumulation may impair the activity of several 2'-O-methyltransferases. Interestingly, our previous studies implicated a 2'-O-methylation modification (mcm^5Um) in selenoproteome regulation in endothelial cells. We found

that excess SAH decreased mcm^{5}Um content of selenocysteine-tRNA, impairing the synthesis of key antioxidant selenoproteins in endothelial cells and promoting oxidative stress and a pro-inflammatory response (8). Additional examination of the effects of SAH on the activity of 2'-O-methyltransferases could clarify their sensitivity to this metabolite. Unfortunately, several human RNA methyltransferases, including 2'-O-methyltransferases, still remain uncharacterized (42). Thus, much is left to discover about specific RNA methylations, their regulation, and significance for diseases, including homocysteine-associated pathologies.

In summary, our work suggests that intracellular SAH can alter the activity of RNA methyltransferases *in vitro* and *in vivo*. Interestingly, SAH accumulation can result in both hypo- and hyper-methylation depending on the RNA modification. Additionally, we found that SAH-induced effects on RNA methylation are tissue-specific.

The great number and complexity of RNA methylation modifications adds to the challenges of understanding their biological roles. Nonetheless, our study revealed additional mechanisms by which SAH may modulate cell homeostasis during hyperhomocysteinemia. Additional studies are necessary to determine whether these alterations in RNA methylation have significant biological effects.

FUNDING

This work was supported by the EMBO grant ASTF 21 – 2014 to MB.

CONFLICTS OF INTEREST

The authors have no conflict of interest.

REFERENCES

1. Castro, R., Rivera, I., Blom, H. J., Jakobs, C., and Tavares de Almeida, I. (2006) Homocysteine metabolism, hyperhomocysteinaemia and vascular disease: an overview. *J. Inherit. Metab. Dis.* **29**, 3–20
2. Durand, P., Prost, M., Loreau, N., Lussier-Cacan, S., and Blache, D. (2001) Impaired Homocysteine Metabolism and Atherothrombotic Disease. *Lab. Investig.* **81**, 645–672
3. Ansari, R., Mahta, A., Mallack, E., and Luo, J. J. (2014) Hyperhomocysteinemia and neurologic disorders: a review. *J. Clin. Neurol.* **10**, 281–8
4. Esse, R., Imbard, A., Florindo, C., Gupta, S., Quinlivan, E. P., Davids, M., Teerlink, T., Tavares de Almeida, I., Kruger, W. D., Blom, H. J., and Castro, R. (2014) Protein arginine hypomethylation in a mouse model of cystathionine β-synthase deficiency. *FASEB J.* **28**, 2686–95
5. Sokolová, J., Janosíková, B., Terwilliger, J. D., Freiberger, T., Kraus, J. P., and Kozich, V. (2001) Cystathionine beta-synthase deficiency in Central Europe: discrepancy between biochemical and molecular genetic screening for homocystinuric alleles. *Hum. Mutat.* **18**, 548–9
6. McCully, K. S., and Wilson, R. B. (1975) Homocysteine theory of arteriosclerosis. *Atherosclerosis*. **22**, 215–27

7. Moat, S. J. (2008) Plasma total homocysteine: instigator or indicator of cardiovascular disease? *Ann. Clin. Biochem.* **45**, 345–8

8. Barroso, M., Florindo, C., Kalwa, H., Silva, Z., Turanov, A. A., Carlson, B. A., de Almeida, I. T., Blom, H. J., Gladyshev, V. N., Hatfield, D. L., Michel, T., Castro, R., Loscalzo, J., and Handy, D. E. (2014) Inhibition of cellular methyltransferases promotes endothelial cell activation by suppressing glutathione peroxidase 1 protein expression. *J. Biol. Chem.* **289**, 15350–62

9. Wagner, C., and Koury, M. J. (2007) S-Adenosylhomocysteine: a better indicator of vascular disease than homocysteine? *Am. J. Clin. Nutr.* **86**, 1581–5

10. Xiao, Y., Zhang, Y., Wang, M., Li, X., Su, D., Qiu, J., Li, D., Yang, Y., Xia, M., and Ling, W. (2013) Plasma S-adenosylhomocysteine is associated with the risk of cardiovascular events in patients undergoing coronary angiography: a cohort study. *Am. J. Clin. Nutr.* **98**, 1162–9

11. Castro, R., Rivera, I., Struys, E. A., Jansen, E. E. W., Ravasco, P., Camilo, M. E., Blom, H. J., Jakobs, C., and Tavares de Almeida, I. (2003) Increased homocysteine and S-adenosylhomocysteine concentrations and DNA hypomethylation in vascular disease. *Clin. Chem.* **49**, 1292–6

12. Esse, R., Rocha, M. S., Barroso, M., Florindo, C., Teerlink, T., Kok, R. M., Smulders, Y. M., Rivera, I., Leandro, P., Koolwijk, P., Castro, R., Blom, H. J., and de Almeida, I. T. (2013) Protein arginine methylation is more prone to inhibition by S-adenosylhomocysteine than DNA methylation in vascular endothelial cells. *PLoS One*. **8**, e55483

13. Esse, R., Florindo, C., Imbard, A., Rocha, M. S., de Vriese, A. S., Smulders, Y. M., Teerlink, T., Tavares de Almeida, I., Castro, R., and Blom, H. J. (2013) Global protein and histone arginine methylation are affected in a tissue-specific manner in a rat model of diet-induced hyperhomocysteinemia. *Biochim. Biophys. Acta*. **1832**, 1708–14

14. Motorin, Y., and Helm, M. (2011) RNA nucleotide methylation. *Wiley Interdiscip. Rev. RNA*. **2**, 611–31

15. Motorin, Y., and Helm, M. (2010) tRNA stabilization by modified nucleotides. *Biochemistry*. **49**, 4934–44

16. Glick, J. M., Ross, S., and Leboy, P. S. (1975) S-adenosylhomocysteine inhibition of three purified tRNA methyltransferases from rat liver. *Nucleic Acids Res.* **2**, 1639–51

17. Leboy, P. S., Glick, J. M., Steiner, F. G., Haney, S., and Borchardt, R. T. (1978) S-adenosylhomocysteine analogues as inhibitors of specific tRNA methylation. *Biochim. Biophys. Acta - Nucleic Acids Protein Synth.* **520**, 153–163

18. Hildesheim, J., Hildesheim, R., Blanchard, P., Farrugia, G., and Michelot, R. (1973) Studies on synthetic inhibitors of t-RNA methyl transferases: analogs of S-adenosyl homocysteine. *Biochimie*. **55**, 541–6

19. Niu, Y., Zhao, X., Wu, Y.-S., Li, M.-M., Wang, X.-J., and Yang, Y.-G. (2013) N6-methyl-adenosine (m6A) in RNA: an old modification with a novel epigenetic function. *Genomics. Proteomics Bioinformatics*. **11**, 8–17

20. Jia, G., Fu, Y., and He, C. (2013) Reversible RNA adenosine methylation in biological regulation. *Trends Genet.* **29**, 108–15

21. Wang, L., Chen, X., Tang, B., Hua, X., Klein-Szanto, A., and Kruger, W. D. (2005) Expression of mutant human cystathionine beta-synthase rescues neonatal lethality but not homocystinuria in a mouse model. *Hum. Mol. Genet.* **14**, 2201–8

22. Klassen, R., Grunewald, P., Thüring, K. L., Eichler, C., Helm, M., and Schaffrath, R. (2015) Loss of anticodon wobble uridine modifications affects tRNA(Lys) function and protein levels in Saccharomyces cerevisiae. *PLoS One*. **10**, e0119261

23. Kellner, S., Ochel, A., Thüring, K., Spenkuch, F., Neumann, J., Sharma, S., Entian, K.-D., Schneider, D., and Helm, M. (2014) Absolute and relative quantification of RNA modifications via biosynthetic isotopomers. *Nucleic Acids Res.* **42**, e142

24. Gjerde, D. T., Hoang, L., and Hornby, D. (2009) *RNA Purification and Analysis*, Wiley-VCH Verlag GmbH & Co. KGaA, Weinheim, Germany, 10.1002/9783527627196

25. Barroso, M., Rocha, M. S., Esse, R., Gonçalves, I., Gomes, A. Q., Teerlink, T., Jakobs, C., Blom, H. J., Loscalzo, J., Rivera, I., Tavares de Almeida, I., and Castro, R. (2012) Cellular hypomethylation is

associated with impaired nitric oxide production by cultured human endothelial cells. *Amino Acids*. **42**, 1903–11

26. Lee, Y. S., Shibata, Y., Malhotra, A., and Dutta, A. (2009) A novel class of small RNAs: tRNA-derived RNA fragments (tRFs). *Genes Dev.* **23**, 2639–49

27. Magalhães, P. J., Andreu, A. L., and Schon, E. A. (1998) Evidence for the presence of 5S rRNA in mammalian mitochondria. *Mol. Biol. Cell*. **9**, 2375–82

28. Blanco, S., and Frye, M. (2014) Role of RNA methyltransferases in tissue renewal and pathology. *Curr. Opin. Cell Biol.* **31**, 1–7

29. Machnicka, M. A., Milanowska, K., Osman Oglou, O., Purta, E., Kurkowska, M., Olchowik, A., Januszewski, W., Kalinowski, S., Dunin-Horkawicz, S., Rother, K. M., Helm, M., Bujnicki, J. M., and Grosjean, H. (2013) MODOMICS: a database of RNA modification pathways--2013 update. *Nucleic Acids Res.* **41**, D262–7

30. Rodriguez-Corona, U., Sobol, M., Rodriguez-Zapata, L. C., Hozak, P., and Castano, E. (2015) Fibrillarin from Archaea to human. *Biol. Cell*. **107**, 159–174

31. Backlund, P. S., Carotti, D., and Cantoni, G. L. (1986) Effects of the S-adenosylhomocysteine hydrolase inhibitors 3-deazaadenosine and 3-deazaaristeromycin on RNA methylation and synthesis. *Eur. J. Biochem.* **160**, 245–51

32. Glick, J. M., Averyhart, V. M., and Leboy, P. S. (1978) Purification and characterization of two tRNA-(guanine)-methyltransferases from rat liver. *Biochim. Biophys. Acta*. **518**, 158–71

33. Decatur, W. A., and Fournier, M. J. (2003) RNA-guided nucleotide modification of ribosomal and other RNAs. *J. Biol. Chem.* **278**, 695–8

34. Green, T. J., Skeaff, C. M., McMahon, J. A., Venn, B. J., Williams, S. M., Devlin, A. M., and Innis, S. M. (2010) Homocysteine-lowering vitamins do not lower plasma S-adenosylhomocysteine in older people with elevated homocysteine concentrations. *Br. J. Nutr.* **103**, 1629–34

35. Wagner, C., and Koury, M. J. (2008) Plasma S-Adenosylhomocysteine Versus Homocysteine as a Marker for Vascular Disease. *J. Nutr.* **138**, 980

36. Basu, A., Das, P., Chaudhuri, S., Bevilacqua, E., Andrews, J., Barik, S., Hatzoglou, M., Komar, A. A., and Mazumder, B. (2011) Requirement of rRNA methylation for 80S ribosome assembly on a cohort of cellular internal ribosome entry sites. *Mol. Cell. Biol.* **31**, 4482–99

37. Decatur, W. A., and Fournier, M. J. (2002) rRNA modifications and ribosome function. *Trends Biochem. Sci.* **27**, 344–351

38. Caudill, M. A., Wang, J. C., Melnyk, S., Pogribny, I. P., Jernigan, S., Collins, M. D., Santos-Guzman, J., Swendseid, M. E., Cogger, E. A., and James, S. J. (2001) Intracellular S-adenosylhomocysteine concentrations predict global DNA hypomethylation in tissues of methyl-deficient cystathionine beta-synthase heterozygous mice. *J. Nutr.* **131**, 2811–8

39. Friedman, A. N., Bostom, A. G., Selhub, J., Levey, A. S., and Rosenberg, I. H. (2001) The kidney and homocysteine metabolism. *J. Am. Soc. Nephrol.* **12**, 2181–9

40. Wu, C.-C., Zheng, C.-M., Lin, Y.-F., Lo, L., Liao, M.-T., and Lu, K.-C. (2012) Role of homocysteine in end-stage renal disease. *Clin. Biochem.* **45**, 1286–94

41. Blanco, S., Dietmann, S., Flores, J. V., Hussain, S., Kutter, C., Humphreys, P., Lukk, M., Lombard, P., Treps, L., Popis, M., Kellner, S., Holter, S. M., Garrett, L., Wurst, W., Becker, L., Klopstock, T., Fuchs, H., Gailus-Durner, V., Hrabe de Angelis, M., Karadottir, R. T., Helm, M., Ule, J., Gleeson, J. G., Odom, D. T., and Frye, M. (2014) Aberrant methylation of tRNAs links cellular stress to neuro-developmental disorders. *EMBO J.* **33**, 2020–2039

42. Towns, W. L., and Begley, T. J. (2012) Transfer RNA methytransferases and their corresponding modifications in budding yeast and humans: activities, predications, and potential roles in human health. *DNA Cell Biol.* **31**, 434–54

Supplementary material

Supplemental Table 1 - Dynamic multiple reaction monitoring parameters used for identification and quantification of the ribonucleosides. Detection of the various nucleosides was performed in positive ion mode, and the cell accelerator voltage was set for 2 V.

Modified nucleoside	Precursor ion (m/z)	Product ion (m/z)	Fragmentor voltage (V)	Collision energy (eV)	Retention time (min)
m^1A	282	150	92	17	7
m^5C	258	126	40	9	8.2
m^7G	298	166	82	9	8.7
Cm	258	112	60	9	8.9
m^1G	298	166	82	9	12.7
m^2G	298	166	82	9	13.3
Gm	298	152	72	5	12.1
Am	282	136	92	13	15.6
m^6A	282	150	92	17	16.7
m_2^6A	296	164	102	17	18.9
m^5U	259	127	76	5	10.0
Um	259	113	66	5	11.8

CHAPTER

5

The Role of DNA Hypomethylation in S-Adenosylhomocysteine-Induced Endothelial Activation

The Role of DNA Hypomethylation in S-Adenosylhomocysteine-Induced Endothelial Activation

Madalena Barroso[a,b], Cristina Florindo[a], Isabel Tavares de Almeida[a], Joseph Loscalzo[b], Diane E. Handy[b], and Rita Castro[a,c].

[a] *The research Institute for Medicines (iMed.ULisboa), Faculty of Pharmacy, University of Lisbon, Lisbon, Portugal;*
[b] *Cardiovascular Division, Department of Medicine, Brigham and Women's Hospital and Harvard Medical School, Boston, MA, USA;*
[c] *Department of Biochemistry and Human Biology, Faculty of Pharmacy, University of Lisbon, Lisbon, Portugal.*

ABSTRACT

S-Adenosylhomocysteine (SAH) is a potent methylation inhibitor that has been associated with atherosclerosis. Our aim was to investigate the effects of SAH in endothelial activation, and assess whether DNA hypomethylation contributes to these effects. Intracellular SAH accumulation was induced in endothelial cells and cell activation was assessed by monitoring adhesion molecule expression and leukocyte transmigration in co-culture. A DNA-methyltransferase (DNMT) inhibitor was used to address the role of DNA hypomethylation in endothelial cell activation.

Excess SAH increased the expression of several adhesion molecules, favored leukocyte transmigration, and lessened global DNA methylation ($p<0.05$). DNMT inhibition reproduced the up-regulation of ICAM-1 (intercellular adhesion molecule-1; $p<0.05$), suggesting that hypomethylation of the *ICAM1* promoter may contribute to its up-regulation. However, detailed methylation analysis revealed that the *ICAM1* promoter was fully demethylated prior to SAH accumulation or DNMT inhibition.

We show that DNA hypomethylation can partially recapitulate the adverse effects of SAH in endothelial cells, but does so by mechanisms independent of adhesion molecule promoter hypomethylation. Our study confirms the physiological relevance of SAH-mediated endothelial cell activation showing that it favors leukocyte transmigration.

Key Words: **S-adenosylhomocysteine, DNA hypomethylation, endothelial activation, leukocyte transmigration, promoter methylation.**

1. INTRODUCTION

Hyperhomocysteinemia is an independent risk factor for cardiovascular disease (CVD) by mechanisms still incompletely defined (1). During hyperhomocysteinemia, the homocysteine precursor, S-adenosylhomocysteine (SAH), accumulates (2). Due, in part, to its ability to inhibit methyltransferases, SAH may contribute to the vascular toxicity of hyperhomocysteinemia (3–5).

The endothelium plays a complex role in vascular biology. Endothelial dysfunction is an early step in the development of atherosclerosis and it is characterized by a redox imbalance and reduced bioavailability of vasodilators (6). Endothelial dysfunction usually progresses to a cell activation stage, in which an up-regulation of pro-inflammatory cytokines and cell adhesion molecules is observed (6). This pro-inflammatory response favors leukocyte adhesion to the endothelium, in which selectins, intercellular adhesion molecule-1 (ICAM-1), and vascular adhesion molecule-1 (VCAM-1) are key players (7). In a subsequent and determinant step in the formation of the atheroma plaque, leukocytes transmigrate through the endothelial cell layer, a process in which platelet endothelial cell adhesion molecule-1 (PECAM-1) is critical (8).

Epigenetic modulation of gene expression has been widely associated with atherosclerosis (9, 10). Methylation of cytosine residues, usually found in a CpG dinucleotide context, is the main epigenetic modification present in DNA, and is usually associated with gene repression (10, 11). CpG islands are short DNA sequences with a high GC and CpG content that are predominantly nonmethylated in transcriptionally active genes (10).

In the present study our goal was to investigate the role of excess SAH in endothelial activation and assessed whether SAH-induced DNA hypomethylation contributes to these effects. Here, we show that SAH-induced hypomethylating stress led to the up-regulation of key adhesion molecules and increased leukocyte transmigration. Importantly, the increased expression of adhesion molecules was partially replicated by the use of a specific DNA methylation inhibitor, suggesting a potential role for SAH-induced epigenetic alterations in homocysteine-associated pro-atherogenic responses in endothelial cells.

2. MATERIALS AND METHODS

Cell Culture and Treatments – Human umbilical vein endothelial cells (HUVEC) (Lonza) were cultured as previously reported (12). Intracellular SAH accumulation was achieved by SAH hydrolase inhibition using adenosine-2',3'-dialdehyde (ADA) (20 μmol/L; Sigma) for 48 h (5, 12). The DNA methyltransferase (DNMT) inhibitor 5'-aza-2-deoxycytidine (5-aza-dC) (Sigma) was used at a final concentration of 5 μmol/L for 48 h.

Flow cytometry – Flow cytometry was used to assess the expression of adhesion molecules in the cell surface as in (5). Adhesion molecules were stained independently with specific fluorescent-conjugated antibodies for ICAM-1 (Santa Cruz Biotechnology), VCAM-1 (R&D Systems), E-selectin, and PECAM-1 (BioLegend).

Quantitative RT-PCR – RNA isolation, cDNA synthesis, and real-time PCR were performed as described in (5), using the following gene expression primers (Life Technologies): *ACTB* (4352935E), *ICAM1* (Hs00164932_m1), *VCAM1* (Hs00365485_m1), *SELE* (Hs00950401_m1), *PECAM1* (Hs00169777_m1).

Transmigration assay – Transendothelial migration of leukocytes was monitored using the QCM™ leukocyte transendothelial migration colorimetric assay (Millipore). Leukocytes isolated from whole blood from three healthy individuals (after their informed consent) were incubated with HUVEC for 8 h.

Global DNA methylation – 5-Methylcytosine (5-mC) levels were detected using the 5-mC DNA ELISA Kit (Zymo).

Targeted bisulfite sequencing – The number and distribution of CpG islands in the *ICAM1* gene (NCBI Reference Sequence: NC_000019.10, chr19:10268500-10273000) were determined using the MethPrimer program (13). A genomic sequence (NCBI Reference Sequence: NC_000019.10, chr19: 10269583-10271319) including 138 CpG sites and comprising the *ICAM1* gene promoter and first exon (−1565 to +160, relative to the transcription start site at +1) was selected for targeted bisulfite sequencing. DNA was isolated (DNeasy Blood & Tissue Kit; Qiagen) from ADA or 5-aza-dC treated and untreated cells in duplicate from three independent experiments. Following bisulfite treatment and amplification of the target sequence, next generation sequencing was performed, followed by sequence alignment and data analysis (Zymo Research Corporation, Irvine, CA, USA). A methylation ratio (MR) was calculated using the number of detected methylated CpGs divided by the total number of CpGs covered for every CpG site across the designated sequence.

Statistical Analysis – Results are shown as mean ± standard deviation. Statistical significance was determined using the Student's *t* test.

3. RESULTS

SAH-induced cell activation – In order to promote intracellular SAH accumulation, SAH hydrolase activity was inhibited with ADA. We have previously observed that HUVEC exposure to ADA increases intracellular SAH levels by more than 6-fold (5, 12). Moreover, excess SAH increased ICAM-1 and VCAM-1 expression (5). Accordingly, ICAM-1 and VCAM-1 were increased on the surface of ADA-treated cells by 2.1±0.5- and 1.3±0.5-fold, respectively ($p<0.05$; Fig. 1A). Additionally, PECAM-1 (1.3±0.1-fold, $p<0.05$) and E-selectin (1.2±0.1-fold, $p<0.05$) were both up-regulated at the cell surface. However, although ADA significantly increased ICAM-1, VCAM-1, and E-selectin mRNA levels by 2.8±0.7-, 2.7±1.0-, and 2.0±0.3-fold ($p<0.005$), respectively, PECAM-1 mRNA levels were decreased by 30.1±21.3 % ($p=0.05$, Fig. 1B). Pre-treatment with ADA significantly increased (2.2±1.3-fold, $p<0.05$ *versus* control; Fig. 1C) leukocyte migration across the endothelial cell monolayer ($p<0.05$ *versus* control; Fig. 1C).

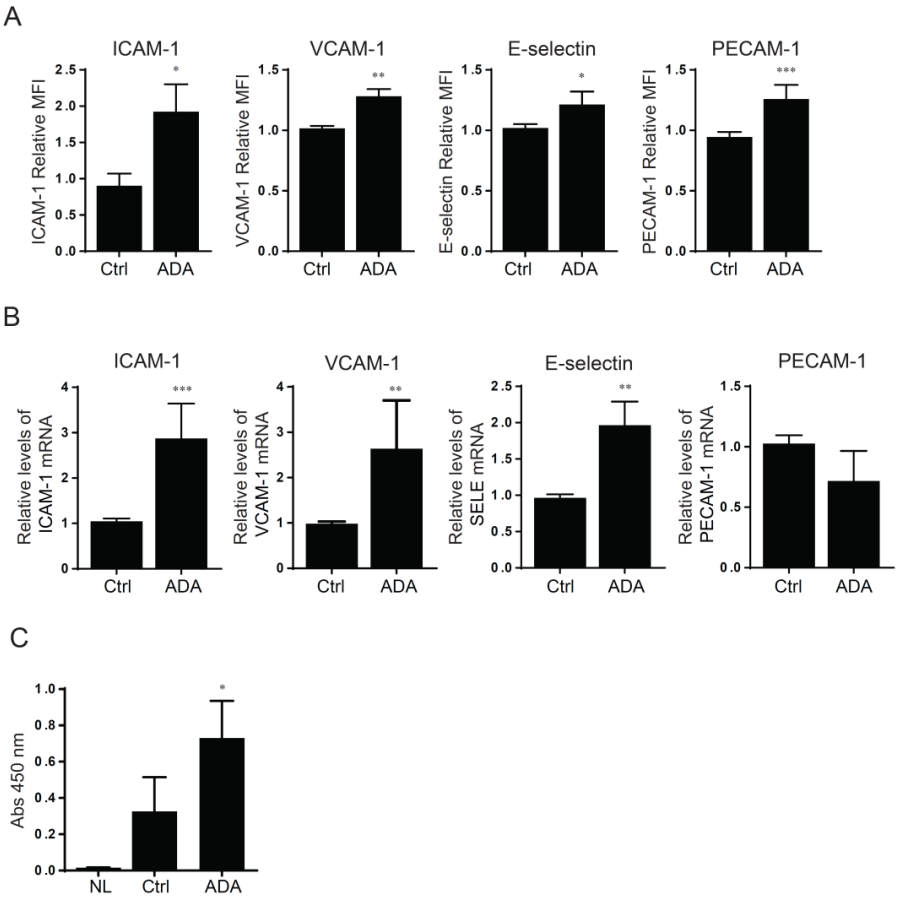

Figure 1 - **SAH accumulation and cell activation. (A)**, Flow cytometry was used to detect the relative cell-surface expression of ICAM-1, VCAM-1, E-selectin, and PECAM-1, in control (Ctrl) and ADA treated HUVEC (ADA) (n=3-6). MFI, mean fluorescence intensity. **(B)**, mRNA expression levels of *ICAM1*, *VCAM1*, *SELE* and *PECAM1*, were measured by quantitative RT-PCR to determine the effects of ADA compared to control (48 h; n=3-5). *, $p < 0.05$, **, $p < 0.005$, ***, $p < 0.0005$ *versus* control. **(C)**, The ADA effect on the number of leukocytes that transmigrate through the endothelial monolayer was analyzed by a transendothelial migration colorimetric assay (n=3). NL, no leukocytes added. Absorbance was measured at 450 nm. *, $p < 0.05$, **, $p < 0.005$, ***, $p < 0.0005$, *versus* control.

DNA hypomethylation and endothelial cell activation – Our previous studies demonstrated that excess SAH induces global DNA hypomethylation in HUVEC (2, 14). Accordingly, ADA treatment decreased 5-mC content by 22.3±6.3% ($p<0.005$; Fig. 2A). To address specifically the potential role of DNA hypomethylation in ADA-induced activation, cells were treated with a potent inhibitor of DNMTs, 5-aza-dC, which significantly ($p<0.05$) increased mRNA levels of ICAM-1 and E-selectin by 2.3±0.2- and 2.5±0.7-fold, respectively, without affecting VCAM-1 expression (Fig. 2B). The E-selectin coding gene, *SELE*, lacks a CpG rich promoter (15), therefore, in order to assess whether SAH-induced DNA hypomethylation could decrease specific promoter methylation, we focused our analysis on the *ICAM1* gene (NCBI Gene ID:3383). Four CpG islands were identified in a region comprising the *ICAM1* promoter and first exon (Fig. 2C). To examine CpG methylation in this region, we used targeted bisulfite sequencing and compared the cytosine methylation levels in DNA isolated from control, ADA-, and 5-aza-dC-treated cells. The average MR for the 138 detected CpGs sites was 0.009±0.03 (n=12), 0.008±0.03 (n=6), and 0.009±0.04 (n=6), for control, ADA, and 5-aza-dC treated cells, respectively. CpG sites with a MR below the 0.2 threshold are often considered as unmethylated (16). Thus, our results show extremely low levels of 5-mC in *ICAM1* gene CpG rich region in control cells with no significant changes in methylation following ADA or 5-aza-dC treatment.

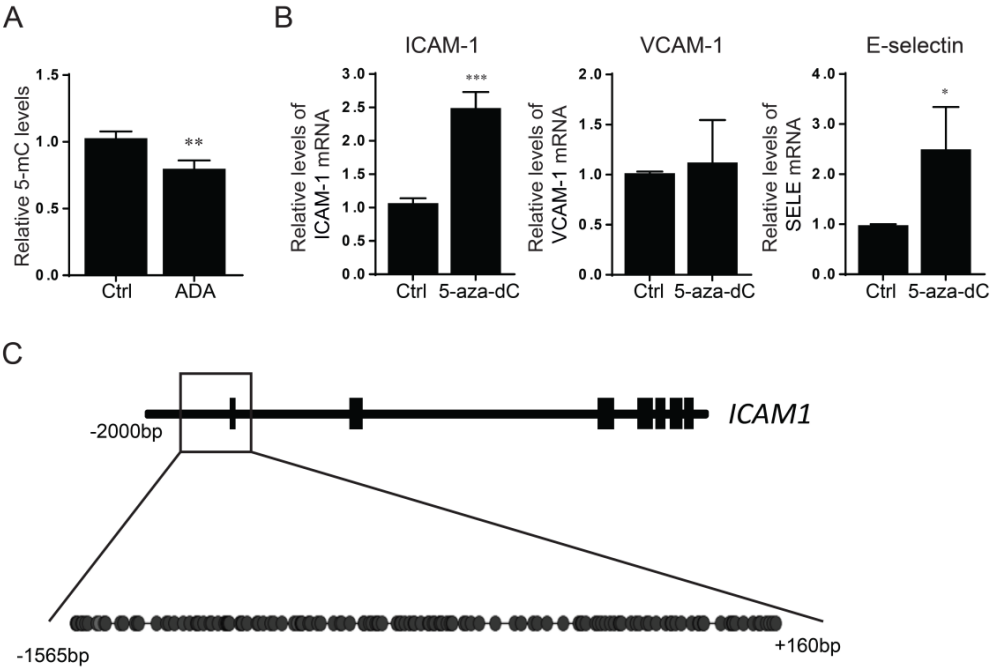

Figure 2 - DNA hypomethylation effects and endothelial cell activation. (A), Relative 5-mC levels in DNA samples, from control and ADA treated cells (n=4), were determined by an ELISA assay using a specific anti-5-mC antibody. **(B)**, *ICAM1*, *VCAM1* and *SELE* expression changes induced by 5-aza-dC, were monitored by quantitative RT-PCR (n=3-4). **(C)**, Schematic representation of *ICAM1* gene (NCBI Gene ID:3383) and promoter region. Vertical black bars represent the seven *ICAM1* exons. The promoter and gene region included in the square (□) were analyzed by targeted bisulfite sequencing; the methylation ratios of the CpG sites (black circles) were all below 0.2 for control and treated samples (12 control, 6 ADA and 6 AZA treated samples) with no significant changes among treatments.

4. DISCUSSION

Impaired methylation has been associated with several diseases, including CVD (17–20). Our research has explored the impact of excess SAH in endothelial dysfunction (2, 5, 14). In the present study, we examined the endothelial expression of key cell-surface proteins involved in the adhesion and transmigration processes to identify targets that may be up-regulated by SAH-induced DNA hypomethylation. ICAM-1, VCAM-1, and E-selectin contribute to the early stages of leukocyte adhesion, whereas PECAM-1 is more important for their transmigration (7). We found that excess SAH increases the cell surface expression of all the aforementioned adhesion molecules. Similar to our previous studies (5), ICAM-1 and VCAM-1 mRNA levels were increased following ADA treatment. E-selectin transcript levels were also increased, although PECAM-1 mRNA levels were slightly decreased. Interestingly, the amount of PECAM-1 in the cell surface may not reflect the levels of PECAM-1 synthesis. In fact, in resting conditions, PECAM-1 is stored in intracellular compartments near the plasma membrane and, upon endothelial cell activation, PECAM-1 may translocate to the cell membrane, contributing to leukocyte transmigration (8, 21).

DNA methylation is an important epigenetic mechanism of gene expression regulation, which we previously found to be impaired by excess SAH (2, 14). Here, we used an additional methodology to confirm the SAH-induced DNA hypomethylation in endothelial cells. Excess SAH can impair the methylation of several targets, such as proteins, RNA, and DNA (5, 14). To address specifically the role of DNA hypomethylation in up-regulating adhesion molecule gene expression, we inhibited DNMT activity using 5-aza-dC. Similar to ADA, 5-aza-dC treatment increased the expression levels of *ICAM1* and *SELE*, suggesting that these genes are potential targets for regulation by SAH-induced DNA hypomethylation. PECAM-1 mRNA levels were unaffected by excess SAH and, therefore, PECAM-1 expression is less likely to be regulated by DNA hypomethylation under ADA treatment. For this reason, the effects of 5-aza-dC on PECAM-1 were not examined. VCAM-1 expression was not significantly altered by DNMT inhibition. This observation may be explained by the lack of a CpG rich promoter in the *VCAM1* gene. The *SELE* promoter, however, does not have CpG islands; yet, its expression was increased following 5-aza-dC treatment. This observation may be explained by long-distance epigenetic activation or indirect mechanisms of epigenetic regulation (as discussed further below) (11, 22).

ICAM1, which has a CpG-rich promoter, was up-regulated by both ADA and 5-aza-dC treatments. To address whether *ICAM1* promotor hypomethylation could explain these observations, we assessed its methylation status. The regulation of *ICAM1* expression by alterations in its promoter methylation has been reported previously for tumor-conditioned endothelial cells, which had significantly higher *ICAM1* promoter methylation with an associated repression of *ICAM1* expression, compared to HUVEC (23, 24). Moreover, increased expression of ICAM-1 was correlated with decreased promoter 5-mC content in endothelial cells of Keshan disease patients (25). Compared to

these previous studies, we analyzed an extended region of the promoter as well as the first exon of the *ICAM1* gene. We found that CpG methylation was virtually undetectable in HUVEC under control conditions; neither ADA nor 5-aza-dC altered the methylation status at the 138 CpG sites analyzed. We cannot exclude the possibility that these agents may alter methylation in other regions of the *ICAM1* gene or that they altered the expression of other regulatory molecules important for ICAM-1 expression. In fact, it was reported that ICAM-1 expression can be induced in response to p66shc up-regulation due to promoter hypomethylation (22).

Previously, we found that SAH-induced expression of adhesion molecules increased leukocyte adhesion to endothelial cells (5). Here, we show that SAH-mediated cell activation also favors leukocyte transmigration. We provide evidence that excess SAH promotes DNA hypomethylation, which may contribute to the up-regulation of ICAM-1 and E-selectin by mechanisms that are still unclear. DNA hypomethylation did not alter the methylation status of the *ICAM1* promoter CpG islands, which were found to be unmethylated under basal conditions. Further analysis is needed to fully address the key methylation targets impaired by excess SAH.

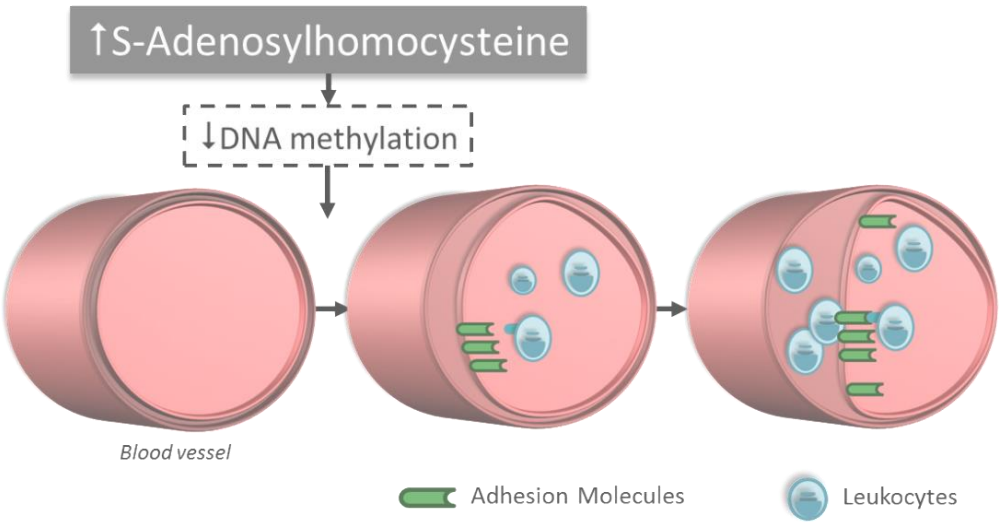

Figure 3 –Schematic representation of SAH induced-endothelial activation and transmigration.

ACKNOWLEDGEMENT

We are very thankful to Isabel Rivera (iMed.ULisboa, Lisbon, Portugal) for her support and scientific advising.

FUNDING

This work was supported by Fundação para a Ciência e a Tecnologia grants PTDC/SAU-ORG/112683/2009 and UID/DTP/04138/2013 (iMed.ULisboa), and SFRH/BD/73021/2010 (MB), and by NIH grants HL0671795, HL048743, HL108630 and HL119145 (JL).

CONFLICTS OF INTEREST

The authors have no conflict of interest.

REFERENCES

1. Boers, G. H. (2000) Mild hyperhomocysteinemia is an independent risk factor of arterial vascular disease. *Semin. Thromb. Hemost.* **26**, 291–5
2. Castro, R., Rivera, I., Struys, E. A., Jansen, E. E. W., Ravasco, P., Camilo, M. E., Blom, H. J., Jakobs, C., and Tavares de Almeida, I. (2003) Increased homocysteine and S-adenosylhomocysteine concentrations and DNA hypomethylation in vascular disease. *Clin. Chem.* **49**, 1292–6
3. Wagner, C., and Koury, M. J. (2008) Plasma S-Adenosylhomocysteine Versus Homocysteine as a Marker for Vascular Disease. *J. Nutr.* **138**, 980
4. Xiao, Y., Huang, W., Zhang, J., Peng, C., Xia, M., and Ling, W. (2015) Increased plasma S-adenosylhomocysteine-accelerated atherosclerosis is associated with epigenetic regulation of endoplasmic reticulum stress in apoE-/- mice. *Arterioscler. Thromb. Vasc. Biol.* **35**, 60–70
5. Barroso, M., Florindo, C., Kalwa, H., Silva, Z., Turanov, A. A., Carlson, B. A., de Almeida, I. T., Blom, H. J., Gladyshev, V. N., Hatfield, D. L., Michel, T., Castro, R., Loscalzo, J., and Handy, D. E. (2014) Inhibition of cellular methyltransferases promotes endothelial cell activation by suppressing glutathione peroxidase 1 protein expression. *J. Biol. Chem.* **289**, 15350–62
6. Davignon, J., and Ganz, P. (2004) Role of endothelial dysfunction in atherosclerosis. *Circulation*. **109**, III27–32
7. Muller, W. A. (2002) Leukocyte-Endothelial Cell Interactions in the Inflammatory Response. *Lab. Investig.* **82**, 521–534
8. Mamdouh, Z., Kreitzer, G. E., and Muller, W. A. (2008) Leukocyte transmigration requires kinesin-mediated microtubule-dependent membrane trafficking from the lateral border recycling compartment. *J. Exp. Med.* **205**, 951–66
9. Aavik, E., Lumivuori, H., Leppänen, O., Wirth, T., Häkkinen, S.-K., Bräsen, J.-H., Beschorner, U., Zeller, T., Braspenning, M., van Criekinge, W., Mäkinen, K., and Ylä-Herttuala, S. (2014) Global DNA methylation analysis of human atherosclerotic plaques reveals extensive genomic hypomethylation and reactivation at imprinted locus 14q32 involving induction of a miRNA cluster. *Eur. Heart J.* **36**, 993–1000
10. Handy, D. E., Castro, R., and Loscalzo, J. (2011) Epigenetic modifications: basic mechanisms and role in cardiovascular disease. *Circulation*. **123**, 2145–56
11. Aran, D., Sabato, S., and Hellman, A. (2013) DNA methylation of distal regulatory sites characterizes dysregulation of cancer genes. *Genome Biol.* **14**, R21
12. Barroso, M., Rocha, M. S., Esse, R., Gonçalves, I., Gomes, A. Q., Teerlink, T., Jakobs, C., Blom, H. J., Loscalzo, J., Rivera, I., Tavares de Almeida, I., and Castro, R. (2012) Cellular hypomethylation is associated with impaired nitric oxide production by cultured human endothelial cells. *Amino Acids*. **42**, 1903–11
13. Li, L.-C., and Dahiya, R. (2002) MethPrimer: designing primers for methylation PCRs. *Bioinformatics*. **18**, 1427–31

14. Esse, R., Rocha, M. S., Barroso, M., Florindo, C., Teerlink, T., Kok, R. M., Smulders, Y. M., Rivera, I., Leandro, P., Koolwijk, P., Castro, R., Blom, H. J., and de Almeida, I. T. (2013) Protein arginine methylation is more prone to inhibition by S-adenosylhomocysteine than DNA methylation in vascular endothelial cells. *PLoS One*. **8**, e55483

15. Du, X., Han, L., Guo, A.-Y., and Zhao, Z. (2012) Features of methylation and gene expression in the promoter-associated CpG islands using human methylome data. *Comp. Funct. Genomics*. **2012**, 598987

16. Hackenberg, M., Barturen, G., and Oliver, J. L. (2011) NGSmethDB: a database for next-generation sequencing single-cytosine-resolution DNA methylation data. *Nucleic Acids Res.* **39**, D75–9

17. Pogribny, I. P., and Beland, F. A. (2009) DNA hypomethylation in the origin and pathogenesis of human diseases. *Cell. Mol. Life Sci.* **66**, 2249–61

18. Lü, C.-X., Xu, R.-D., Cao, M., Wang, G., Yan, F.-Q., Shang, S.-S., Wu, X.-F., Ruan, L., Quan, X.-Q., and Zhang, C.-T. (2013) FOXP3 demethylation as a means of identifying quantitative defects in regulatory T cells in acute coronary syndrome. *Atherosclerosis*. **229**, 263–70

19. Fleming, J. L., Phiel, C. J., and Toland, A. E. (2012) The role for oxidative stress in aberrant DNA methylation in Alzheimer's disease. *Curr. Alzheimer Res.* **9**, 1077–96

20. Castro, R., Barroso, M., Rocha, M., Esse, R., Ramos, R., Ravasco, P., Rivera, I., and de Almeida, I. T. (2010) The TCN2 776CNG polymorphism correlates with vitamin B(12) cellular delivery in healthy adult populations. *Clin. Biochem.* **43**, 645–9

21. Bonecchi, R. (2008) Transmigration at the borders: Recycling and trafficking of adhesion molecules. *Cell Adh. Migr.* **2**, 55–6

22. Kim, C.-S., Kim, Y.-R., Naqvi, A., Kumar, S., Hoffman, T. A., Jung, S.-B., Kumar, A., Jeon, B.-H., McNamara, D. M., and Irani, K. (2011) Homocysteine promotes human endothelial cell dysfunction via site-specific epigenetic regulation of p66shc. *Cardiovasc. Res.* **92**, 466–75

23. Hellebrekers, D. M. E. I., Castermans, K., Viré, E., Dings, R. P. M., Hoebers, N. T. H., Mayo, K. H., Oude Egbrink, M. G. A., Molema, G., Fuks, F., van Engeland, M., and Griffioen, A. W. (2006) Epigenetic regulation of tumor endothelial cell anergy: silencing of intercellular adhesion molecule-1 by histone modifications. *Cancer Res.* **66**, 10770–7

24. Hellebrekers, D. M. E. I., Melotte, V., Viré, E., Langenkamp, E., Molema, G., Fuks, F., Herman, J. G., Van Criekinge, W., Griffioen, A. W., and van Engeland, M. (2007) Identification of epigenetically silenced genes in tumor endothelial cells. *Cancer Res.* **67**, 4138–48

25. Yang, G., Zhu, Y., Dong, X., Duan, Z., Niu, X., and Wei, J. (2014) TLR2-ICAM1-Gadd45α axis mediates the epigenetic effect of selenium on DNA methylation and gene expression in Keshan disease. *Biol. Trace Elem. Res.* **159**, 69–80

CHAPTER

6

S-Adenosylhomocysteine Induces Inflammation Through NFkB: a Possible Role for EZH2 in Endothelial Cell Activation

Biochim Biophys Acta. 2015 *(under revision)*

S-Adenosylhomocysteine Induces Inflammation Through NFkB: a Possible Role for EZH2 in Endothelial Cell Activation

Madalena Barroso[a,b], Derrick Kao[a], Isabel Tavares de Almeida[b], Rita Castro[b,c], Joseph Loscalzo[a], and Diane E. Handy[a*].

[a] *Cardiovascular Division, Department of Medicine, Brigham and Women's Hospital and Harvard Medical School, Boston, MA, USA;*
[b] *The Research Institute for Medicines (iMed.ULisboa), Faculty of Pharmacy, University of Lisbon, Lisbon, Portugal.*
[c] *Department of Biochemistry and Human Biology, Faculty of Pharmacy, University of Lisbon, Lisbon, Portugal.*

ABSTRACT

S-Adenosylhomocysteine (SAH) can induce endothelial dysfunction and activation, contributing to atherogenesis; however, its role in the activation of the inflammatory mediator NFkB has not been explored. Our aim was to determine the role of NFkB in SAH-induced activation of endothelial cells. Furthermore, we examined whether SAH, as a potent inhibitor of S-adenosylmethionine-dependent methyltransferases, suppresses the function of EZH2 methyltransferase to contribute to SAH-induced endothelial cell activation. We found that excess SAH increases the expression of adhesion molecules and cytokines in human coronary artery endothelial cells. Importantly, this up-regulation was suppressed in cells expressing a dominant negative form of the NFkB inhibitor, IkB. Moreover, SAH accumulation triggers the activation of both the canonical and non-canonical NFkB pathways and represses EZH2 activity, decreasing histone H3 lysine 27 trimethylation. EZH2 knockdown recapitulated the effects of excess SAH on endothelial activation, i.e., it induced NFkB activation and the subsequent up-regulation of adhesion molecules and cytokines. Our findings suggest that suppression of the epigenetic regulator EZH2 by excess SAH may contribute to NFkB activation and the consequent vascular inflammatory response. These studies unveil new targets of SAH regulation, demonstrating that EZH2 suppression and NFkB activation mediated by SAH accumulation may contribute to its adverse effects in the vasculature.

Key Words: ***S-adenosylhomocysteine, endothelial activation, adhesion molecules, NFkB, methylation, EZH2.***

1. INTRODUCTION

S-Adenosylhomocysteine (SAH) is an inhibitor of cell methyltransferases that accumulates during hyperhomocysteinemia. SAH-induced hypomethylation of DNA, protein, and RNA have been associated with vascular disease (1–4). Elevated homocysteine in plasma is an independent risk factor for cardiovascular diseases (5). We and others have suggested that SAH is a key mediator of homocysteine-associated atherogenesis (1, 6, 7). Our previous studies show that SAH can induce endothelial cell dysfunction and activation by decreasing nitric oxide production and increasing oxidative stress and leukocyte adhesion (1, 8). The molecular mechanisms by which SAH induces a pro-inflammatory phenotype are, however, not completely understood. Several studies have reported a role for the nuclear transcription factor kB (NFkB) in endothelial dysfunction and atherosclerosis (9–11).

NFkB is a major regulator of important cell processes, such as inflammation, immunity, cellular proliferation, and apoptosis (12, 13). NFkB complexes are composed of homo- or heterodimers of various NFkB family members, including p50, p52, p65 (RelA), RelB, and c-Rel (12, 14). The NFkB pathway can be triggered by several stimuli, including inflammatory cytokines such as tumor necrosis factor-α (TNF-α) and interleukin-1β (IL-1β), which initiate the classical pathway; or other stimuli such as the CD40 ligand, and lymphotoxin β, which trigger the alternative NFkB pathway (12, 13).

DNA and histones are well studied targets of methyltransferases that can modulate important cellular processes. Enhancer of Zeste homolog 2 (EZH2) is the catalytic core of the Polycomb repressive complex (PRC) 2 and establishes the major mark of transcriptional repression in mammalian cells: the trimethylation of lysine 27 on histone H3 (H3K27me3) (15). As an S-adenosylmethionine-dependent methyltransferase, EZH2 is a target for SAH-mediated inhibition. EZH2 modulates many cellular processes, including inflammation and cell adhesion, by targeting genes such as *IL1B* and *CDH13* (16). The H3K27me3 mark can be removed by the Jumonji domain containing 3 (JMJD3) or the ubiquitously transcribed tetratricopeptide repeat on X chromosome (UTX) demethylases (17–19).

We previously used human umbilical vein endothelial cells (HUVEC) to investigate the role of excess SAH in endothelial activation. Our findings showed that SAH-induced oxidative stress promotes an up-regulation of adhesion molecules (1), however, the molecular mechanisms by which redox changes activate inflammatory responses under excess SAH were not completely resolved. Here, we analyze the effects of SAH on human coronary artery endothelial cells (HCAEC), and demonstrate the role of SAH-mediated hypomethylation on NFkB activation and modulation of pro-inflammatory signals. Additionally, we show that excess SAH suppresses the expression of EZH2 and that EZH2 knockdown mimics the endothelial cell responses to excess SAH, suggesting that the suppression of this methyltransferase may contribute to SAH-mediated endothelial dysfunction.

2. MATERIALS AND METHODS

Cell Culture and Treatments – Human coronary artery endothelial cells (HCAECs) were cultured at 37º C in 5% CO_2. Cells were grown in EBM-2 supplemented (EGM-2-MV) medium (Lonza) without antibiotics. Experiments were performed between passages five and eight and with cells 70 to 80% confluent. Treatments with adenosine-2',3'-dialdehyde (ADA) (Sigma) were performed for 48 h at 20 µM concentration. Tumor necrosis factor-α (TNF-α) treatments (10 ng/mL; R&D systems) were performed for 24h.

Real-Time PCR – RNeasy Mini kit (Qiagen) was used for RNA extraction. DNase (Qiagen) treatment was performed during the RNA extraction protocol, according to the manufacturer's instructions. After reverse-transcription using the Advantage RT-for-PCR kit (Clontech), cDNA was used for real-time PCR reactions with TaqMan Universal PCR Master Mix (Life Technologies) and specific gene expression primers (Life Technologies): *ACTB* (β-actin) (4352935E); *ICAM1* (Hs00164932_m1); *SELE* (Hs00950401_m1); *VCAM1* (Hs00365485_m1); *PECAM1* (Hs00169777_m1); *RELA* (Hs00153294_m1); *NFKB1* (Hs00231653_m1); *NFKB2* (Hs00174517_m1); *IL1B* (Hs01555410_m1); *TNFA* (Hs01113624_g1); *EZH2* (Hs00544833_m1); *JMJD3* (Hs00996325_g1); *CDKN1A* (Hs00355782_m1); *CDKN2A* (Hs00923894_m1). PCR reactions were performed using a PRISM 7900 HT Sequence Detector (Applied Biosystems). The ΔΔCT method was used for relative quantification using β-actin as the endogenous control.

Nuclear Protein Extraction – Nuclear protein extracts were obtained with the NE-PER nuclear and cytoplasmic extraction reagents (Thermo Scientific) following the kit protocol.

NFKB Inhibition – The dominant negative IkBα adenovirus (AdIkBDN) (Vector Biolabs) was used to overexpress a recombinant form of the *IKBα,* which is resistant to its phosphorylation-induced degradation. HCAEC infection with AdIkBDN was performed simultaneously with ADA treatments. An empty adenoviral vector was used as a control (AdCtrl) (Vector Biolabs).

Luciferase and β-galactosidase Assays – A luciferase adenoviral expression vector (AdNFkB-Luc) (Vector Biolabs) controlled by a promoter containing five repeats of the NFkB enhancer element (TGGGGACTTTCCGC) was used to infect HCAECs that were simultaneously infected with a β -galactosidase expression vector (Vector Biolabs). HCAEC were infected with adenovirus for 24 h prior to treatments. Cell lysates were obtained using the reporter lysis buffer (Promega) and promptly used for the luciferase and β-galactosidase enzyme assays (Promega). Firefly luciferease activity was

measured using the 20/20^n luminometer (Turner Biosystems), while β-galactosidase activity was measured by absorbance detection at 420 nm (SPECTRA MAX 190, Molecular Devices).

Histone Extraction – Histone extracts were prepared using EpiQuik total histone extraction kit (Epigentek) following the manufacturer's instructions.

siRNA Transfections – Transfections with small interference RNA (siRNA) were performed in OPTI-MEM medium (Life Technologies) using lipofectamine 2000 (Life Technologies) and a stealth siRNA to EZH2 (5'-GACCACAGUGUUACCAGCAUUUGGA-3') or a scrambled control siRNA (5'-GGUAGCGCCAAUCCUUACGUCUCUU-3'). The final siRNA concentration used was 52 nM.

Statistical Analysis – All of the experiments were repeated three to five times. Results are shown as mean ± standard deviation. Statistical significance of the differences between means was determined by Student's *t* test or ANOVA followed by post-hoc multiple comparisons using the Newman-Keuls test for experiments with two or more conditions, respectively.

3. RESULTS

Endothelial cell activation by excess SAH – We previously showed that ADA-induced SAH hydrolase inhibition reduces the S-adenosylmethionine/SAH ratio over 6-fold in endothelial cells due to a significant accumulation of SAH. In HUVEC, this treatment results in increased expression of adhesion molecules (1). In Figure 1, we examined whether ADA modulates the expression of adhesion molecules in human endothelial cells derived from coronary artery (HCAECs), a type of endothelial cells more relevant to atherosclerotic vascular disease than HUVECs. After 48h of incubation with the SAH hydrolase inhibitor (ADA), HCAECs had a 4.0 ± 1.1- and 2.5 ± 0.5-fold increase in the mRNA levels of the adhesion molecules ICAM-1 (intercellular adhesion molecule-1) and VCAM-1 (vascular adhesion molecule-1) ($p < 0.005$), respectively (Fig. 1A), similar to our previous findings in HUVECs (1). Two additional adhesion molecules were studied: E-selectin and PECAM-1 (platelet endothelial cell adhesion molecule-1). E-selectin transcripts were also increased by 5.2 ± 1.0-fold ($p < 0.005$), whereas ADA significantly decreased PECAM-1 transcript levels by 37.4 ± 13.4 % ($p < 0.0005$) (Fig. 1A). Accordingly, ICAM-1 and VCAM-1 protein levels were up-regulated by 2.2 ± 0.4- and 3.5 ± 0.8-fold ($p < 0.0005$), respectively, in ADA-treated HCAECs (Fig. 1B).

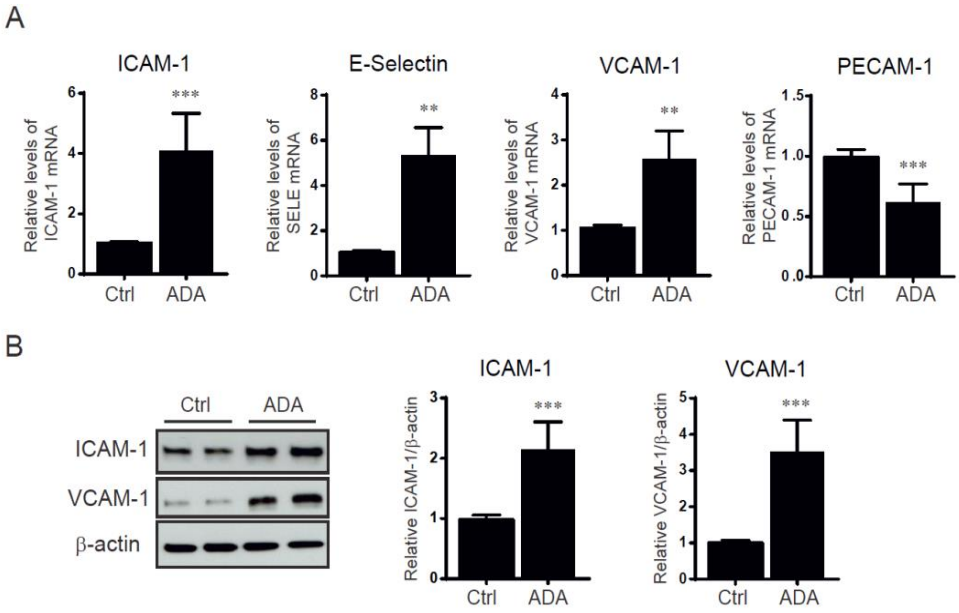

Figure 1 - SAH accumulation and cell activation. (A), mRNA expression levels of ICAM-1, E-Selectin, VCAM-1, and PECAM-1 were measured by quantitative RT-PCR to determine the effects of ADA 20 µmol/L (ADA) compared to control (Ctrl) (n= 3-5). **(B)**, Western blot analysis of ICAM-1 and VCAM-1 following ADA treatment for 48 h. Summary densitometry measurements for five independent experiments is shown on the right of the representative immunoblots. **, $p < 0.005$, ***, $p < 0.0005$ *versus* control.

NFkB pathway activation by excess SAH – We next examined whether ADA treatment activates the NFkB pathway. To do so, we initially monitored p50 and p65, as they are the most abundant NFkB components in the canonical pathway (20). ADA treatment had no significant effect on the expression of the p50 and p65 encoding genes, *NFKB1* and *RELA*, respectively (Fig. 2A). Activation of the canonical pathway is usually marked by the phosphorylation and degradation of the NFkB inhibitory protein IkBα, releasing NFkB and allowing its migration to the nucleus (14). In order to study this process, we assessed IkBα degradation and p65 translocation. After ADA treatment, IkBα levels decreased by 72.2 ± 17.1 % ($p < 0.005$), and a 42.1 ± 17.5 % increase of nuclear p65 protein was observed ($p < 0.05$; Fig. 2B&C). Taken together, these data support the notion that ADA induces activation of the NFkB canonical pathway. To confirm the effects of excess SAH on NFkB-induced transcriptional activation, we used an *NFkB* luciferase reporter construct (Fig. 2D). TNF-α was used as a positive control, as it is a well-known activator of NFkB in endothelial cells (21). As expected, non-infected cells had no detectable luciferase activity, whereas infected cells treated with TNF-α for 24 h had a 4.4 ± 0.6-fold increase in luciferase activity compared with infected cells not exposed to TNF-α or ADA. Similarly, intracellular SAH accumulation significantly increased NFkB-dependent luciferase activity by 2.8 ± 0.3-fold ($p < 0.0005$).

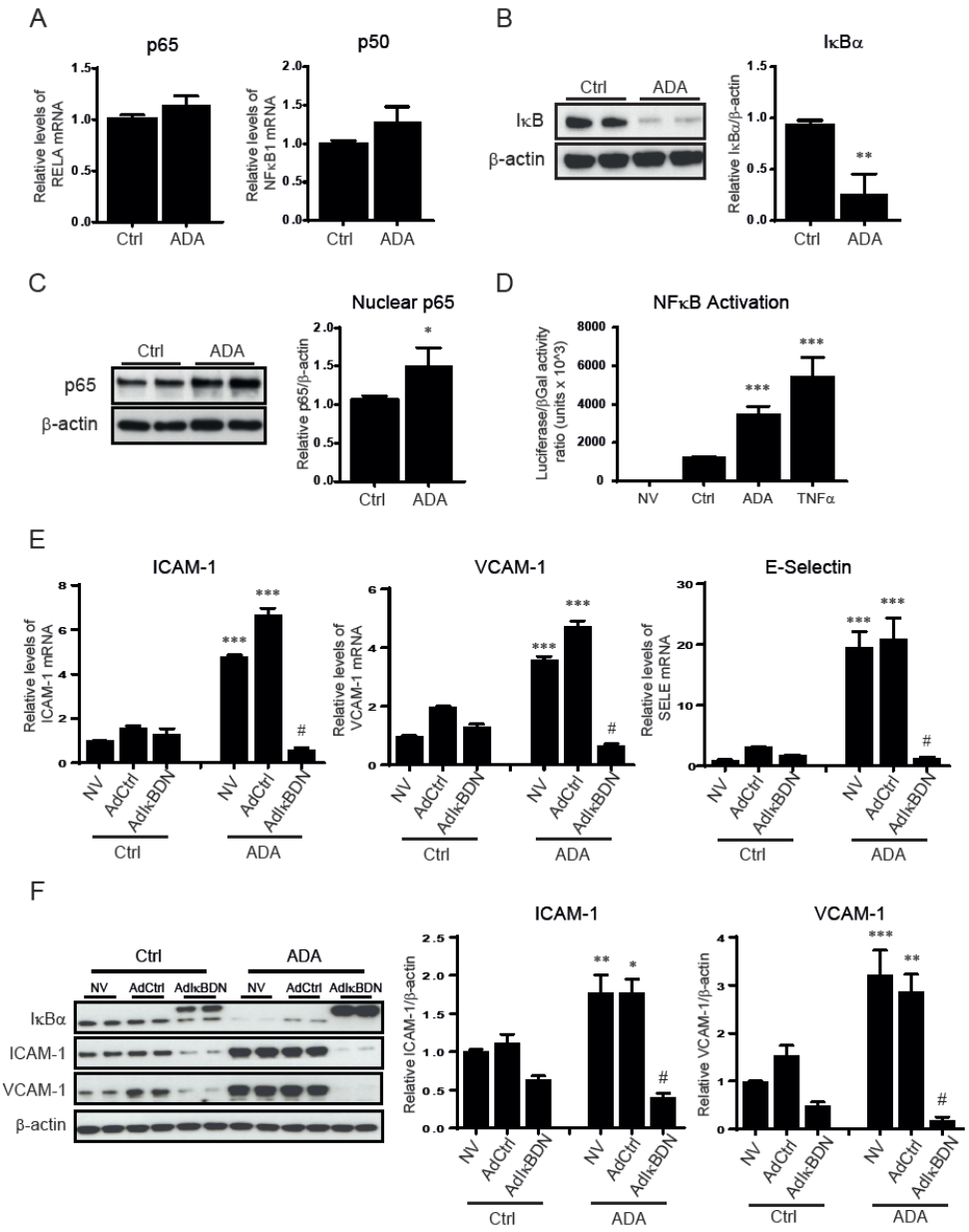

Figure 2 - NFkB pathway activation and its role in SAH-mediated up-regulation of adhesion molecules. (A), ADA-mediated changes in *RELA* (p65) and *NFKB1* (p50) gene expression were measured by quantitative RT-PCR using β-actin as an endogenous control (n=3). **(B)**, IkBα protein degradation induced by ADA was evaluated by Western blot. A representative blot is shown on the left and summary densitometry measurements on the right (n=3). **(C)**, Nuclear levels of p65. Western blot was used to analyze nuclear extracts. Shown are a representative Western blot (left) and a graph of the average densitometry measurements (right, n=3). **(D)**, The ability of ADA to promote NFkB-mediated transcription was analyzed using an NFkB luciferase reporter adenovirus construct simultaneously with a β-galactosidase vector (n=4). Luciferase expression was normalized to β-galactosidase activity. Results are shown for uninfected HCAECs (NV) and infected cells without treatment (Ctrl) or treated with ADA for 48 h (ADA) or TNF-α for 24 h (TNFα). E & F, Cells overexpressing dominant negative IkBα (AdIkBDN), infected with an empty control adenovirus (AdCtrl), and uninfected control cells (NV) were incubated in the presence or absence of ADA. **(E)**, Quantitative RT-PCR was used to study differences in mRNA levels of ICAM-1, VCAM-1, and E-selectin. **(F)**, Protein extracts were used for Western blot analysis. A representative immunoblot (left) and a summary densitometry measurements (right) are shown (n= 3). Note that the recombinant IkBDN migrates more slowly than the endogenous IkBα. A, B and C. *, $p < 0.05$, **, $p < 0.005$, ***, $p < 0.0005$, *versus* control. ANOVA, followed by the Newman-Keuls test for multiple comparisons, was used in the analysis shown in panels D, E and F. *, $p < 0.05$, **, $p < 0.005$, ***, $p < 0.0005$, *versus* the corresponding condition without ADA treatment. #, $p < 0.0005$, *versus* ADA treated cells with no virus or those infected with the AdCrl (ADA- AdCtrl).

IkBα degradation is induced after its phosphorylation at serine residues S32 and S36 (22). To block NFkB activation, we overexpressed the dominant-negative mutant NFkB inhibitor (IkBDN), which lacks S32 and S36 and cannot be targeted for degradation (Fig. 2E&F) (23). Wild type IkBα levels (lower molecular weight) are reduced after ADA treatment whereas the recombinant IkBDN (higher molecular weight) is modestly up-regulated by ADA treatment (Fig. 2F). As shown in Figures 2E&F, baseline adenoviral infection had no effect on the expression of adhesion molecules when compared to non-infected cells (NV). Upon ADA exposure, cells infected with the control adenovirus (AdCtrl) had a 4.2 ± 0.3-fold up-regulation of ICAM-1 mRNA levels ($p < 0.0005$). This effect was inhibited by the presence of the IkBDN ($p < 0.0005$). Similarly, VCAM-1 and E-selectin transcript levels were reduced by IkBDN to 13.7 ± 2.2 % and 6.1 ± 1.5 % ($p < 0.0005$), respectively, in ADA-treated cells. ADA significantly augmented ICAM-1 (1.6 ± 0.2-fold) and VCAM-1 (1.9 ± 0.3-fold) protein expression in cells transduced with the AdCtrl ($p < 0.05$). These effects were attenuated by expression of the IkBDN ($p < 0.0005$, Fig. 2F).

Alternative NFkB pathway activation – Unlike the canonical pathway, the non-canonical or alternative NFkB pathway is independent of IkBα and involves p100 phosphorylation and processing to the NFkB active subunit p52 (24). We analyzed the activation of the non-canonical NFkB pathway by monitoring changes in the expression of *NFKB2* and its gene products, p100 and p52 (Fig. 3). There was a significant increase in *NFKB2* gene expression (1.8 ± 0.2-fold) following ADA treatment ($p < 0.0005$). Western blot analysis revealed a 1.8 ± 0.2-fold concomitant increase in p100 levels ($p < 0.05$) upon ADA exposure with evidence for increased p100 processing, as illustrated by the higher levels of p52 detectable under excess SAH compared to the control (2.5 ± 0.4-fold increase; $p < 0.005$).

We next used the adenoviral vector IkBDN to determine whether the NFkB canonical pathway modulates the non-canonical pathway (Fig. 3C&D). Although the presence of the control virus augmented the ADA-induced up-regulation of *NFKB2* gene expression compared to ADA-treated cells with no virus, ADA treatment further increased *NFkB2* mRNA levels 2.0 ± 0.04-fold ($p < 0.0005$) in the AdCtrl cells. In contrast, ADA-induced expression of *NFKB2* was significantly attenuated by IkBDN ($p < 0.0005$). Accordingly, endothelial cells infected with the AdCtrl also manifested a p52 increase (2.9 ± 0.6-fold; $p < 0.0005$) with ADA treatment, which was abolished by the presence of IkBDN ($p < 0.0005$, Fig. 3D).

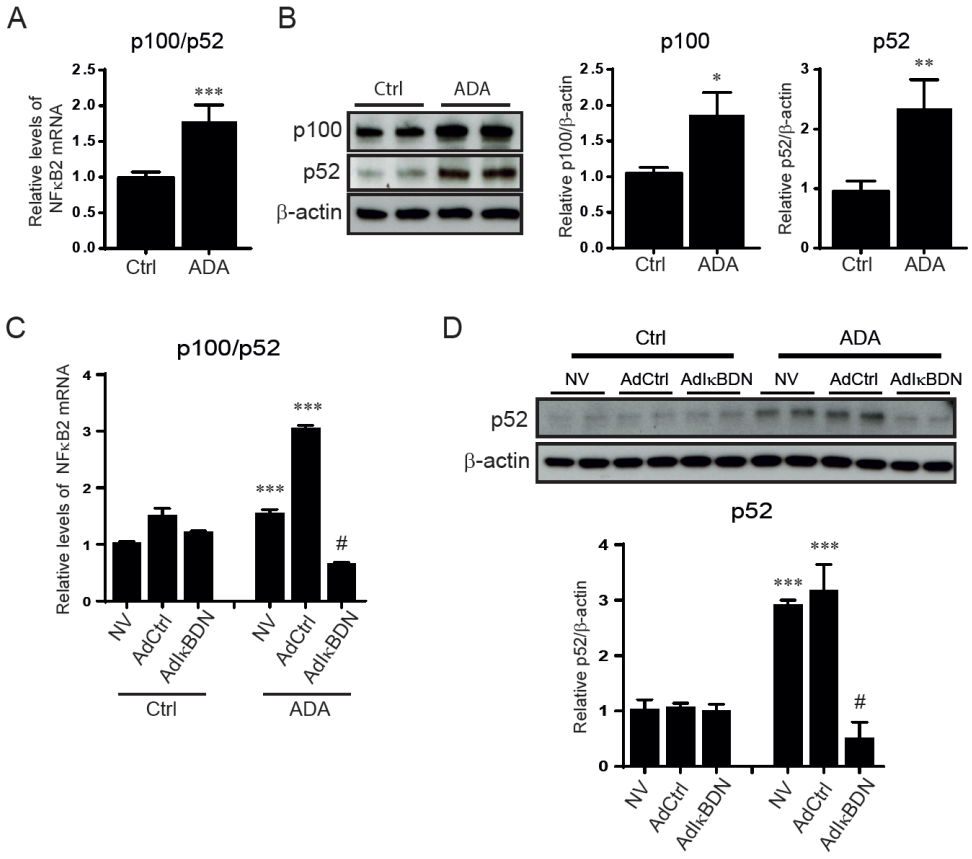

Figure 3 - Activation of the NFkB alternative pathway. (A), *NFKB2* transcript levels from control and ADA-treated cells measured by quantitative RT-PCR (n=4). *, $p < 0.05$, **, $p < 0.005$, ***, $p < 0.0005$, *versus* control. **(B)**, Protein expression of p100 and p52 in HCAECs control and with ADA treatment. Representative Western blots (left) and summary densitometry analysis (right) are shown (n=3). The statistical analysis was performed as in A. **(C)**, *NFKB2* mRNA levels under SAH accumulation, analyzed by quantitative RT-PCR, for cells infected with AdIkBDN, the control adenovirus (AdCtrl), or control uninfected cells (NV) (n=3). ANOVA with multiple comparisons was used for statistical significance analysis. ***, $p<0.0005$ *versus* the correspondent no ADA condition. #, $p < 0.0005$ *versus* ADA treated cells with no virus or infected with the AdCtrl. **(D)**, Western blot analysis of p52 expression in cells infected with the AdIkBDN, the AdCtrl, or NV that were treated or untreated with ADA. Representative blot is shown (top) with the densitometry measurements (below, n=3). Statistical analysis was performed as in C.

SAH accumulation results in increased expression of pro-inflammatory cytokines – Interestingly, inflammatory cytokines, such as TNF-α or IL-1β, are not only NFkB activators, but also its downstream transcriptional targets (22, 25). ADA treatment increased the expression of *IL1B* and *TNFA* genes by 73.3 $\pm$ 20.8- and 5.9 $\pm$ 0.6-fold, respectively ($p < 0.0005$; Fig. 4A). Notably, quantitative RT-PCR results showed very low basal expression of these cytokines in control cells. Likewise, the IL-1β cytokine is almost undetectable by Western blot in control cells (Fig. 4B), although its expression is significantly augmented by ADA (50.4 $\pm$ 4.8-fold; $p < 0.0005$). We next examined whether inhibiting NFkB pathways modulates ADA-induced cytokine expression (Fig. 4C). Unexpectedly, the ADA-induced up-regulation of *IL1B* expression was 63.1 $\pm$ 3.2 % lower when the cells were infected with AdCtrl (compared to uninfected cells exposed to ADA), but still significantly

increased compared with cells not exposed to the SAH hydrolase inhibitor (12.8 ± 1.1-fold; $p < 0.0005$). IkBDN reduced the ADA-induced expression of *IL1B* by 63.4 ± 2.4 % compared to the ADA-treated AdCtrl ($p < 0.0005$); however, IkBDN failed to eliminate completely ADA-induced *IL1B* up-regulation as *IL1B* expression remained 7.7 ± 0.5-fold higher in IKBDN expressing cells with ADA compared to untreated IkBDN expressing cells ($p < 0.005$). ADA-treated cells infected with the AdCtrl had substantially greater expression of *TNFA* when compared with uninfected cells exposed to ADA ($p < 0.0005$; Fig. 4C); nonetheless, *TNFA* up-regulation by ADA was completely abolished by IkBDN expression ($p < 0.0005$).

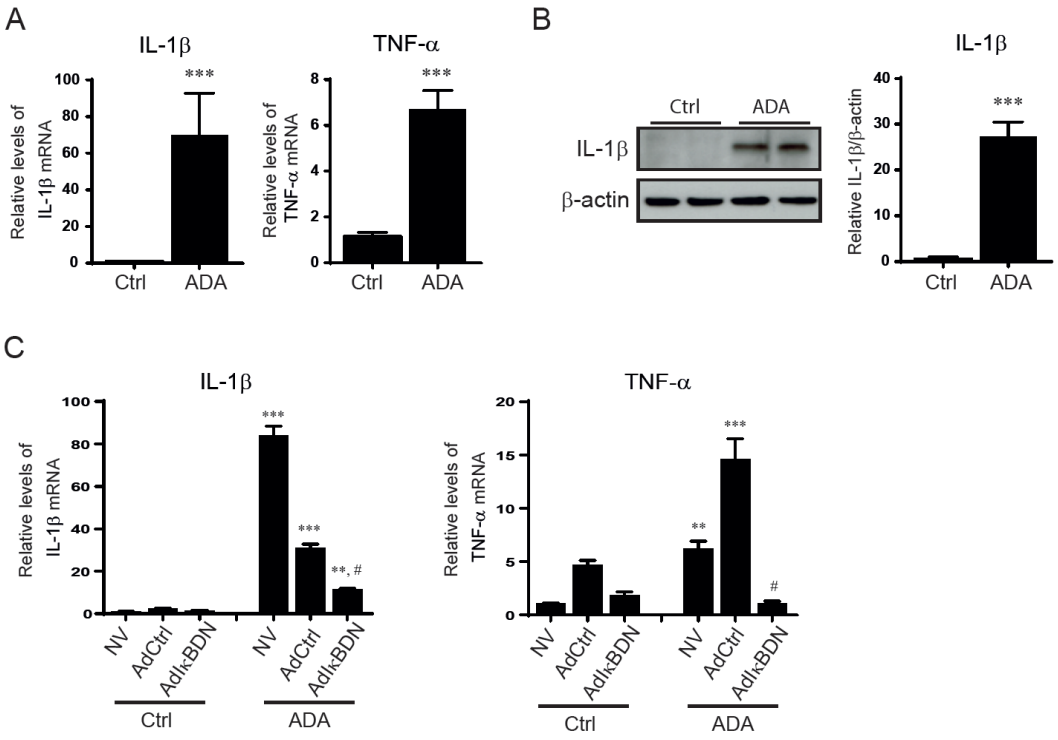

Figure 4 - Expression of proinflammatory cytokines under SAH accumulation. (A), The mRNA levels of IL-1β and TNFα were measured by quantitative RT-PCR for control and ADA-treated cells (n=4). ***, $p < 0.0005$, *versus* control. **(B)**, Western blot analysis of IL-1β protein expression induced by ADA treatment. A representative blot is shown. Mean densitometry results are presented. Statistical significance was measured as for A. **(C)**, Cytokine mRNA expression was determined for control and ADA treated cells infected with the adenovirus IkBDN (AdIkBDN), a control adenovirus (AdCtrl), or no virus (NV) by quantitative RT-PCR (n=3-4). A multiple comparison ANOVA statistical analysis was performed, and the significance of the differences between the means is indicated. ***, $p < 0.0005$, **, $p<0.005$ *versus* corresponding condition without ADA; #, $p < 0.005$, compared to ADA treated no virus or ADA treated AdCtrl.

Excess SAH disturbs EZH2 and EZH2-related proteins – Previous studies have shown that SAHH inhibitors can suppress the activity of the S-adenosylmethionine-dependent methytransferase EZH2 (26). The balance between the activity of EZH2 and the demethylase JMJD3 modulates epigenetic regulation through H3K27me3. EZH2 is known to suppress the expression of the senescence markers, cyclin-dependent kinase inhibitor 1A (CDKN1A/p21) and 2A (CDKN2A/p16) (27).

To determine whether EZH2 was altered by SAHH inhibition in HCAEC, we investigated the effects of ADA on the expression of EZH2; the EZH2-regulated genes, CDKN1A and CDKN2A; and the demethylase JMJD3 (Fig. 5A). ADA treatment resulted in a 58.0 ± 11.7 and 68.4 ± 7.7 % reduction of EZH2 and JMJD3 mRNA levels, respectively ($p < 0.005$). CDKN1A gene expression was 2.1 ± 0.3-fold higher after ADA treatment ($p < 0.005$), whereas CDKN2A expression was not significantly changed. EZH2 protein levels decreased by 59.8 ± 0.1 % with ADA treatment ($p < 0.005$; Fig. 5B). SAH accumulation also decreased H3K27me3 content by 25.5 ± 0.2 % ($p < 0.05$; Fig. 5C), consistent with a decrease in cellular EZH2 activity. Figure 5D suggests that SAH-mediated changes in EZH2 expression and activity are independent of NFkB activation, as the presence of IkBDN had no effect on ADA-induced suppression of EZH2 nor did it alter the ADA-induced increase of CDKN1A.

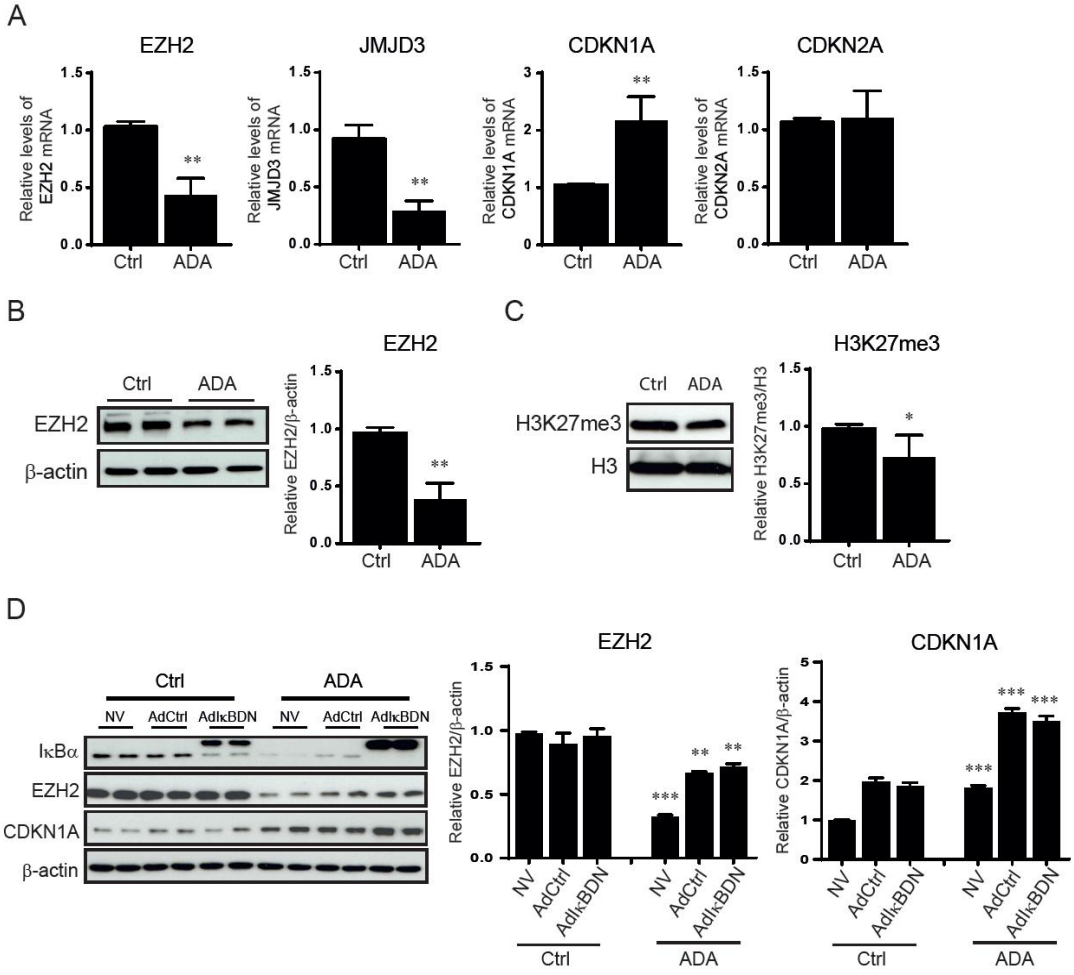

Figure 5 - Effects of excess SAH on EZH2 and EZH2-related proteins. (A), EZH2, JMJD3, CDKN1A, and CDKN2A mRNA levels were studied by quantitative RT-PCR following ADA treatment (n=3). **, $p < 0.005$, *versus* control. **(B)**, Total protein extracts from control and ADA treated cells were used for Western blot detection of EZH2. A representative blot is shown on the left and the summary of densitometry analysis on the right (n= 3). Statistical analysis was performed as in A. **(C)**, Western blot analysis of histone H3K27 tri-methylation (H3K27me3) after ADA treatment. Data are analyzed as in A. *, $p < 0.05$, *versus* control. **(D)**, EZH2 and CDKN1A protein expression was evaluated, by Western blot, in noninfected cells (NV) or those infected with the adenovirus IkBDN or adenovirus control (AdCtrl) in the presence or absence of ADA treatment. Representative blots are presented along with densitometry analysis (n=3-4). An ANOVA multiple comparisons test was used to analyze the statistically significant differences between means. **, $p < 0.005$, ***, $p < 0.0005$, *versus* the corresponding condition without ADA treatment.

EZH2 knockdown mimics SAH-mediated effects on cell activation – To determine whether ADA-induced EZH2 suppression could contribute to the pro-inflammatory activation of endothelial cells, we knocked down EZH2 using a targeted siRNA (siEZH2) and analyzed the expression of adhesion molecules, CDKN1A, and IL-1β, another known target of EZH2-associated epigenetic regulation (16). EZH2 knockdown resulted in a 94.1 ± 0.9 and 73.3 ± 8.9 % reduction of EZH2 mRNA and protein levels, respectively ($p < 0.005$ vs siCtrl; Fig. 6).

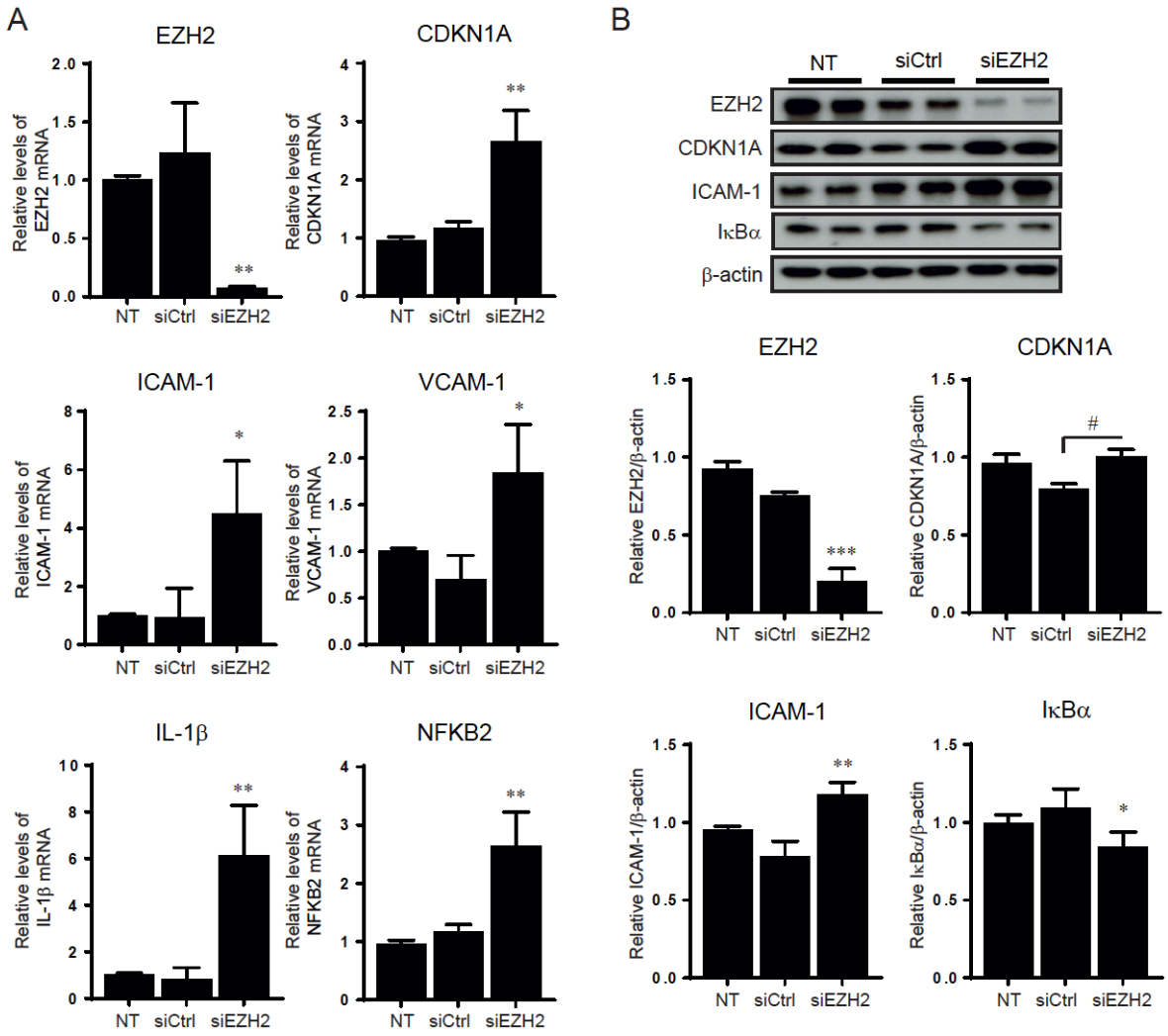

Figure 6 - Effects of EZH2 knockdown on NFkB and endothelial cell activation. (A), Quantitative RT-PCR results are presented for non-transfected (NT) and transfected cells with either a scrambled siRNA (siCtrl) or an siRNA directed to EZH2 (siEZH2) (n=3-4). **(B)**, Western blot analysis was performed after knockdown of EZH2. Representative blots (top), along with densitometry analysis (below) are shown (n=3). Statistically significant differences between the means were determined by an ANOVA multiple comparisons test for panel A and B. *, $p < 0.05$, **, $p < 0.005$, ***, $p < 0.0005$, *versus* the non-transfected and siCtrl conditions. #, $p < 0.0005$ significant only against siCtrl.

Suppression of EZH2 expression increased CDKN1A mRNA and protein levels when compared to siCtrl treated cells by 2.3 ± 0.4- and 1.3 ± 0.1-fold, respectively ($p < 0.005$). [The up-regulation of CDKN1A gene expression was also significant when comparing the siEZH2 and nontransfected cells,

but the protein levels were not significantly different between these groups.] A significant increase of 4.8 ± 1.4- and 2.6 ± 0.5-fold was also observed for ICAM1 and VCAM1 expression following EZH2 knockdown compared to siCtrl conditions ($p < 0.05$). The role of EZH2 on the expression of adhesion molecules was further confirmed by Western blot, where EZH2 knockdown resulted in a 1.5 ± 0.1-fold increase of ICAM-1 expression ($p < 0.0005$, Fig. 6B). EZH2 knockdown also resulted in a 7.3 ± 2.1-fold increase of IL-1β mRNA levels ($p < 0.005$).

To determine whether EZH2 inhibition could promote NFkB activation, we monitored IkBα degradation after EZH2 knockdown. Cells transfected with siEZH2 showed 23.0 ± 7.6 % less IkBα than those transfected with the siCtrl ($p < 0.05$). Furthermore, EZH2 knockdown increased NFKB2 gene expression 2.3 ± 0.4-fold, supporting a possible role for EZH2 in modulating NFkB pathways in endothelial cells.

4. DISCUSSION

The role of homocysteine as a risk factor for cardiovascular disease (CVD) has been widely debated. SAH, as a functionally important metabolite of homocysteine metabolism, has been suggested as a potentially more accurate indicator and determinant of CVD risk (28–30). Our work has focused on targets that are impaired by excess SAH that may contribute to vascular disease development. We have shown that SAH hydrolase inhibition using ADA induces intracellular accumulation of SAH and that excess SAH disturbs nitric oxide production and antioxidant systems in HUVECs (1, 8). Here, we used primary endothelial cells derived from coronary arteries (HCAECs) to examine the mechanisms by which SAH promotes inflammatory activation. The adhesion of leukocytes to endothelial cells, which occurs during inflammatory diseases such as atherosclerosis, is complex and involves multiple interactions among endothelial and leukocyte surface molecules. We monitored the expression of *ICAM1* and *VCAM1*, as well as the expression of *SELE,* which encodes E-selectin, an adhesion molecule involved mainly in the early stages of the adhesion process, and *PECAM1*, which is required during the transmigration stage (31). *SELE*, *ICAM1*, and *VCAM1* are all target genes for NFkB and their mRNA levels were all significantly increased by ADA, suggesting that NFkB may be activated by excess SAH (Fig. 1). By contrast, *PECAM1* expression was significantly decreased by ADA treatment. Down-regulation of *PECAM1* expression upon cell activation has been shown previously in various cell models, including endothelial cells (32–35). Notably, although its global expression may be decreased, its redistribution to the cell surface to favor leukocyte transmigration is likely (32–34, 36). In fact, in our previous work in HUVECs, we found evidence for increased cell surface expression of this adhesion molecule following cell activation by excess SAH (1).

We report a novel link between the hypomethylating agent SAH and NFkB activation. Using an NFkB luciferase reporter construct, we confirmed that ADA induced NFkB-dependent transcriptional activation. Our data support an activation of both the canonical and non-canonical NFkB pathways in endothelial cells. Thus, IkBα degradation and p65 nuclear migration were up-regulated and the expression and processing of p100 were enhanced by ADA. The crosstalk between canonical and non-canonical NFkB pathways is reported to exist at several different points in these activation cascades (37). We found that the increased expression of the *NFKB2* gene (Fig. 3) was dependent on the activation of the canonical pathway following ADA treatment (Fig. 3C). The regulation of the *NFKB2* gene by the canonical NFkB pathway has been previously described; however, studies suggest that increased expression of p100 may have a positive or negative effect on the subsequent activation of the non-canonical pathway (37). p100 is the precursor of p52 and required for non-canonical pathway activation, but its accumulation (without degradation to p52) can paradoxically lead to the suppression of RelB nuclear translocation (37, 38). In our cell system, excess SAH not only resulted in an NFkB-dependent *NFKB2* up-regulation, but also in increased processing of p100 to p52. The non-canonical NFkB pathway is largely involved in lymphoid organ development and adaptive immune responses. Its role in endothelial cell function is largely unknown (38, 39). Interestingly, the expression of CXCL2, which is a pro-inflammatory cytokine involved in lymphocyte transendothelial migration, was reported to be dependent on activation of the non-canonical NFkB pathway in endothelial cells (40, 41). Further investigation is necessary to clarify the role of the non-canonical NFkB pathway and *CXCL2* expression in SAH-induced endothelial cell activation.

NFkB pathways can be triggered by several factors, including pathogen exposure, inflammatory cytokines, radiation, and other stress signals (14, 42). Interestingly, pro-inflammatory cytokines, such as IL-1β and TNF-α, are not only NFkB targets, but also NFkB activators via their receptor-mediated actions. We found that SAH accumulation caused a significant increase in the expression of *IL1B* and *TNFA* (Fig. 4). IL-1β is synthesized as a precursor 33 kDa protein, which is cleaved by caspase-1, inducing the extracellular release of the processed 17 kDa form (43). Only the precursor form was detectable by Western blot following ADA treatment (Fig. 4B). [The mature form of IL-1β was below the detection limit of the Western blot, possibly owing to its release from the cell and/or its low levels of production.] In order to understand whether increased cytokine production is a consequence of NFkB activation, we used the recombinant IkBDN. Our results show that IkBDN completely suppressed the ADA-induced increase of *TNFA*. IKBDN also significantly reduced, but did not eliminate, ADA-induced up-regulation of *IL1B*, as it remained elevated in comparison to untreated samples (Fig. 4C). These findings suggest that intracellular accumulation of SAH leads to cytokine production in response to NFkB activation, which may continue to augment and prolong cellular activation by promoting cytokine receptor-mediated activation of NFkB.

It is unclear why IkBDN failed to completely block the up-regulation of *IL1B* by ADA; however, the *IL1B* promoter may be additionally regulated by other pathways, independent of NFkB. Our previous studies showed that ADA induced oxidant stress in endothelial cells (1, 13). Specifically, hypomethylation led to the suppression of GPx1 and other selenocysteine containing enzymes, which play an important role on the maintenance of cell redox balance (1, 44). Other studies, including our own in microvascular endothelial cells, indicate that decreased GPx1 expression can enhance inflammatory signaling in response to cytokines and endotoxins by increasing oxidants (45, 46). In HCAECs, the use of antioxidants confirmed that oxidative stress also contributes to SAH-induced inflammatory activation; however, antioxidants were unable to eliminate ADA's effects on adhesion molecule up-regulation and they failed to block ADA-induced IkB degradation in HCAECs (data not shown).

To understand better the effects of excess SAH on endothelial cell activation, we considered other pathways that might contribute to endothelial activation. Recently, decreased levels of H3K27me3 were positively correlated with the progression of atherosclerosis (47). Here, we report that SAH accumulation can induce H3K27 hypomethylation (Fig. 5). The H3K27me3 repressive mark is maintained by EZH2 and can be removed by JMJD3. We investigated the endothelial changes in *EZH2* and *JMJD3* expression under SAH accumulation promoted by ADA. EZH2 is a possible target for SAH-directed inhibition, and our findings show that its gene expression is also decreased by excess SAH via an as-yet unknown mechanism. Furthermore, *JMJD3* gene expression was down-regulated with excess SAH, suggesting that a feedback mechanism may be triggered due to lack of substrate. Interestingly, it was recently reported in cancer cell lines that JMJD3 suppression can be mediated by miRNA-941, which is up-regulated with DNA hypomethylation (48). Similarly, EZH2 expression has been shown to be suppressed by microRNAs that may normally be transcriptionally repressed by DNA methylation (49). Thus, similar mechanisms could contribute to JMJD3 or EZH2 suppression by excess SAH.

EZH2 is known to mediate transcriptional repression of the cyclin-dependent kinase inhibitor *CDKN1A* and *CDKN2A* genes. CDKN1A and CDKN2A inhibit different cyclin-dependent kinases, contributing to a senescent phenotype by blocking cell cycle progression (27). Expression of *CDKN1A*, but not *CDKN2A*, was found to be significantly increased with SAH accumulation, most likely due to EZH2 inhibition, and suggesting that a senescent phenotype might be activated. Endothelial cell senescence has been associated with atherogenesis and could be another mechanism by which SAH contributes to vascular disease (50).

Little is known about EZH2 interaction with NFkB pathway, especially in endothelial cells. In breast cancer cells, the EZH2 protein caused an activation or repression of NFkB pathways depending on the estrogen receptor (ER) status of the cancer cells (51). In ER-negative cancer cells, EZH2 physically interacted with NFkB heterodimers to promote the expression of a subset of NFkB

target genes; whereas in ER-positive cells, ER recruited EZH2-containing complexes to NFkB target genes to epigenetically silence them via histone methylation. A different interaction was found between NFkB and EZH2 in endothelial cells infected with Kaposi sarcoma-associated herpesvirus in which latent viral genes were found to activate NFkB, leading to increased expression of EZH2 (52). In primary endothelial cells, we found a different association between EZH2 and NFkB that was caused by a *loss* of functional EZH2. In fact, NFkB had no effect on EZH2 expression in HCAECs; rather, the loss of EZH2 promoted NFkB activation, with a concomitant increase of NFkB2 mRNA levels.

In support of a role for EZH2 suppression in ADA-induced activation of NFkB, knockdown of EZH2 (Fig. 6) recapitulated the effects of ADA, activating NFkB and increasing the expression of adhesion molecules, and the pro-inflammatory cytokine *IL1B*. Although the pro-inflammatory effects of EZH2 knockdown are less robust than those induced by SAH hydrolase inhibition, the knockdown caused many of the same inflammatory responses. It is likely that the magnitude of these responses is lower with EZH2 knockdown as additional pathways (such as oxidative stress) that also contribute to endothelial cell dysfunction may be activated by SAH-accumulation. Nonetheless, our results support a role for EZH2 suppression in the effects of excess SAH, and suggest that EZH2 suppression may contribute to NFKB activation in endothelial cells.

In conclusion, our studies implicate homocysteine's precursor, SAH, in the activation of the canonical and non-canonical NFkB pathways. Furthermore, excess SAH suppresses EZH2, decreasing the global levels of the repressive H3K27me3 mark. Based on these results, we believe that EZH2 suppression promotes the expression of inflammatory cytokines, such as IL-1β, due to a decrease of the epigenetic mark H3K27me3 at the *IL1B* promoter (16, 25). Up-regulation of IL-1β may promote the continued stimulation of the NFkB pathway via activation of the IL-1β receptor. Thus, we suggest that SAH-induced EZH2 suppression can contribute to pro-inflammatory changes favoring atherogenesis. Our results reveal an important link between NFkB and PRC2 epigenetic regulation, which may be relevant to vascular disease (Fig.7).

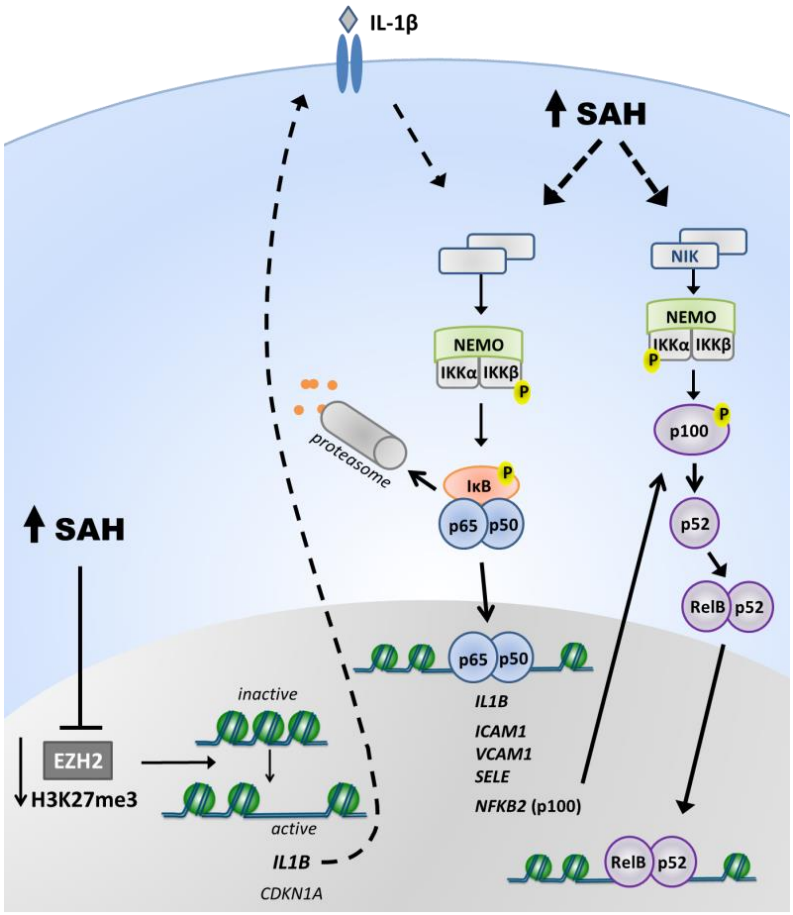

Figure 7 - Potential mechanism(s) by which SAH causes endothelial activation. SAH can inhibit EZH2 activity, decreasing the repressive histone mark H3K27me3. H3K27me3 suppresses the expression of a number of genes, including *CDKN1A* and *IL1B*. By stimulating its receptor, IL-1β can contribute to NFkB activation. Exposure to excess SAH activates both the canonical and non-canonical NFkB pathways. The canonical pathway involves IκB kinase complex (IKK) activation to induce IkB phosphorylation, triggering its ubiquitination-mediated degradation by the proteasome. Following IkB degradation, NFkB complexes (p65/p50) are free to migrate to the nucleus, activating transcription of its target genes. SAH induces NFkB-mediated transcription of cytokines (such as IL-1β, which can sustain further NFkB activation), adhesion molecules, and *NFkB2*. The non-canonical pathway relies on the activation of NFkB-interacting kinase (NIK) and IKKα which mediates the phosphorylation of the *NFkB2* gene product, p100, leading to its processing to p52, and subsequent migration of RelB/p52 to the nucleus. SAH augments the accumulation of p52, which may contribute to endothelial cell activation.

ACKNOWLEDGEMENT

We are very thankful to Ms. Stephanie Tribuna for her expert technical assistance in preparing this manuscript.

FUNDING

This work was supported by NIH grants HL671795, HL084743, HL108630 and HL119145 (to JL) and by the Portuguese Fundação para a Ciência e a Tecnologia grant SFRH/BD/73021/2010 (to MB).

CONFLICTS OF INTEREST

The authors have no conflict of interest.

REFERENCES

1. Barroso, M., Florindo, C., Kalwa, H., Silva, Z., Turanov, A. A., Carlson, B. A., de Almeida, I. T., Blom, H. J., Gladyshev, V. N., Hatfield, D. L., Michel, T., Castro, R., Loscalzo, J., and Handy, D. E. (2014) Inhibition of cellular methyltransferases promotes endothelial cell activation by suppressing glutathione peroxidase 1 protein expression. *J. Biol. Chem.* **289**, 15350–62

2. Caudill, M. A., Wang, J. C., Melnyk, S., Pogribny, I. P., Jernigan, S., Collins, M. D., Santos-Guzman, J., Swendseid, M. E., Cogger, E. A., and James, S. J. (2001) Intracellular S-adenosylhomocysteine concentrations predict global DNA hypomethylation in tissues of methyl-deficient cystathionine beta-synthase heterozygous mice. *J. Nutr.* **131**, 2811–8

3. Esse, R., Florindo, C., Imbard, A., Rocha, M. S., de Vriese, A. S., Smulders, Y. M., Teerlink, T., Tavares de Almeida, I., Castro, R., and Blom, H. J. (2013) Global protein and histone arginine methylation are affected in a tissue-specific manner in a rat model of diet-induced hyperhomocysteinemia. *Biochim. Biophys. Acta*. **1832**, 1708–14

4. Castro, R., Rivera, I., Struys, E. A., Jansen, E. E. W., Ravasco, P., Camilo, M. E., Blom, H. J., Jakobs, C., and Tavares de Almeida, I. (2003) Increased homocysteine and S-adenosylhomocysteine concentrations and DNA hypomethylation in vascular disease. *Clin. Chem.* **49**, 1292–6

5. Clarke, R., Daly, L., Robinson, K., Naughten, E., Cahalane, S., Fowler, B., and Graham, I. (1991) Hyperhomocysteinemia: an independent risk factor for vascular disease. *N. Engl. J. Med.* **324**, 1149–55

6. Xiao, Y., Huang, W., Zhang, J., Peng, C., Xia, M., and Ling, W. (2015) Increased plasma S-adenosylhomocysteine-accelerated atherosclerosis is associated with epigenetic regulation of endoplasmic reticulum stress in apoE-/- mice. *Arterioscler. Thromb. Vasc. Biol.* **35**, 60–70

7. Zawada, A. M., Rogacev, K. S., Hummel, B., Berg, J. T., Friedrich, A., Roth, H. J., Obeid, R., Geisel, J., Fliser, D., and Heine, G. H. (2014) S-adenosylhomocysteine is associated with subclinical atherosclerosis and renal function in a cardiovascular low-risk population. *Atherosclerosis*. **234**, 17–22

8. Barroso, M., Rocha, M. S., Esse, R., Gonçalves, I., Gomes, A. Q., Teerlink, T., Jakobs, C., Blom, H. J., Loscalzo, J., Rivera, I., de Almeida, I. T., and Castro, R. (2012) Cellular hypomethylation is associated with impaired nitric oxide production by cultured human endothelial cells. *Amino Acids*. **42**, 1903–11

9. Gareus, R., Kotsaki, E., Xanthoulea, S., van der Made, I., Gijbels, M. J. J., Kardakaris, R., Polykratis, A., Kollias, G., de Winther, M. P. J., and Pasparakis, M. (2008) Endothelial cell-specific NF-kappaB inhibition protects mice from atherosclerosis. *Cell Metab.* **8**, 372–83

10. Handy, D. E., Lubos, E., Yang, Y., Galbraith, J. D., Kelly, N., Zhang, Y.-Y., Leopold, J. A., and Loscalzo, J. (2009) Glutathione peroxidase-1 regulates mitochondrial function to modulate redox-dependent cellular responses. *J. Biol. Chem.* **284**, 11913–21

11. Pamukcu, B., Lip, G. Y. H., and Shantsila, E. (2011) The nuclear factor--kappa B pathway in atherosclerosis: a potential therapeutic target for atherothrombotic vascular disease. *Thromb. Res.* **128**, 117–23

12. Madonna, R., and De Caterina, R. (2012) Relevance of new drug discovery to reduce NF-κB activation in cardiovascular disease. *Vascul. Pharmacol.* **57**, 41–7

13. Gloire, G., Legrand-Poels, S., and Piette, J. (2006) NF-kappaB activation by reactive oxygen species: fifteen years later. *Biochem. Pharmacol.* **72**, 1493–505

14. Hinz, M., and Scheidereit, C. (2014) The IκB kinase complex in NF-κB regulation and beyond. *EMBO Rep.* **15**, 46–61

15. Deb, G., Singh, A. K., and Gupta, S. (2014) EZH2: Not EZHY (Easy) to Deal. *Mol. Cancer Res.* **12**, 639–653

16. Dreger, H., Ludwig, A., Weller, A., Stangl, V., Baumann, G., Meiners, S., and Stangl, K. (2012) Epigenetic regulation of cell adhesion and communication by enhancer of zeste homolog 2 in human endothelial cells. *Hypertension*. **60**, 1176–83

17. Hübner, M. R., and Spector, D. L. (2010) Role of H3K27 demethylases Jmjd3 and UTX in transcriptional regulation. *Cold Spring Harb. Symp. Quant. Biol.* **75**, 43–9

18. Agger, K., Cloos, P. A. C., Christensen, J., Pasini, D., Rose, S., Rappsilber, J., Issaeva, I., Canaani, E., Salcini, A. E., and Helin, K. (2007) UTX and JMJD3 are histone H3K27 demethylases involved in HOX gene regulation and development. *Nature*. **449**, 731–4

19. Williams, K., Christensen, J., Rappsilber, J., Nielsen, A. L., Johansen, J. V., and Helin, K. (2014) The histone lysine demethylase JMJD3/KDM6B is recruited to p53 bound promoters and enhancer elements in a p53 dependent manner. *PLoS One*. **9**, e96545

20. Harte, M. T., Gorski, J. J., Savage, K. I., Purcell, J. W., Barros, E. M., Burn, P. M., McFarlane, C., Mullan, P. B., Kennedy, R. D., Perkins, N. D., and Harkin, D. P. (2014) NF-κB is a critical mediator of BRCA1-induced chemoresistance. *Oncogene*. **33**, 713–23

21. Mackay, F. (1993) Tumor necrosis factor alpha (TNF-alpha)-induced cell adhesion to human endothelial cells is under dominant control of one TNF receptor type, TNF-R55. *J. Exp. Med.* **177**, 1277–1286

22. Hoesel, B., and Schmid, J. A. (2013) The complexity of NF-κB signaling in inflammation and cancer. *Mol. Cancer*. **12**, 86

23. Leychenko, A., Konorev, E., Jijiwa, M., and Matter, M. L. (2011) Stretch-induced hypertrophy activates NFkB-mediated VEGF secretion in adult cardiomyocytes. *PLoS One*. **6**, e29055

24. Choudhary, S., Kalita, M., Fang, L., Patel, K. V, Tian, B., Zhao, Y., Edeh, C. B., and Brasier, A. R. (2013) Inducible tumor necrosis factor (TNF) receptor-associated factor-1 expression couples the canonical to the non-canonical NF-κB pathway in TNF stimulation. *J. Biol. Chem.* **288**, 14612–23

25. Maleszewska, M., Gjaltema, R. A. F., Krenning, G., and Harmsen, M. C. (2015) Enhancer of zeste homolog-2 (EZH2) methyltransferase regulates transgelin/smooth muscle-22α expression in endothelial cells in response to interleukin-1β and transforming growth factor-β2. *Cell. Signal.* **27**, 1589–96

26. Kung, P.-P., Huang, B., Zehnder, L., Tatlock, J., Bingham, P., Krivacic, C., Gajiwala, K., Diehl, W., Yu, X., and Maegley, K. (2015) SAH derived potent and selective EZH2 inhibitors. *Bioorg. Med. Chem. Lett.* **25**, 1532–7

27. Bai, J., Chen, J., Ma, M., Cai, M., Xu, F., Wang, G., Tao, K., and Shuai, X. (2014) Inhibiting enhancer of zeste homolog 2 promotes cellular senescence in gastric cancer cells SGC-7901 by activation of p21 and p16. *DNA Cell Biol.* **33**, 337–44

28. Wagner, C., and Koury, M. J. (2007) S-Adenosylhomocysteine: a better indicator of vascular disease than homocysteine? *Am. J. Clin. Nutr.* **86**, 1581–5

29. Xiao, Y., Zhang, Y., Wang, M., Li, X., Su, D., Qiu, J., Li, D., Yang, Y., Xia, M., and Ling, W. (2013) Plasma S-adenosylhomocysteine is associated with the risk of cardiovascular events in patients undergoing coronary angiography: a cohort study. *Am. J. Clin. Nutr.* **98**, 1162–9

30. Liu, C., Wang, Q., Guo, H., Xia, M., Yuan, Q., Hu, Y., Zhu, H., Hou, M., Ma, J., Tang, Z., and Ling, W. (2008) Plasma S-adenosylhomocysteine is a better biomarker of atherosclerosis than homocysteine in apolipoprotein E-deficient mice fed high dietary methionine. *J. Nutr.* **138**, 311–5

31. Muller, W. A. (2002) Leukocyte-Endothelial Cell Interactions in the Inflammatory Response. *Lab. Investig.* **82**, 521–534

32. Newman, P. J., Hillery, C. A., Albrecht, R., Parise, L. V, Berndt, M. C., Mazurov, A. V, Dunlop, L. C., Zhang, J., and Rittenhouse, S. E. (1992) Activation-dependent changes in human platelet PECAM-1: phosphorylation, cytoskeletal association, and surface membrane redistribution. *J. Cell Biol.* **119**, 239–46

33. Stewart, R. J., Kashour, T. S., and Marsden, P. A. (1996) Vascular endothelial platelet endothelial adhesion molecule-1 (PECAM-1) expression is decreased by TNF-alpha and IFN-gamma. Evidence for cytokine-induced destabilization of messenger ribonucleic acid transcripts in bovine endothelial cells. *J. Immunol.* **156**, 1221–8

34. Sawa, Y., Sugimoto, Y., Ueki, T., Ishikawa, H., Sato, A., Nagato, T., and Yoshida, S. (2007) Effects of TNF-alpha on leukocyte adhesion molecule expressions in cultured human lymphatic endothelium. *J. Histochem. Cytochem.* **55**, 721–33

35. Zehnder, J. L., Hirai, K., Shatsky, M., McGregor, J. L., Levitt, L. J., and Leung, L. L. (1992) The cell adhesion molecule CD31 is phosphorylated after cell activation. Down-regulation of CD31 in activated T lymphocytes. *J. Biol. Chem.* **267**, 5243–9

36. Romer, L. H., McLean, N. V, Yan, H. C., Daise, M., Sun, J., and DeLisser, H. M. (1995) IFN-gamma and TNF-alpha induce redistribution of PECAM-1 (CD31) on human endothelial cells. *J. Immunol.* **154**, 6582–92

37. Sun, S.-C. (2012) The noncanonical NF-κB pathway. *Immunol. Rev.* **246**, 125–40

38. Sun, S.-C. (2011) Non-canonical NF-κB signaling pathway. *Cell Res.* **21**, 71–85

39. Noort, A. R., van Zoest, K. P. M., Weijers, E. M., Koolwijk, P., Maracle, C. X., Novack, D. V, Siemerink, M. J., Schlingemann, R. O., Tak, P. P., and Tas, S. W. (2014) NF-κB-inducing kinase is a key regulator of inflammation-induced and tumour-associated angiogenesis. *J. Pathol.* **234**, 375–85

40. Madge, L. A., Kluger, M. S., Orange, J. S., and May, M. J. (2008) Lymphotoxin-alpha 1 beta 2 and LIGHT induce classical and noncanonical NF-kappa B-dependent proinflammatory gene expression in vascular endothelial cells. *J. Immunol.* **180**, 3467–77

41. Noort, A.-R., van Zoest, K. P., Koolwijk, P., Tak, P.-P., and Tas, S. W. (2012) NF-kappaB inducing kinase (NIK) is a key regulator of inflammation-induced angiogenesis. *J. Transl. Med.* **10**, O1

42. Liu, F., Xia, Y., Parker, A. S., and Verma, I. M. (2012) IKK biology. *Immunol. Rev.* **246**, 239–53

43. Schönbeck, U., Mach, F., Bonnefoy, J. Y., Loppnow, H., Flad, H. D., and Libby, P. (1997) Ligation of CD40 activates interleukin 1beta-converting enzyme (caspase-1) activity in vascular smooth muscle and endothelial cells and promotes elaboration of active interleukin 1beta. *J. Biol. Chem.* **272**, 19569–74

44. Papp, L. V., Lu, J., Holmgren, A., and Khanna, K. K. (2007) From selenium to selenoproteins: synthesis, identity, and their role in human health. *Antioxid. Redox Signal.* **9**, 775–806

45. Lubos, E., Mahoney, C. E., Leopold, J. A., Zhang, Y.-Y., Loscalzo, J., and Handy, D. E. (2010) Glutathione peroxidase-1 modulates lipopolysaccharide-induced adhesion molecule expression in endothelial cells by altering CD14 expression. *FASEB J.* **24**, 2525–32

46. Lubos, E., Kelly, N. J., Oldebeken, S. R., Leopold, J. A., Zhang, Y.-Y., Loscalzo, J., and Handy, D. E. (2011) Glutathione peroxidase-1 deficiency augments proinflammatory cytokine-induced redox signaling and human endothelial cell activation. *J. Biol. Chem.* **286**, 35407–17

47. Wierda, R. J., Rietveld, I. M., van Eggermond, M. C. J. A., Belien, J. A. M., van Zwet, E. W., Lindeman, J. H. N., and van den Elsen, P. J. (2014) Global histone H3 lysine 27 triple methylation levels are reduced in vessels with advanced atherosclerotic plaques. *Life Sci.* 10.1016/j.lfs.2014.10.010

48. Zhang, P.-P., Wang, X.-L., Zhao, W., Qi, B., Yang, Q., Wan, H.-Y., Shuang, Z.-Y., Liu, M., Li, X., Li, S., and Tang, H. (2014) DNA methylation-mediated repression of miR-941 enhances lysine (K)-specific demethylase 6B expression in hepatoma cells. *J. Biol. Chem.* **289**, 24724–35

49. So, A.-Y., Jung, J.-W., Lee, S., Kim, H.-S., and Kang, K.-S. (2011) DNA methyltransferase controls stem cell aging by regulating BMI1 and EZH2 through microRNAs. *PLoS One*. **6**, e19503

50. Wang, J. C., and Bennett, M. (2012) Aging and atherosclerosis: mechanisms, functional consequences, and potential therapeutics for cellular senescence. *Circ. Res.* **111**, 245–59

51. Lee, S. T., Li, Z., Wu, Z., Aau, M., Guan, P., Karuturi, R. K. M., Liou, Y. C., and Yu, Q. (2011) Context-specific regulation of NF-κB target gene expression by EZH2 in breast cancers. *Mol. Cell*. **43**, 798–810

52. He, M., Zhang, W., Bakken, T., Schutten, M., Toth, Z., Jung, J. U., Gill, P., Cannon, M., and Gao, S.-J. (2012) Cancer angiogenesis induced by Kaposi sarcoma-associated herpesvirus is mediated by EZH2. *Cancer Res.* **72**, 3582–92

CHAPTER

7

General Discussion and Perspectives

Hyperhomocysteinemia is considered a risk factor for cardiovascular diseases; however, treatments that lower homocysteine have not yielded the anticipated protective effects in clinical studies. An alternative theory proposes that S-adenosylhomocysteine (SAH), the homocysteine precursor, rather than homocysteine itself, is a more accurate measure of the disease risk associated with hyperhomocysteinemia (1–3).

Endothelial dysfunction and activation are early steps in the development of atherosclerosis; thus, understanding the effects of SAH on endothelial function is necessary to clarify its role in the molecular and pathological basis of vascular disease.

As a strong inhibitor of most cell methyltransferases, SAH can affect different biomolecules by modulating their methylation state. DNA, RNA, and histone protein methylation relies on S-adenosylmethionine (SAM)-dependent methyltransferases and, therefore, these modifications are potential targets for SAH-mediated inhibition. Methylation of these biomolecules can modulate gene expression. While DNA and histone methylation are widely recognized as epigenetic factors that regulate gene expression, the effects of RNA methylation on gene expression are less understood. Nonetheless, several reports have recognized that RNA methylation is important for the control of translation and RNA processing (4, 5).

Our work was mainly focused on the harmful effects of SAH, as an inhibitor of methylation reactions, to the endothelium. During our studies (Chapters 3-6) intracellular SAH accumulation was promoted by pharmacological inhibition of SAH hydrolase. This approach led to a robust increase in intracellular SAH, independently of homocysteine accumulation, and resulted in a reduction of the SAM/SAH (methylation) ratio[1], an indicator of cell hypomethylation. Under these conditions, we examined the molecular consequences of excess SAH and its role as a hypomethylating agent. In Chapter 4, to confirm that these effects were due to the suppression of SAH hydrolase activity, an siRNA was used to decrease the expression of SAH hydrolase. Importantly, the molecular knockdown approach yielded results similar to those obtained with the pharmacologically-based suppression of SAH hydrolase.

Our results demonstrated that excess SAH can contribute to endothelial dysfunction by decreasing nitric oxide (NO) bioavailability (Chapter 3) and promoting oxidative stress (Chapter 4). Moreover, excess SAH can further sustain the progression of atherosclerosis by triggering an inflammatory response in endothelial cells (Chapters 4-6). Thus, SAH accumulation can increase the expression of adhesion molecules and cytokines. Finally, endothelial accumulation of SAH favored leukocyte adhesion and transmigration through the endothelium, supporting a functional role of the molecular alterations observed in the endothelial cells.

[1]Biochemical characterization of the model, with quantification of relevant metabolites, is shown in Chapter 3.

Excess SAH and Endothelial Dysfunction

As mentioned in Chapter 1, although hyperhomocysteinemia has been shown to promote endothelial dysfunction, the molecular mechanisms underlying this association remain unclear. Our results provide evidence for a role of excess SAH in endothelial damage, supporting the hypothesis that it may be a mediator in the association between homocysteine and vascular disease. In Chapter 3, we demonstrated that excess SAH decreases endothelial nitric oxide synthase (eNOS) protein levels and NO bioavailability. Nitric oxide is a major anti-atherothrombotic molecule, and within its pleiotropic effects to the endothelial layer (see Chapter 1 for more detail), it can protect against oxidative stress and inflammation, disturbances that are induced under excess SAH (Chapters 4-6). Moreover, an oxidative environment can also contribute to eNOS impairment (6). In Chapter 4, we showed that an SAH-induced hypomethylation environment can lead to the impairment of antioxidant systems and increase oxidative stress. Several reports demonstrate the role of reactive oxygen species (ROS) in the reduction of bioactive NO by chemical inactivation to form peroxynitrite and by inducing eNOS uncoupling (7). In fact, decreased eNOS expression and activity, as shown in Chapter 3, was previously observed in an oxidative environment (7). Furthermore, the homocysteine-induced increase of hydrogen peroxide (H_2O_2) was previously suggested to render NO more susceptible to oxidative inactivation (8). Thus, SAH-mediated oxidative stress could also contribute to decreased NO bioavailability.

Interestingly, although we observed decreased protein levels of eNOS, *NOS3* gene expression (eNOS mRNA) was up-regulated (Chapter 3). Remarkably, it was recently reported that the *NOS3* gene may be regulated by histone methylation. Specifically, its expression was inversely correlated with the histone methyltransferase activity of EZH2 (enhancer of zeste homolog 2) and the presence of the repression mark H3K27me3 (trimethylation of histone H3 on lysine 27) on the *NOS*3 promoter (9, 10). Therefore, EZH2 suppression and the resulting H3K27me3 down-regulation, which we observed under excess SAH (Chapter 6), may contribute to increased *NOS3* gene expression. The basis for the SAH-mediated decrease in eNOS protein levels remains to be determined. However, previous findings implicated protein kinase C (PKC) pathways in the degradation of the eNOS protein under high homocysteine levels in aortic endothelial cells (11); possibly, SAH may similarly activate this pathway in our cell system. Nonetheless, studies of eNOS phosphorylation by PKC, and the possible rescue of eNOS expression by PKC inhibitors, are necessary to confirm this hypothesis.

Oxidative stress is another key feature of endothelial dysfunction observed under excess SAH (Chapter 4). Redox balance is essential in maintaining cellular homeostasis and, under physiologic conditions, cells maintain this balance through the production and elimination of ROS. Major ROS producers include the mitochondrial electron transport chain, the endoplasmic reticulum system, and NAD(P)H oxidase (NOX) complexes (12). Major ROS-scavenging enzymes include glutathione peroxidases, catalase, and superoxide dismutases (SOD) (12). The impairment of antioxidant

systems results in the accumulation of naturally produced ROS, including H_2O_2. We found that SAH-mediated down-regulation of glutathione peroxidase-1 (GPx-1) and potentially the suppression of other antioxidant selenoproteins, such as selenoprotein H (SelH), selenoprotein M (SelM), and methionine sulfoxide reductase B1 (MsrB1), can lead to increased accumulation of intra- and extracellular H_2O_2. Interestingly, decreased expression of GPx-1 was previously observed under hyperhomocysteinemia (13). Our recent work clarified the role of SAH in this previously established association, and illustrated the role of GPx-1 in the SAH-mediated inflammatory response (see below).

Others have reported that catalase activity was decreased under increased homocysteine levels in human cultured cells (14). Likewise, homocysteine decreased the binding of extracellular-SOD to endothelial cell surfaces, leading to a reduced ability to protect endothelial cell surfaces from oxidative stress (15). However, the role of SAH in these alternative antioxidant pathways was not explored in our studies.

Excess SAH and Endothelial Activation

Endothelial cells undergo an activation process during the onset and progression of atherosclerosis. This activation is part of an inflammatory response that results in the expression of chemokines, cytokines, and adhesion molecules which mediate the interaction of the endothelium with leukocytes and platelets (16). The increased expression of cytokines and adhesion molecules prompts leukocyte homing, adhesion, and migration into the sub-endothelial space, favoring the progression of the atherosclerotic process (16).

We have found that excess SAH mediates endothelial cell activation (Chapters 4-6) through oxidative stress-dependent (Chapter 4) and -independent mechanisms (discussed below). In Chapter 4, we demonstrated that the SAH-induced down-regulation of the antioxidant GPx-1 resulted in increased expression of adhesion molecules, such as ICAM-1 (intercellular adhesion molecule-1) and VCAM-1 (vascular adhesion molecule-1), in human umbilical vein endothelial cells (HUVECs). Chapters 5 and 6 confirmed that SAH-induced the up-regulation of ICAM-1 and VCAM-1 and also provided evidence that additional adhesion molecules, specifically, E-selectin and/or PECAM-1, are up-regulated by SAH in HUVECs as well as endothelial cells from other vascular beds, such as the coronary artery (HCAECs). Importantly, we found that the up-regulation of these adhesion molecules resulted in their increased presence at the cell surface where they enhanced leukocyte adhesion (Chapter 4.1) and transmigration (Chapter 5), indicating that these SAH-induced changes can contribute to the atherogenic process. Moreover, we have also established the ability of SAH accumulation to induce the expression of the inflammatory cytokines IL-1β (interleukin-1 beta) and TNF-α (tumor necrosis factor alpha) (Chapter 6).

Oxidative stress is a known activator of inflammation; ROS-activated transcription factors, such as NFkB and AP-1, mediate the expression of adhesion molecules and cytokines at the transcriptional level (16). In Chapter 4, we initially reported that SAH-induced oxidative stress promoted adhesion molecule expression. Our findings in Chapter 6 indicate that the up-regulation of the adhesion molecules and cytokines is highly dependent on the activation of the NFkB canonical pathway. The NFkB pathway is considered a prototypical pro-inflammatory signaling pathway. The possibility of NFkB being activated by the SAH-induced oxidative stress was likely. However, co-treatments with an antioxidant (N-acetylcysteine) showed that oxidative stress only partially contributed to the observed inflammatory response in HCAECs as the reduced environment was not sufficient to suppress NFkB activation and, although, ICAM-1 up-regulation was decreased by the presence of exogenous antioxidants, it was not completely suppressed by this treatment (Supplemental Fig. 1). Conversely, during our studies in HUVEC (Chapter 4), antioxidants more completely suppressed inflammatory responses. Further investigation is necessary to understand the differences between these cell types. Although we measured ROS production in HUVEC following SAH exposure, the effects of SAH on ROS production was not examined in HCAEC. Thus, levels of ROS production in HCAECs should be assessed to determine if oxidant production (or impairment of antioxidant systems) differs between these cells. Moreover, many inflammatory responses require both AP-1 as well as NFkB activation, and the relative importance of each of these pathways in inflammatory signaling, as well as the effects of antioxidants on these pathways, may differ between HCAEC and HUVEC.

The initiator for the activation of the NFkB canonical pathway in HCAECs remains to be ascertained. Nonetheless, we observed that IL-1β, a known activator of the NFkB pathway, was not completely suppressed when the canonical pathway was blocked by a dominant negative inhibitor. Thus, IL-1β up-regulation could be mediated by other SAH-induced mechanisms and may contribute to the initial activation of the NFkB pathway, which could then be further activated and sustained by the subsequent NFkB-mediated transcription of cytokine genes, including those encoding IL-1β (*IL1B*) and TNF-α (*TNFA*).

We considered other pathways that could contribute to the endothelial cell inflammatory response that may be targets of SAH-mediated inhibition. One possibility was EZH2. EZH2 is a histone methyltransferase, which is part of the epigenetic regulator polycomb repressive complex PRC2. Recent analysis of a whole-genome mRNA expression array showed that EZH2 represses the expression of several inflammatory genes in endothelial cells, including *IL1B* (17), by adding the repressive histone mark H3K27me3 at these *loci* (18). We found that SAH-mediated hypomethylation suppresses H3K27me3, therefore, this pathway may, in part, contribute to the up-regulation of IL-1β by SAH.

Furthermore, our studies revealed a novel interaction between EZH2 and NFkB activation in endothelial cells. We found that targeted knockdown of EZH2 can promote NFkB activation and induce an inflammatory response, suggesting that SAH may promote inflammatory responses, in part, via its suppression of EZH2 activity. Interestingly, SAH also decreased the mRNA and protein levels of EZH2. These mechanisms of SAH-induced EZH2 suppression, as well as those involved in NFkB activation, warrant further investigation. Nonetheless, IL-1β, a known target of EZH2-mediated suppression and an activator of NFkB, was up-regulated by EZH2 knockdown, and may mediate the link between EZH2 and NFkB.

In summary, we found evidence that SAH can mediate homocysteine's associated endothelial dysfunction and activation, two critical factors for the onset of atherosclerosis. A prolonged exposure to these stresses can also cause the dysfunctional endothelium to lose integrity, and progress to senescence (16). Senescence has been commonly found in atherosclerosis (16, 19). Interestingly, the H3K27me3 mark also represses the expression of the cell cycle regulator CDKN1A, and its up-regulation is a marker of cell senescence. We found that CDKN1A was up-regulated by SAH accumulation (Chapter 6), suggesting that suppression of EZH2 by SAH may contribute to cell senescence.

S-Adenosylhomocysteine-Induced Hypomethylation

SAH toxicity is associated with its ability to inhibit SAM-dependent methyltransferases. As mentioned in Chapter 1, accumulation of SAH has been associated with DNA, RNA, and protein hypomethylation. In the presented studies, we found evidence for impaired methylation of RNA (Chapter 4), DNA (Chapter 5), and protein (Chapter 6), which may contribute to the harmful effects of SAH on the endothelium.

RNA Methylation

RNA is one of the major targets of SAM-dependent methyltransferases and, therefore, a potential target of SAH-mediated inhibition. However, the role of RNA methylation in hyperhomocysteinemia was not previously examined. One reason that may explain why this area has not attracted much attention is the limited knowledge regarding RNA modifications. Except for a few well studied modifications, the function of RNA methylation is poorly understood. The most well-known mRNA modification is the methylation cap on the mRNA 5'-end (m^7G methylation), which is part of mRNA maturation process and is required for its stability, efficient gene expression, and cell viability (20, 21). More recently, m^6A (N6-methyladenosine) and m^5C (5-methylcytidine) modifications of mRNA were found to have a role in the circadian cycle, cancer, and neuronal development (20, 22, 23). A common link among these studies is that they involved the analysis of m^7G, m^6A, and m^5C

modifications in mRNA molecules. Compared with tRNA and rRNA, mRNA is much less modified, which can make the study of its specific modifications easier. tRNA is the most highly methylated RNA species and within one tRNA molecule a large diversity of methylation modifications can be found. Furthermore, in most cases, a particular modification is found at more than one position and in different types of RNAs (4). Most tRNA and rRNA methylations have been found to be important for their structure as well as for their mRNA decoding functions (24–26). Additionally, it is important to realize that the number of RNA methylation modifications is close to one hundred and that the biological role for most of these modifications is still unknown (27). The highly demanding techniques necessary for the study of these modifications may have limited the volume of research done in this field (4).

In Chapter 4, we examined the importance of a specific RNA methylation modification, mcm^5Um (5-methoxycarbonylmethyl-2′-O-methyluridine), in endothelial dysfunction induced by excess SAH. mcm^5Um is present in the mammalian selenocysteine tRNA, at the wobble position of the anticodon, and it is necessary for translation of a subset group of selenoproteins. As shown in Chapter 4, the impairment of the translation of these proteins, especially GPx-1, can contribute to SAH-mediated oxidative stress. Importantly, the methyltransferase that catalyzes the final step in mcm^5Um formation (i.e., methylation of the mcm^5U to mcm^5Um) is still unknown. Analysis of known methyltransferases indicated that the SPOUT family of methyltransferases target 2'-O-ribose methylations; however, none of the known enzymes have been shown to mediate the mcm^5Um methylation (4, 27–29).

Our findings uniquely show a possible role for RNA hypomethylation in endothelial dysfunction, that may potentially contribute to vascular disease in the context of hyperhomocysteinemia (Chapter 4.1).

DNA and protein methylation were previously found to be inhibited by SAH accumulation and the hypomethylation of these biomolecules was observed previously in the context of hyperhomocysteinemia (30–35). Thus, in Chapter 4.2 we expanded our studies to examine additional forms of RNA methylation. We found that SAH accumulation can also impair other RNA methyl modifications in endothelial cells. Excess SAH reduced the content of several specific RNA methyl modifications, many of which were also targeted to the ribose 2'-OH-site of the ribonucleotide. As most of the known mammalian RNA methyltransferases are SAM-dependent, this study supports the concept that excess SAH can impair intracellular global methylation, including RNA methylation. However, the identification of the specific methyltransferases responsible for these modifications is essential to allow for further study of their inhibition by SAH and the biological roles of their modifications. At the present time, major obstacles remain to achieve these goals: firstly, many methyltransferases still lack characterization; secondly, some modifications are catalyzed by more than one methyltransferases while some methyltransferases mediate more than one modification; and

lastly, some RNA-methyltransferases have specific RNA targets, while others can methylated different nucleotides and/or RNA species.

In Chapter 4.2 studies, in addition to studying RNA methylation in endothelial cells, we examined RNA methylation in Cbs-deficient hyperhomocysteinemic mice. Liver and kidney, organs associated with homocysteine metabolism, showed suppression of some RNA methylations that overlapped with our findings in human endothelial cells. A surprising observation, however, was the increased RNA methylation in brain of hyperhomocysteinemic mice compared to wild type mice. In addition to vascular diseases, hyperhomocysteinemia has been strongly associated with neurologic disorders (36), associations that may also be modulated by SAH accumulation. The possible existence of tissue-specific methyltransferases that are less sensitive to SAH accumulation, along with the fact that increased SAM levels are found in the brain of these hyperhomocysteimenic mice in comparison to wild type (33), could help to explain the increased methylation of RNA in these mice. Additionally, differential homocysteine and SAH metabolism in brain, or differences in the regulation of the RNA methyltransferases or demethylases may also contribute to these tissue-specific differences. The biological relevance of human RNA demethylases has been reported for m^6A (37), but no other demethylases were yet identified for the methylation modifications studied, neither in mouse nor human (27).

RNA methylation is known to affect basic cellular processes, such as RNA decoding and synthesis, maturation, transport, and splicing. Our findings support the possibility that SAH-induced impairment of some RNA methylation reactions may be relevant in a disease context (4).

DNA Methylation

The most extensively studied epigenetic mark is DNA methylation, which can regulate gene expression by modulating the chromatin structure and transcription factor binding (38). Several studies have reported the hypomethylating effects of SAH on DNA (35). In Chapter 5 we showed that endothelial cell accumulation of SAH resulted in reduced global DNA methylation.

DNA methylation is mainly associated with gene repression when present at gene promoters. During our studies we questioned whether the observed up-regulation of *NOS3* gene expression under increased SAH concentrations (Chapter 3) could be a result of gene promoter hypomethylation caused by SAH-mediated inhibition of DNA methyltransferases (DNMTs). However, an examination of the literature revealed that the *NOS3* promoter is mainly hypomethylated in endothelial cells (39).

In Chapter 5, we examined *ICAM1* promoter methylation after finding that ICAM-1 was up-regulated by either accumulation of SAH, or the use of a specific DNMT inhibitor. A few studies previously reported that ICAM1 gene expression was regulated by promoter methylation in endothelial cells, but only in the context of cancer or other disease states (40–42). In our analysis, we found that the *ICAM1* gene promoter was already hypomethylated in untreated endothelial cells. It is interesting

that although ICAM-1 is not highly expressed in unactivated endothelial cells, its promoter is mainly demethylated. Nonetheless, the *ICAM1* promoter has several binding sites for different transcription factors and its regulation can be extremely complex (43). Transcription regulation by the activation of transcription factors may facilitate a quicker response to inflammatory signals than that regulated by changes in DNA methylation. Nevertheless, we observed ICAM-1 up-regulation under inhibition of DNMTs, suggesting that decreases in DNA methylation can still increase *ICAM1* gene expression, either by modulating genomic regions that were not included in our analysis to directly modulate *ICAM1* transcription, or by affecting the expression of other regulators of *ICAM1* expression (such as transcription factors).

Importantly, the consequences of SAH-induced DNA hypomethylation in cultured cells, genetically determined hyperhomocysteinemia, and, hyperhomocysteinemia acquired by malnutrition, may differ. In fact, most DNA methylation marks are settled during development and DNA methylation is considered a relatively stable epigenetic mark. Additionally, the endothelium is a quiescent monolayer with an estimated replication rate of 0.1 to 0.4% *per* day (44). Therefore, the effects of excess SAH on DNA hypomethylation on individuals with genetically determined hyperhomocysteinemia may be different from those who are exposed to higher SAH only during the later stages of life. Nevertheless, DNA methylation changes are associated with different diseases like cancer, and the sudden activation of specific genes could still be determinant for disease risk. Additionally, the relevance of DNA hypomethylation in vascular disease was further supported by a recently conducted genome-wide analysis to identify differentially methylated genes in human atherosclerotic lesions (45). The analysis revealed that hypomethylation of chromosomal DNA predominates in atherosclerotic plaques in comparison to healthy mammary arteries. Nevertheless, atherosclerotic plaques may contain a variety of cells, some of which may be more susceptible to changes in DNA methylation due to their relative rates of cell division or their differential expression of other factors that influence DNA methylation, such as the ten-eleven translocation (TET) enzymes that may promote hydroxymethylation and the subsequent removal of methylcytosines (46).

Protein Methylation

Our work identified several targets of SAH-induced hypomethylation while investigating the molecular pathways by which SAH promotes cellular dysfunction. Thus, our studies lead to the discovery that the histone modification H3K27me3 was also altered by SAH accumulation in endothelial cells (Chapter 6). H3K27me3 is the major epigenetic mark associated with Polycomb group (PcG)-mediated gene-repression. As mentioned previously, we observed that SAH decreased cellular H3K27me3 and suppressed the expression of the EZH2 methyltransferase, which is responsible for this histone methylation. EZH2 maintains the pluripotency of human stem cells, and its excess activity promotes tumor growth, but its function in differentiated cells is poorly understood

(17, 47). Recently, EZH2 suppression, via modifications in the H3K27me3 mark, was suggested to promote the expression of a variety of genes involved in adhesion of endothelial cells to fibronectin, and genes involved in angiogenesis (17). Interestingly, this report did not find an up-regulation of the adhesion molecules studied in this thesis (e.g. ICAM-1 and VCAM-1) following EZH2 knockdown; however, they reported that lack of EZH2 altered normal endothelial function by impairing cell-to-cell communication and angiogenic properties of these cells. Similar to our findings, they found that EZH2 suppression led to an increase in the expression of cytokines, such as IL-1β.

Our findings demonstrated SAH-mediated suppression of EZH2, and showed that its suppression may contribute to activation of inflammatory genes as well as the up-regulation of the *CDKN1A* gene, which is associated with a senescent phenotype.

Like H3K27me3, the trimethylation of histone H3K9 has been associated with cardiovascular disease (48). G9a and G9a-Like Protein (GLP) are the two methyltransferases primarily responsible for H3K9 methylation (49). Although the crosstalk between H3K9 and H3K27 methylation was previously suggested, only recently has their actual functional interplay been shown (50). Mozzetta *et al.* demonstrated that EZH2 and G9a/GLP share a high number of common genomic targets and that G9a activity can modulate EZH2 recruitment to a subset of target genes. Since G9a/GLP are also SAM-dependent methyltransferases, SAH accumulation may also inhibit G9a and GLP, further contributing to the impairment of EZH2 function. In fact, a recent study (51) suggests that *in vivo* administration of the same SAH hydrolase inhibitor that we have used in our studies, or the use of a short hairpin RNA construct targeted to SAH hydrolase, specifically decreased H3K9me3 in the aortic sinus of $ApoE^{-/-}$ mice. Interestingly, these *in vivo* treatments, that significantly increased plasma SAH and reduced SAM/SAH ratio, were associated with increased vascular lesion size. However, as we have shown, many targets can be modified by increased SAH. Taken together, these and our own findings suggest the importance of further analysis to better understand the role of histone methylation in endothelial homeostasis and vascular disease.

Methylation is a common post-translational modification in proteins, which can modulate their function and expression; therefore, many non-histone proteins may be affected by excess SAH-induced hypomethylation. For example, Forkhead-box-O transcription factors (FOXOs) are emerging transcriptional regulators in endothelial cells, which may be modulated by methylation. Several studies have established an important role of FOXOs in cell proliferation, oxidative stress, and in the regulation of eNOS (52–54), suggesting that compromised activity of these transcription factors may contribute to impaired endothelial homeostasis. Furthermore, the regulation of FOXO factors by the SAM-dependent methyltransferase protein arginine methyltransferases-1 (PRMT1) was recently reported (52, 55). Thus, further investigation of the effects of SAH on the methylation and function of proteins, including FOXOs, may potentially uncover additional targets modified by excess SAH that contribute to hyperhomocysteinemia-related vascular dysfunction.

PERSPECTIVES

Our studies have contributed to the understanding of the role of SAH as a mediator in hyperhomocysteinemia-associated vascular disease. Interestingly, some of the molecular disturbances found in the endothelium could similarly alter the function of other vascular cell types and their analysis may also uncover novel targets that can be relevant in vascular disease.

Our findings also suggest other avenues of exploration, including the role of SAH and EZH2 suppression in cell senescence that may impair cell cycle progression, contributing to vascular disease. Importantly, an accelerated endothelial cell senescent phenotype was observed in endothelial cells exposed to high homocysteine levels (56). In addition, inhibition of other histone methyltransferases by increased SAH levels may also alter gene expression and contribute to vascular disease. Therefore, the analysis of differentially methylated histone marks, such as H3K27me3 and H3K9me3, by chromatin immunoprecipitation and promoter arrays under conditions of excess SAH, or in *in vivo* hyperhomocysteinemia models, could uncover relevant gene targets involved in disease.

The role of RNA methylation in SAH-mediated vascular dysfunction is another open field of research. Our studies suggest that the identification of the 2'-O-methyltransferases, which were mostly affected by SAH, could help to define new relevant targets of SAH-mediated inhibition. Following methyltransferase identification and characterization under excess SAH, antibodies to these methyltransferases can be used to pull down specific RNAs that they target (RNA-immunoprecipitation) and molecular techniques, such as microarrays or RNA sequencing, can be used to subsequently identify these subsets of RNAs.

We believe that large-scale metabolomic studies of patient populations may clarify whether plasma SAH concentrations are a good biomarker for vascular disease. Nonetheless, it is not clear whether plasma levels of SAH are a good indicator of its intracellular concentrations. An alternative would be to measure intracellular SAH in leukocytes. Although studies of vascular tissue would be more informative, these would be difficult to perform in patient-based studies. Alternatively, the use of a hyperhomocysteinemic animal model, or an animal model in which pharmacological inhibitors are used to induce SAH accumulation, could provide new insights into the physiological relevance of the targets that are altered by excess SAH.

In addition, it is important that cell biology studies of molecular mechanisms are integrated with clinical studies to identify the factors that contribute to human vascular disease. For example, although the use of plasma and peripheral blood cells have limitations, they could be used in parallel with cardiovascular tissue (e.g., samples obtained from patients with cardiovascular disease when subjected to surgical intervention) to better determine the correlations between elevated SAH, homocysteine, and disease in humans. Furthermore, these samples could be used to determine whether the key targets defined in our studies, such as eNOS, GPx-1, cytokines, adhesion molecules,

EZH2, and histone modifications correlate with the biochemical parameters, namely with SAH, and disease.

Cardiovascular diseases are the leading cause of death in developed countries. Therefore, it is important to understand better the factors that contribute to these multifactorial diseases in order to accelerate the development of new drugs and improve prevention and treatment approaches.

Our research has examined the biological importance of SAH accumulation in endothelial dysfunction and activation, considering the question of whether homocysteine is the real culprit of its associated vascular damage. Our results implicate SAH in the pathophysiology of homocysteine-associated vascular disorders, as they demonstrate that excess SAH promotes an endothelial pro-atherogenic phenotype. Nevertheless, our understanding of the role of homocysteine and its metabolites in cardiovascular disease is still incomplete, demanding further investigation.

REFERENCES

1. Liu, C., Wang, Q., Guo, H., Xia, M., Yuan, Q., Hu, Y., Zhu, H., Hou, M., Ma, J., Tang, Z., and Ling, W. (2008) Plasma S-adenosylhomocysteine is a better biomarker of atherosclerosis than homocysteine in apolipoprotein E-deficient mice fed high dietary methionine. *J. Nutr.* **138**, 311–5
2. Wagner, C., and Koury, M. J. (2007) S-Adenosylhomocysteine: a better indicator of vascular disease than homocysteine? *Am. J. Clin. Nutr.* **86**, 1581–5
3. Green, T. J., Skeaff, C. M., McMahon, J. A., Venn, B. J., Williams, S. M., Devlin, A. M., and Innis, S. M. (2010) Homocysteine-lowering vitamins do not lower plasma S-adenosylhomocysteine in older people with elevated homocysteine concentrations. *Br. J. Nutr.* **103**, 1629–34
4. Motorin, Y., and Helm, M. (2011) RNA nucleotide methylation. *Wiley Interdiscip. Rev. RNA*. **2**, 611–31
5. Motorin, Y., and Helm, M. (2010) tRNA stabilization by modified nucleotides. *Biochemistry*. **49**, 4934–44
6. Karbach, S., Wenzel, P., Waisman, A., Munzel, T., and Daiber, A. (2014) eNOS uncoupling in cardiovascular diseases--the role of oxidative stress and inflammation. *Curr. Pharm. Des.* **20**, 3579–94
7. Förstermann, U. (2010) Nitric oxide and oxidative stress in vascular disease. *Pflugers Arch.* **459**, 923–39
8. Upchurch, G. R., Welch, G. N., Fabian, A. J., Freedman, J. E., Johnson, J. L., Keaney, J. F., and Loscalzo, J. (1997) Homocyst(e)ine decreases bioavailable nitric oxide by a mechanism involving glutathione peroxidase. *J. Biol. Chem.* **272**, 17012–7
9. Mitic, T., Anannya, O., and Emanueli, C. (2013) Abstract 12890: Epigenetic Modulation of Endothelial Cell Responses to Hypoxia and Post-ischemic Angiogenesis by the Component of Polycomb Repressive Complex 2 (PRC2), Enhancer of Zest Homology (EZH2). *Circulation*. **128**, A12890–
10. Mitić, T., Caporali, A., Floris, I., Meloni, M., Marchetti, M., Urrutia, R., Angelini, G. D., and Emanueli, C. (2015) EZH2 modulates angiogenesis in vitro and in a mouse model of limb ischemia. *Mol. Ther.* **23**, 32–42
11. Jiang, X., Yang, F., Tan, H., Liao, D., Bryan, R. M., Randhawa, J. K., Rumbaut, R. E., Durante, W., Schafer, A. I., Yang, X., and Wang, H. (2005) Hyperhomocystinemia impairs endothelial function and eNOS activity via PKC activation. *Arterioscler. Thromb. Vasc. Biol.* **25**, 2515–21
12. Trachootham, D., Lu, W., Ogasawara, M. A., Nilsa, R.-D. V., and Huang, P. (2008) Redox regulation of cell survival. *Antioxid. Redox Signal.* **10**, 1343–74
13. Handy, D. E., Zhang, Y., and Loscalzo, J. (2005) Homocysteine down-regulates cellular glutathione peroxidase (GPx1) by decreasing translation. *J. Biol. Chem.* **280**, 15518–25

14. Milton, N. G. N. (2008) Homocysteine Inhibits Hydrogen Peroxide Breakdown by Catalase. *Open Enzym. Inhib. J.*

15. Yamamoto, M., Hara, H., and Adachi, T. (2000) Effects of homocysteine on the binding of extracellular-superoxide dismutase to the endothelial cell surface. *FEBS Lett.* **486**, 159–62

16. Deanfield, J. E., Halcox, J. P., and Rabelink, T. J. (2007) Endothelial function and dysfunction: testing and clinical relevance. *Circulation*. **115**, 1285–95

17. Dreger, H., Ludwig, A., Weller, A., Stangl, V., Baumann, G., Meiners, S., and Stangl, K. (2012) Epigenetic regulation of cell adhesion and communication by enhancer of zeste homolog 2 in human endothelial cells. *Hypertension*. **60**, 1176–83

18. Maleszewska, M., Gjaltema, R. A. F., Krenning, G., and Harmsen, M. C. (2015) Enhancer of zeste homolog-2 (EZH2) methyltransferase regulates transgelin/smooth muscle-22α expression in endothelial cells in response to interleukin-1β and transforming growth factor-β2. *Cell. Signal.* **27**, 1589–96

19. Minamino, T. (2002) Endothelial Cell Senescence in Human Atherosclerosis: Role of Telomere in Endothelial Dysfunction. *Circulation*. **105**, 1541–1544

20. Li, S., and Mason, C. E. (2014) The pivotal regulatory landscape of RNA modifications. *Annu. Rev. Genomics Hum. Genet.* **15**, 127–50

21. Jia, G., Fu, Y., and He, C. (2013) Reversible RNA adenosine methylation in biological regulation. *Trends Genet.* **29**, 108–15

22. Lokody, I. (2014) Gene regulation: RNA methylation regulates the circadian clock. *Nat. Rev. Genet.* **15**, 3

23. Sibbritt, T., Patel, H. R., and Preiss, T. (2013) Mapping and significance of the mRNA methylome. *Wiley Interdiscip. Rev. RNA*. **4**, 397–422

24. Porrua, O., and Libri, D. (2013) RNA quality control in the nucleus: the Angels' share of RNA. *Biochim. Biophys. Acta*. **1829**, 604–11

25. Phizicky, E. M., and Hopper, A. K. (2010) tRNA biology charges to the front. *Genes Dev.* **24**, 1832–60

26. Decatur, W. A., and Fournier, M. J. (2002) rRNA modifications and ribosome function. *Trends Biochem. Sci.* **27**, 344–351

27. Machnicka, M. A., Milanowska, K., Osman Oglou, O., Purta, E., Kurkowska, M., Olchowik, A., Januszewski, W., Kalinowski, S., Dunin-Horkawicz, S., Rother, K. M., Helm, M., Bujnicki, J. M., and Grosjean, H. (2013) MODOMICS: a database of RNA modification pathways--2013 update. *Nucleic Acids Res.* **41**, D262–7

28. Rodriguez-Corona, U., Sobol, M., Rodriguez-Zapata, L. C., Hozak, P., and Castano, E. (2015) Fibrillarin from Archaea to human. *Biol. Cell*. **107**, 159–174

29. Petrossian, T. C., and Clarke, S. G. (2011) Uncovering the human methyltransferasome. *Mol. Cell. Proteomics*. **10**, M110.000976

30. Castro, R., Rivera, I., Struys, E. A., Jansen, E. E. W., Ravasco, P., Camilo, M. E., Blom, H. J., Jakobs, C., and Tavares de Almeida, I. (2003) Increased homocysteine and S-adenosylhomocysteine concentrations and DNA hypomethylation in vascular disease. *Clin. Chem.* **49**, 1292–6

31. Caudill, M. A., Wang, J. C., Melnyk, S., Pogribny, I. P., Jernigan, S., Collins, M. D., Santos-Guzman, J., Swendseid, M. E., Cogger, E. A., and James, S. J. Intracellular S-Adenosylhomocysteine Concentrations Predict Global DNA Hypomethylation in Tissues of Methyl-Deficient Cystathionine β-Synthase Heterozygous Mice

32. Mandaviya, P. R., Stolk, L., and Heil, S. G. (2014) Homocysteine and DNA methylation: a review of animal and human literature. *Mol. Genet. Metab.* **113**, 243–52

33. Esse, R., Imbard, A., Florindo, C., Gupta, S., Quinlivan, E. P., Davids, M., Teerlink, T., Tavares de Almeida, I., Kruger, W. D., Blom, H. J., and Castro, R. (2014) Protein arginine hypomethylation in a mouse model of cystathionine β-synthase deficiency. *FASEB J.* **28**, 2686–95

34. Esse, R., Florindo, C., Imbard, A., Rocha, M. S., de Vriese, A. S., Smulders, Y. M., Teerlink, T., Tavares de Almeida, I., Castro, R., and Blom, H. J. (2013) Global protein and histone arginine methylation are

affected in a tissue-specific manner in a rat model of diet-induced hyperhomocysteinemia. *Biochim. Biophys. Acta*. **1832**, 1708–14

35. Esse, R., Rocha, M. S., Barroso, M., Florindo, C., Teerlink, T., Kok, R. M., Smulders, Y. M., Rivera, I., Leandro, P., Koolwijk, P., Castro, R., Blom, H. J., and de Almeida, I. T. (2013) Protein arginine methylation is more prone to inhibition by S-adenosylhomocysteine than DNA methylation in vascular endothelial cells. *PLoS One*. **8**, e55483

36. Ansari, R., Mahta, A., Mallack, E., and Luo, J. J. (2014) Hyperhomocysteinemia and neurologic disorders: a review. *J. Clin. Neurol.* **10**, 281–8

37. Niu, Y., Zhao, X., Wu, Y.-S., Li, M.-M., Wang, X.-J., and Yang, Y.-G. (2013) N6-methyl-adenosine (m6A) in RNA: an old modification with a novel epigenetic function. *Genomics. Proteomics Bioinformatics*. **11**, 8–17

38. Moore, L. D., Le, T., and Fan, G. (2013) DNA methylation and its basic function. *Neuropsychopharmacology*. **38**, 23–38

39. Chan, Y., Fish, J. E., D'Abreo, C., Lin, S., Robb, G. B., Teichert, A.-M., Karantzoulis-Fegaras, F., Keightley, A., Steer, B. M., and Marsden, P. A. (2004) The cell-specific expression of endothelial nitric-oxide synthase: a role for DNA methylation. *J. Biol. Chem.* **279**, 35087–100

40. Hellebrekers, D. M. E. I., Castermans, K., Viré, E., Dings, R. P. M., Hoebers, N. T. H., Mayo, K. H., Oude Egbrink, M. G. A., Molema, G., Fuks, F., van Engeland, M., and Griffioen, A. W. (2006) Epigenetic regulation of tumor endothelial cell anergy: silencing of intercellular adhesion molecule-1 by histone modifications. *Cancer Res.* **66**, 10770–7

41. Hellebrekers, D. M. E. I., Melotte, V., Viré, E., Langenkamp, E., Molema, G., Fuks, F., Herman, J. G., Van Criekinge, W., Griffioen, A. W., and van Engeland, M. (2007) Identification of epigenetically silenced genes in tumor endothelial cells. *Cancer Res.* **67**, 4138–48

42. Yang, G., Zhu, Y., Dong, X., Duan, Z., Niu, X., and Wei, J. (2014) TLR2-ICAM1-Gadd45α axis mediates the epigenetic effect of selenium on DNA methylation and gene expression in Keshan disease. *Biol. Trace Elem. Res.* **159**, 69–80

43. Roebuck, K. A., and Finnegan, A. (1999) Regulation of intercellular adhesion molecule-1 (CD54) gene expression. *J. Leukoc. Biol.* **66**, 876–88

44. Jaffe, E. A. (2012) *Biology of Endothelial Cells*, Springer Science & Business Media

45. Aavik, E., Lumivuori, H., Leppänen, O., Wirth, T., Häkkinen, S.-K., Bräsen, J.-H., Beschorner, U., Zeller, T., Braspenning, M., van Criekinge, W., Mäkinen, K., and Ylä-Herttuala, S. (2014) Global DNA methylation analysis of human atherosclerotic plaques reveals extensive genomic hypomethylation and reactivation at imprinted locus 14q32 involving induction of a miRNA cluster. *Eur. Heart J.* **36**, 993–1000

46. Kohli, R. M., and Zhang, Y. (2013) TET enzymes, TDG and the dynamics of DNA demethylation. *Nature*. **502**, 472–9

47. Ezhkova, E., Pasolli, H. A., Parker, J. S., Stokes, N., Su, I., Hannon, G., Tarakhovsky, A., and Fuchs, E. (2009) Ezh2 orchestrates gene expression for the stepwise differentiation of tissue-specific stem cells. *Cell*. **136**, 1122–35

48. Kim, G. H., Ryan, J. J., and Archer, S. L. (2013) The role of redox signaling in epigenetics and cardiovascular disease. *Antioxid. Redox Signal.* **18**, 1920–36

49. Shinkai, Y., and Tachibana, M. (2011) H3K9 methyltransferase G9a and the related molecule GLP. *Genes Dev.* **25**, 781–8

50. Mozzetta, C., Pontis, J., Fritsch, L., Robin, P., Portoso, M., Proux, C., Margueron, R., and Ait-Si-Ali, S. (2014) The histone H3 lysine 9 methyltransferases G9a and GLP regulate polycomb repressive complex 2-mediated gene silencing. *Mol. Cell*. **53**, 277–89

51. Xiao, Y., Huang, W., Zhang, J., Peng, C., Xia, M., and Ling, W. (2015) Increased plasma S-adenosylhomocysteine-accelerated atherosclerosis is associated with epigenetic regulation of endoplasmic reticulum stress in apoE-/- mice. *Arterioscler. Thromb. Vasc. Biol.* **35**, 60–70

52. Yamagata, K., Daitoku, H., Takahashi, Y., Namiki, K., Hisatake, K., Kako, K., Mukai, H., Kasuya, Y., and Fukamizu, A. (2008) Arginine methylation of FOXO transcription factors inhibits their phosphorylation by Akt. *Mol. Cell*. **32**, 221–31

53. Yang, X.-F., Fang, P., Meng, S., Jan, M., Xiong, X., Yin, Y., and Wang, H. (2009) The FOX transcription factors regulate vascular pathology, diabetes and Tregs. *Front. Biosci. (Schol. Ed).* **1**, 420–36

54. Wang, Y., Chen, S., and Li, H. (2010) Hydrogen peroxide stress stimulates phosphorylation of FoxO1 in rat aortic endothelial cells. *Acta Pharmacol. Sin.* **31**, 160–4

55. Michalek, R. D., and Rathmell, J. C. (2008) Methed-up FOXOs can't in-Akt-ivate. *Mol. Cell*. **32**, 160–2

56. Xu, D., Neville, R., and Finkel, T. (2000) Homocysteine accelerates endothelial cell senescence. *FEBS Lett.* **470**, 20–4

Supplemental Material

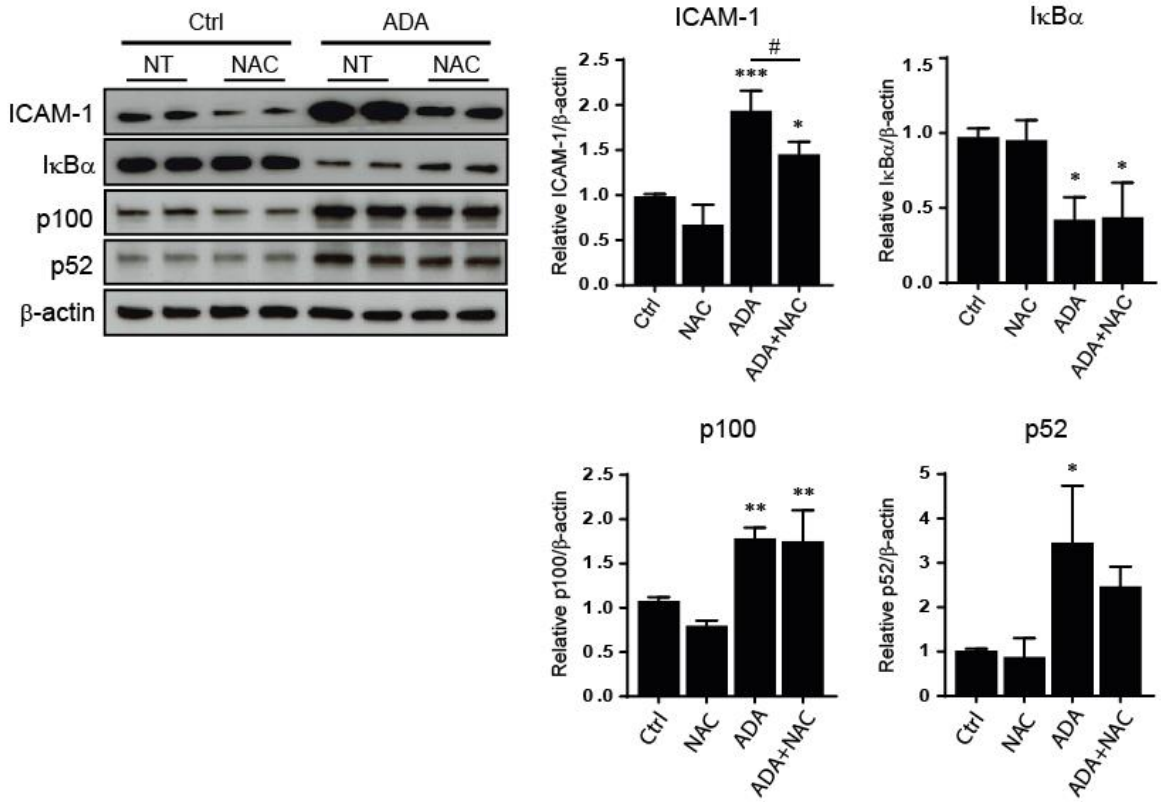

Suppl. Figure 1 – The effects of oxidative stress on NFkB activation by SAH. SAH accumulation was induced in human coronary endothelial cells using adenosine-2′,3′-dialdehyde (ADA; 20 µmol/L). Cells were additionally incubated with eight mmol/L of the antioxidant N-acetylcysteine (NAC) or in the absence of the antioxidant (NT). Incubations were performed for 48h. ICAM-1, IkBα, p100, and p52 proteins were monitored by Western blot. A representative blot is shown on the left and summary densitometry measurements on the right (n=3). ANOVA, followed by the Newman-Keuls test for multiple comparisons, was used in the analysis shown. *, $p < 0.05$, **, $p < 0.005$, ***, $p < 0.0005$, *versus* control or NAC treated cells. #, $p < 0.05$ for co-treatment (ADA+NAC) *versus* ADA treated cells.

LIST OF PUBLICATIONS

1. Barroso, M., Kao, D., Tavares de Almeida, I., Castro, R., Loscalzo, J., and Handy, D.E. S-Adenosylhomocysteine induces inflammation through NFkB: a possible role for EZH2 in endothelial cell activation. *Submitted to Biochim Biophys Acta.* (July 8th, 2015).

2. Barroso, M., Florindo, C., Kalwa, H., Silva, Z., Turanov, A. A., Carlson, B. A., de Almeida, I. T., Blom, H. J., Gladyshev, V. N., Hatfield, D. L., Michel, T., Castro, R., Loscalzo, J., and Handy, D. E. (2014) Inhibition of cellular methyltransferases promotes endothelial cell activation by suppressing glutathione peroxidase 1 protein expression. *J. Biol. Chem.* 289, 15350–62.

3. Esse, R., Rocha, M. S., Barroso, M., Florindo, C., Teerlink, T., Kok, R. M., Smulders, Y. M., Rivera, I., Leandro, P., Koolwijk, P., Castro, R., Blom, H. J., and de Almeida, I. T. (2013) Protein arginine methylation is more prone to inhibition by S-adenosylhomocysteine than DNA methylation in vascular endothelial cells. *PLoS One*. 8, e55483.

4. Barroso, M., Rocha, M. S., Esse, R., Gonçalves, I., Gomes, A. Q., Teerlink, T., Jakobs, C., Blom, H. J., Loscalzo, J., Rivera, I., Tavares de Almeida, I., and Castro, R. (2012) Cellular hypomethylation is associated with impaired nitric oxide production by cultured human endothelial cells. *Amino Acids*. 42, 1903–11.

5. Castro, R., Barroso, M., Rocha, M., Esse, R., Ramos, R., Ravasco, P., Rivera, I., and de Almeida, I. T. (2010) The *TCN2* 776C>G polymorphism correlates with vitamin B(12) cellular delivery in healthy adult populations. *Clin. Biochem.* 43, 645–9.

"If I have seen further, it is by standing upon the shoulders of giants."
"Se eu vi mais longe, foi por estar sobre ombros de gigantes"
Isaac Newton

ACKNOWLEDGEMENTS / AGRADECIMENTOS

Se esta tese fosse um gene a ser expresso, bateria o record do número de ativadores que teriam contribuído para a sua expressão. Agradeço a todos os que, na minha condição de polimerase que nada pode fazer sozinha, contribuíram para a minha atividade e determinaram as condições favoráveis para que este trabalho pudesse ser desenvolvido.

If this thesis was a gene to be expressed, it would beat a record on the number of activators that were involved in its expression. Being a polymerase that can't do much by herself, I am thankful to everyone that made it possible for this work to be developed.

O meu primeiro agradecimento vai para as minhas orientadoras que me colocaram e mantiveram no caminho certo, sendo sempre a minha "capacidade de *proof-reading*" e garantindo que este gene tivesse um produto final. Obrigada. Esta tese também é vossa.

My first acknowledgement goes to my supervisors who have put me and kept me on the right path, being always my "proof-reading ability" and making sure that this gene would have a final product. Thank you. This thesis is also yours.

A Professora Rita Castro foi sem dúvida o promotor deste gene. Obrigada por me ter introduzido na vida científica, por todo o seu apoio, ensinamentos e amizade. Acima de tudo, obrigada por ter acreditado sempre em mim.

Diane, I am sure this gene would be much shorter without you. Thank you very much for being always so helpful and full of ideas that kept me in a non-stop mode. Thank you for your scientific advising and friendship.

Dr. Loscalzo, thank your constant help and support. I am grateful for the opportunity I had to work in your Lab. Thank you for welcoming me into your group in Boston and for sharing your knowledge and be always so nice and helpful.

Professora Isabel Tavares de Almeida, obrigada por me ter dado a oportunidade de iniciar a minha vida científica no Grupo de Metabolismos e Genética, por todo o seu apoio e incentivo ao longo deste anos. Obrigada pelos sábios conselhos e também pela amizade.

Agradeço também às Professoras Isabel Rivera e Paula Leandro por estarem sempre disponíveis para dar apoio e aconselhamento nos nossos trabalhos mais “genéticos” ou “proteicos”. Um muito obrigada também à Professora Fátima Ventura. Quem sabe se estaria aqui se um dia, naquela entrevista, não tivesse sugerido que a minha ajuda era bem-vinda no grupo? Obrigada também às Professoras Maria João e Margarida Silva, por estarem sempre disponíveis para ajudar, e também pela sua amizade e simpatia.

Um agradecimento especial para os meus colegas do Met&Gen. É com saudade que recordo os tempos em que estávamos todos (ou quase todos) juntos no “cepas”. Cátia, Paula, Sara, Inês Faustino, João Leandro, Ana Pinheiro, Sandra, Ana Isabel, Paulo, Marisa, Henrique, Ruben R., Ana Serrão, Hana, Israel e Marco, obrigada por todos os bons momentos e dores de cabeça partilhados. Obrigada por, com a vossa boa disposição, nunca permitirem que um Western-blot me tirasse um sorriso por muito mais de um minuto (era +/- o tempo de subir as escadas). Obrigada também Ângelita por me teres aturado e por seres sempre tão boa menina!

Conceição, eu fico feliz de fazer sorrir os outros. Mas amigo amigo é aquele que fica feliz de ouvir a nossa gargalhada. Obrigada pela sua amizade. Eu também fico sempre feliz de ouvir a sua. Obrigada também por toda a ajuda com as burocracias!

Mónica e Ruben ”S”, obrigada pelo apoio do início ao fim deste trabalho. Obrigada por terem sido sempre um exemplo a seguir. Obrigada pela amizade e por terem valorizado o poder do SAH antes de eu chegar aqui!

Cristina, por seres assim e pela tua amizade, obrigada! Foi um prazer trabalhar contigo, mas ainda mais foi partilhar muitos bons momentos de amizade ao longo desta aventura! Obrigada também por toda a ajuda e por estares sempre disponível!

Obrigada também para os restantes colegas do CPM com quem tive oportunidade de conviver, trocar ideias e materiais. Obrigada à dupla Miguel&André pelos momentos de boa disposição! Obrigada às “Doritas” pela partilha agradável das místicas “catacumbas”.

Obrigada também aos amigos que fora do laboratório contribuíram para que tudo isto fosse possível. Obrigada por me apoiarem sempre, quer seja a um ou dois quarteirões, ou a milhares de quilómetros de distância. Um obrigado por serem e manterem a “partilha mundial”. Vocês são os melhores! Um obrigada também à minha Joana por toda a amizade ao longo destes anos.

E qual a maior vantagem de ter vivido em 3 lugares diferentes? Amigos “a triplicar”. Obrigada a todos os meus portugueses em Boston, por toda a amizade e bons momentos passados juntos. Ângela, muito obrigada por me teres acolhido, por me teres mostrado toda a cidade, por todos os *brunches* e bons momentos que fazem esquecer por um bocadinho o trabalho. Obrigada também, por toda a ajuda e especial amizade que tão preciosa foi durante os meus tempos “em terras do tio Sam”, à Inês Tenente (obrigada por todas as longas conversas), à Inês Lima, ao Dário, à Ana Tellechea, à Sofia, ao Randy, à Evi e ao Harold.

Thank you Professor Mark Helm for the opportunity to join your group and learn about RNA modifications biology. Thank you to all the lab members, especially Kathirn and Ludy, for all your help. Helena, thank you for your friendship and for staying late with me in the lab! Thanks for all the good memories I'll keep from Mainz.

Now back to Boston. I want to thank all the members of the Loscalzo Lab for their support and advising. Thank you for being such a good example of how hard work can be rewarding. Ying-Yi, Brad, Steve, Jane, Will, Shiow Shi, Hae-Young, thanks for your constant insights and suggestions that helped to improve my work and to grow as a scientist. Thanks for being so nice and helpful all the time. I am also thankful to all my lab-mates! A special thanks to David, Anjali and Paula, for your help, friendship, and all the good moments we spent together in Boston!

Derrick Kao. What can I say? I could never thank you enough. But, specially, thank you for being such a genuine person and having that child always in you. Thanks for being such a nice friend and thank you for trying to say “bom dia” and turning the lab into a happy place! Thanks for talking with my mum. Oddly, she always felt I was in good hands… You are the best!

Os meus últimos agradecimentos vão para a minha Família. A melhor do mundo. Obrigada aos meus primos, Tota, Didi, João e Joana por serem sempre mais do que amigos, é como se tivesse 5 irmãos. Obrigada pela vossa constante preocupação e disponibilidade. Obrigada por fazerem sempre tudo para estarmos perto, mesmo quando um oceano nos separava. Obrigada também por serem os melhores do mundo.

Tota e Mike, para vocês um agradecimento especial, por me terem dado a melhor coisa que aconteceu durante estes quatro anos, o meu Afonsinho! Foi a minha maior alegria. Obrigada pela forma especial como sempre me mantiveram por perto, mesmo longe.

Obrigada aos titios. Tios Aurora e Saul, obrigada por toda a alegria com que sempre me recebem, com direito a todos os mimos! Obrigada pela amizade e preocupação constante. Obrigada por todo o vosso apoio ao longo desta jornada.

Um especial agradecimento também à minha tia Fátima e ao tio Zé, por me aperfilharem sempre de braços abertos. Por terem sempre sido uns segundos pais. Obrigada por tudo.

Ao meu irmão, João, obrigada pela amizade. Obrigada por me fazeres rir e por transmitires sempre essa “tranquilidade” com o teu espirito prático.

João Coelho, sem ti isto não tinha tido graça nenhuma. Obrigada por toda a ajuda nesta fase final. Obrigada por, mesmo no meio de tanto momento mais difícil, estares sempre aí para o que vem a seguir; porque há sempre um a seguir… Obrigada por acreditares em mim.

E obrigada aos meus pais. Pais, esta tese é para vocês, pois sem vocês não existiria! Obrigada pelo amor incondicional, obrigada por me darem sempre tudo de vocês. Obrigada por serem meus pais. Obrigada por serem os melhores!

Professores, amigos e família, não foram apenas ativadores deste “gene” mas também as modificações pós-tradução de que a polimerase (eu) foi/é alvo e que condicionam a sua estrutura e função. São parte de quem eu sou. Obrigada.

Professors, family, and friends, you were not only the activators for this “gene” to be expressed. You are also like the post-translational modifications that can alter a polymerase structure and function. You are part of who I became. Thank you.